Stony Brook University

A Scaffold Directed Approach to an Aromatic Belt

A Dissertation Presented

by

David Connors

to

The Graduate School

in Partial Fulfillment of the

Requirements

for the Degree of

Doctor of Philosophy

in

Chemistry

Stony Brook University

December 2012

Stony Brook University

The Graduate School

David Connors

We, the dissertation committee for the above candidate for the

Doctor of Philosophy degree, hereby recommend

acceptance of this dissertation.

Nancy Goroff– Dissertation Advisor
Associate Professor, Department of Chemistry

Iwao Ojima - Chairperson of Defense
Distinguished Professor, Department of Chemistry

Andreas Mayr - Third Member of Defense
Professor, Department of Chemistry

Frank Mallory – Outside Member of Defense
W. Alton Jones Research Professor, Department of Chemistry, Bryn Mawr College

This dissertation is accepted by the Graduate School

Charles Taber
Interim Dean of the Graduate School

Abstract of the Dissertation

A Scaffold Directed Approach to an Aromatic Belt

by

David Connors

Doctor of Philosophy

in

Chemistry

Stony Brook University

2012

An aromatic belt, a molecule that has two continuous edges that do not intersect and is fully conjugated, is a synthetic target that has yet to be isolated. Aromatic belts are an attractive target for synthetic chemists, due to their curved pi system. Molecules with curved pi systems, such as fullerenes and carbon nanotubes, have unique physical and chemical properties.

Synthesis of an aromatic belt is challenging, as bending a pi system leads to an increase in strain energy. Our work uses a scaffold to direct the reactions in a controlled manner. The scaffold will allow smaller planer pieces, the "subunits", to be joined together to create a curved precursor. This precursor can then be oxidized to form an aromatic belt. Removal of the scaffold will give the target belt. The scaffold we have chosen is a substituted benzene with three-fold symmetry.

This work discusses the synthetic efforts toward [12]cyclophenacene, an aromatic belt with 12 benzene rings arranged in a zig-zag orientation. The synthesis of the sub-units required the development of a novel synthetic route towards tetrasubstituted phenanthrenes. In addition, some previously unreported difficulties with the Mallory photooxidation were encountered and overcome.

Dedication Page

I would like to dedicate this thesis to the memory of my father, James Patrick Connors.

Table of Contents

List of Figures

List of Schemes

List of Tables

List of Abbreviations

Ac	acetyl
aq	aqueous
bn	benzyl
Bu	butyl
DAN	dialkoxy naphthalene
DFT	density functional theory
DIBAL	diisobutylaluminum hydride
DME	dimethoxyethane, glyme
DMF	N,N-dimethylformamide
dppf	diphenylphosphinoferrocene
DMSO	dimethylsulfoxide
FVP	flash vacuum pyrolysis
Hex	hexyl
HOMO	highest unoccupied molecular orbital
LUMO	lowest unoccupied molecular orbital
Me	methyl
NBS	N-bromosuccinimide
NDI	naphthalene diimide
NMP	N-methyl-2-pyrrolidinone
NMR	nuclear magnetic resonance
Ph	phenyl
r.t. (rt)	room temperature

S-Phos	2-Dicyclohexylphosphino-2',6'-dimethoxybiphenyl
THF	tetrahydrofuran
TLC	thin-layer chromatography
Tos	p-toluenesulfonyl
TsOH	p-toluenesulfonic acid

Acknowledgements

I first would like to thank Dr. Gary Snyder for introducing me to research. He taught me most of what I know about planning and troubleshooting reactions. His enthusiasm about science inspired me to go to grad school.

I also wanted to thank Nancy Goroff for being a great PhD advisor. Not only did she allow me work on such an interesting project, but she always made sure I wasn't discouraged by such a challenging project. She also sent me to many wonderful conferences in which I had to the opportunity to meet and speak with a variety of great scientists.

I also want to thank my other committee members Professors Mayr and Ojima. I appreciate Professor Mayr for always being positive and encouraging anytime we discussed my research or at my third meeting. Professor Ojima was always offering advice and things to try.

I also want to thank Professor Frank Mallory for being my outside member and traveling for my thesis defense. In addition, he provided advice and feedback on the photocyclization reaction at the 2010 Reaction Mechanism conference.

Professor Larry Scott provided a lot of input at the 2009 Physical Organic Gordon conference. He suggested focusing on the McMurry coupling to form the initial macrocycle. He also suggested the use of ether linkages instead of esters, so they don't interfere with the coupling.

Many others have given me useful feedback that has helped this project move forward. Professor Kathleen Kilway suggested the used of the ethyl substituted benzene. Professor Ramesh Jasti suggested the vigorous deoxygenation of the palladium catalyzed reaction with the

S-Phos ligand. I got good feedback from Professor Steven Wheeler on my computational project.

I want to thank the members of the Goroff group. Chris Wilhelm was always around to talk to and is responsible for getting me addicted to coffee. Raquel Campo was a great benchmate and helped pass the time in lab. Allison Black has been my officemate for quite a while and I appreciate her putting up with my messy desk and for good conversation, some work related, but mostly not. I also want to thank Dan Resch for computer help, x-ray help, good suggestions and just interesting conversation in general.

Most importantly I want to thank my wonderful family. My wife Megan has been an incredible source of support while I finished my PhD. My daughter Riley is so fun to be around and she makes me smile whenever I see her. I also want to thank my mom for always telling me I can accomplish anything I put my mind to.

Chapter 1

1-1 An Introduction to Aromatic Belts

Aromatic belts have long fascinated and eluded chemists.[1] An aromatic belt is a hoop shaped macrocycle that is double stranded and conjugated. Figure 1-1 shows some examples of the belts that have been targeted synthetically by chemists. Belt **1-1** is an example of a cyclacene, which is the smallest portion of a zig-zag nanotube. If one were to synthesize a single row armchair carbon nanotube then the result would be belt **1-2**, a cyclophenacene. Other synthetic targets have included the equator of a C_{84} fullerene[2] **1-3**, and a "Vögltle" belt[3] **1-4**. Although other aromatic belts can be targeted, the belts shown in Figure 1-1 have been the main targets for synthetic chemists.

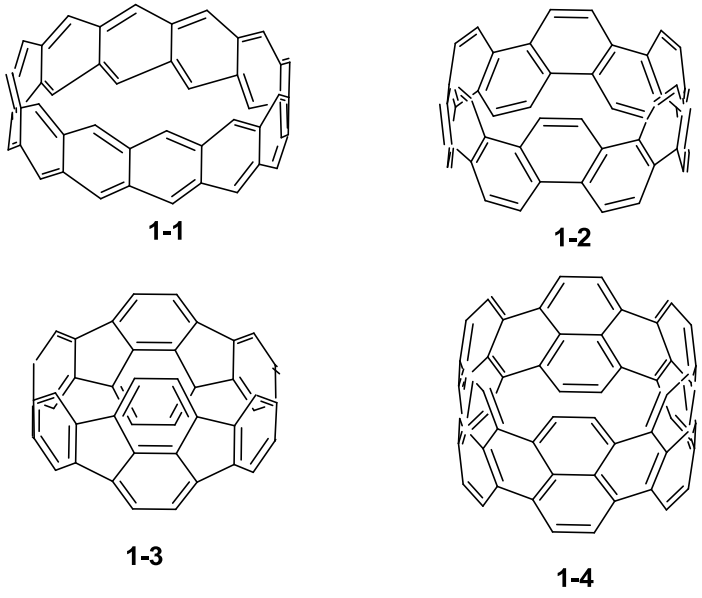

Figure 1-1 – Synthetically target aromatic belts[1]

The history of aromatic belts begins as early as 1954,when the orbital structure of cyclacene (**1-1**) was examined by Heilbronner. [4] One of the first discussions of an aromatic belt

as a synthetic target was in 1983 when Vögltle suggested using the successfully developed cyclophane chemistry to target belts **1-1** and **1-4**.[3] Interest in aromatic belts has only increased since the discovery of fullerenes and carbon nanotubes (CNT).[5]

Aromatic belts have radially oriented p-orbitals or p-orbitals that point towards the center of the molecule (Figure 1-2).[6] This arrangement is in contrast to most aromatic molecules in which the p-orbitals all point perpendicular to the center of the molecule. Molecules with radially oriented p-orbitals have shown interesting complexation abilities,[7] such as in host-guest chemistry due to different attraction of molecules or atoms to the convex or concave face.[1]

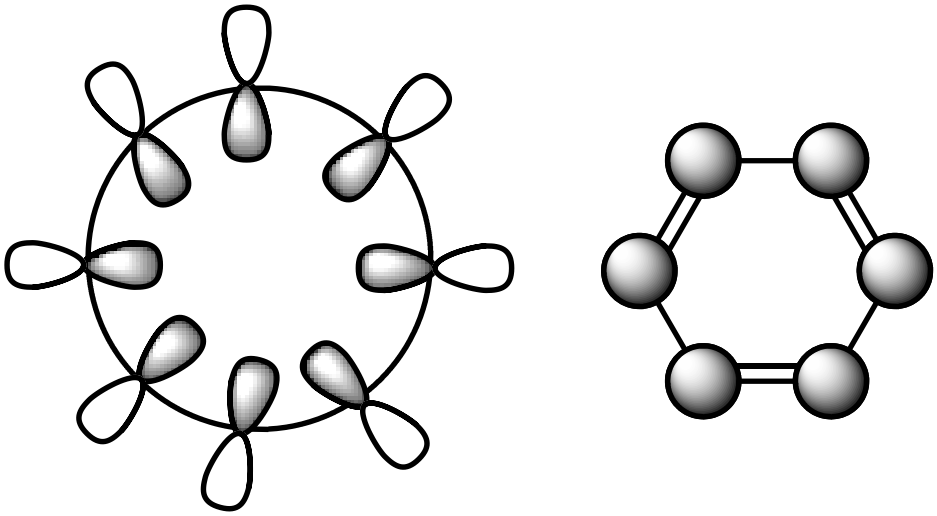

Figure 1-2 – A molecule with radially oriented p-orbitals and the p-orbitals of benzene

In addition to the numerous synthetic efforts that have been undertaken[1] a number of theoretical studies have also been conducted.[8] A major problem with cyclacene belts is that they are predicted to be open-shell singlets, meaning not all of the electrons would be paired.[8a] An open-shell singlet would be reactive because of its radical-like character. Cyclophenacenes, on the other hand, have been predicted to be more stable due to their greater degree of aromaticity.[9] Figure 1-3 below shows the Clar structure of [12]cyclophenacene (**1-2**) and [12]cyclacene (**1-1**).

Cyclacene has no Clar sextets, while cyclophenacene **1-2** has six, meaning cyclophenacene **1-2** is more stabilized by aromaticity than belt **1-1**.

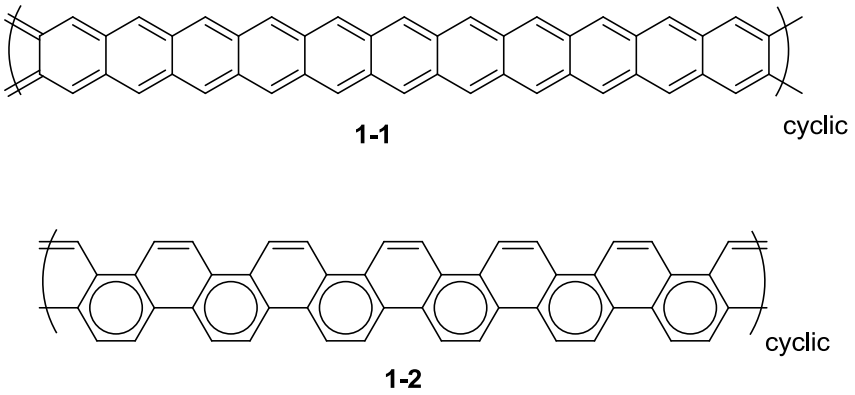

Figure 1-3 – The Clar structure of cyclacene and cyclophenacene

Even though carbon nanotubes were first reported in 1991,[5b] most carbon nanotubes are still obtained as mixtures by extraction from soot.[10] Larry Scott has proposed the use of aromatic belts as templates for the formation of carbon nanotubes with well-defined chirality by a rational method.[11] The chirality of a carbon nanotube affects its electronic properties.[12] Armchair carbon nanotubes (**1-5**), shown in Figure 1-4, are metallic and the others are all semiconductors with varying band gaps.[12] The ability to produce a carbon nanotube with a predefined chirality would

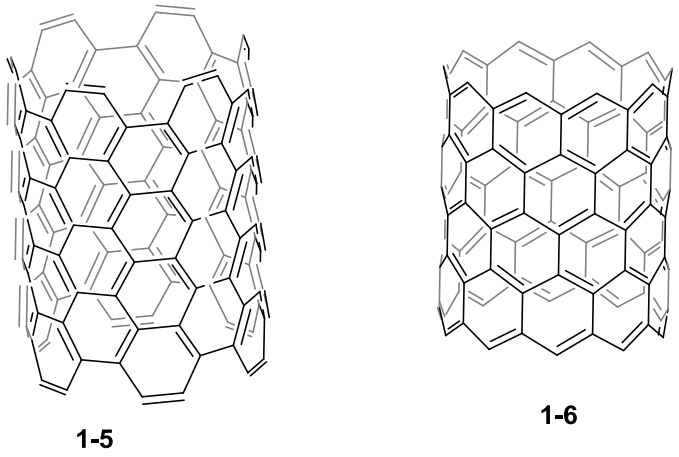

Figure 1-4 – An armchair (**1-5**) and a zig-zag (**1-6**) carbon nanotube

allow for a better understanding of the properties of carbon nanotubes, as well as their further applications.[10]

1-2 Synthetic Efforts Towards Aromatic Belts

In 1991 Vöglte reported on his group's synthetic progress towards an aromatic belt.[13] His strategy relies on a valence isomerism/dehydration sequence (VID) to form pyrene units (Scheme 1-1). The VID reaction to form pyrene was first reported in 1970 by Mitchell and Boekelheide.[14] When cyclophane **1-7** was irradiated with light, it turned green, forming a mixture of dihydropyrene **1-8** and pyrene (**1-9**). Further irradiation or exposure to oxygen led to the complete conversion of the mixture to pyrene.

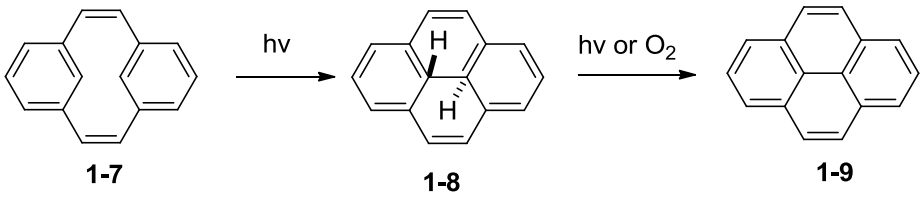

Scheme 1-1 – The VID to form pyrene

Scheme 1-2 shows Vögtle and co-workers' synthetic route towards belt **1-14**.[13] Molecules **1-10** and **1-11** were reacted together in a solution of cesium carbonate. The product of the reaction was macrocycle **1-12**, which was obtained in only 3% yield, presumably due to noncyclized byproducts. The proposed route from macrocycle **1-12** would have involved transformation to polyene **1-13**, followed by the VID sequence to give belt **1-14.** Efforts to perform further chemistry with intermediate **1-12** were not reported.

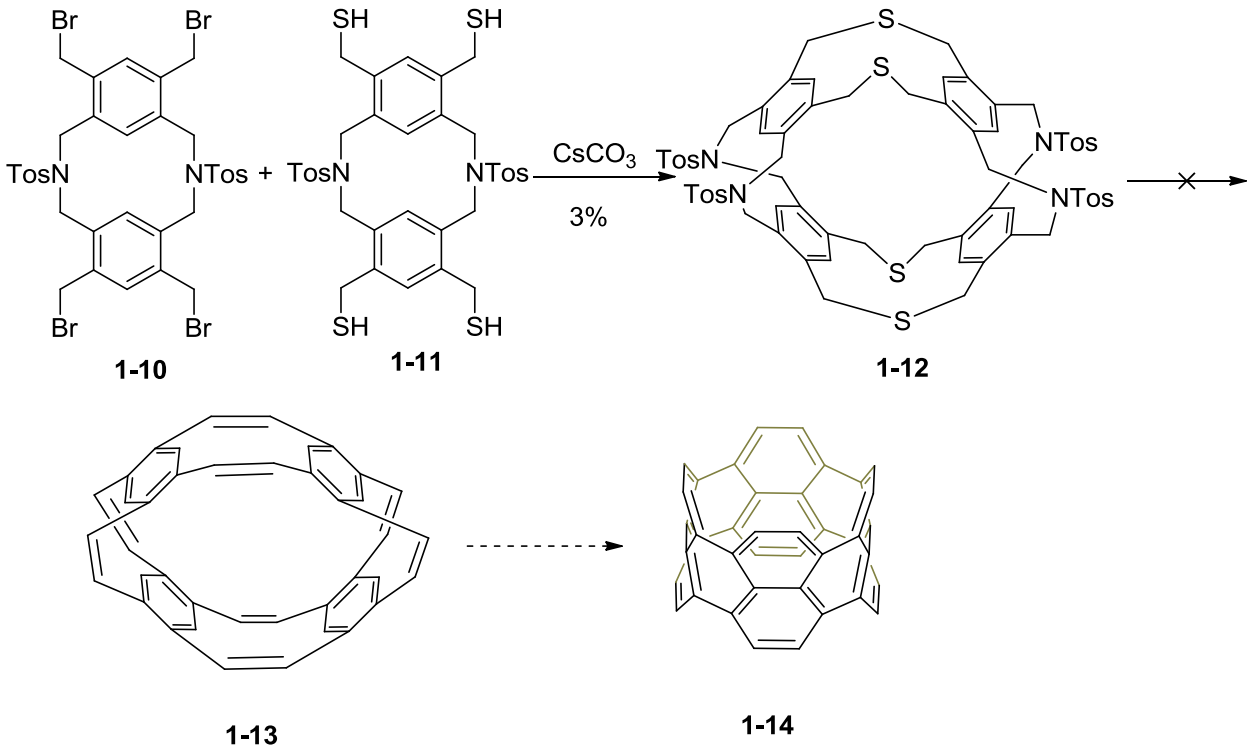

Scheme 1-2 – Vögtle's synthesis of macrocycle 1-12[13]

Starting in 1987, the Stoddart group began reporting on work towards the synthesis of cyclacenes.[15] Their strategy relies on a stereoselective Diels-Alder reaction between the double-sided dienophile **1-15** and tetraene **1-16**, shown in Scheme **1-3**. When the dienophile **1-15** and an excess of **1-16** are heated in toluene, they yield tetraene **1-17** as the only diastereomer. Using high pressure and a second equivalent of the dienophile **1-15** gave macrocycle **1-18**, which they termed "kohnkene". The two conjugated oxygen bridges of compound **1-18** were removed with Ti^0 generated from $TiCl_4$ and $LiAlH_4$, to give macrocycle **1-19**. The remaining oxygen bridges were removed under acidic conditions, but the major product isolated (**1-21**) was an isomer of the expected compound **1-20**.[15e] Compound **1-21** may be less strained than the target macrocycle. A variety of conditions were employed to try to aromatize macrocycle **1-21** fully to [12]cycloacene **1-1**, but these attempts were unsuccessful.[15e]

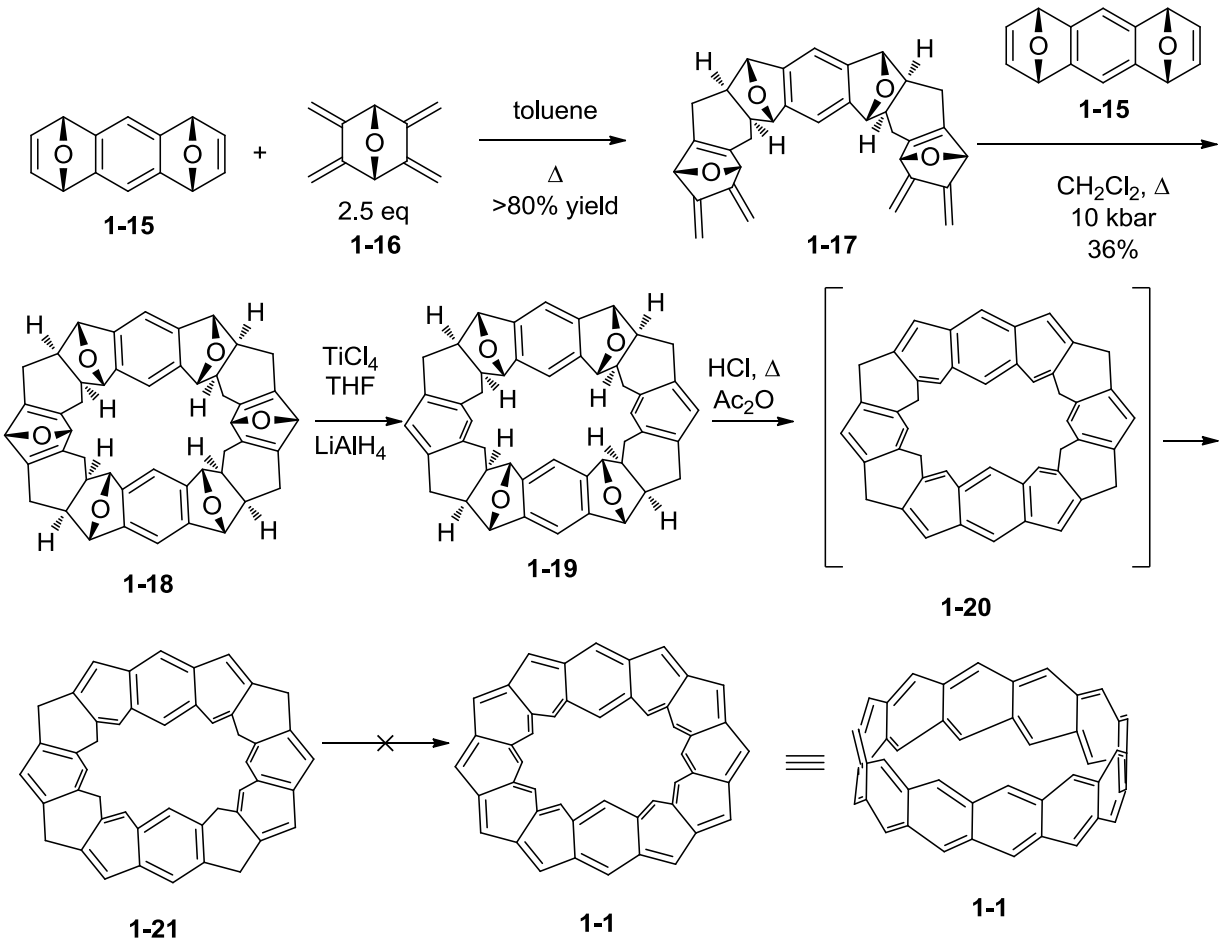

Scheme 1-3 – The Stoddart group's route towards [12]cyclacene[15]

In 1996 the Cory group reported also using a Diels-Alder approach in an effort to synthesize a cyclacene belt.[16] Their strategy was to use flexible precursors and to control reaction conditions such that a macrocycle is formed and not a polymer, as shown in Scheme 1-4. By adding compounds **1-22** and **1-23** dropwise to a flask of boiling dioxane, macrocycle **1-24** was formed in 69% yield. Attempted aromatization with dichlorodicyanoquinone (DDQ) only oxidized one of the rings (**1-25**). Pyridium chlorochromate (PCC) was used to form polyquinone **1-26**, but further efforts to aromatize the molecule to cyclacene **1-27** were unsuccessful.

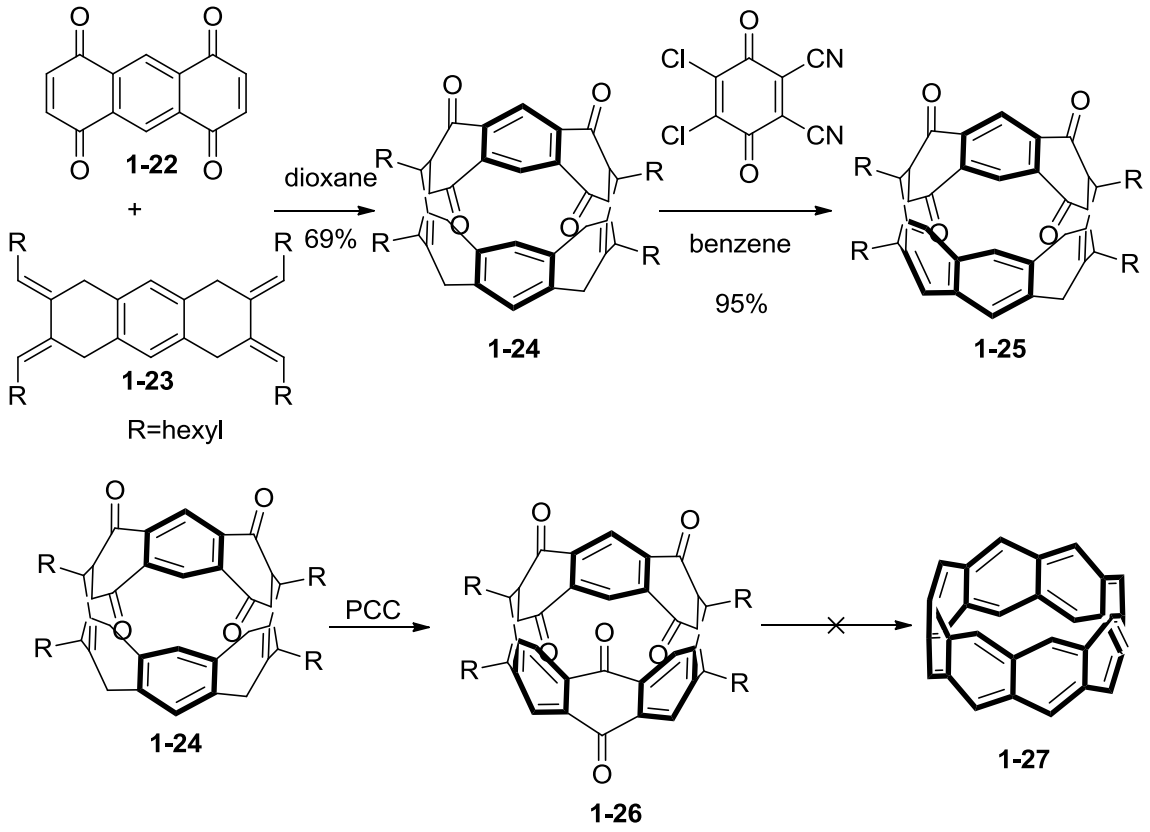

Scheme 1-4 – The Cory group's synthesis of macrocycle **1-24** and its attempted aromatization[16]

In 1990 Iyoda and coworkers reported the synthesis of molecule **1-32**, shown below in Scheme 1-5.[17] The synthetic route to macrocycle **1-32** relies on a pinacol coupling of stilbene **1-28**, which gave a mixture of isomers. The desired syn isomer was formed by using a Swern oxidation to give a diketone followed by a reduction with sodium borohydride to give the diol **1-30**. Diol **1-30** was then converted to thiocarbonate **1-31** with thiocarbonyldiimidazole (TCDI) and compound **1-32** was obtained when **1-31** was heated with 1,3-dimethyl-2-phenyl-1,3,2-diazaphospholidine (DMPD). Oxidation of **1-32** would give [10] cyclophenacene (**1-33**), but when **1-32** was exposed to iodine and light, instead of obtaining the desired cyclophenacene, a side reaction took place giving the unusual molecule **1-34**.[18]

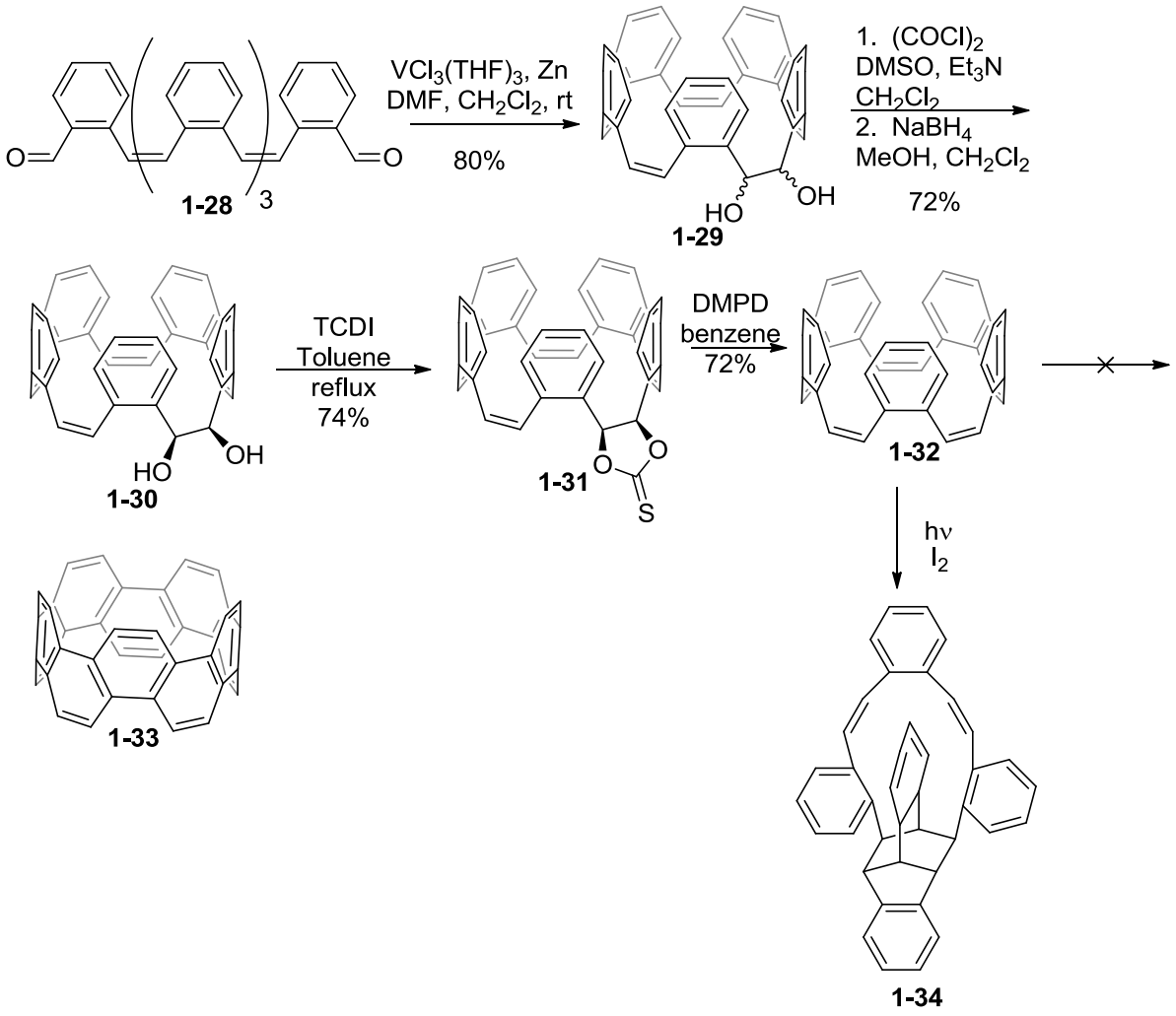

Scheme 1-5 – Iyoda's attempted aromatization of **1-32**[17,18]

Around this time the Scott group was working towards the synthesis of [12]cyclophenacene (**1-2**), shown in Scheme **1-6**.[19] Their strategy was first to synthesize precursor **1-40**, which would then be subjected to flash vacuum pyrolysis (FVP) to form the target belt **1-2**. The Scott group has used FVP to synthesize nonplanar compounds previously, most notably during the rational synthesis of C_{60}.[20] Their synthetic route involves the formation of phenanthrene trimer **1-37** by the Wittig reaction of dialdehyde **1-35** with phosphonium salt **1-36**. The *t*-butyl groups on dialdehyde **1-35** were added in order to increase the solubility of the resulting intermediates. The phenanthrene trimer **1-37** was cyclized by reducing the nitriles to

aldehydes, followed by a McMurry coupling to give macrocycle **1-39** in good yield. The lability of the t-butyl groups in macrocycle **1-39** was expected to inhibit cyclization directly to the [12]cyclophenacene. Attempts to remove the t-butyl groups from **1-39** led to decomposition of the material and no detectable product. Synthesis of **1-40** from a precursor trimer without *t*-butyl groups was also attempted, but poor solubility inhibited this route.

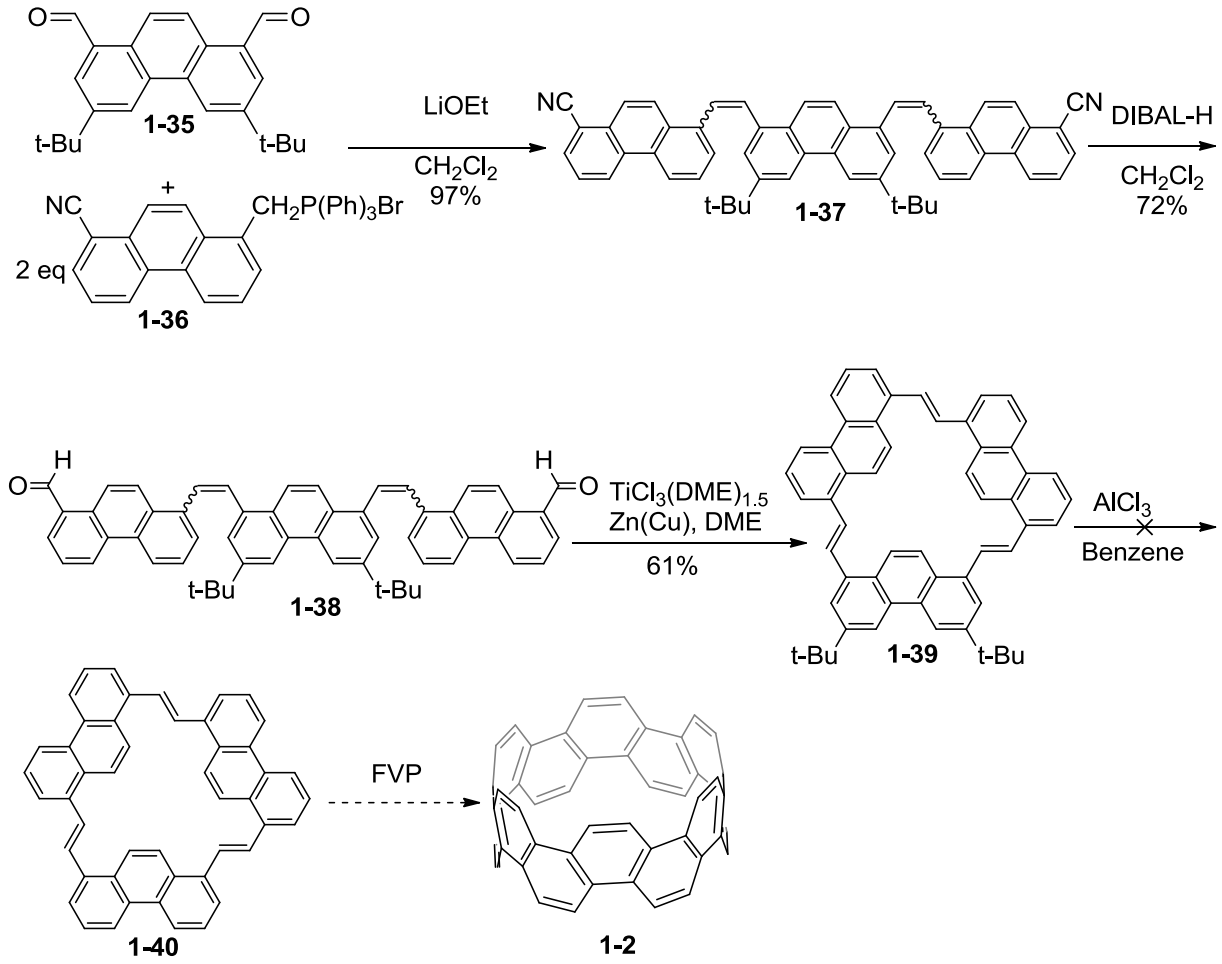

Scheme 1-6 – The Scott group's efforts toward [12]cyclophenacene[19]

Herges and co-workers used a different approach to an aromatic belt, involving ring expansion of smaller strained macrocycles, as shown in Scheme **1-7**.[21] Their route begins from tetradehydrodianthracene (**1-41**), which had previously been reported.[22] Herges and co-workers found that when crystals of **1-41** are suspended in benzene and irradiated with a high-pressure

mercury lamp, they undergo a [2+2]cycloaddition followed by ring opening to give compound **1-43**, which the authors termed a "picotube".[21] Attempts to fully aromatize picotube have been unsuccessful, giving only starting material or unidentifiable products. When picotube **1-43** was subjected to FVP, it rearranged to give compound **1-44**, whose structure was elucidated by X-ray diffraction.[23] One reason this route may have been unsuccessful is that the target molecule would be a portion of a [4,4]carbon nanotube, which smaller and therefore more strained than many of the other belts that have been targeted.

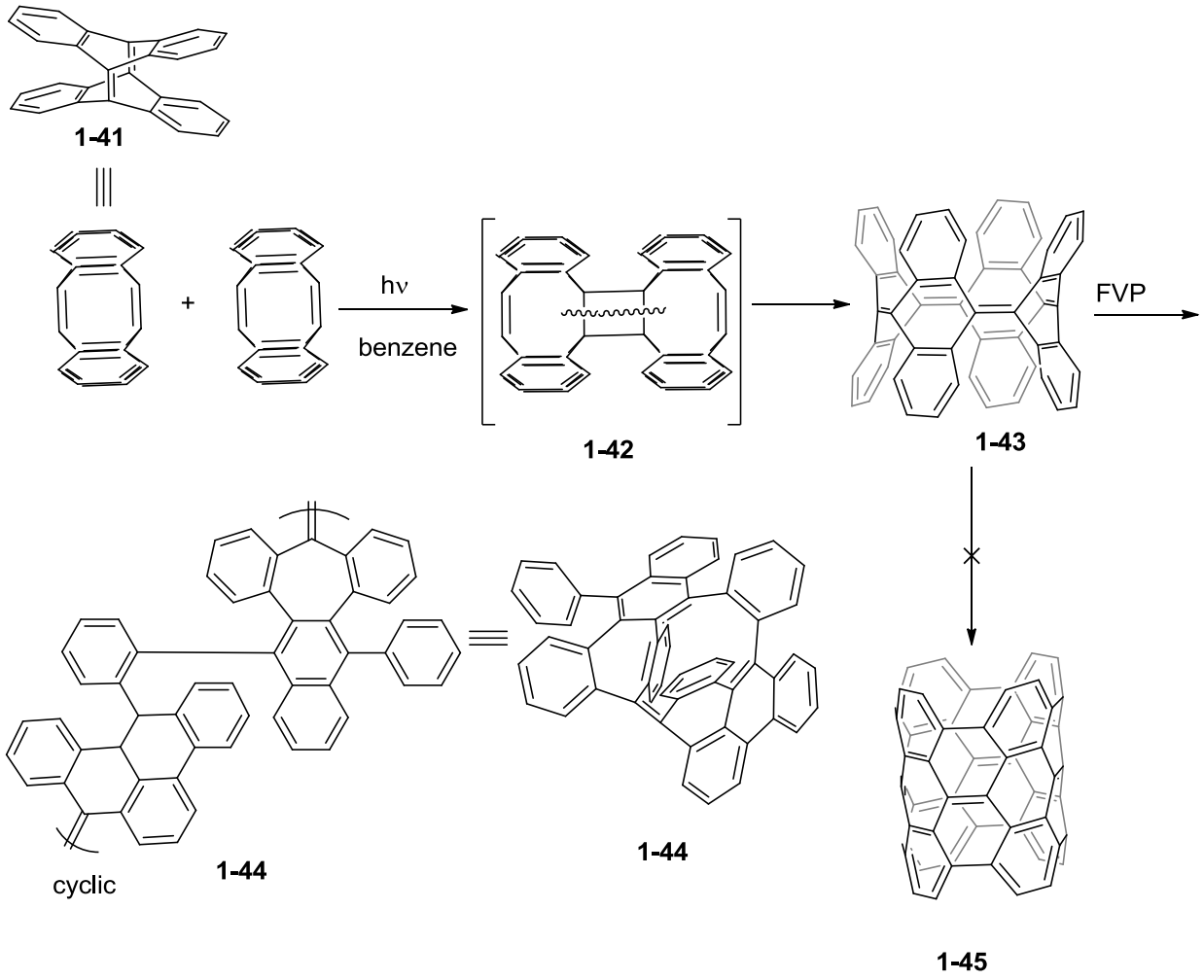

Scheme 1-7 – The synthesis of the "picotube" and its attempted aromatization[23]

In 2004 Nakamura and co-workers isolated the pi system on the equator of C_{60}, which formally is a [10]cyclophenacene unit (Scheme 1-8).[24] They first used a large excess of methyl cuprate to functionalize one pole of the fullerene (**1-46**), to give hexamethylfullerene **1-47**. Next, the lone hydrogen was protected as a nitrile and the resulting compound (**1-48)** was reacted with an excess of phenyl cuprate to get the doubly capped **1-49**, which contains the pi system of [10]cyclophenacene. The nitrile group was removed with lithium naphthalenide to give compound **1-50**. Both compounds **1-49** and **1-50** are stable and isolable, giving further evidence that the pi system of a cyclophenacene is stable. While this is a noteworthy and remarkable synthetic achievement, it is not a true aromatic belt since both the top and bottom of the molecule are capped.

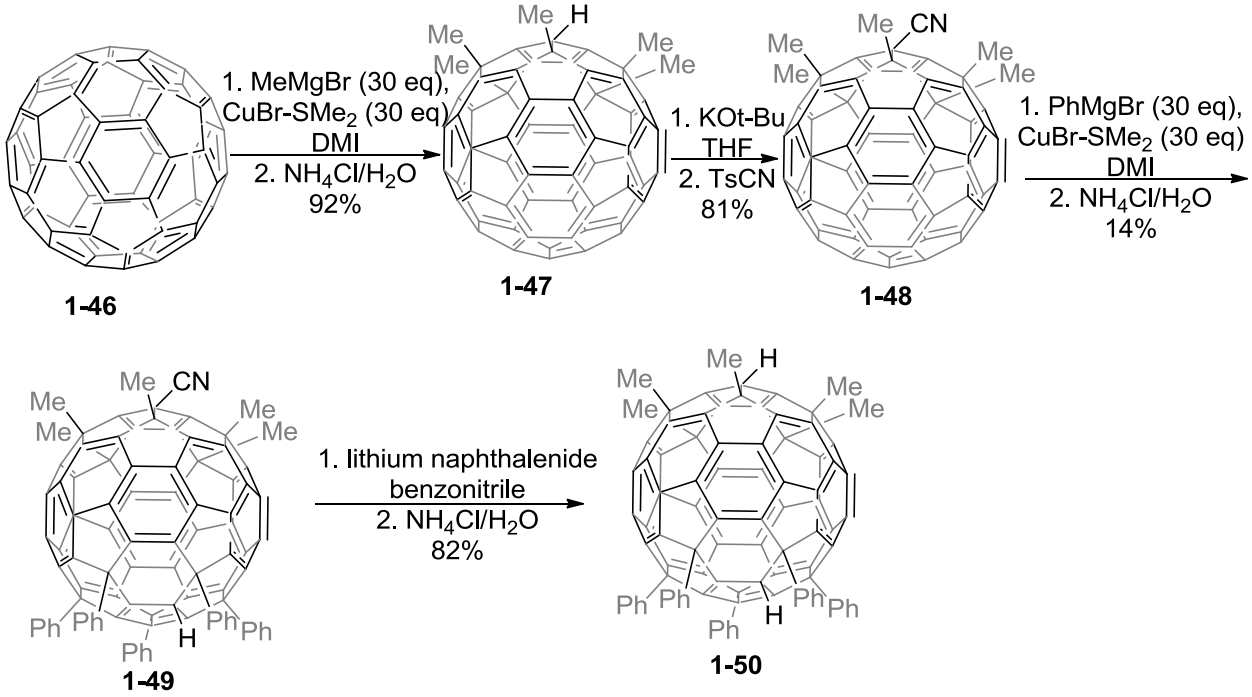

Scheme 1-8 – Nakamura's isolation of a [10]cyclophenacene pi system[24]

In 2004 the Gleiter group reported their synthetic targets [4,8] and [6,8] cyclacenes, where the numbers in brackets refer to the size of the rings in the belt.[25] By using cyclooctatetraenes, the strain would be minimized since cyclooctatetraenes are non-planar. The

formation of macrocyle **1-53**, which is a $[4,8]_3$ cyclacene, was accomplished by irradiation with UV light of compound **1-51** in the presence of cobalt compound **1-52** (Scheme 1-9). This reaction is a trimerization utilizing a [2+2] cycloaddition in which the cobalt is used to stabilize the butadiene units. While all the carbons along the belt are formally conjugated, the degree of conjugation is low since the cyclooctatetraene is bent. Gleiter proposed that the cosine of the angle between a cyclobutadiene unit and an adjacent phenyl ring, may give the degree of conjugation.[25] For molecule **1-53** the angle is 63º, which by this measure would correspond to 43% conjugation in the macrocycle.

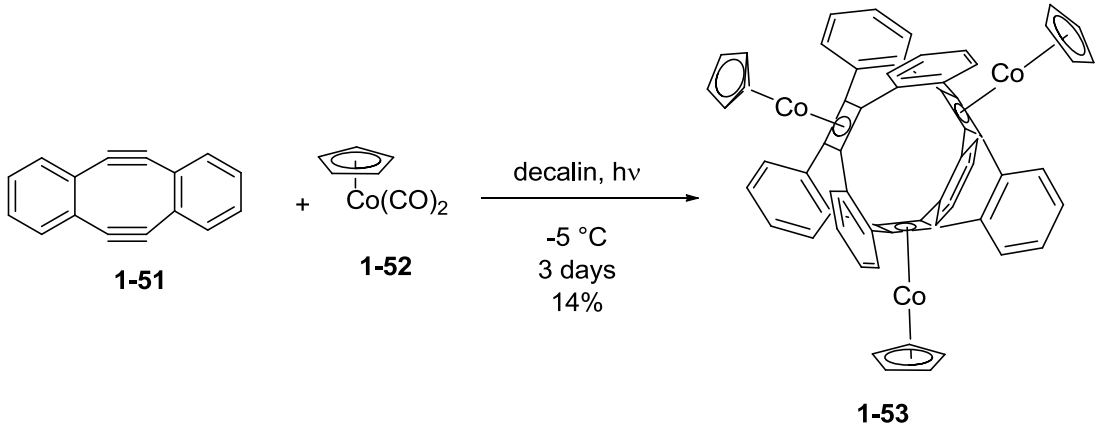

1-51 **1-52** **1-53**

Scheme 1-9 – The synthesis of $[4,8]_3$ cyclacene (**1-53**)

The Gleiter group also accomplished the synthesis of a $[6,8]_3$ cyclacene, according to Scheme 1-10.[26] Trimerization of compound **1-54**, led to a mixture of products **1-55** and **1-56** in low yield. Conversion of the *trans* bond in **1-55** to the desired *cis* bond was accomplished by irradiating the molecule with UV light. Molecule **1-56** was then brominated with n-bromosuccinimide (NBS) and dibenzoyl-peroxide to give hexabromide **1-57**. The benzyl bromides were oxidized directly to aldehydes, using 2-iodoxybenzoic acid (IBX) at 65 ºC. Cyclacene **1-59** was formed by a three-fold McMurry coupling, with a yield of only 8%, and its structure was confirmed by single-crystal X-ray diffraction. The angle between the double bonds

of the cyclooctatetraene and the adjacent aromatic ring is 72º, which, if the conjugation is proportional to the cosine, is a conjugation of only 31% for the belt. Gleiter has since suggested the synthesis of cyclacene-type belts that incorporate heteroatoms, based on his group's computational studies.[27]

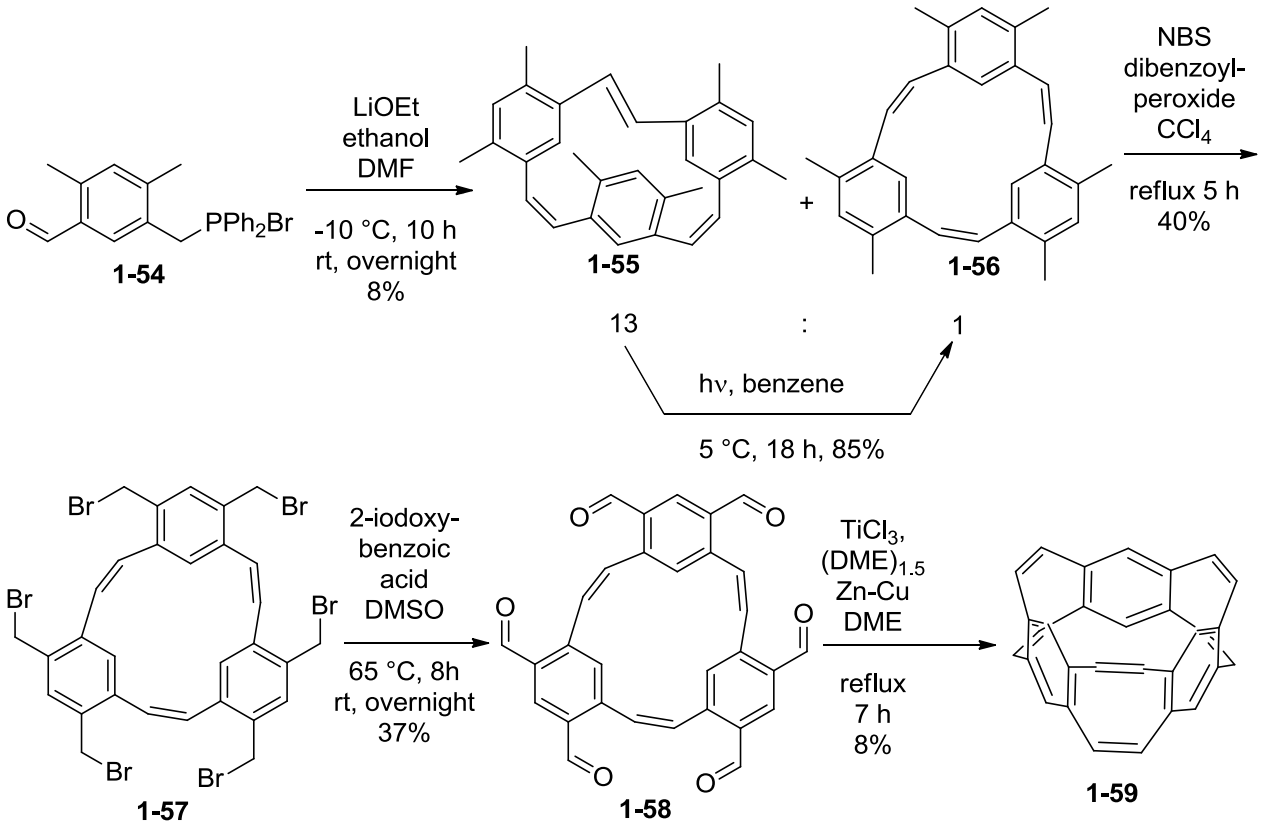

Scheme 1-10 – The synthesis of $[6,8]_3$ cyclacene

The Bodwell group reported their strategy towards an aromatic belt in 2008 (Scheme 1-11).[28] The strategy relies on synthesizing flat molecular boards (**1-66** and **1-67**) and then using the VID reaction to form strained pyrene units.[28] The Bodwell group has utilized the VID reaction during the synthesis of many strained pyrenes.[28-29] A double Sonagashira reaction between aryl bromide **1-60** and diacetylene **1-61** was used to synthesize compound **1-62**, which was reduced with hydrogen and palladium on carbon to give **1-63**. The free positions on the central benzene ring were brominated to give dibromide **1-64**, which then yielded compound **1-**

65 via a palladium-catalyzed C-H bond activation. The ester groups were then reduced to alcohols, which were brominated to give the tetrabromide **1-66**, which is one of the desired molecular boards. Tetrabromide **1-66** could then be converted to tetrathiol **1-67**, giving the second desired molecular board.

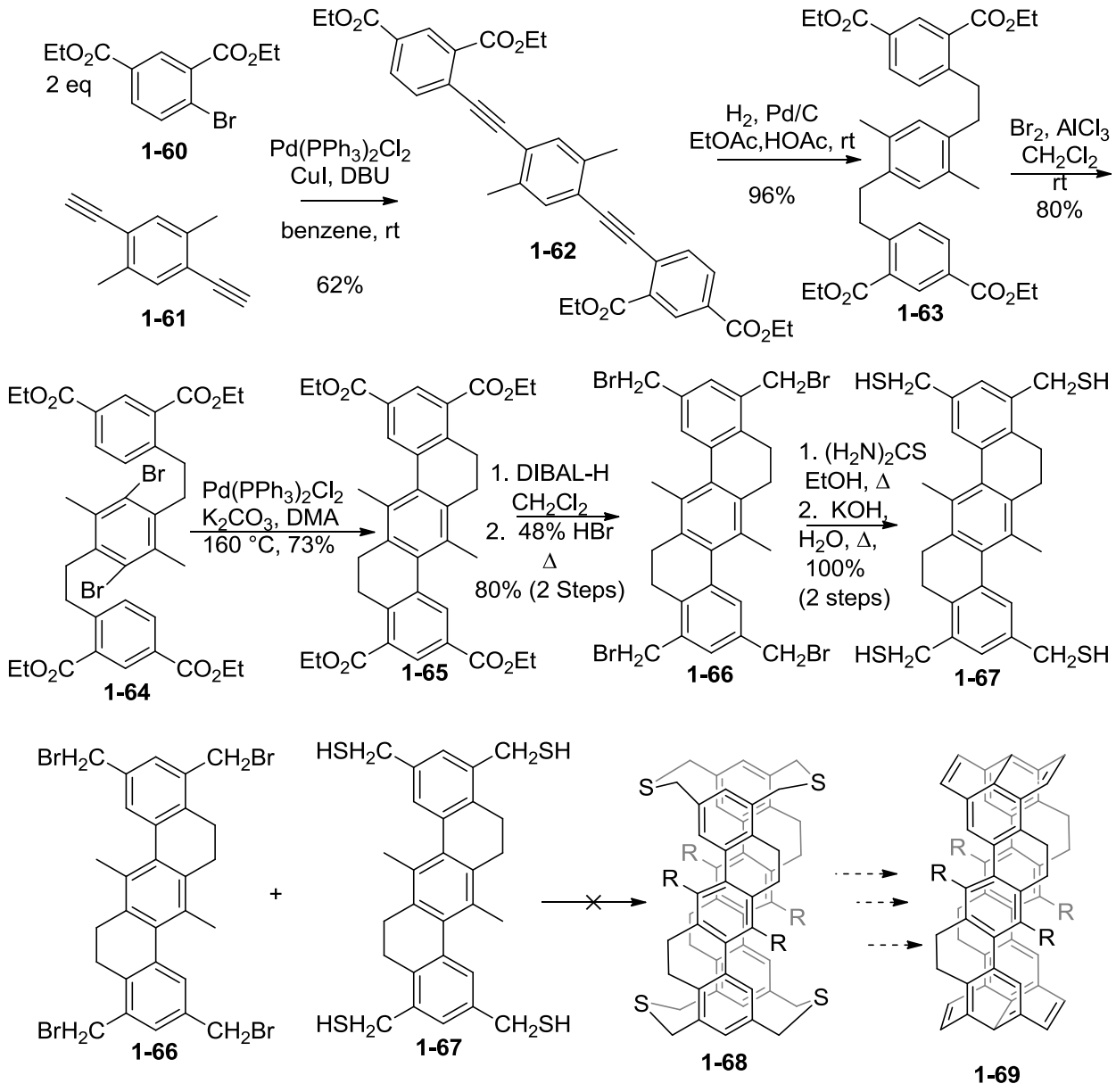

Scheme 1-11 – The Bodwell group's route to molecular boards **1-68** and **1-69**

The insolubility of molecular boards **1-66** and **1-67** inhibited the formation of macrocycle **1-68**. The methyl groups on the central ring were not sufficient to solubilize the molecule.

Although the Bodwell group has since worked out the solubility problems, at least enough to obtain a mass spectrum of the desired belt (**1-69**), they have yet to publish these findings.[30]

In work that was first reported in 2003 and that continued until 2011, the Schlüter group targeted a novel aromatic belt, the equator of a C_{84} fullerene (**1-3**).[2, 31] The skeleton of this belt was constructed by using a series of Diels-Alder (DA) and retro-DA reactions, as shown in Scheme 1-12. In the first step compound **1-71** undergoes a retro-DA to give a furan functional group (not shown) that than reacts with dienophile **1-70** to give compound **1-72**. It should be noted that the reaction gives both an *endo* and an *exo* product. The isomers were separated and both were carried forward, but only the *endo* isomer route is drawn in Scheme 1-12. Oxidation with DDQ of compound **1-72** gives a double bond at the terminal five-membered ring (**1-73**). Treatment of dibromide **1-73** with n-BuLi forms a benzyne in situ , which undergoes a DA reaction with cyclopentadiene to give both the *syn* and *anti* products, **1-74a** and **1-74b** respectively. Both products were carried forward to react with tetracyclone (**1-75**), giving products **1-76a** and **1-76b**. Upon heating, these molecules undergo a double retro-DA reaction, in which the tetacyclone fragment and a C_2 fragment are lost to give intermediate **1-77**. This intermediate then undergoes a double DA dimerization to give macrocycle **1-78**.[2] Aromatization of this macrocycle proved difficult, but reaction with acetic anhydride leads to the aromatization of two of the rings, as well as opening of the remaining two ether units to give the tetraacetate **1-79**.[31a] Tetraacetate **1-79** can be ionized by collision-induced dissociation (CID) and the M+1 peak at 933 m/z, corresponding to **1-80a**, was observed in the mass spectrometer.[31b] Schlüter and coworkers do not claim to have made the desired belt, although the desired peak was detected in the mass spectrometer; it is possible that an isomerization occurred instead.

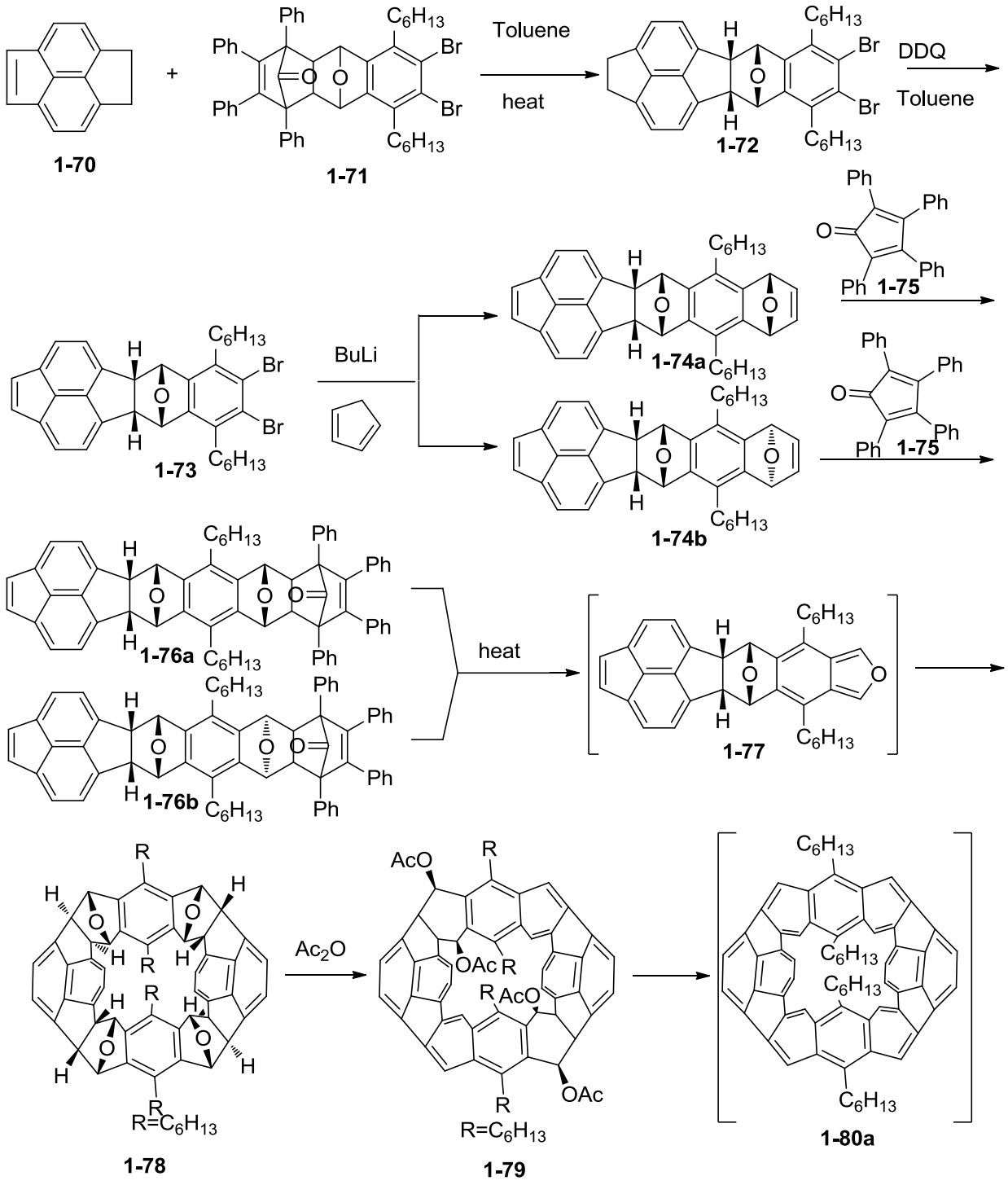

Scheme 1-12 – The Schlüter group's synthesis of the equator of C_{84}

To further investigate these results, a series of calculations were carried out, giving further insight regarding ionization of tetraacetate **1-79**.[31b] Schlüter and co-workers found that a

1,5-hydrogen shift gives a non-conjugated macrocycle (**1-80b**) that is lower in energy than belt **1-80a** (B3LYP, 6-311G*). They also found that a double hydrogen shift (**1-80c**) is even more favored, because it decreases the strain energy of the macrocycle. In order to prevent the isomerization, tetraacetate precursors to belts **1-3** and **1-73b** were synthesized a similar route. The molecular ions of belts **1-3** and **1-73b** were detected by mass spectrometry, but all efforts to isolate themwere unsuccessful.[31c] These belts thus can exist in the gas phase, but either cannot form or decompose in solution under the conditions used.

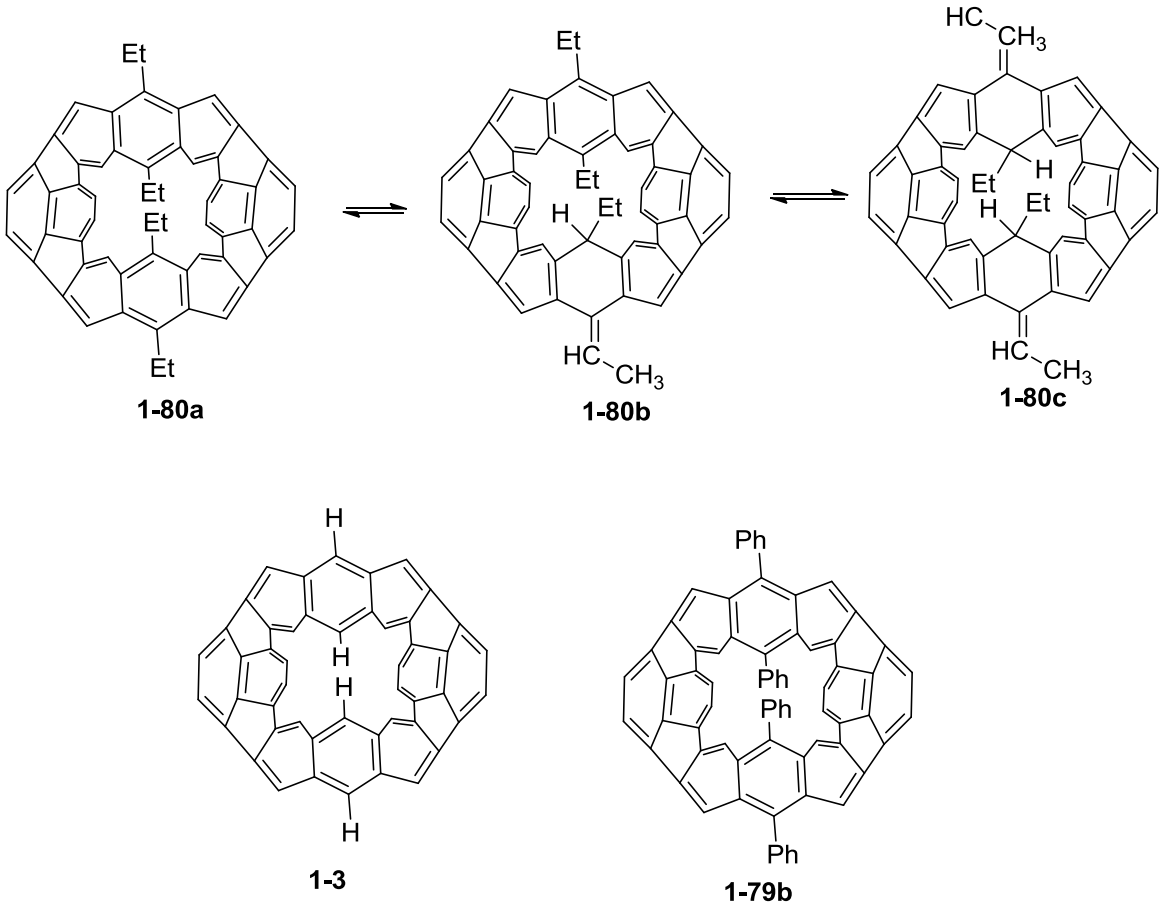

Figure 1-5 – The rearranged macrocyles and the new macrocycles that were targeted

1-3 A New Approach to an Aromatic Belt

In spite of a tremendous amount of synthetic effort, a fully conjugated belt-shaped molecule has not been isolated to date. The Goroff group chose to utilize a scaffold to aid in the construction of belt **1-2**. Scheme 1-14 shows the retrosynthetic analysis of the approach. A scaffold could be used to favor macrocyclization and oxidation of the macrocycle to a belt. Removal of the scaffold would give the target belt. The scaffold will favor macrocyclization over polymerization, since the couplings are all intramolecular. Also the synthesis should be more straightforward, since the couplings will be done in one step and not sequentially. The details of this approach and the progress made will be described in the following chapters.

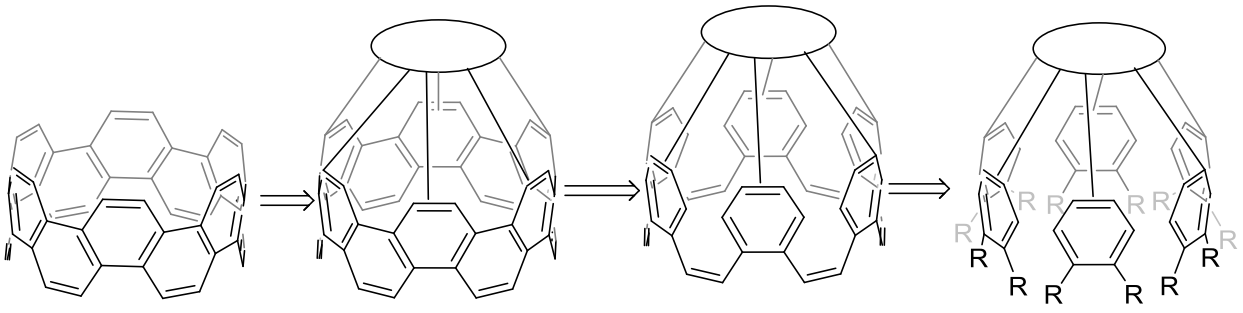

Scheme 1-13 – Using a scaffold to synthesize a belt

1-4 References

1. Eisenberg, D.; Shenhar, R.; Rabinovitz, M., Synthetic approaches to aromatic belts: building up strain in macrocyclic polyarenes. *Chem. Soc. Rev.* **2010,** *39* (8), 2879-2890.
2. Neudorff, W. D.; Lentz, D.; Anibarro, M.; Schlüter, A. D., The Carbon Skeleton of the Belt Region of Fullerene C84 (D2). *Chem. Eur. J.* **2003,** *9* (12), 2745-2757.
3. Vögtle, F., Concluding remarks. *Top. Curr. Chem.* **1983,** *115*, 157-159.
4. Heilbronner, E., Molecular Orbitals in homologen Reihen mehrkerniger aromatischer Kohlenwasserstoffe: I. Die Eigenwerte yon LCAO-MO's in homologen Reihen. *Helv. Chim. Acta* **1954,** *37* (3), 921-935.
5. (a) Kroto, H. W.; Heath, J. R.; O'Brien, S. C.; Curl, R. F.; Smalley, R. E., C_{60}: Buckminsterfullerene. *Nature* **1985,** *318*, 162-164; (b) Iijima, S., Helical microtubules of graphitic carbon. *Nature* **1991,** *354* (6348), 56-58.
6. Scott, L. T., Conjugated belts and nanorings with radially oriented π orbitals. *Angew. Chem. Int. Ed.* **2003,** *42*, 4133-4135.

7. Kawase, T.; Kurata, H., Ball-, bowl-, and belt-shaped conjugated systems and their complexing abilities: Exploration of the concave-convex pi-pi interaction. *Chem. Rev.* **2006,** *106* (12), 5250-5273.
8. (a) Houk, K. N.; Lee, P. S.; Nendel, M., Polyacene and cyclacene geometries and electronic structures: Bond equalization, vanishing band gaps, and triplet ground states contrast with polyacetylene. *J. Org. Chem.* **2001,** *66* (16), 5517-5521; (b) Fokin, A. A.; Jiao, H.; Schleyer, P. v. R., From dodecahedrapentaene to the "[n]trannulenes". A new in-plane aromatic family. *J. Am. Chem. Soc.* **1998,** *120*, 9364-9365; (c) Choi, H. S.; Kim, K. S., Structures, Magnetic Properties, and Aromaticity of Cyclacenes. *Angew. Chem. Int. Ed.* **1999,** *38* (15), 2256-2258; (d) Turker, L.; Celebi, N., Some properties of cyclacenes and silacyclacenes. *Bull. Soc. Chim. Belg.* **1997,** *106* (4), 201-204; (e) Turker, L., AM1 treatment of cyclacene tubes. *Theochem* **1999,** *490*, 55-60; (f) Türker, L., Zigzag cyclopolyacenes: a theoretical study. *Theochem* **1999,** *491* (1–3), 275-280.
9. Aihara, J.-i., Aromaticity and superaromaticity in cyclopolyacenes. *J. Chem. Soc. Perk. Trans. 2* **1994,** (5), 971-974.
10. Baughman, R. H.; Zakhidov, A. A.; de Heer, W. A., Carbon Nanotubes--the Route Toward Applications. *Science* **2002,** *297* (5582), 787-792.
11. (a) Fort, E. H.; Donovan, P. M.; Scott, L. T., Diels−Alder Reactivity of Polycyclic Aromatic Hydrocarbon Bay Regions: Implications for Metal-Free Growth of Single-Chirality Carbon Nanotubes. *J. Am. Chem.Soc.* **2009,** *131* (44), 16006-16007; (b) Steinberg, B. D.; Scott, L. T., New Strategies for Synthesizing Short Sections of Carbon Nanotubes. *Angew. Chem. Int. Ed.* **2009,** *48* (30), 5400-5402; (c) Fort, E.; Scott, L., One-Step Conversion of Aromatic Hydrocarbon Bay Regions into Unsubstituted Benzene Rings: A Reagent for the Low-Temperature, Metal-Free Growth of Single-Chirality Carbon Nanotubes. *Angew. Chem. Int. Ed.* **2010,** *49* (37), 6626-6628; (d) Fort, E. H.; Scott, L. T., Carbon nanotubes from short hydrocarbon templates. Energy analysis of the Diels-Alder cycloaddition/rearomatization growth strategy. *J. Mat. Chem.* **2011,** *21* (5), 1373-1381; (e) Fort, E. H.; Scott, L. T., Gas-phase Diels–Alder cycloaddition of benzyne to an aromatic hydrocarbon bay region: Groundwork for the selective solvent-free growth of armchair carbon nanotubes. *Tetrahedron Lett.* **2011,** *52* (17), 2051-2053.
12. Louie, S. G., Electronic properties, junctions, and defects of carbon nanotubes. *Carbon Nanotubes* **2001,** *80*, 113-145.
13. Vögtle, F.; Schröder, A.; Karbach, D., Strategy for the Synthesis of Tube-Shaped Molecules. *Angew. Chem. Int. Ed. Eng.* **1991,** *30* (5), 575-577.
14. Mitchell, R. H.; Boekelheide, V., Syntheses of [2.2]metacyclophane-1,9-diene and trans-15,16-dihydropyrene. *J. Am. Chem. Soc.* **1970,** *92* (11), 3510-3512.
15. (a) Ashton, P. R.; Brown, G. R.; Isaacs, N. S.; Giuffrida, D.; Kohnke, F. H.; Mathias, J. P.; Slawin, A. M. Z.; Smith, D. R.; Stoddart, J. F.; Williams, D. J., Molecular LEGO. 1. Substrate-directed synthesis via stereoregular Diels-Alder oligomerizations. *J. Am. Chem. Soc.* **1992,** *114* (16), 6330-6353; (b) Mathias, J. P.; Stoddart, J. F., Constructing a Molecular Lego Set. *Chem. Soc. Rev.* **1992,** *21* (4), 215-225; (c) Ashton, P. R.; Girreser, U.; Giuffrida, D.; Kohnke, F. H.; Mathias, J. P.; Raymo, F. M.; Slawin, A. M. Z.; Stoddart, J. F.; Williams, D. J., Molecular belts. 2. Substrate-directed syntheses of belt-type and cage-type structures. *J. Am. Chem. Soc.* **1993,** *115* (13), 5422-5429; (d) Kohnke, F. H.; Slawin, A. M. Z.; Stoddart, J. F.; Williams, D. J., Molecular Belts and Collars in the Making: A Hexaepoxyoctacosahydro[12]cyclacene Derivative. *Angew. Chem. Int. Ed. Eng.* **1987,** *26* (9), 892-894; (e) Ashton, P. R.; Isaacs, N. S.; Kohnke, F. H.; Slawin, A. M. Z.; Spencer, C. M.;

Stoddart, J. F.; Williams, D. J., Towards the Making of [12]Collarene. *Angew. Chem. Int. Ed. Eng.* **1988,** *27* (7), 966-969.
16. (a) Cory, R. M.; McPhail, C. L., Transformations of a macrocyclic cyclophane belt into advanced [8]cyclacene and [8]cyclacene triquinone precursors. *Tetrahedron Lett.* **1996,** *37* (12), 1987-1990; (b) Cory, R. M.; McPhail, C. L.; Dikmans, A. J.; Vittal, J. J., Macrocyclic cyclophane belts via double diels-alder cycloadditions: Macroannulation of bisdienes by bisdienophiles. Synthesis of a key precursor to an [8]cyclacene. *Tetrahedron Lett.* **1996,** *37* (12), 1983-1986.
17. Kuwatani, Y.; Yoshida, T.; Kusaka, A.; Iyoda, M., All-Z-Tribenzo[12]-, tetrabenzo[16]- and pentabenzo[20]annulenes. *Tetrahedron Lett.* **2000,** *41* (3), 359-363.
18. Kuwatani, Y.; Yoshida, T.; Igarashi, J.-I.; Iyoda, M. In *Synthesis and properties of ALL-Z-pentabenzo[20]- and hexabenzo[24]annulenes*, 10th International Symposium on Novel Aromatics, San Diego, CA, August 4-8, 2001; San Diego, CA, 2001.
19. (a) Brooks, M. A. 1,2-Shifts in Aryl Radicals and Synthetic Routes Toward Cyclo[12]phenacene: A Molecular Belt. Dissertation, Boston College, Chestnut Hill, MA, 1998; (b) St.Martin-Davis, H. M. Synthetic Routes Towards Cyclo[N]phenacenes and [8]Circulene: Molecular Belts and Saddles. Dissertation, Boston College, Chestnut Hill, MA, 2002.
20. Scott, L. T.; Boorum, M. M.; McMahon, B. J.; Hagen, S.; Mack, J.; Blank, J.; Wegner, H.; de Meijere, A., A rational chemical synthesis of C_{60} *Science* **2002,** *295*, 1500-1503.
21. Kammermeier, S.; Jones, P. G.; Herges, R., Ring-Expanding Metathesis of Tetradehydro-anthracene—Synthesis and Structure of a Tubelike, Fully Conjugated Hydrocarbon. *Angew. Chem. Int. Ed. Eng.* **1996,** *35* (22), 2669-2671.
22. Viavattene, R. L.; Greene, F. D.; Cheung, L. D.; Majeste, R.; Trefonas, L. M., 9,9',10,10'-Tetradehydrodianthracene. Formation, protection, and regeneration of a strained double bond. *J. Am. Chem. Soc.* **1974,** *96* (13), 4342-4343.
23. Deichmann, M.; Näther, C.; Herges, R., Pyrolysis of a Tubular Aromatic Compound. *Org. Lett.* **2003,** *5* (8), 1269-1271.
24. Matsuo, Y.; Tahara, K.; Sawamura, M.; Nakamura, E., Creation of hoop- and bowl-shaped benzenoid systems by selective detraction of 60 fullerene conjugation. 10 cyclophenacene and fused corannulene derivatives. *J. Am. Chem. Soc.* **2004,** *126* (28), 8725-8734.
25. Gleiter, R.; Esser, B.; Kornmayer, S. C., Cyclacenes: Hoop-Shaped Systems Composed of Conjugated Rings. *Acc. Chem. Res.* **2009,** *42* (8), 1108-1116.
26. Esser, B.; Bandyopadhyay, A.; Rominger, F.; Gleiter, R., From Metacyclophanes to Cyclacenes: Synthesis and Properties of [6.8]3Cyclacene. *Chem. Eur. J.* **2009,** *15* (14), 3368-3379.
27. Kornmayer, S. C.; Esser, B.; Gleiter, R., DFT Calculations on Heterocyclacenes. *Org. Lett.* **2009,** *11* (3), 725-728.
28. Yao, T.; Yu, H.; Vermeij, R. J.; Bodwell, G. J., Nonplanar aromatic compounds. Part 10: A strategy for the synthesis of aromatic belts - all wrapped up or down the tubes? *Pure and Appl. Chem.* **2008,** *80*, 533-546.
29. Zhang, B.; Gregory P. Manning; Michał A. Dobrowolski; Cyranski, M. K.; Bodwell, G. J., Nonplanar aromatic compounds. 9. Synthesis, structure, and aromaticity of 1:2,13:14-dibenzo[2]paracyclo[2](2,7)-pyrenophane-1,13-diene. *Org. Lett.* **2008,** *10*, 273-376.
30. Bodwell, G., Personal Communication. 2009.

31. (a) Stuparu, M.; Lentz, D.; Rüegger, H.; Schlüter, A. D., Exploring the Chemistry of a Double-Stranded Cycle with the Carbon Skeleton of the Belt Region of the C84 Fullerene. *Eur. J. Org. Chem.* **2007,** *2007* (1), 88-100; (b) Denekamp, C.; Etinger, A.; Amrein, W.; Stanger, A.; Stuparu, M.; Schlüter, A. D., Towards a Fully Conjugated, Double-Stranded Cycle: A Mass Spectrometric and Theoretical Study. *Chem. Eur. J.* **2008,** *14* (5), 1628-1637; (c) Standera, M.; Hafliger, R.; Gershoni-Poranne, R.; Stanger, A.; Jeschke, G.; van Beek, J. D.; Bertschi, L.; Schluter, A. D., Evidence for Fully Conjugated Double-Stranded Cycles. *Chem. Eur. J.* **2011,** *17* (43), 12163-12174.

Chapter 2

2-1 A Cyclodextrin-Based Scaffold Towards Cyclophenacenes

The synthesis of an aromatic belt using a scaffold requires two separate pieces: the scaffold and the subunits. The subunits make up the aromatic core and attach to the other subunits, while the scaffold holds the subunits in place. These pieces are synthesized separately and then joined together.

The work described in this chapter was a collaboration among three graduate students in the Goroff group: Zachary Katsamanis,[1] Li Cui,[2] and Lu Zhou.[3] Initial work focused on using α

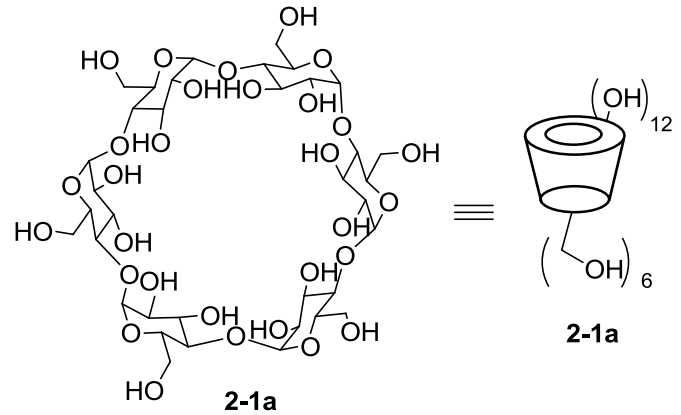

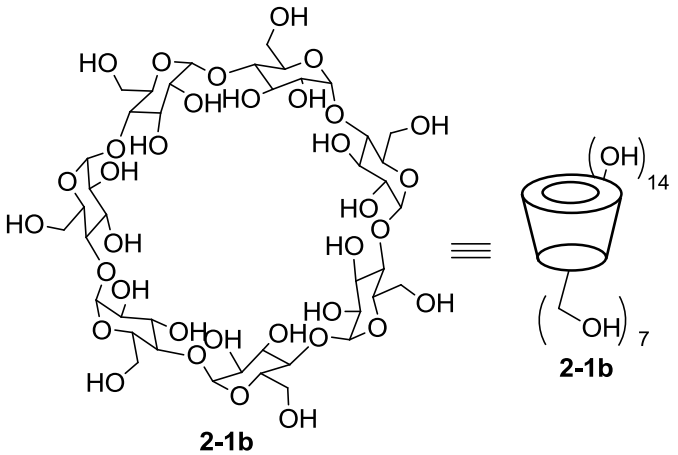

Figure 2-1 – The parent structures of α and β cyclodextrin (**2-1a** and **2-1b**).

and β-cyclodextrin (**2-1a** and **21b**, respectively) as scaffolds for the synthesis of cyclophenacenes. Cyclodextrins are naturally occurring cyclic oligomers of glucose, with α-cyclodextrin consisting of six glucose monomers and β-cyclodextrin containing seven glucose monomers.[4] Cyclodextrins have two faces: one face contains one primary alcohol on each glucose unit of the cyclodextrin and the other face has two secondary alcohols on each glucose unit**.** Figure 2-1 shows the structures of the cyclodextrins and the schematic images that are used to represent them

The work to functionalize the cyclodextrins (Scheme 2-1) was performed by previous lab member Zachary Katsamanis.[1] The difference in reactivity between the primary alcohols and the secondary alcohols allows the faces of the cyclodextrin to be functionalized separately. The chemistry of α and β cyclodextrin is similar, so conditions only had to be optimized once for both. The synthesis begins from commercially available α and β-cyclodextrin (**2-1a** and **2-1b),** with selective protection of the primary alcohols with tert-butyldimethylsilyl (TBS) groups. The

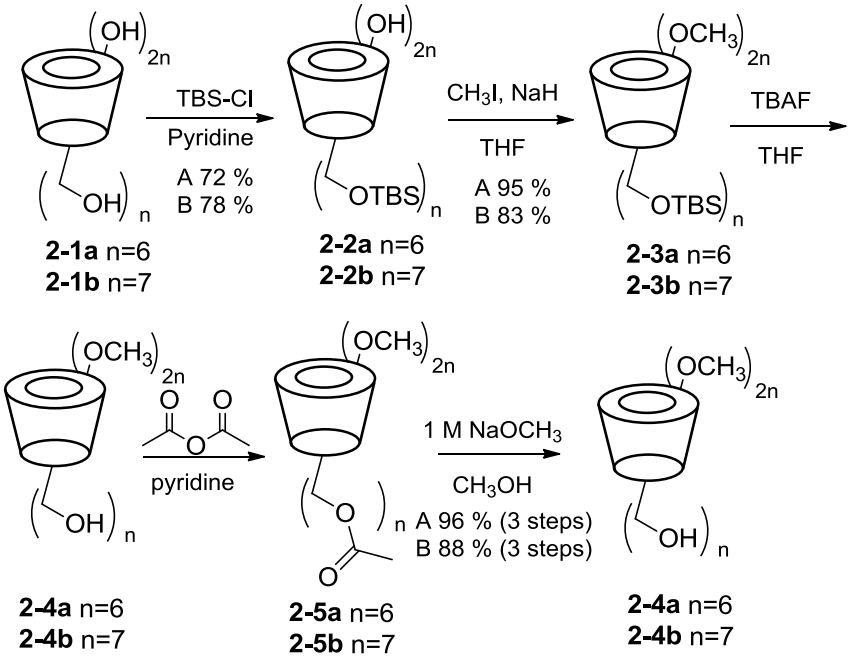

Scheme 2-1 – The synthetic route to the cyclodextrin scaffolds.

twelve (or fourteen) secondary alcohols are then methylated in good yield to give compounds **2-3a** and **2-3b**. Removal of the TBS groups gives **2-4a** and **2-4b,** which are difficult to purify due to butyl impurities. The alcohols are then acetylated to ease purification, and the product is purified by column chromatography to give pure samples of **2-5a and 2-5b**. The acetyl groups are removed cleanly giving the targeted scaffold precursors **2-4a** and **2-4b**.[1]

With the synthesis of the scaffold precursors complete, the attention shifts to the subunits. The subunit requires three basic components: an attachment point to the scaffold, an aromatic core, and functional groups that can be coupled to the other subunits. Divinylacid **2-11** was chosen as the initial subunit because it meets the above requirements and it is synthetically accessible. The synthesis of the subunit for the cyclodextrin scaffold was performed by former

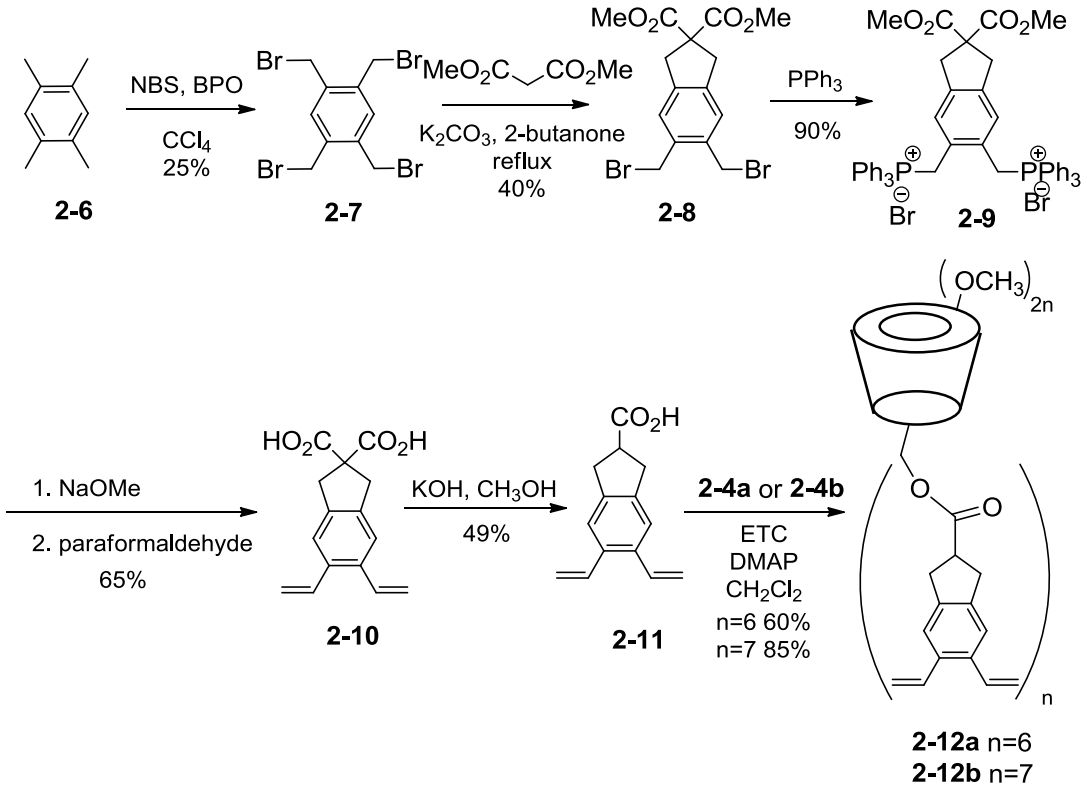

Scheme 2-2 – The route to the orthosubstituted subunits **2-11**

group members Li Cui and Lu Zhou.[2-3] The synthesis begins with tetrabromination of durene (**2-6**) which gives the desired product **2-7**, but the yield suffers due to both under and overbromination. Formation of a five-membered ring is accomplished with dimethymalonate to give diester **2-8** in 40% yield. The remaining benzyl bromides are then converted to olefins by using the Wittig reaction, followed by a decarboxylation gave the target molecule (**2-11**). Subunit **2-11** was attached to scaffolds **2-4a** and **2-4b** in good yield, giving the coupling-ready precursors **2-12a** and **2-12b**.[2-3]

With compounds **2-12a** and **2-12b** in hand, the first test of the scaffolding approach was attempted. Compound **2-12a** was treated with ruthenium catalyst **2-13** in dichloromethane (Scheme 2-3), but even after stirring the reaction mixture for one week with 60 mol% (5 mol% per vinyl group) of catalyst, ^{1}H NMR indicated the presence of the vinyl groups of the starting material. The desired metathesis reaction did not occur. To gain information about the reaction, the scaffold was hydrolyzed, giving a mixture of products, but primarily cyclodextrin derivative **2-4a** and unreacted subunit **2-11**. A ^{1}H and ^{32}P NMR study was then conducted to explore the metathesis reaction. A stoichiometric amount of the ruthenium catalyst (**2-13**) was mixed with *ortho*-divinylbenzene (**2-14**) in a NMR tube, and the ^{1}H NMR spectrum showed new peaks at 16.31, 16.51, 20.63 and 20.80 ppm. None of these peaks appeared during the reaction of catalyst **2-13** and styrene. The conclusion from the experiment was that a stable complex (**2-15**) is formed between the ruthenium complex and the *o*-divinylbenzene. The Grubbs group later obtained a crystal structure of compound **2-15** confirming the proposed structure (Scheme 2-3).[5]

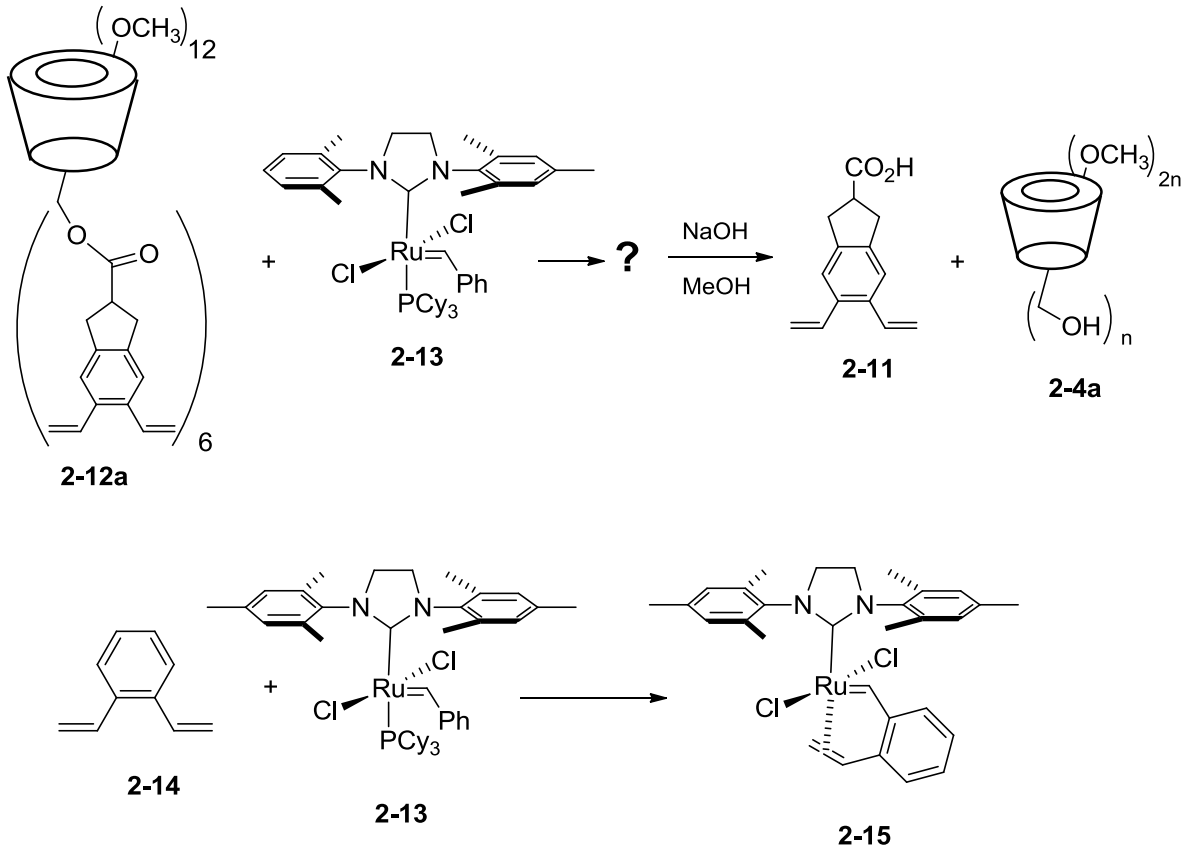

Scheme 2-3 – The attempted coupling to form the belt precursor

2-2 A Cyclodextrin-Based Scaffold Approach Toward Kekulene

The failure of the *ortho*-divinyl subunits to undergo olefin metathesis does not rule out cyclodextrin's validity as a scaffold. To determine if cyclodextrin could be used to construct a polycyclic aromatic hydrocarbon, the subunits were changed to *meta*-divinylbenzenes. *Meta*-divinylbenzene was stirred with the metathesis catalyst, forming polymeric product **2-17**

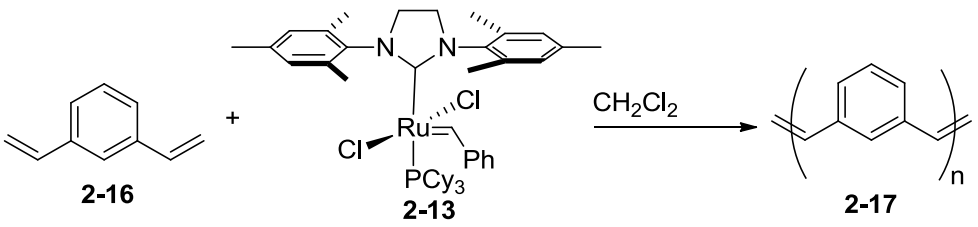

Scheme 2-4 – The reaction of metadivinyl benzene with catalyst **2-13**

(Scheme 2-4), which demonstrated these subunits are compatible with the coupling reaction. The connectivity of the subunit would not give a cyclophenacene, but instead will give a derivative of kekulene.[6]

The retrosynthesis of kekulene is shown below in Scheme 2-5. Using α–cyclodextrin, the ring closure would lead to a kekulene precursor. The precursor could then be oxidized to the final product. The previously synthesized compound **2-4a** can be used as the scaffold. The new subunit is slightly simpler since the symmetry does not require a five-membered ring to attach to the scaffold (**2-22**).

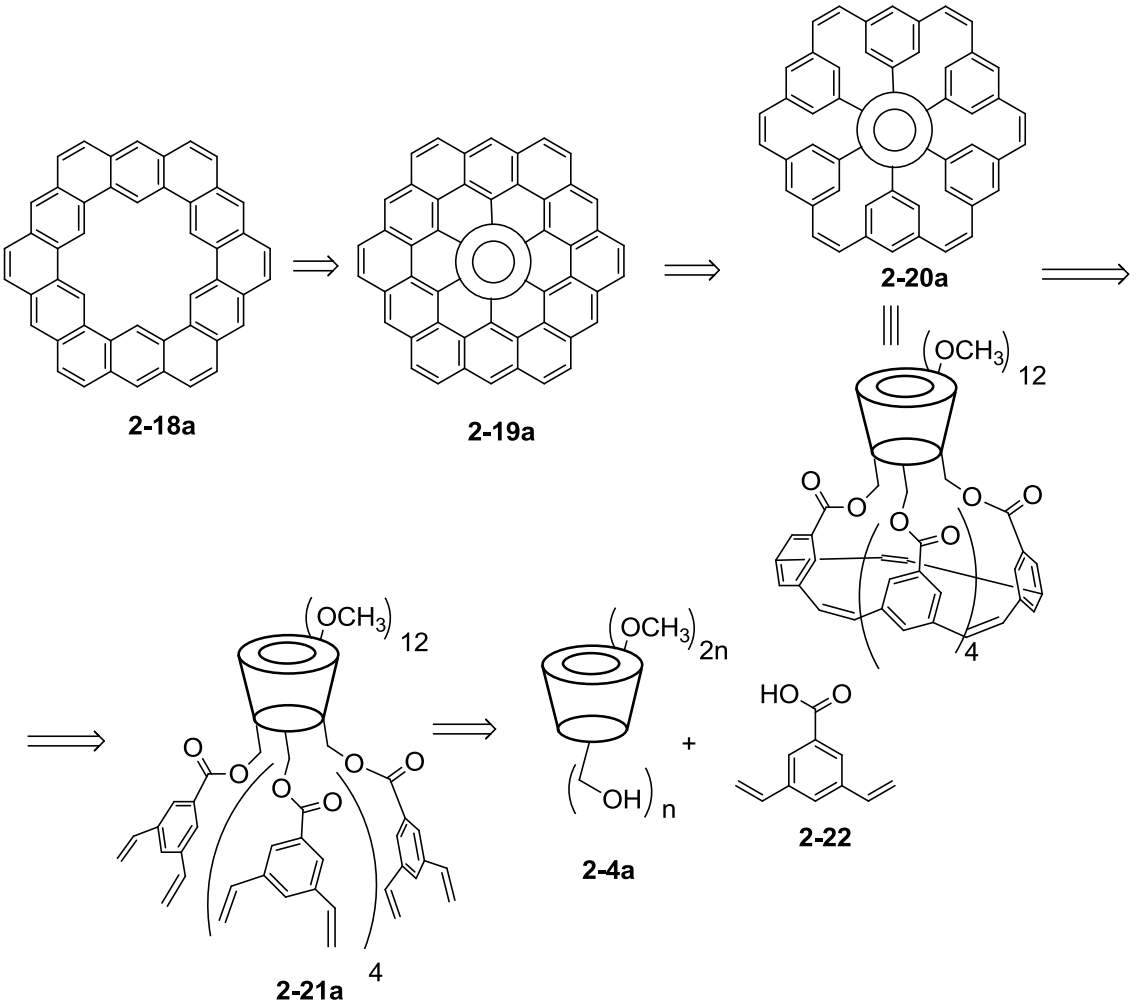

Scheme 2-5 – The restrosynthesis of kekulene

Lu Zhou carried out the synthesis of subunit **2-22** (Scheme 2-6).[3] Commercially available carboxylic acid **2-23** was esterified under acidic conditions with methanol to give compound ester **2-24** in good yield. Radical bromination of the benzylic positions of **2-24** gave the desired dibromide (**2-25**), although in low yield. The final step involved conversion of the bromides to vinyl groups with a Wittig reaction to give the target subunit **2-22**. Zachary Katsamanis then attached the new subunit **2-22** to the scaffold precursors **2-4a** and **2-4b** using ETC and 4-Dimethylaminopyridine to give kekulene precursors **2-21a** and **2-21b**.[1]

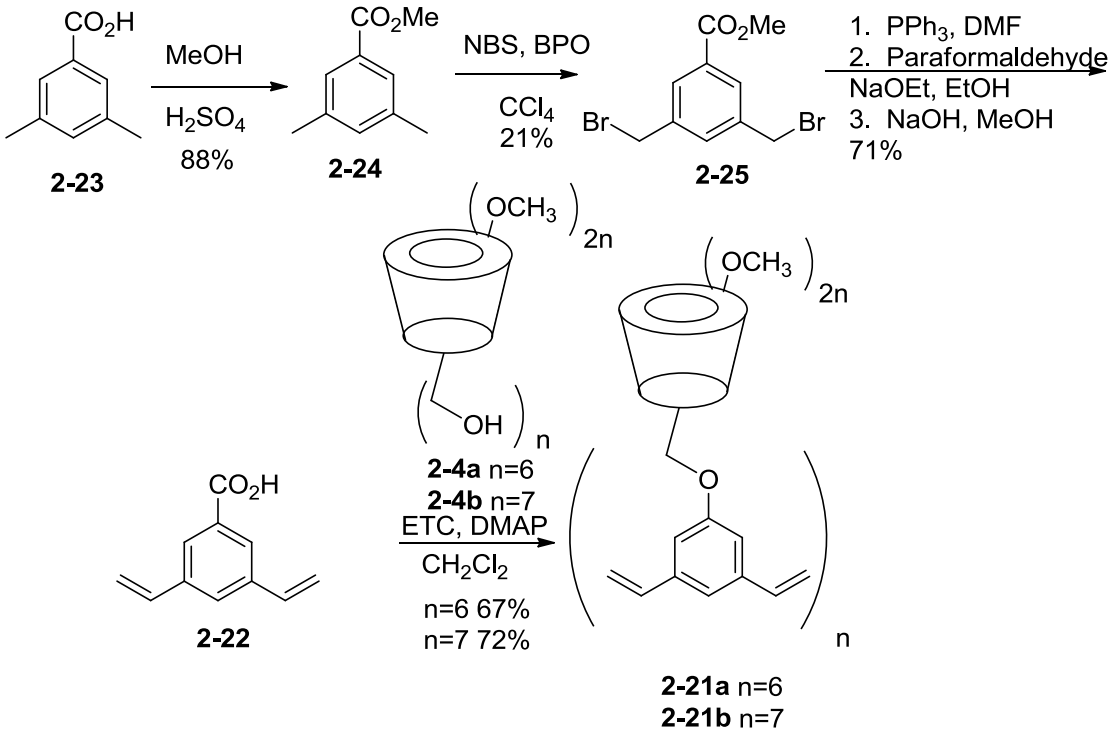

Scheme 2-6 – The synthesis of *meta*-substituted subunit **2-22** and its attachment to the scaffold

The belt precursors **2-21a** and **2-21b** were each allowed to react with 60 mol% ruthenium catalyst **2-13** for one week at 45 ºC. Analysis of each reaction by TLC showed the consumption of starting material, but the TLC contained no distinct spots, just a long streak in each. To simplify interpretation of the reaction, the product mixture from reaction of β-cyclodextrin derivative **2-21b** was detached from the scaffold using sodium methoxide in methanol. The

resulting mixture was analyzed by GC/MS, and the spectrum showed a major peak at 348 m/z, which was assigned to the dimer **2-26**. The other major peak at 298 m/z was not identified.

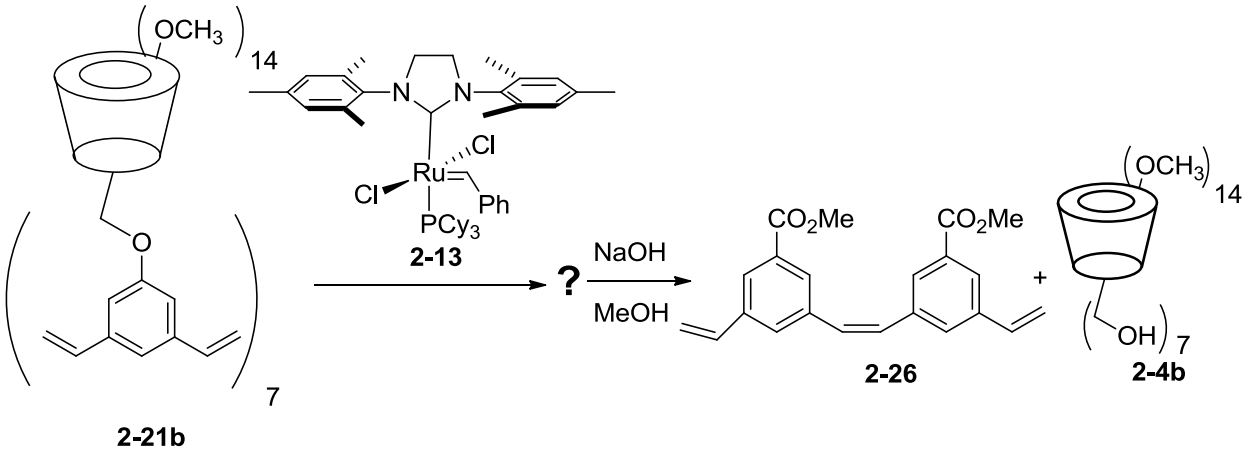

Scheme 2-7 – The failure of compound **2-21b** to form a macrocycle

To help understand why the reaction did not go to completion, Li Cui performed a computational analysis of the possible reaction products (conformational analysis performed with the Merck Molecular Force Field, MMFF, using the program MacroModel).[2] The product of each of the couplings shown below in Figure 2-2 was examined separately, and the global

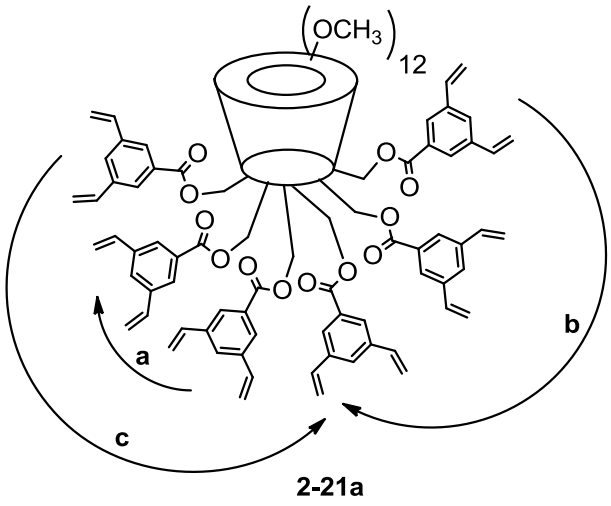

Figure 2-2 – The connections that were tested computationally

energy minimum for each was determined by conformational search. The global minimum was analyzed because the metathesis reaction is reversible, so the product is determined by thermodynamics and not kinetics. A summary of the results is shown below in Table 2-1. In order for the scaffold to produce a macrocycle, coupling to the adjacent subunit must be favored, an **a** type coupling. For both α and β cyclodextrin the desired **a**-type coupling is not the thermodynamic minimum.

Number of units	**a** type connection	**b** type connection	**c** type connection
6	5.3 kcal/mol	15.8 kcal/mol	0 kcal/mol
7	3.6 kcal/mol	0 kcal/mol	6.5kcal/mol

Table 2-1 – The results of the computations to determine which couplings were favored[7]

Since the desired coupling is not favored, cyclodextrin cannot be used as a scaffold in this instance as it allows non-adjacent subunits to be too close together. While the subunits should be in close proximity to their adjacent neighbor, they should be distanced from the other subunits. In order for this approach to be successful, all of the subunits must react with the nearest neighbor, and the scaffold must be rigid as to prevent interaction with any other subunits.

2-3 A Benzene Scaffold Approach Toward [12]cyclophenacene

With the inability of the cyclodextrin scaffold to be used in the construction of an aromatic belt, Zachary Katsamanis proposed using a scaffold with only three-fold symmetry.[6] The advantage of using three-fold symmetry is that the first coupling is always productive. A tri-substututed benzene was chosen as the new scaffold.

Höger and coworkers have previously used a tri-substituted benzene as a scaffold for the formation of macrocycles (Scheme 2-8).[8] They focused on obtaining compound **2-28**, the trimer of compound **2-27**but when the compound **2-27** was subjected to alkyne-alkyne coupling conditions, a mixture of compounds was observed. The desired trimer **2-28** was formed in only

25% yield. The main byproducts were proposed to be higher order macrocycles such as tetramer, pentamer, and polymeric products. When the same coupling was carried out with compound **2-29**, in which the couplings will all be intramolecular, the yield for the trimer was over 90%. The scaffold gave a more than threefold improvement in the yield, and was removed easily to give the desired product.

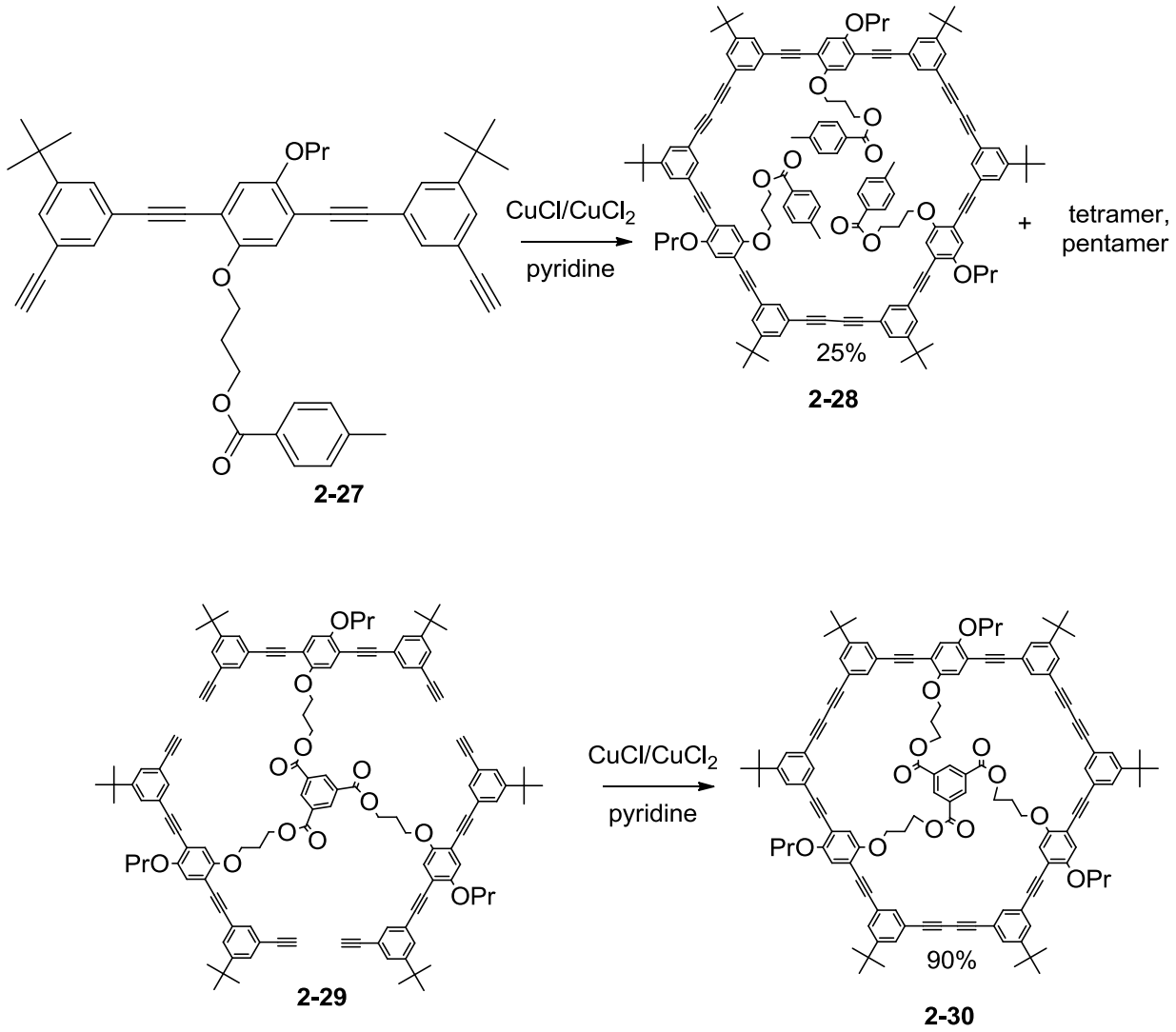

Scheme 2-8 – The Höger group's macrocyclizations, unscaffolded and scafolded

The use of a new scaffold made it necessary to redesign the subunits. Since the scaffold only connects three subunits, each subunit of the aromatic belt must be larger. Molecular modeling was performed by Li Cui in order to which scaffolds and subunits would form the

desired *cis* double bonds needed to synthesize the belt and to see what tether length was optimum between the scaffold and the subunits.[2] The conformational analysis was performed with the Merck Molecular Force Field, MMFF, and the generalized Born/surface area (GB/SA) model for chloroform, using the program MacroModel 8.1. Figure 2-3 below shows the compounds that were targeted initially due to both promising computational results and synthetic accessibility.

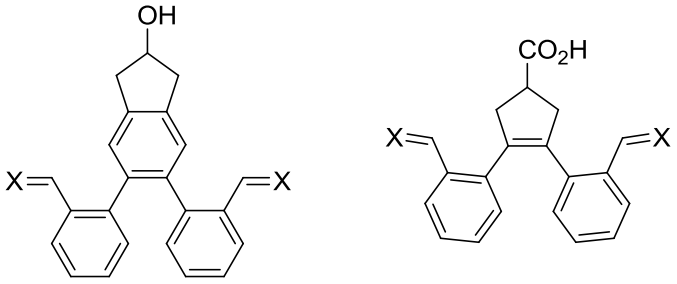

2-31a X=O
2-31b X=CH_2

2-32a X=O
2-32b X=CH_2

Figure 2-3 – The initial subunits for the benzene scaffold

Li Cui then carried out the synthesis of compound **2-31b**.[2] The synthesis begins from 2-indanol, the alcohol is protected with acetic anhydride, and then the compound is brominated with n-bromosuccinimide (NBS) and bromine to give dibromide **2-35**. The alcohol is deprotected before the double Suzuki-Miyaura coupling, because Li Cui found that the acetyl group was partially hydrolyzed during the coupling. The Suzuki-Miyaura coupling of 2-formylphenylboronic acid and dibromide **2-6** yielded subunit **2-31a**. Li Cui chose to convert the aldehydes to vinyl groups with a Wittig reaction, to obtain subunit **2-31b**,[7] because the ruthenium catalyst **2-13** is less sensitive to reaction conditions, including the presence of water, than the McMurry coupling.[9]

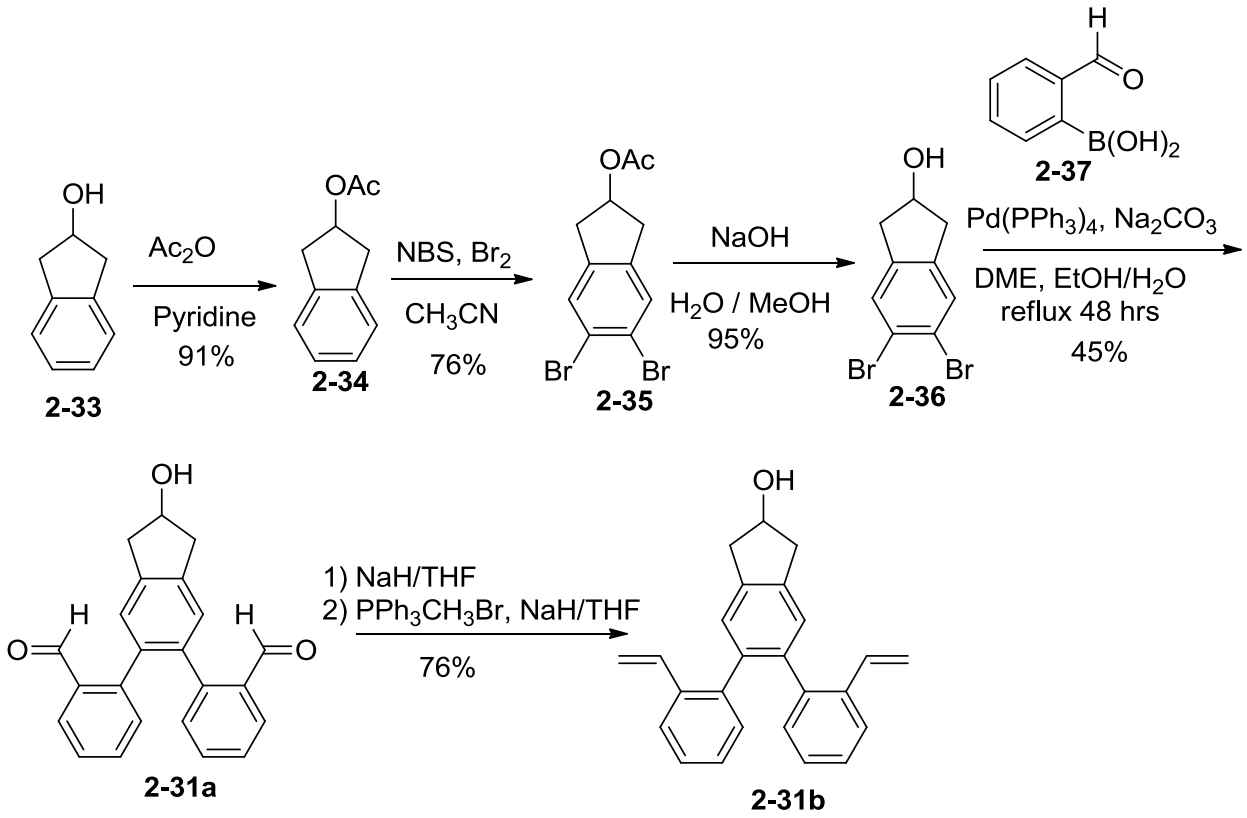

Scheme 2-9 – The synthesis of the new subunit

After trying many different reaction conditions, Li found that a Mitsunobu reaction was best to attach the subunits to the benzene scaffold (**2-38**). When **2-39** reacted with ruthenium catalyst **2-13** TLC showed the presence of starting material after four days, so the solution was heated to reflux for another two days. The reaction mixture was difficult to interpret so the ester linkages were hydrolyzed to simplify the mixture. The only identifiable compounds after preparative TLC was the original subunit **2-30b** and cyclooctatetraene **2-40**, which resulted from self-cyclization of the subunits.

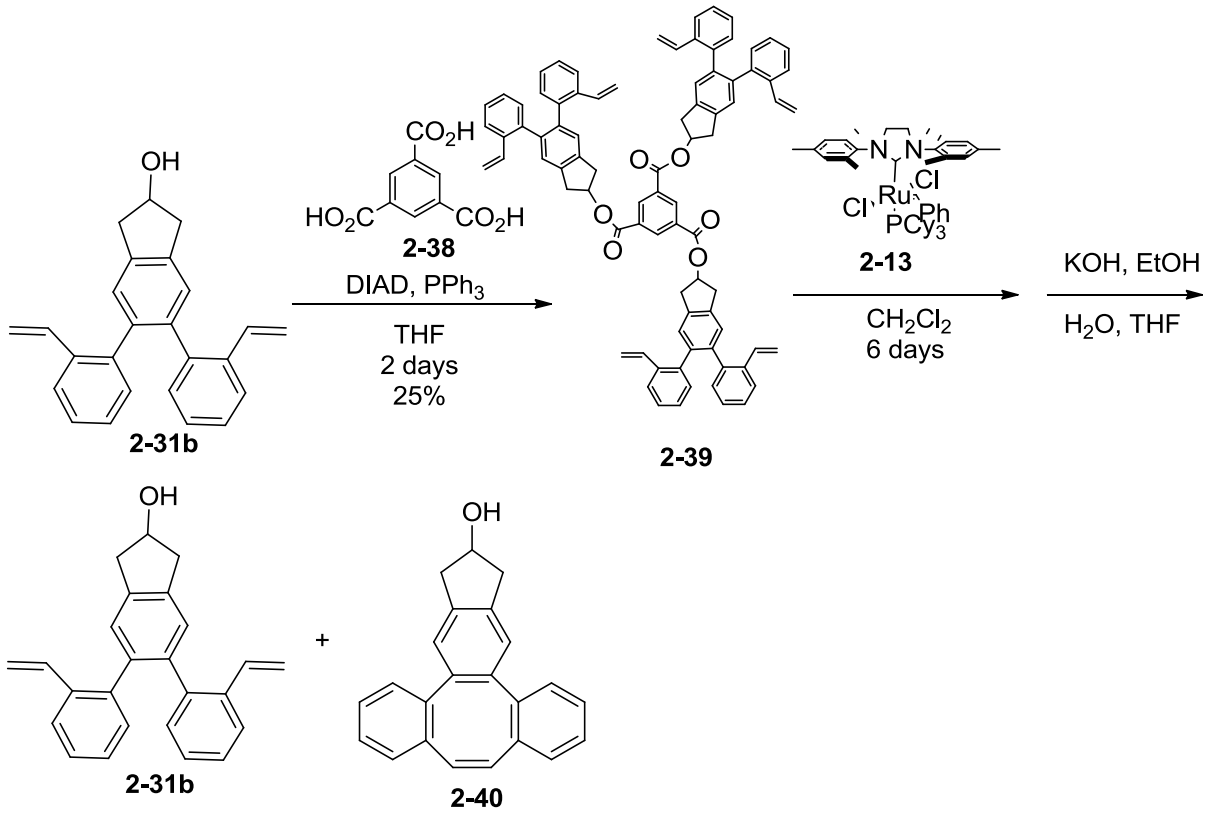

Scheme 2-10 – The attachment of the subunit to the scaffold and its attempted macrocyclization

It seems that subunit **2-31b** is not appropriate to form an aromatic belt, since the reaction to form a cyclooctatetraene is favored over macrocycle formation. At this point Li Cui graduated and the attention shifted to subunit **2-32b**, since molecular modeling showed it as the most promising subunit.

2-4 References

1. Katsamanis, Z. E. Designing a Template-Directed Synthesis of Nonplanar Polycyclic Aromatic Belts. Stony Brook University, Stony Brook, NY, 2005.
2. Cui, L. Buckybelt Synthesis: Template Directed Approach Towards Cyclophenacene. Stony Brook University, Stony Brook, NY, 2006.
3. Zhou, L. Synthesis Different Tethered Compounds for Cylindrically Conjugated Organic Belts and Synthesis of Three-Dimensional Assemblies of Chromophores of FRET Studies. Stony Brook University, Stony Brook, NY, 2006.

4. Szejtli, J., Introduction and general overview of cyclodextrin chemistry. *Chem. Rev.* **1998,** *98* (5), 1743-1753.
5. Anderson, D. R.; Hickstein, D. D.; O'Leary, D. J.; Grubbs, R. H., Model Compounds of Ruthenium−Alkene Intermediates in Olefin Metathesis Reactions. *J. Am. Chem. Soc.* **2006,** *128* (26), 8386-8387.
6. Diederich, F.; Staab, H. A., Benzenoid versus Annulenoid Aromaticity: Synthesis and Properties of Kekulene. *Angew. Chem., Int. Ed. Engl.* **1978,** *17* (5), 372-374.
7. McMurry, J. E., Carbonyl-coupling reactions using low-valent titanium. *Chem. Rev.* **1989,** *89* (7), 1513-1524.
8. Höger, S.; Meckenstock, A.-D.; Pellen, H., High-yield macrocyclization via Glaser coupling of temporary covalent templated bisacetylenes. *J. Org. Chem.* **1997,** *62*, 4556-4557.
9. Trnka, T. M.; Grubbs, R. H., The development of $L_2X_2Ru{=}CHR$ olefin metathesis catalysts: An organometallic success story. *Acc. Chem. Res.* **2001,** *34* (1), 18-29.

Chapter 3

3-1 Computational Studies of the Strain Energy of [12]cyclophenacene

In order to better assess the plausibility of synthesizing an aromatic belt, initial calculations were performed to estimate the strain energy in [12]cyclophenacene. In order to accomplish this, an isodesmic equation was used as shown in Scheme 3-1 in which the energy of belt **3-1** was compared to a series of phenacenes.[1] The equilibrium geometry and energy of a series of phenacenes was calculated (n=1-5) and as n increases, the energy increases linearly (Table 3-1). The linear increase in energy of the phenacenes can be multiplied by twelve to serve as the unstrained equivalent to **3-1**. The strain energy is estimated to be 114 kcal/mol (Table 3-2). In order to compare [12]cyclophenacene to other compounds the strain energy can be expressed on a per carbon basis, which is 2.4 kcal/mol per carbon atom. The heat of formation of C_{60} (relative to graphite) can be taken as its strain energy since it is a comparison to an unstrained reference. The heat of formation of C_{60} is 556 kcal/mol[2] or 9.3 kcal/mol per carbon atom, which is much larger than the strain energy of the belt (2.4 kcal/mol per carbon atom). This means that [12]cyclophenacene is a viable synthetic target since C_{60} has a much larger strain energy and it has been rationally synthesized.[3]

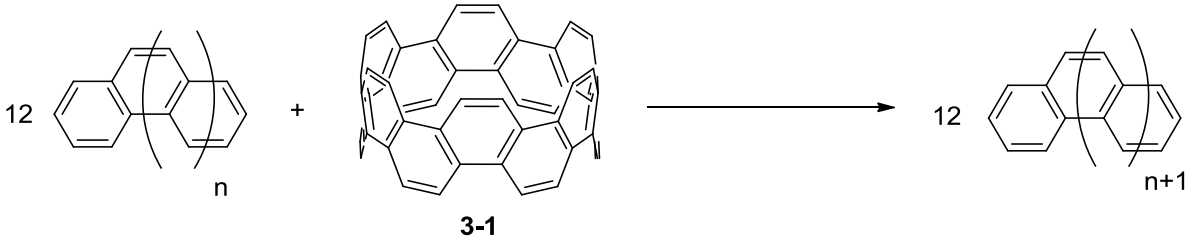

Scheme 3-1 – The isodesmic equation used to estimate the strain energy

n	Rel. E. (kcal/mol)	E_n-E_{n-1} (kcal/mol)
1	0	0
2	-96412.64	-96412.64
3	-192826.11	-96413.47
4	-289239.13	-96413.02
5	-385652.55	-96413.42
avg	-	-96413.14

Table 3-1 – The relative energies of several phenacenes and their energy difference

	12* [E_n-E_{n-1}]	**3-1**	Difference	Difference per carbon atom
Energy (kcal/mol)	1156956	1157070	114	2.4

Table 3-2 – Comparison of [12]cyclophenacene to its unstrained model

Another question that computations helped answer was how difficult would it be to form the last three bonds to make **3-1**. These computations were all carried out by an undergraduate in our group, Michelle Lacoske. Scheme 3-2 shows the isodesmic equation that was used to calculate the strain energy involved in the formation of the last three bonds. Scheme 3-2 only shows the isodesmic equation for the formation of the first of the final three bonds, but the other energies are calculated the same way. The first carbon-carbon bond to form would be 22 kcal/mol higher than in a planar system. The formation of the second carbon-carbon bond would have 9 kcal/mol of strain energy and the final carbon-carbon bond has a strain energy of 15 kcal/mol (HF/3-21G, using SPARTAN 08).

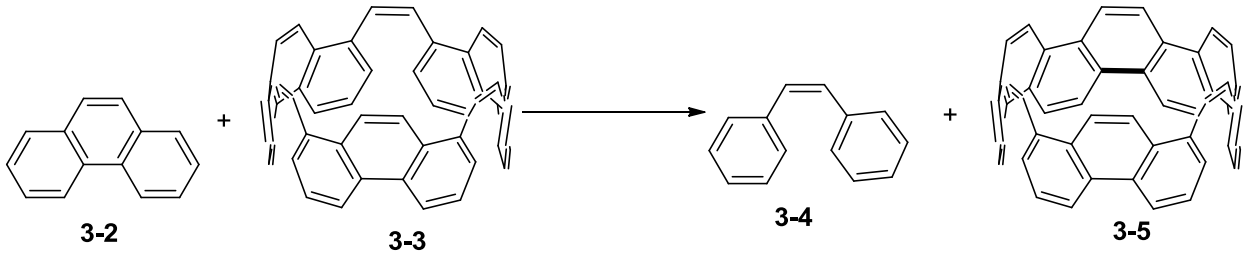

Scheme 3-2 – The isodesmic equation to estimate the strain in the final bonds formation

3-2 Synthesis of a Dibromocyclopentene

Li Cui's work showed that stibene **3-6** was not an ideal subunit because when placed on a molecular scaffold it reacted to form cycloctatetraene **3-7** instead of forming a larger macrocycle (Scheme 3-3). Subunit **3-8** was chosen as the new synthetic target because it seemed more promising computationally.[4] To circumvent the possible self-cyclization of subunit **3-8** to give cyclooctatetraene **3-9**, phenanthrene **3-10** was chosen as the synthetic target.

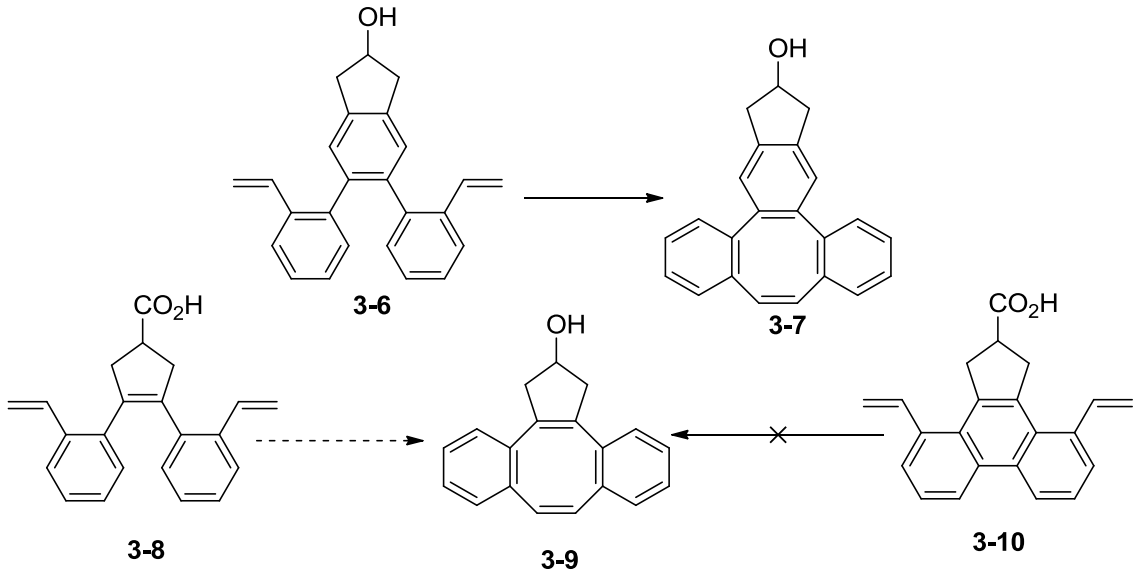

Scheme 3-3 – Redesigning the subunit to avoid a self-cyclization

A retrosynthetic analysis of subunit **3-10** is shown in scheme 3-4. Divinylphenanthrene **3-10** could be synthesized via stilbene **3-11**, which in turn could be synthesized from dibromide **3-12** and an appropriate boronic acid (**3-13**).

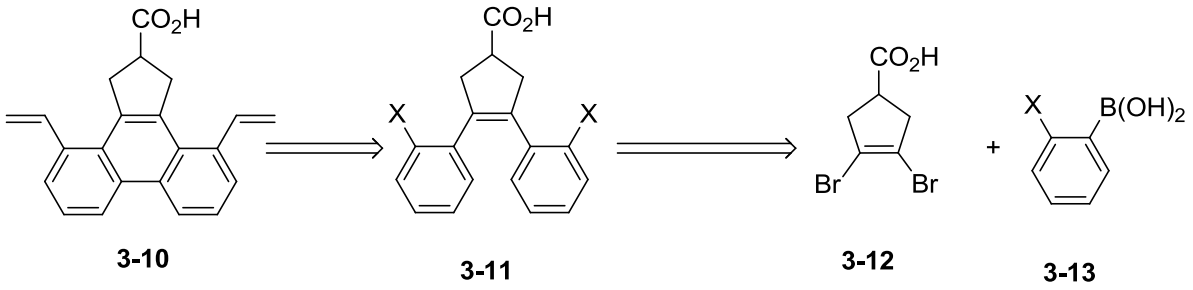

Scheme 3-4 – The retrosynthetic analysis of subunit **3-10**

A published synthetic route was found to dibromocyclopentene **3-19** (Scheme 3-5).[5] The starting material for the synthetic route is mucobromic acid (**3-14**), which exists in equilibrium between an open form (**3-14a)** and a closed form (**3-14b**). Ethylation under acidic conditions will trap it in the closed form (**3-15**). Ethyl ether **3-15** is then reduced with DIBAL-H to give diol **3-16**, and the alcohols are then replaced with chlorines using thionyl chloride. A cyclopentene ring was formed by allowing dichloride **3-17** to react with diethyl malonate to give cyclopentene **3-18**. Decarboxylation gave compound **3-19** in five steps and 26% overall yield. To obtain the desired subunit **3-12** the molecule would have to be hydrolyzed. Unfortunately the literature report has no experimental data, the schemes were the only information given about the synthesis.[5]

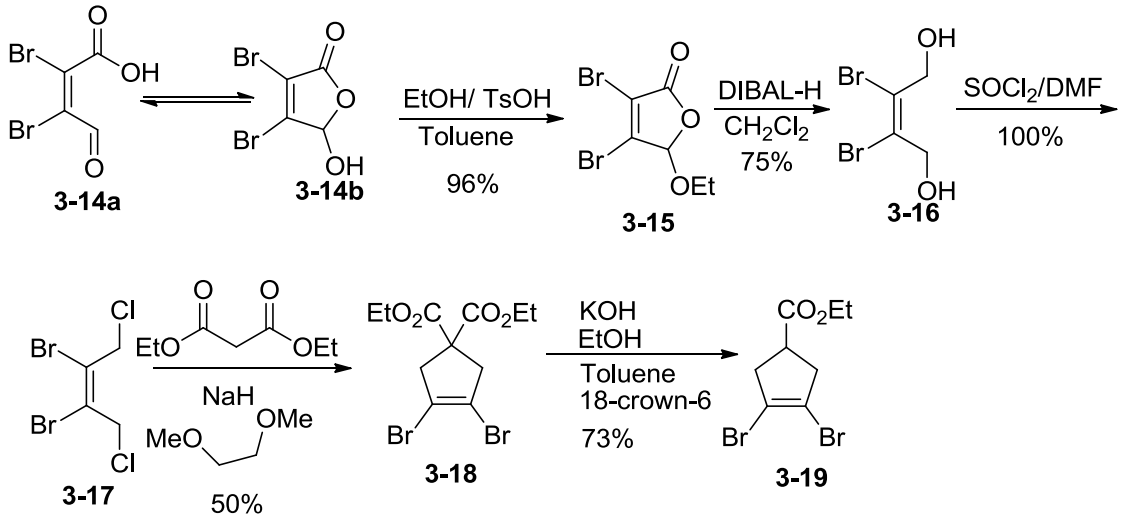

Scheme 3-5 – The published route to molecule **3-19**[5]

The first two steps to synthesize diol **3-16,** proceeded as reported. However, the chlorination with thionyl chloride to give dichloride **3-17** returned only starting material (Scheme 3-6). When **3-14** reacted with PBr_3 only a complicated mixture was obtained. Diol **3-16** was successfully ditosylated to give **3-20**, but in moderate yield. The reaction of the diol with triphenylphosphine and bromine gave 79% yield of dibromide **3-21**. Since these conditions had

the highest yield, they were chosen for the synthetic route. The use of tetrabromide **3-21** instead of the dichloride **3-17** did not change the planned chemistry of the following step.

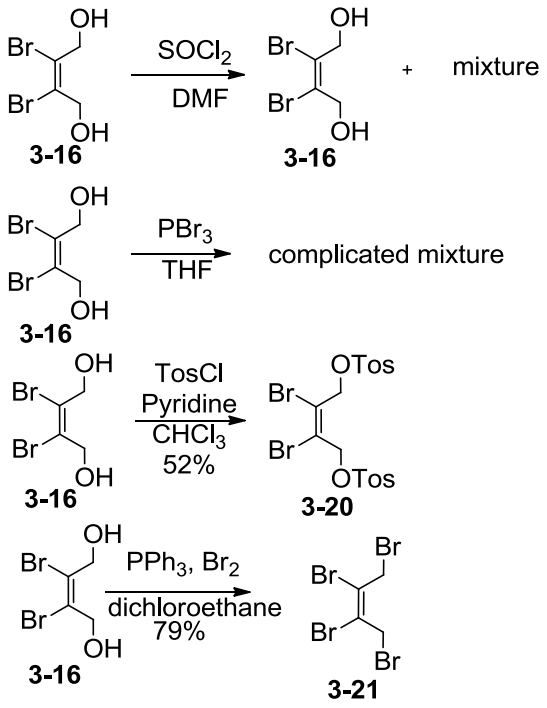

Scheme 3-6 – Attempts to functionalize diol **3-16**

The reaction between tetrabromide **3-21** and dimethyl malonate, with sodium hydride as a base gave only a 20% yield of the desired cyclopentene **3-22**. The low yield was thought to be due to the age of the sodium hydride or the dimethyl malonate, so diethyl malonate was used in the following reactions. The use of sodium ethoxide and diethyl malonate gave only a slight improvement in the yield. When potassium carbonate was used as a base, cyclopentene **3-18** was obtained in 65% yield, which is higher than the literature report.[5a]

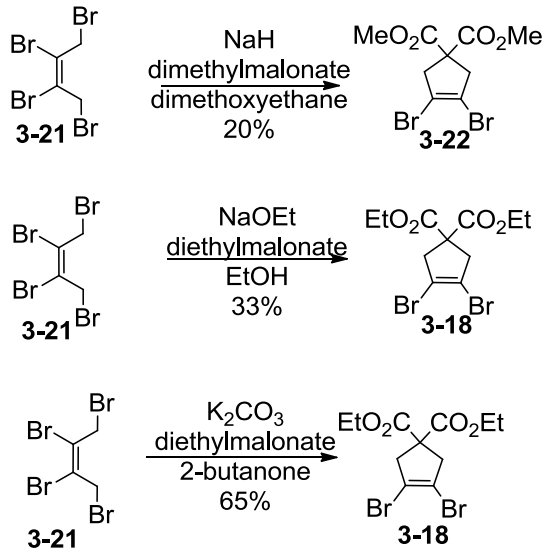

Scheme 3-7 – Different conditions to form cyclopentene diesters **3-18** and **3-22**

Scheme 3-8 shows several attempts to decarboxylate diester **3-18**. Reaction with sodium chloride in a mix of water and ethanol only returned starting material. However, hydrolysis of diester **3-18** with potassium hydroxide in water in ethanol gave the crude diacid. Heating this crude material in a flask, neat, to the melting point, led to the evolution of gas and gave monoacid **3-6** in 80% yield for the two steps.

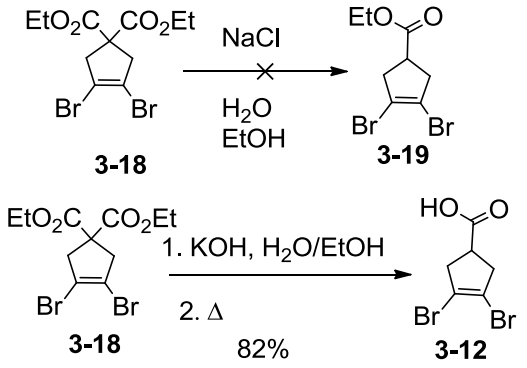

Scheme 3-8 –Attempted decarboxylations to synthesize carboxylic acid **3-12**

The final synthetic route to dibromocyclopentene **3-12** is shown in Scheme 3-9. The synthesis was a 33% yield over five steps. After these conditions had already been worked out, a patent was found that contained experimental details for some of these steps.[6]

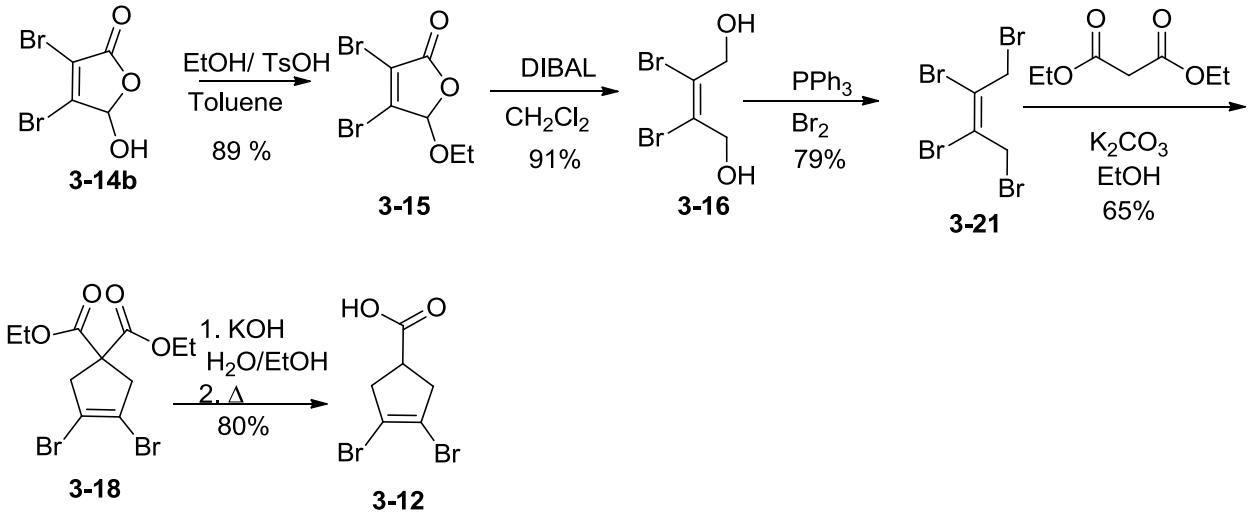

Scheme 3-9 – The route to dibromocyclopentene **3-12**

With the desired dibromide **3-12** in hand a Suzuki-Miyaura coupling was attempted with 2-formylboronic acid (**3-23**), as shown in Scheme 3-10. The reaction returned only starting material even after heating and prolonging the reaction time. Literature searching showed that carboxylic acids are generally protected as esters during a Suzuki-Miyaura coupling. Compound **3-18** was allowed to react under similar conditions but no product was detected. However, this

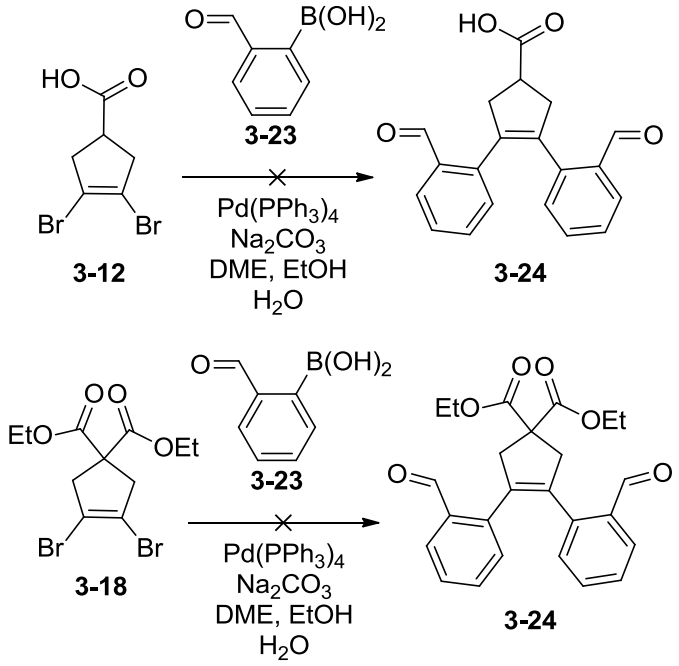

Scheme 3-10 –Attempted coupling of **3-12** and **3-18**

reaction was not explored any further. Instead focus shifted to a subunit based on divinyl indanol **3-6**, which had been previously synthesized by Li Cui.[4]

3-3 The Dibromoindanol Route

Dibromoindanol (**3-28**) was a known compound[7] and Li Cui was able to repeat the literature synthesis.[4] The route (Scheme 3-11) begins from commercially available 2-indanol (**3-25**), which is protected with acetic anhydride. The molecule is brominated with NBS and bromine, to give dibromide **3-27** in 40% yield after five days. The acetyl group is then hydrolyzed in excellent yield giving the target dibromoindanol (**3-28**) in 34% overall yield.

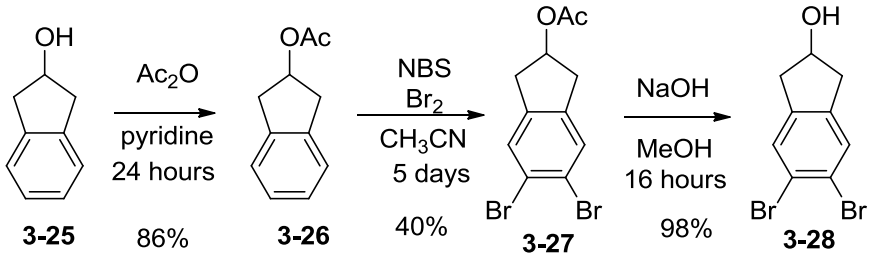

Scheme 3-11 – The route to dibromoindanol **3-28**

With dibromide **3-28** in hand, the next step is to perform a coupling reaction with 2-formylphenylboronic acid (**3-23**). Li Cui had previously performed this reaction, and reported a 45% yield. When the same reaction conditions were initially used only starting material was isolated, but after degassing all of the solvents in the reaction with argon, a 15% yield of the monosubstituted product **3-29** was isolated (Scheme 3-12). One difference between the recent attempts and those performed by Li Cui is that she synthesized boronic acid **3-23**, and we used purchased material. Another possible reason for the difference in products could be the age of the palladium catalyst, since it is oxygen sensitive it becomes less active over time. A solution to the catalyst decomposition was the use of the PEPPSI catalyst because it is more active catalyst

than tetrakis(triphenylphosphine) palladium and it is air stable.[8] Unfortunately the reaction returned only starting material. Since the coupling reaction was unsuccessful, this synthetic route was abandoned.

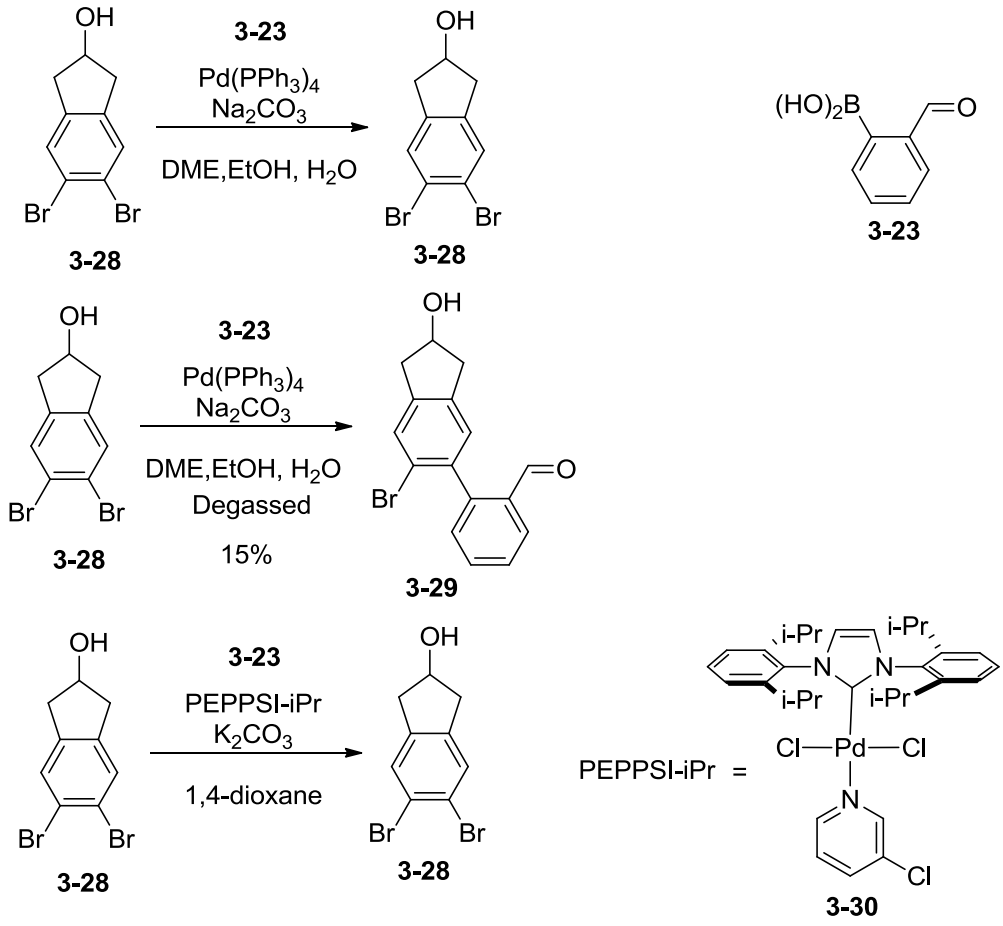

Scheme 3-12 – Attempted Suzuki-Miyaura couplings of dibromoindanol **3-28**

3-4 A New Route Starting from a McMurry Reaction

To avoid the problem of partial reaction describe above, a new route was designed that did not rely on a Suzuki-Miyaura coupling to build up the stilbene core (Scheme 3-13). The route begins from commercially available 2'-bromoacetophenone (**3-31**), forming a dimer via a McMurry coupling to give stilbene **3-32**.[9] Stilbene **3-32** was then irradiated in the presence of

iodine, but the reaction returned only starting material. Increasing the reaction time did not lead to any changes. This route was abandoned at this point.

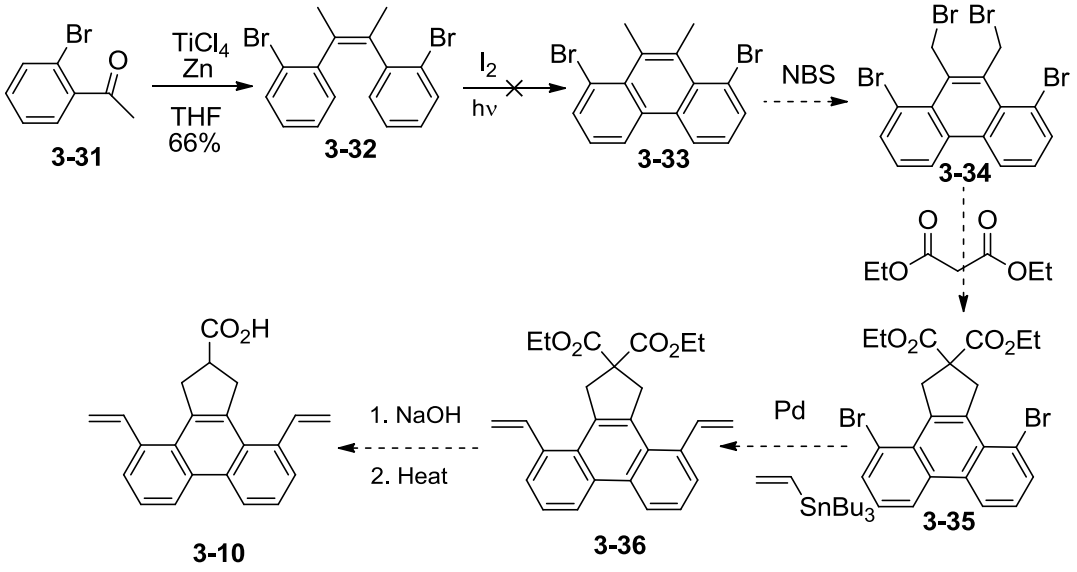

Scheme 3-13 – The new route to subunits **3-10**

The inability for stilbene **3-32** to form phenanthrene **3-33** was surprising since there are literature reports of the formation of 1,8-dibromophenanthrene (**3-37**) in excellent yield (Scheme 3-14).[1b] One possible reason that tetrasubstituted stilbene **3-32** fails to react may be that the

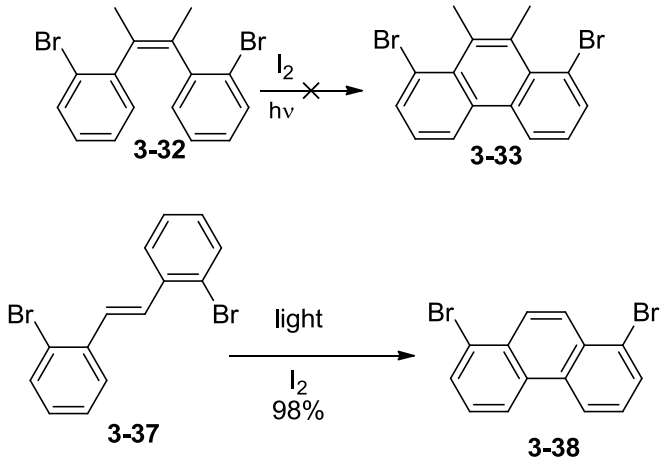

Scheme 3-14 – The photocyclization of some bromostilbenes

steric hindrance of having substituents so close together interferes with the molecule's ability to cyclize.

3-5 Changes to the Route

Around this time it was decided to focus on the McMurry coupling to form the initial macrocycle instead of an olefin metathesis. The McMurry coupling has more literature precedent for forming strained macrocycles.[10]

Another change was altering the scaffold from a simple trisubstituted benzene into a hexasubstituted benzene with ethyl groups at the 1, 3 and 5 positions and attachment points at the 2, 4, and 6 positions. The steric crowding of the molecule causes the substituents to alternate which face of the benzene they are on (Figure 3-1).[11] The subunits would all be on the same face of the benzene and this should favor intramolecular coupling.

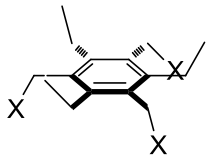

3-38

Figure 3-1 –The new hexasubstituted benzene scaffold

With all of these changes it was decided to move forward and attempt to synthesize a subunit in a route that does not involve a Suzuki-Miyaura coupling. The new synthetic route is discussed in Chapter 4.

3-6 Experimental

3,4-Dibromo-5-ethoxy-2,5-dihydrofuran-2-one **(3-15)**

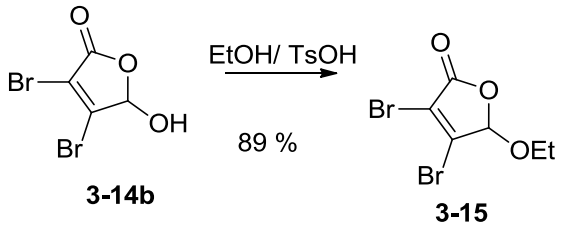

Mucobromic acid (**3-14b,** 2.00 g, 7.8 mmol) was placed in a 50-mL round-bottomed flask. Absolute ethanol (20 mL) was added along with a magnetic stirring bar. p-Toluenesulfonic acid (.046 g, 0.24 mmol, 3 mol %) was added to the solution, a reflux condenser was attached and the solution was placed under Ar. The flask was then placed in a 105 °C oil bath. After 24 h, the flask was cooled to room temperature and the solvent was removed *in vacuo* to give an orange liquid. The liquid was then dissolved in 30 mL CH_2Cl_2 and washed with 20 mL $NaHCO_3$ (aq, sat.). The aqueous layer was then subjected to extraction with CH_2Cl_2 (3x 25 mL). The organic layers were combined, dried over $MgSO_4$, and filtered. The solvent was removed *in vacuo* to give **3-15** as a colorless liquid (1.97 g, 89% yield). ^{1}H NMR (400 MHz, $CDCl_3$) δ 5.81 (s, 1H), 3.95-3.70 (m, 2H), 1.30 (t, *J*=7.2 Hz, 3H). ^{13}C NMR (100 MHz $CDCl_3$) δ 164.2, 143.5, 118.9, 103.3, 66.1, 15.1. ^{1}H NMR matches the reported spectrum.[6]

(2Z)-2,3-Dibromobut-2-ene-1,4-diol (**3-16**)

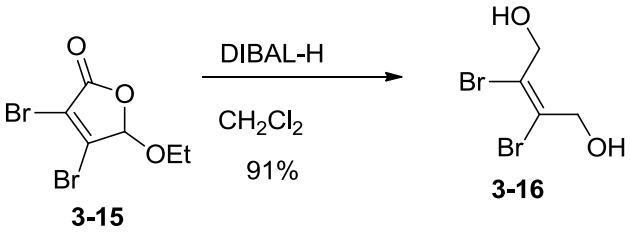

Compound **3-15** (1.60 g, 5.6 mmol) was placed in an oven-dried 50-mL round bottomed flask. 1 M DIBAL-H in CH_2Cl_2 (22.2 mL) was added at 0°C. The solution was warmed to room

temperature and was stirred overnight under Ar. Methanol (5 mL) was added, and bubbling was observed. The solution was then transferred to a separatory funnel containing 50 mL of 1 M HCl (*aq*). A solid precipitate formed in the separatory funnel, that then slowly dissolved and more bubbling was observed. Aqueous K_2CO_3 (40%) was added until the pH=7. The aqueous layer was then extracted with ethyl acetate (3 x 100 mL). The organic layers were combined, dried over $MgSO_4$ and the solvent was removed *in vacuo* to give **3-16** (1.25 g, 91%) as a white solid. M.p. 79-82°C. ^{1}H NMR (300 MHz, DMSO-d^6) δ 5.54 (t, *J*=3.3 Hz, 2H), 4.35 (d, *J*=3.3 Hz, 4H). ^{13}C NMR (75 MHz, DMSO-d^6) δ 131.7, 63.8. ^{1}H NMR matches the reported spectrum.[6]

(Z)-2,3-Dibromobut-2-ene-1,4-diyl bis(4-methylbenzenesulfonate) (**3-20**)

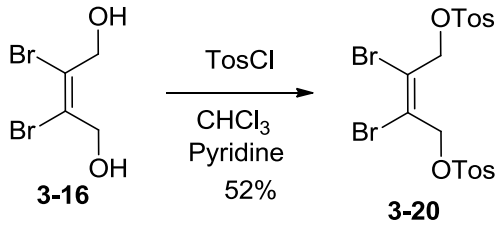

In an oven dried flask was added **3-16** (0.100 g, 0.41 mmol) and 2 mL of chloroform. Toluenesulfonyl chloride (0.311 g, 1.60 mmol) was added to the light yellow solution. Pyridine (0.20 mL, 2.4 mmol) was injected and the solution was stirred under Ar overnight. It was then diluted with 15 mL of diethyl ether and 15 mL of water. The layers were separated and the organic layer was washed with aq. HCl (0.5 M, 20 mL) and then 20 mL $NaHCO_3$ (satd, aq.). The organic layer was dried over $MgSO_4$, filtered and the solvent removed *in vacuo* to give crude **3-20** (0.116 g, 52%) as a brown oil. ^{1}H NMR (300 MHz, $CDCl_3$) δ 7.79 (d, *J*=8.4 Hz, 4H), 7.34 (d, *J*=7.8 Hz, 4H), 4.47 (s, 4H), 2.45 (s, 4H). ^{13}C NMR (100 MHz $CDCl_3$) δ 146.8, 129.8, 128.0, 127.8, 127.0, 45.6, 21.6.

(2Z)-1,2,3,4-Tetrabromobut-2-ene (**3-21**)

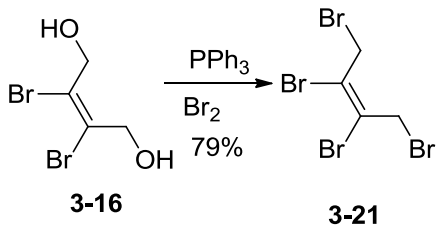

3-16 **3-21**

PPh_3 (0.317 g, 1.21 mmol) was dissolved in 2 mL 1,2-dichlorethane. Br_2 (0.06 mL, 1.21 mmol) was added at 0 °C and the solution was stirred for 5 min. Diol **3-16** (0.100 g, 0.41 mmol) was added and the solution was warmed to room temperature. The solution was stirred overnight, and the next day the solvent was removed *in vacuo*. The solid was then dissolved in CH_2Cl_2 and absorbed onto silica purified by column chromatography (SiO_2, hexanes) to give compound **3-21** as a yellow solid (0.120 g, 79% yield) . ^{1}H NMR (300 MHz, $CDCl_3$) δ 4.39 (s, 4H). ^{13}C NMR (100 MHz $CDCl_3$) δ 127.6, 32.0.

1,1-Diethyl 3,4-dibromocyclopent-3-ene-1,1-dicarboxylate (**3-18**)

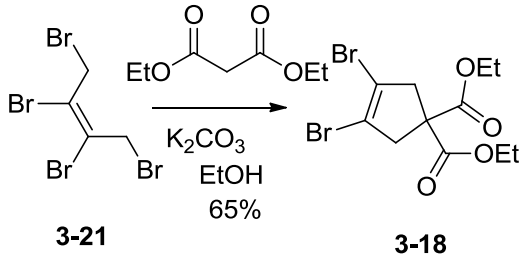

3-21 **3-18**

Tetrabromide **3-21** (0.688 g, 1.85 mmol) was placed in a 25 mL round bottomed flask with a stir bar. 10 mL of 2-butanone was added. Diethyl malonate (0.296 g, 1.85 mmol) was added along with K_2CO_3 (1.53 g. 11.1 mmol). The solution was refluxed under Ar for 20 h. The solution was concentrated *in vacuo* and poured into a separatory funnel charged with 15 mL water and 25 mL ethyl acetate. The aqueous layers were acidified with 2M HCl and extracted with ethyl acetate (3x 25 mL). The organic layers were combined, washed with brine, dried over $MgSO_4$, and the solvent was removed *in vacuo*. The resulting brown oil was then purified by column

chromatography on silica gel to give compound (**3-16**) as a colorless oil (0.31 g, 65% yield) . ^{1}H NMR (300 MHz, $CDCl_3$) δ 4.22 (q, *J*=7 Hz, 4H), 3.26 (s, 4H), 1.26 (t, *J*=7 Hz, 6H). ^{13}C NMR (100 MHz $CDCl_3$) δ 170.1, 117.9, 62.3, 57.2, 45.9, 13.9.

3,4-Dibromocyclopent-3-ene-1-carboxylic acid (**3-12**)

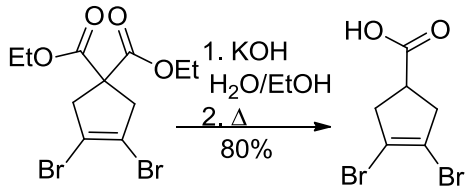

3-18 **3-12**

Compound **3-18** (0.194 g, 0.52 mmol) was placed in a 25 mL flask. KOH (0.073 g, 1.31 mmol) was added along with 10 mL 80% EtOH (*aq*). The reaction mixture was then heated to reflux overnight under Ar. The solvent was then removed *in vacuo* and the resulting oil was dissolved in ethyl acetate (25 mL) and water (25 mL). The layers were separated and the aqueous layer was acidified with 2M HCl until pH reached 1. The aqueous layer was then extracted with ethyl acetate (3 x 50 mL). The organic layers were combined, dried over $MgSO_4$ and the solvent was removed *in vacuo* to give 0.160 g (98% yield) of a white solid. The product was used in the next step without further purification or characterization.

The resulting white solid (0.160 g, 0.51 mmol) was placed in a 50 mL round bottomed flask and placed in a 180° C oil bath for 15 min. Bubbling was observed and a solid began to form on the sides of the flask. The flask was then cooled and the solid was purified by column chromatography (SiO_2) to give **3-12** as a white solid (0.116 g, 85 % yield). ^{1}H NMR (400 MHz, $CDCl_3$) δ 3.36 (m, 1H), 2.94 (m, 4H). ^{13}C NMR (100 MHz, $CDCl_3$) δ 178.7, 119.7, 42.0, 40.4.

2,3-Dihydro-1H-inden-2-yl acetate (**3-26**)

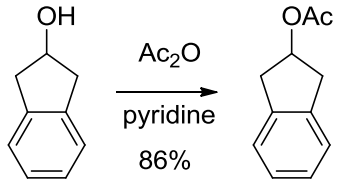

2-Indanol (**3-25**, 5.00 g, 37.3 mmol) was dissolved in 5 mL of pyridine. Acetic anhydride (7.3 mL, 74.6 mmol) was added, and the solution was stirred under Ar. After 24 h the solvent was removed *in vacuo*. The remaining liquid was then purified by vacuum distillation to give compound **3-26** as a colorless oil (5.83 g, 90% yield). bp 80 °C under vacuum. ^{1}H NMR (400 MHz, $CDCl_3$) δ 7.24 (m, 4H), 5.55 (m, 1H), 3.33 (dd, *J*=6.4, 3.2 Hz, 2H), 3.03 (dd, *J*= 16.8, 3.2 Hz, 2 H), 2.03 (s, 3H). ^{13}C NMR (100 MHz, $CDCl_3$) δ 170.9, 140.3, 126.7, 124.5, 75.2, 39.5, 21.2. ^{13}C spectrum matches the literature report.[7]

5,6-Dibromo-2,3-dihydro-1H-inden-2-yl acetate (**3-27**)

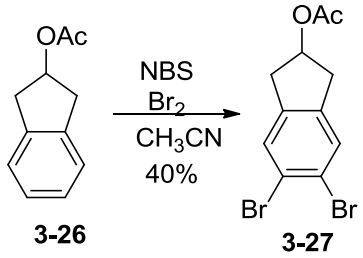

In a 250 mL flask, 100 mL dry acetonitrile (freshly distilled from P_2O_5) and compound **3-26** (3.72 g, 21.6 mmol) were added with a magnetic stir bar. *N*-Bromosuccinamide (9.62 g, 54.1 mmol) and bromine (1.4 mL, 27 mmol) were added and the flask was covered with aluminum foil, capped with a stopper and stirred for 5 days. The solvent was then removed *in vacuo*, and the resulting brown oil was dissolved in 50 mL dichloromethane and washed with saturated Na_2CO_3 (*aq*, 3 x 75 mL). The organic layer was then dried over $MgSO_4$, filtered and the solvent was removed *in vacuo*. The brown oil was then put through a plug of silica gel with 1:1

hexanes:ethyl acetate as the eluent. Evaporation of the solvent let to a brown solid which was recrystallized from hot ethyl ether to give **3-27** as yellow crystals (2.87 g, 40% yield). ^{1}H NMR (300 MHz, $CDCl_3$) δ 2.01 (s, 3H), 2.95 (dd, *J*=17.1, 2.7 Hz, 2H), 3.24 (ddd, *J*=17.4, 6.3, .6 Hz, 2H), 5.50 (tt, *J*=6.3, 2.7 Hz, 1H), 7.49 (s, 2H). ^{13}C NMR (100 MHz, $CDCl_3$) δ 170.7, 141.7, 120.6, 122.5, 75.0, 39.0, 21.1. ^{1}H and ^{13}C NMR match the reported spectra.[7]

5,6-Dibromo-2,3-dihydro-1H-inden-2-ol (**3-28**)

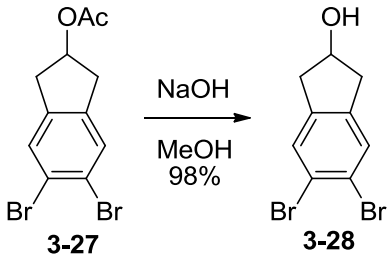

3-27 **3-28**

To a 50 mL flask charged with a stir bar was added compound **3-27** (2.87 g, 8.6 mmol) and 15 mL methanol. To this mixture was added 5 mL of 10% NaOH in water. The flask became warm and a white precipitate formed. The reaction mixture was allowed to stir overnight. The solvent was removed *in vacuo*, and the solid was dissolved in 20 mL water and 25 mL dichloromethane. The layers were separated and the aqueous layer was extracted with dichloromethane (2 x 25 mL). The organic layers were combined, dried over $MgSO_4$, filtered and the solvent was removed *in vacuo* to give 2.45 g (98% yield) of **3-28** as a white solid. . ^{1}H NMR 400 MHz ($CDCl_3$) δ 7.49 (s, 2H), 4.72 (bs, 2H), 3.14 (dd, *J*=17, 6 Hz, 2H), 2.85 (dd, *J*=17, 3 Hz, 2H), 1.73 (s, 1H). ^{1}H NMR matches the reported spectrum.[7]

2-(6-Bromo-2-hydroxy-2,3-dihydro-1H-inden-5-yl)benzaldehyde (**3-29**)

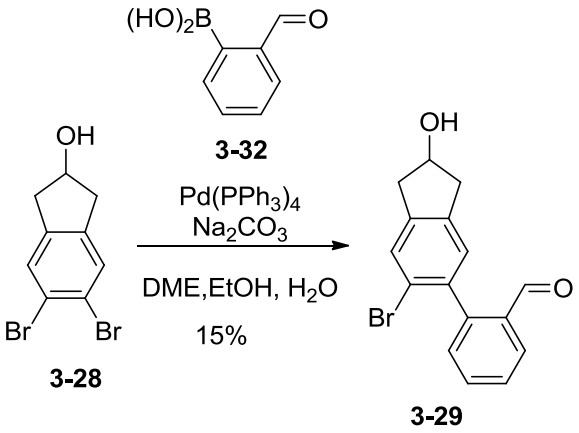

A 25 mL flask with a stir bar was charged with 6 mL dimethoxyethane and **3-28** (0.174 g, 0.6 mmol) and Ar was bubbled through the solution for 30 min to remove oxygen. Palladium tetrakis(triphenylphosphine) (0.058 g, 0.06 mmol, 10 mol %) was added to the solution and the solution became light brown. After 30 min a solution of ethanol (4 mL) and 2-formyl boronic acid (**3-23**, 0.320 g, 2.1 mmol, 3.5 eq) was added to the reaction flask. (The EtOH solution had Ar bubbled through it for 15 min prior to addition.) The reaction mixture turned yellow and was stirred for 15 min. A solution of Na_2CO_3 (0.7 g, 6.5 mmol) in 3 mL water, Ar bubbled through the solution for 15 min) was added to the reaction flask, and a white precipitate formed. After a few minutes the reaction mixture became an orange-red color. The solution was stirred under Ar and put in a 65° oil bath. After 24 h TLC showed no starting dibromide, so the black solution was poured in a separatory funnel with 25 mL water and 25 mL ether. The layers were separated and the aqueous layer was extracted with ether (2 x 25 mL). The organic layers were combined and dried over $MgSO_4$, filtered and the solvent was removed *in vacuo*. The brown oil was then purified by column chromatography (SiO_2, 4:1 Hex:EtOAc) to give compound **3-29** as a white solid (0.026 g, 15%yield). ^{1}H NMR (300 MHz, $CDCl_3$) δ 9.9 (d, *J*=6.0 Hz, 1 H) 8.1 (d, *J*=5.8

Hz, 1 H), 7.5-7.8 (m, 3H), 7.4 (m, 2H), 4.8 (m, 1H) 3.2-3.4 (m, 2H), 2.9-3.1 (m, 2H). ^{1}H matches the reported spectrum.[4]

1-Bromo-2-[3-(2-bromophenyl)but-2-en-2-yl]benzene (**3-31**)

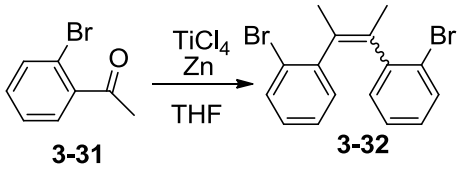

3-31 **3-32**

To a stirred oven-dried 2-necked flask under Ar, zinc dust (1.27 g, 20 mmol, 4 eq) was added. Dry THF (20 mL) was injected into the flask, and the mixture was stirred. The flask was cooled in an ice water bath and $TiCl_4$ (1.11 mL, 10 mmol, 2 eq) was added dropwise. A yellow gas formed, and the solution turned a purple black color. The mixture was stirred for 15 min, then 2'-bromoactophenone (**3-31**, 0.68 mL, 5.0 mmol) was added dropwise. After the addition, the solution was heated to reflux for 3 h. Then 20 mL water was added, and the solution bubbled. The reaction mixture was extracted with hexanes (3 x 50 mL), the organic layers were combined, dried over $MgSO_4$, filtered and the solvent was removed *in vacuo*. This led to 1.1 g of a brown oil, which was adsorbed onto silica and purified with a short column (SiO_2, hexanes) to give compound **3-32** as a 6:1 mixture of the *cis*:*trans* iosmers (0.603 g, 66% yield). The mixture can be separated by recrystallization from hexanes; the soluble compound is the cis isomer. ^{1}H NMR (300 MHz, $CDCl_3$) δ trans isomer 1.67 (s, 4 H), 1.70 (s, 2H), 7.12-7.34 (m, 6H), 7.61 (dd, *J*=8, 1.2 Hz, 2 H). cis isomer 2.10 (s, 6H) 6.88 (dt, *J*=8, 2 Hz, 2H), 6.98 (dt, *J*=7, 1 Hz, 2H), 7.09 (dd, *J*=7.5, 1.5 Hz, 2 H), 7.39 (d, *J*=7,5Hz) ^{1}H NMR matches the reported spectra.[9]

1,8-Dibromo-9,10-dimethylphenanthrene **3-33**

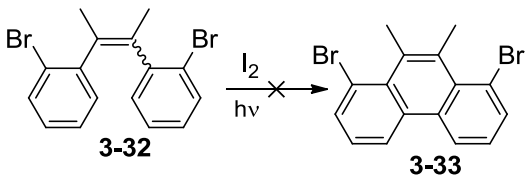

3-32 **3-33**

Compound **3-32** (0.058 g, 0.16 mmol) was dissolved in 200 mL hexanes in a quartz photochemical reaction vessel. Iodine (0.04 g, 0.16 mmol) was added and Ar was bubbled through the solution for 30 min. Then propylene oxide (2.21 mL, 31.7 mmol) was added and the solution was irradiated with stirring in a Rayonet photolysis chamber (300 nm). After the disappearance of the iodine color (~72 h) the solution was transferred to a flask and the solvent was removed *in vacuo*. ^{1}H NMR of the reaction showed a significant amount of unreacted starting material, with only a trace amount of product.

The reaction was repeated, using 254 nm lamps, but this experiment led to no detectable product formation and more byproducts.

3-7 References

1. (a) Mallory, F. B.; Butler, K. E.; Evans, A. C.; Mallory, C. W., Phenacenes: A family of graphite ribbons. 1. Syntheses of some [7]phenacenes by stilbene-like photocyclizations. *Tetrahedron Lett.* **1996,** *37* (40), 7173-7176; (b) Mallory, F. B.; Butler, K. E.; Evans, A. C.; Brondyke, E. J.; Mallory, C. W.; Yang, C. Q.; Ellenstein, A., Phenacenes: A family of graphite ribbons. 2. Syntheses of some [7]phenacenes and an [11]phenacene by stilbene-like photocyclizations. *J. Am. Chem. Soc.* **1997,** *119* (9), 2119-2124; (c) Mallory, F. B.; Butler, K. E.; Berube, A.; Luzik, E. D.; Mallory, C. W.; Brondyke, E. J.; Hiremath, R.; Ngo, P.; Carroll, P. J., Phenacenes: a family of graphite ribbons. Part 3: Iterative strategies for the synthesis of large phenacenes. *Tetrahedron* **2001,** *57* (17), 3715-3724.
2. Beckhaus, H. D.; Verevkin, S.; Ruechardt, C.; Diederich, F.; Thilgen, C.; ter Meer, H. U.; Mohn, H.; Mueller, W., C70 is as stable as C60: experimental determination of the heat of formation of C70. *Angew. Chem., Int. Ed. Engl.* **1994,** *33* (9), 996-8.
3. Scott, L. T.; Boorum, M. M.; McMahon, B. J.; Hagen, S.; Mack, J.; Blank, J.; Wegner, H.; de Meijere, A., A rational chemical synthesis of C_{60} *Science* **2002,** *295*, 1500-1503.
4. Cui, L. Buckybelt Synthesis: Template Directed Approach Towards Cyclophenacene. Stony Brook University, Stony Brook, NY, 2006.
5. (a) Lerstrup, K.; Bailey, A.; McCullough, R.; Mays, M.; Cowan, D.; Kistenmacher, T., The synthesis and study of new selenium and tellurium heterocyclic w-donors. *Synth. Met.* **1987,** *19*, 647-652; (b) Bailey, A. B.; McCullough, R. D.; Mays, M. D.; Cowan, D. O.; Lerstrup, K. A., New organic π-donors: Analogues of HMTSF and HMTTeF. *Synth. Met.* **1988,** *27* (3-4), 425-430.
6. Huang, H.-C.; Reitz, D. R. Substituted cyclopentadienyl compounds for the treatment of inflammation. 5663180, 1997.

7. Süleyman, G.; Hasan, S., Concise syntheses of 2-aminoindans via indan-2-ol. *Tetrahedron* **2005,** *61* (28), 6801-6807.
8. Kantchev, E. A. B.; O'Brien, C. J.; Organ, M. G., Palladium Complexes of N-Heterocyclic Carbenes as Catalysts for Cross-Coupling Reactions—A Synthetic Chemist's Perspective. *Angew. Chem. Int. Ed.* **2007,** *46* (16), 2768-2813.
9. Yamazaki, S.; Yoshimura, T.; Yamabe, S.; Arai, T.; Tamura, H., Synthesis and unusual selenium extrusion reaction of a cyclic triselenide. *J. Org. Chem.* **1990,** *55* (1), 263-269.
10. McMurry, J. E., Titanium-induced dicarbonyl-coupling reactions. *Acc. Chem. Res.* **1983,** *16* (11), 405-411.
11. Kilway, K. V.; Siegel, J. S., Control of functional group proximity and direction by conformational networks: synthesis and stereodynamics of persubstituted arenes. *Tetrahedron* **2001,** *57* (17), 3615-3627.

Chapter 4

4-1 A Route to a New Subunit 4-1

The challenges of the Suzuki-Miyaura approach led us to reexamine the synthesis of subunit **4-1**. Locking the molecule in the *cis* conformation (as in intermediate **4-3**) would favor the Mallory photocyclization. A McMurry coupling on a 1,5-diketone would provide access to compound **4-3**. The aldol reaction between two equivalents of a substituted acetophenone and an ethyl formate equivalent could generate diketone **4-4**.

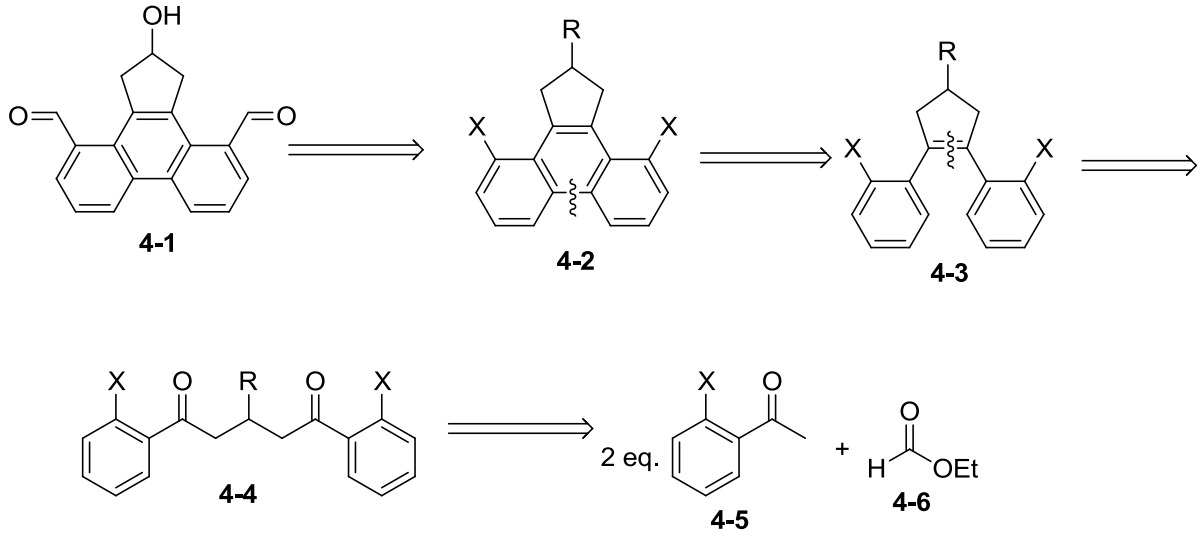

Scheme 4-1 – A new retrosynthesis of subunit **4-1**

A search of the literature revealed that the synthesis of diketone **4-4** could be accomplished by a Mukaiyama-aldol reaction (Scheme 4-2).[1] By utilizing the silyl enol ether of acetophenone (**4-7**), trimethyl orthoformate (**4-8**) as the electrophile, and bistrifluoromethanesulfonimide (**4-9)** as a catalytic acid, diketone **4-10** was reported in moderate yield under mild conditions. This reaction provided a viable starting point for the route to phenanthrene dialdehyde **4-1**.

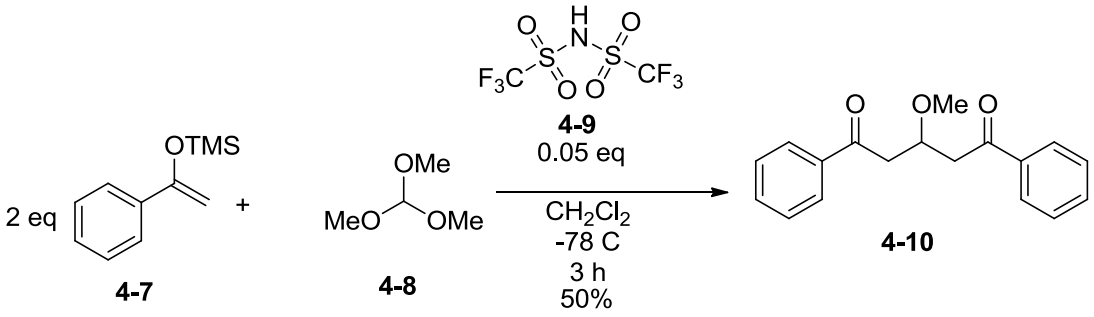

Scheme 4-2 – The literature report to 1,5-diketone **4-10**

In order to test the reproducibility of the reaction to form diketone **4-10,** a series of model reactions were performed (Scheme 4-3). Formation of silyl enol ether **4-7** occurred in low yield because the triethylamine used in the reaction was old and wet, but enough material was produced to continue the route.[2] The next step was a repeat of the literature procedure to synthesize diketone **4-10**, which proceeded with similar yield, although twice as much of the acid **4-9** was used.[1] The literature report used 5 mol% acid **4-9** for the reaction with one equivalent of silyl enol ether **4-27** and the yield was 92% of the monosubstituted product(not shown). When two equivalents of silyl enol ether **4-27** were used, the amount of acid **4-9** was kept the same and the yield of the diketone **4-10** was only 50%. It was thought that increasing the amount of acid **4-9** would increase the yield, but this was not the case.

With diketone **4-10** in hand, a McMurry coupling was performed, which proceeded in low yield due to a miscalculation of the stoichiometry. Nonetheless, enough material was obtained to proceed. Stilbene **4-11** was then photocyclized using the modified conditions developed by Katz, in which a stoichiometric amount of iodine is used and an excess of propylene oxide is added to scavenge the HI produced during the reaction.[3] The photocyclization proceeded well to give the target phenanthrene **4-12** in excellent yield. The final step in the model route was removal of the methyl group on the oxygen, but due to the

small amount of material isolated, it was decided to model that step on a simpler molecule. With the model route validated, attention shifted to making phenanthrene dialdehyde **4-1**.

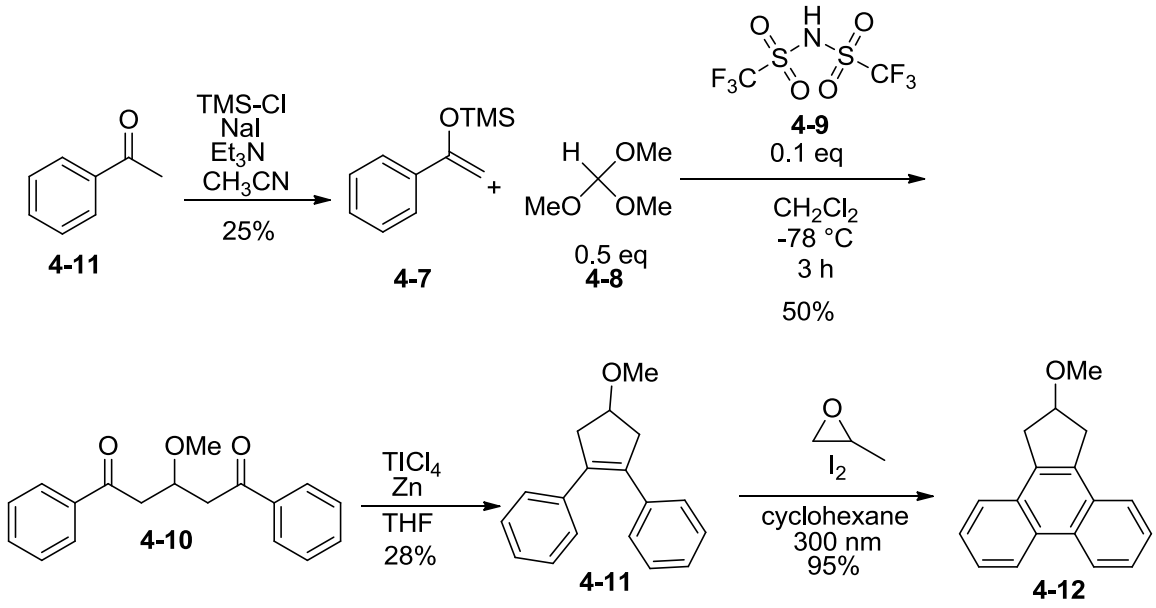

Scheme 4-3 – The model route using trimethyl orthoformate

The route to the phenanthrene dialdehyde **4-1** (Scheme 4-4) begins with 2'-bromoacetophenone (**4-13)**. Formation of silyl enol ether **4-14** was accomplished by reaction with lithium hexamethyldisilazane (LHMDS) followed by trimethylsilylchloride (TMS-Cl), instead of the triethylamine used in the model reaction.[4] The Mukaiyama-aldol addition to form diketone **4-15** proceeded in better yield than the model reaction, and the McMurry coupling gave stilbene **4-16** in excellent yield. Unfortunately the photolysis of stilbene **4-16** at 300 nm in the presence of iodine returned only starting material, even after 3 days.

The attempted photooxidation of stilbene **4-16** to form phenanthrene **4-17** was repeated several times under different conditions (Scheme 4-5). If cyclohexane was used as the solvent the iodine color disappeared in 48 hours, but the reaction mixture contained mostly unreacted starting material. However, when the solvent used in the reaction was toluene, a phenanthrene

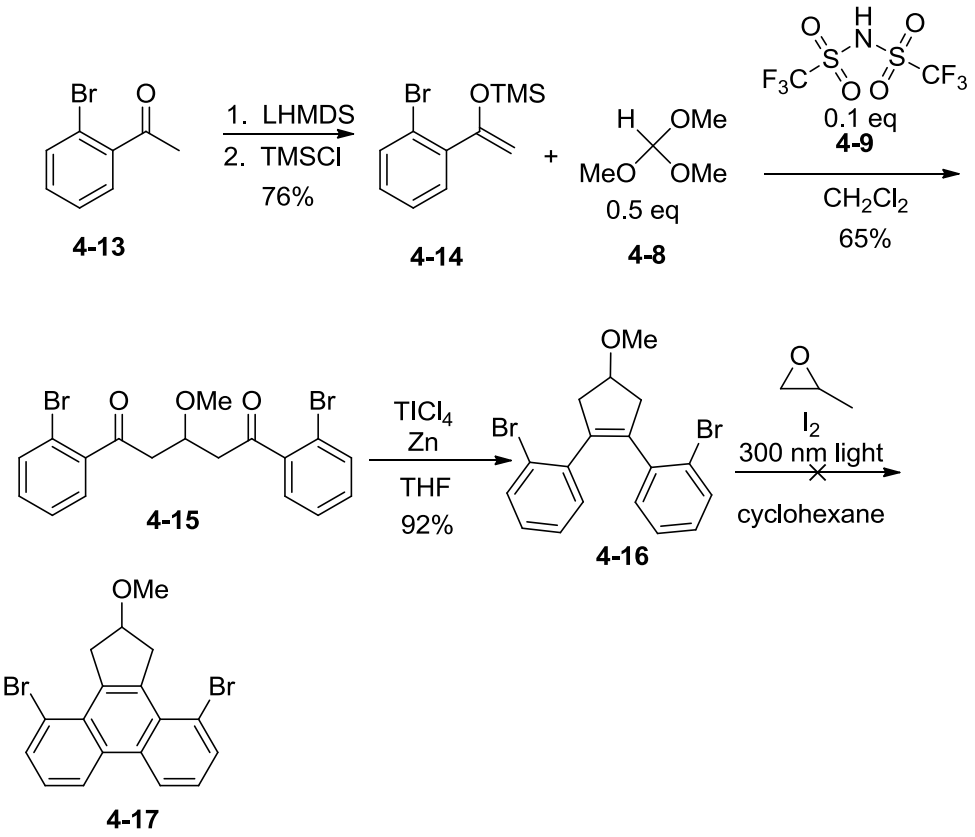

Scheme 4-4 – The route to dialdehyde **4-1** from 2'-bromoacetophenone

(4-12) was formed, but the bromines were lost. It has been reported that iodines can be removed over the course of a photoxidation,[5] but no reports were found of aryl bromides undergoing debromination. However, other stilbenes with similar substitution patterns have also failed to close to the desired phenanthrene. Irradiation of dinaphthyl stilbene **4-18** in the presence of iodine did not give the desired [5]phenacene **4-19**.[6] The lack of cyclization is likely due to the steric crowding of the hydrogen atoms on the cyclopentene and the *ortho*-substituent on the benzene rings. The steric crowding prevents the required geometry needed for the photocyclization. Pillai and coworkers have reported a successful Mallory photooxidation with the same substituent pattern (**4-20**).[7] Compound **4-20** has an imidazole ring and chlorines in place of the bromines on **4-16**. The use of chlorine atoms in the photocyclization has at least two

advantages over the use of bromines: a carbon-chlorine bond is stronger than a carbon-bromine bond, so less likely to be cleaved photolytically, and a chlorine atom is smaller, so it should interfere less with the geometry of the reaction.

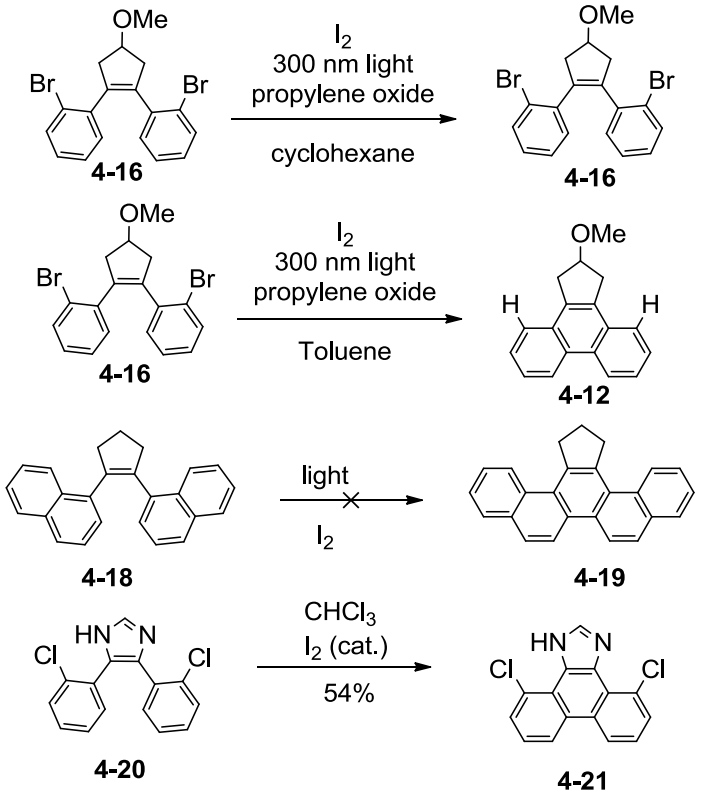

Scheme 4-5 – Some photooxidations of similar stilbenes

It should be noted that dibromophenantherene **4-17** was later formed in small quantities by using 254 nm light during the photolysis (Scheme 4-6). The desired product (**4-17**) was obtained as part of a mixture with the monobrominated and unbrominated phenanthrenes **4-23** and **4-12**. Purification was difficult, as the three compounds have very similar R_f's on silica gel, so dibromophenanthrene **4-17** has not been isolated as a pure compound.

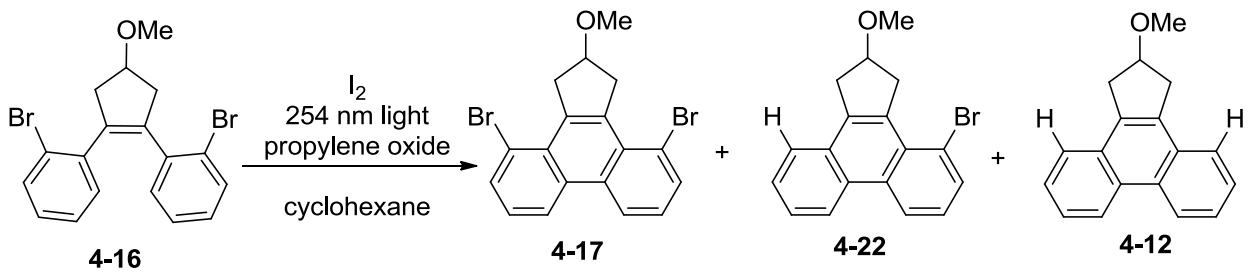

Scheme 4-6 – The synthesis of dibromophenanthrene **4-17**

In light of the literature precedent to synthesize chlorophenanthrene **4-21**,[7] we decided to approach subunit **4-1** via 2'-chloroacetophenone (Scheme 4-7). The route proceeded smoothly and the photooxidation gave the desired dichlorophenanthrene **4-27**. The main byproduct of the photocyclization was the mono-chlorophenanthrene **4-28**. The separation of the two phenanthrenes **4-27** and **4-28** by silica gel chromatography was difficult, due to the similar polarities of the two molecules. Dichlorophenthrene **4-27** was isolated in 52% yields after column chromatography, but many mixed fractions were also obtained. In order to improve the isolated yield, a recrystallization was attempted on a mixture of phenantherenes **4-27** and **4-28**, but the ratio of the two phenanthrenes did not change.

With the synthesis of dichlorophenanthrene **4-27** complete, the next step was to transform the chlorine positions into aldehydes. Unfortunately aryl chlorides are significantly less reactive than aryl bromides. Table 3-1 shows some of the conditions that were attempted and their results. The target molecule is dialdehyde (**4-29**), but vinyl groups (**4-30**) or nitriles (**4-33**) can be converted to aldehydes, so these functional groups were also targeted (Scheme 4-8). Entries 1, 2 and 4 were attempted lithium halogen exchanges, but the reactions returned only starting material. Entry 3 was a literature procedure in which aryl chlorides are subjected to sonication in the presence of DMF to give benzaldehydes[8], but the reaction mixture yielded mostly unreacted dichlorophenanthrene **4-27**. Since phenanthrene **4-27** failed to react, the reaction of

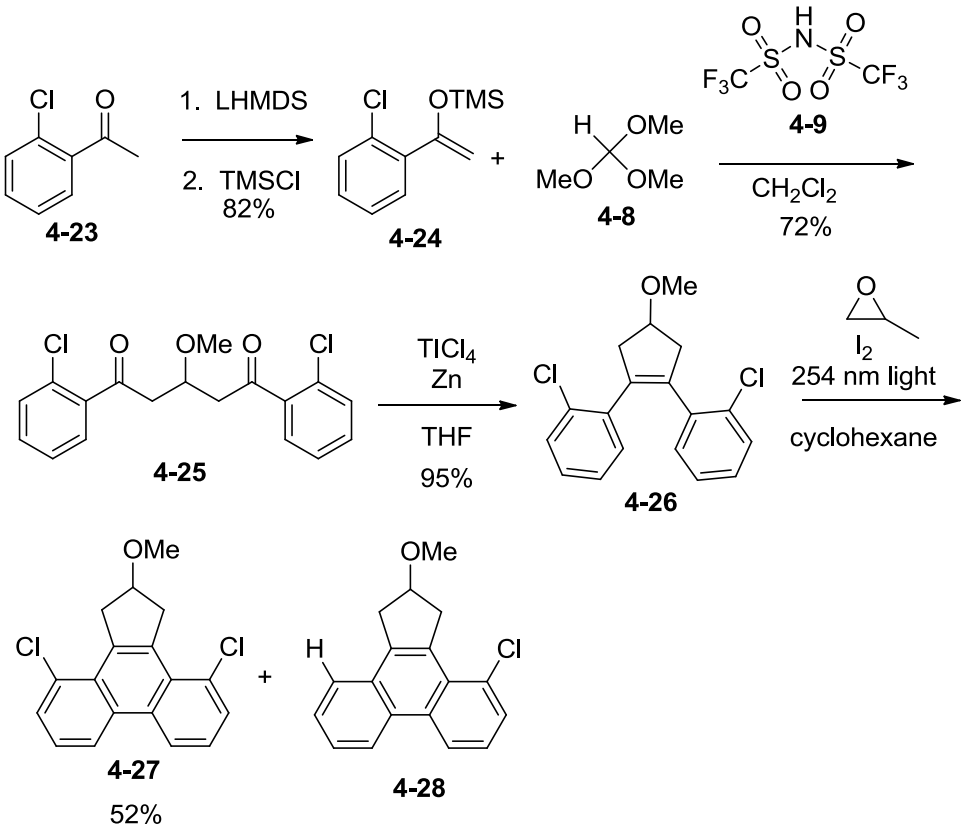

Scheme 4-7 – The synthetic route to dichlorophenanthrene **4-26**

dichlorostilbene **4-26** with t-BuLi was attempted (entry 5), but the reaction also yielded only unreacted starting material. The next reaction attempted was a Stille coupling of dichlorophenanthrene **4-27** with tributylvinyltin, in which a small amout of mono-vinyl product (**4-31)** was formed (entry 6). Entry 7 shows the attempted substitution of the chlorines with copper cyanide, which proceeded poorly even after 48 hours at 200 °C. The final entry is a Stille coupling with cesium fluoride added to activate the tin.[9]

Entry	Starting Material	Conditions	Product
1	**4-27**	n-BuLi in THF for one hour then DMF	**4-27**
2	**4-27**	n-BuLi in THF with TMEDA then DMF	**4-27**
3	**4-27**	Li^0 and DMF in THF sonicated	**4-27**
4	**4-27**	t-BuLi in THF then DMF	**4-27**
5	**4-26**	t-BuLi in THF then DMF	**4-26**
6	**4-27**	Tributyl(vinyl)tin $Pd(PPh_3)_4$ in toluene	**4-27** with a small amount of **4-31**
7	**4-27**	CuCN in NMP 200 °C for 48 hours	**4-27** with a trace of **4-34**
8	**4-27**	Tributyl(vinyl)tin $Pd(PPh_3)_4$ in dioxane with CsF	A mix of compounds with vinyl protons

Table 4-1 – Attempted functionalization of **4-26**

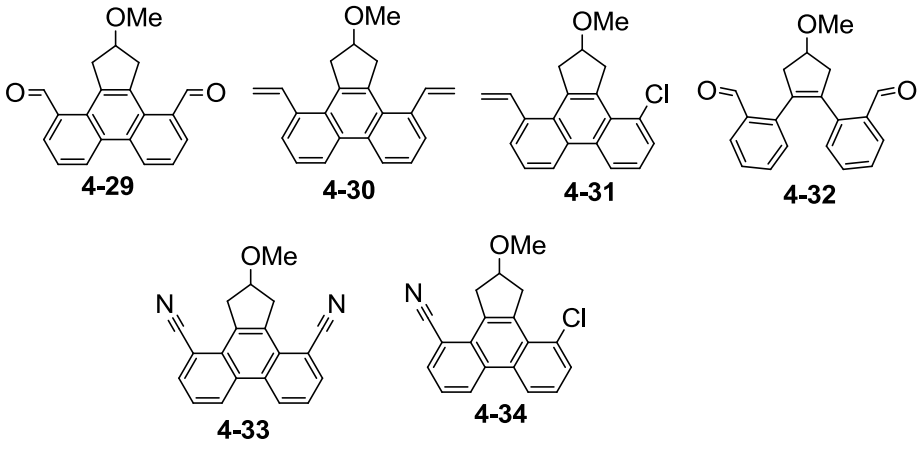

Scheme 4-8 – Possible products of the functionalization of **4-27** and **4-26**

Chobanian and coworkers reported a convenient method for converting aryl chlorides to aryl nitriles (Scheme 4-9).[10] Aryl chloride **4-35** undergoes a palladium catalyzed cyanation with zinc cyanide in the presence of Buchwald's S-Phos ligand.[11] The S-Phos ligand has also been shown to give excellent reactivity of aryl chlorides in Suzuki-Miyaura couplings.

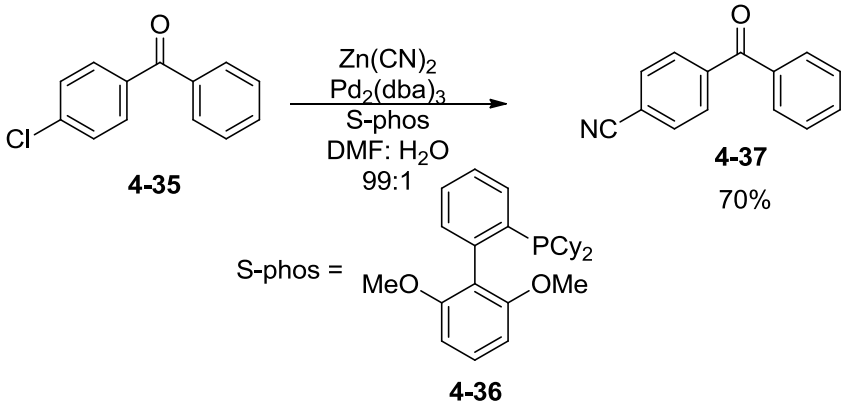

Scheme 4-9 – A palladium catalyzed cyanation with S-Phos.[10]

When these reaction conditions were applied to the functionalization of dichloride **4-27**, the desired product dinitrile **4-33** was isolated in 45% yield (Scheme 4-10). However, upon repeating the reaction, only starting material was recovered. The reaction was repeated several more times with no success. In order to rule out decomposition or degradation of the starting materials, a new bottle of $Pd_2(dba)_3$ was purchased along with new zinc cyanide. The reaction still showed no conversion. The most likely reason the reaction did not work was that the catalyst decomposed by reacting with oxygen. The palladium catalyst with the S-Phos ligand is very active in cross-couplings, but it is also very reactive towards any oxygen present. The reaction mixture shown in Scheme 4-9 was degassed after all of the components were dissolved in solvent by bubbling argon through the solvent for 15 minutes. A more rigorous method of degassing is to freeze-pump-thaw the solvent. When the solvent is degassed using the freeze-pump-thaw techniques the cyanation is reproducible in 40% yield.

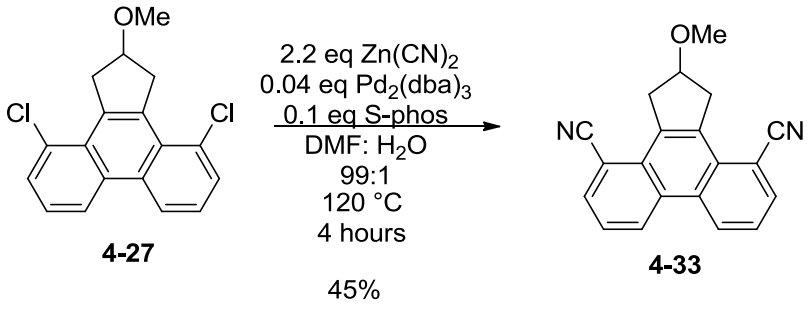

Scheme 4-10 – The palladium-catalyzed cyanation of **4-27**

4-2 Investigation of a *para*-Substituted Subunit

Because of the difficulty in functionalizing the dichlorophenanthrene **4-27**, we also investigated the use of a *para*-substituted acetophenone to synthesize a new subunit (Scheme 4-11). Phenanthrenes with substituents on the 1,8,9 and 10 positions are difficult to form due to the steric hindrance, but if the substituents are moved from the 1 and 8 positions to the 3,and 6 positions, then they should not interfere with the photocyclization.

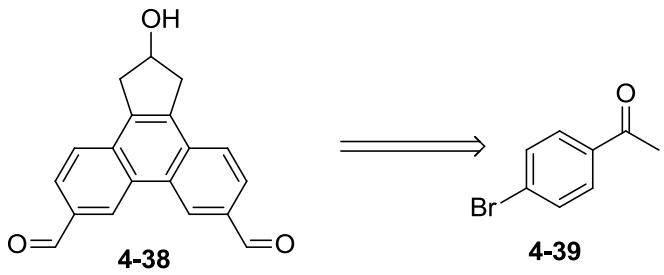

Scheme 4-11 – *para*-Substituted subunit **4-38** and *para*-bromoacetophenone **4-39**

The belt that would be made from subunit **4-38** would not be a cyclophenacene, but instead would have a slightly different connectivity (Figure 4-1). Before any synthetic work was performed, this belt (**4-40**) was examined computationally. The calculations showed that the belt **4-40** is only 4 kcal/mol higher in total energy than [12]cyclophenacene, and that the HOMO-LUMO gap is 3.0 eV (B3LYP/6-31G*), compared to 3.1 eV for [12]cyclophenacene. A much

smaller HOMO-LUMO gap might indicate that the belt is not stable. With the computations showing that belt **4-40** is comparable to [12]cyclophenacene in terms of energy and HOMO-LUMO gap, phenanthrene **4-38** was targeted synthetically.

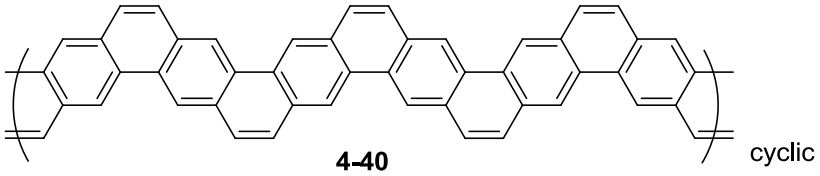

4-40

Figure 4-1 – The belt formed from a *para*-substituted acetophenone

The synthetic route to subunit **4-38** is shown in Scheme 4-12. *p*-Bromoacetophenone **4-39** is converted to its silyl enol ether **4-41** with trimethylsilyl chloride, sodium iodide and triethylamine. Compared to lithium hexamethyldisilazide, triethylamine is better for large scale reactions because triethylamine is less reactive and easier to handle on a large scale. Silyl enol ether **4-41** is purified by simply removing the volatiles from the reaction mixture and running the resulting mixture through a plug of silica gel with hexanes. The silyl enol ether is then used immediately in the next step to form diketone **4-42** in 80% yield. Hydrolysis of the silyl enol ether to acetophenone **4-39** occurs after a few hours on the benchtop. After the Mukaiyama aldol, the McMurry coupling proceeds smoothly, giving the desired cyclopentene **4-43**. The photocyclization reaction gave a 90% yield of the desired phenanthrene **4-44,** confirming the hypothesis that the substitution pattern plays a major role in the cyclization.

Lithium-halogen exchange of the bromines on **4-44**, followed by treatment with DMF gave only a 20% yield of the target dialdehyde **4-45**. There was no evidence of unreacted dibromide **4-44**, but there was evidence of unsymmetric phenanthrenes in the ^{1}H NMR. Further efforts to increase the yield by changing the stoichiometry and temperature showed no change in the yield.

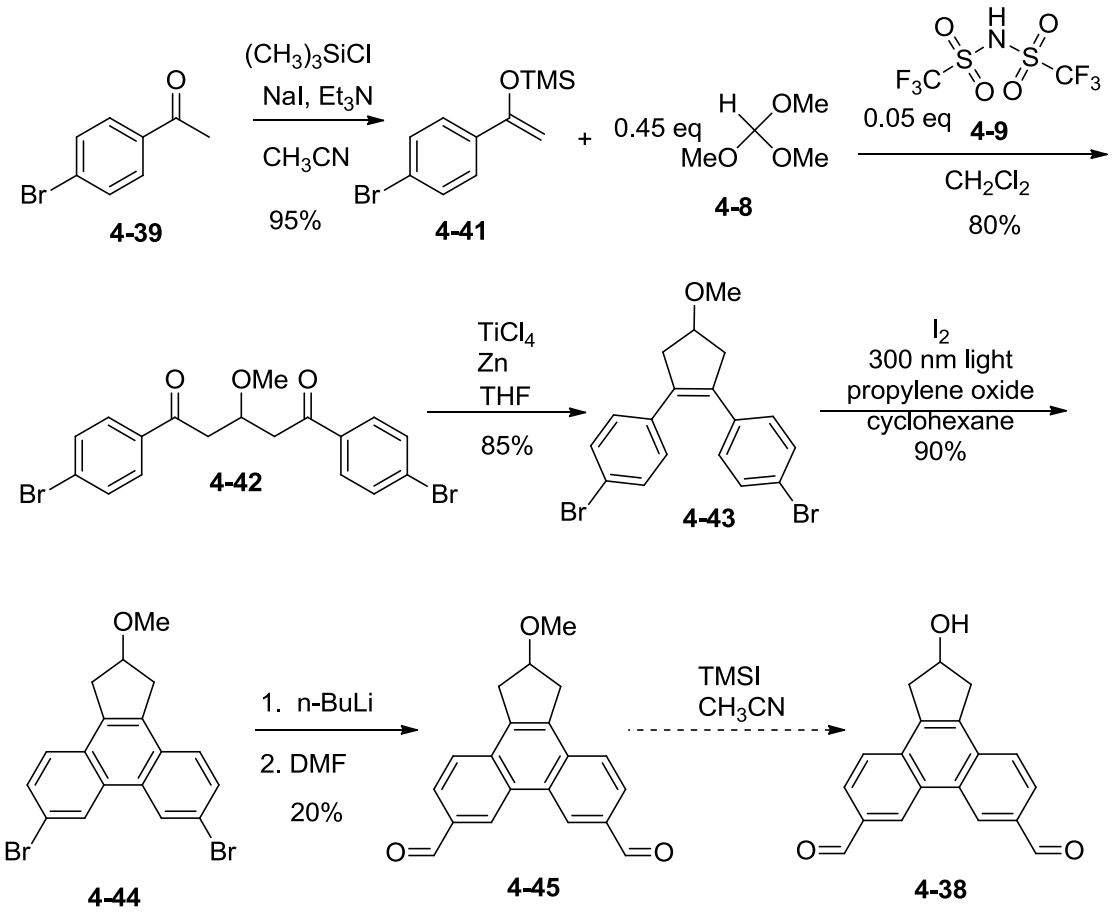

Scheme 4-12 – The synthetic route to subunit **4-38.**

4-3 Removal of the Methyl Ether

One step that had not been worked out in the model route (Scheme 4-3) was removal of the methyl ether. The alcohol is needed to attach the subunit to the scaffold precursor, making removal of the methyl group a necessary step. To model this reaction, we examined the synthetically accessible methyl ether of 2-indanol (**4-47**). Michelle Lacoske, an undergraduate in the Goroff group, conducted the initial experiments on the deprotection of the model compound **4-47**. Lacoske first prepared compound **4-47** in 76% yield by the treatment of 2-indanol (**4-46**) with potassium *tert*-butoxide, followed by methyl iodide (Scheme 4-13).

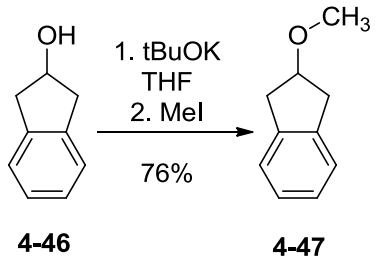

4-46 **4-47**

Scheme 4-13 – The synthesis of model compound **4-47**

The most prevalent method in the literature for the cleavage of methyl ethers is the use of BBr_3, but when Lacoske used those conditions, only a complicated mixture was obtained and no starting material or product was isolated (Scheme 4-14). Reaction with trimethylsilyl iodide[12] in dichloromethane gave some conversion of the starting material to product, but there were also unidentified byproducts formed. Changing the solvent to acetonitrile brought the isolated yield

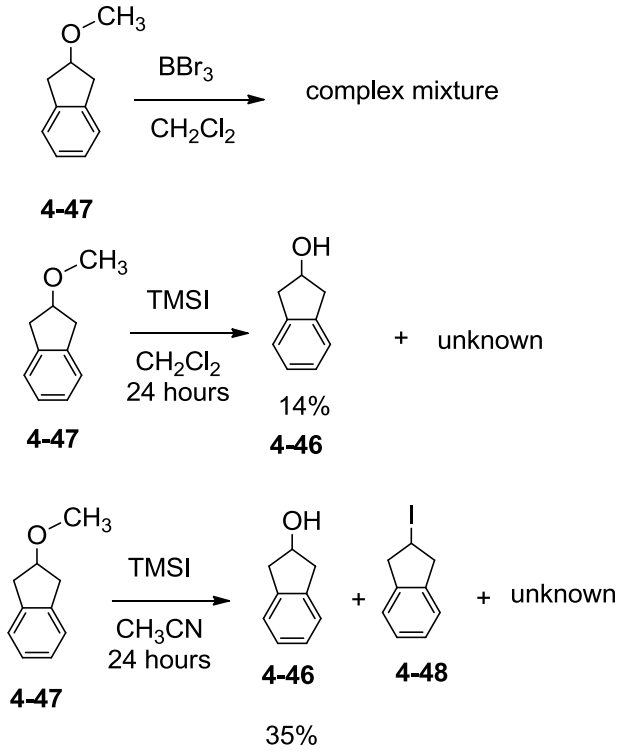

Scheme 4-14 – Some of the results in the model demethylation

up to 35%. In order to identify some of the unknown byproducts, mass spectrometry was performed on the reaction mixture, giving major peaks at 244 m/z and 344 m/z. The peak at 244 m/z was attributed to **4-48**, 2-iodoindane, but the peak at 344 m/z was not assigned.

Upon reexamination of the literature, it was found that the demethylation can be monitored by ^{1}H NMR.[12] When methyl indanyl ether **4-47** is dissolved in $CDCl_3$ and 1.3 eq. of TMSI is added, after 24 hours the peaks for **4-47** disappear and the peaks for the silyl ether **4-49** were present. During the course of the reaction, the free alcohol is not produced; instead it is trapped as the silyl ether **4-49** (Scheme 4-15). During reaction, the methyl group is converted to methyl iodide, making it possible to monitor the reaction by the disappearance of the ether methyl in the NMR and by the appearance of methyl iodide. Upon completion of the reaction, the mixture is poured into methanol, which hydrolyzes the silyl ether to give alcohol **4-46**. By ^{1}H NMR, the conversion is 100% after 24 hours, but the isolated yield is only 70%.

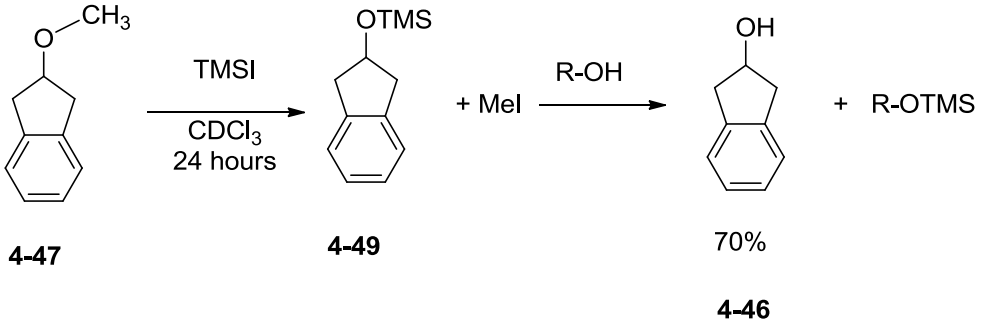

Scheme 4-15 – The basic mechanism of the demethylation with TMSI

Because TMSI gave at least a moderate yield for the model reaction, an experiment under the same conditions was carried out with dialdehyde **4-45**, in an NMR tube (Scheme 4-16). After 1 hour, a significant amount of solid had precipitated from the reaction. ^{1}H NMR showed the disappearance of the starting material peaks and formation of methyl iodide, but the intensity of the peaks corresponding to compound **4-38** was very low. It was assumed that the solid

precipitate was the silyl ether of subunit **4-38**, so the reaction was poured into methanol, but the black solid did not dissolve as expected. It seems that dialdehyde **4-45** decomposes in the presence of TMSI. This observation was unexpected, given that there were literature reports of TMSI deprotections in the presence of aldehydes.[13]

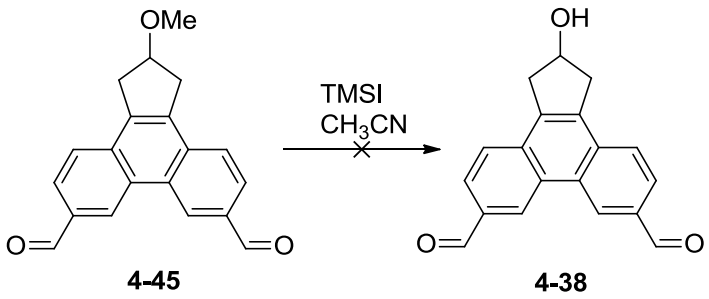

4-45 **4-38**

Scheme 4-16 – The attempted deprotection of **4-45**

Since dialdehyde **4-45** decomposed during the attempted demethylation, the deprotection reaction was attempted on stilbene **4-43**. The reaction gave only decomposition of the starting material. The previously attempted demethylation conditions, such as BBr_3 and TMSI in acetonitrile, were all performed again on stilbene **4-43**, but none showed anything promising.

The methyl ether cleavage was problematic, so the use of other functionalities was investigated. To install a benzyl group on the molecule, the corresponding silyl enol ether would have to react with tribenzyl orthoformate (**4-52**) (Scheme 4-16). Tribenzyl orthoformate is not commercially available, but has been reported in the literature.[14] The literature method for synthesis of **4-52** is simply an exchange reaction between triethyl orthoformate and benzyl alcohol in the presence of trifluoroacetic acid (TFA). To isolate tribenzylorthoformate **4-52**, the reaction mixture is first distilled under vacuum with a water aspirator to remove the TFA and toluene and then under high vacuum to remove the benzyl alcohol, leaving the desired product in the reaction flask. The reaction proceeded smoothly in 95% yield. Silyl enol ether **4-41** was

then mixed with orthoformate **4-52** in the presence of 5 mol% acid **4-9**, but no reaction occurred. This experiment was repeated several times, but it only returned starting material. No literature precedent was found for the use of tribenzyl orthoformate **4-52** in an aldol reaction, perhaps because it does not react. With the failure of tribenzylorthoformate **4-52** to react, this idea was put aside and other demethylation conditions were investigated.

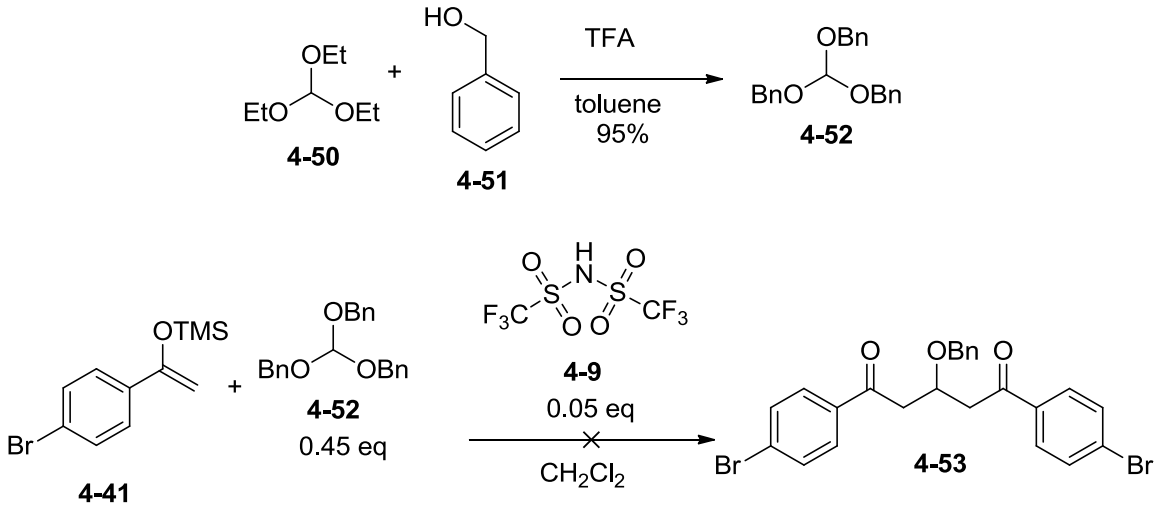

Scheme 4-17 – Synthesis of tribenzyl orthoformate and its attempted reaction

Ozaki and coworkers have described another set of demethylation conditions (Scheme 4-18), involving a large excess of aluminum trichloride and tetrabutyl ammonium iodide (TBAI).[15] Using 20 equivalents of $AlCl_3$ and 20 equivalents of TBAI, demethylation of **4-43** did occur, although the reaction did not go to completion. Longer reaction times showed consumption of the starting material, but did not change the yield. One reason for the low yield may be the difficulty of removing TBAI from the desired alcohol **4-54**. TBAI is not soluble in water, so it stays with the product in the organic layer during the workup. The only effective way found to remove the TBAI and purify the reaction mixture was to subject the products of the reaction to

sonication in ethyl acetate and filter out the solid. The solid is TBAI, and the alcohol **4-54** is in the filtrate.

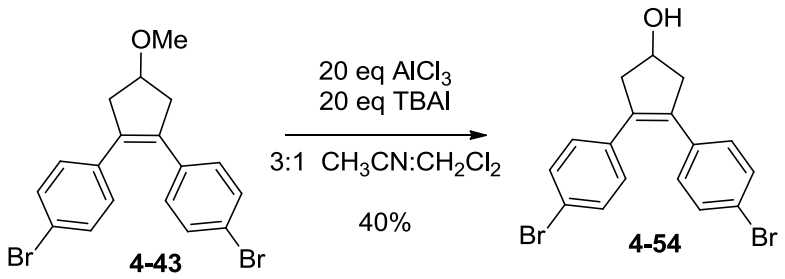

Scheme 4-18 – Formation of **4-54** with $AlCl_3$ and TBAI[12]

A variation of the reaction with $AlCl_3$ and TBAI has been reported, using sodium iodide instead of TBAI.[16] Utilizing this procedure did not change the yield, but isolation of the product was greatly simplified, since the excess sodium iodide dissolves in water during workup. However, a careful analysis of the product mixture showed that 42% of the material had lost the alcohol group, forming cyclopentene **4-55** (Scheme 4-19). This sort of reduction reaction has been reported for substrates with electron withdrawing groups, such as ketones, alpha to the methoxy ether,[17] but we have not found any references for an aliphatic alcohol such as **4-54**.

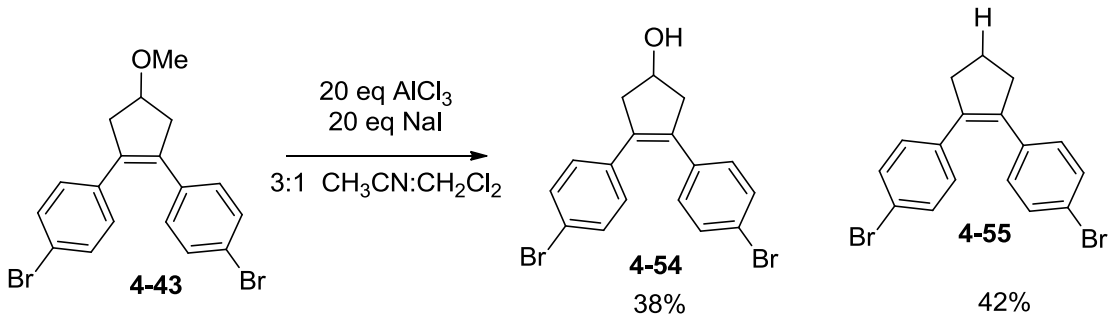

Scheme 4-19 – The new demethylation reaction and the unexpected byproduct

With the deprotection reaction working in moderate yield, the route to the *p*-bromo-substituted subunit **4-38** was continued. Alcohol **4-54** was subjected to the photocyclization

reaction, but solubility problems for the product of this reaction hindered characterization and further analysis (Scheme 4-20). All efforts to get the compound into solution for NMR analysis have been unsuccessful.

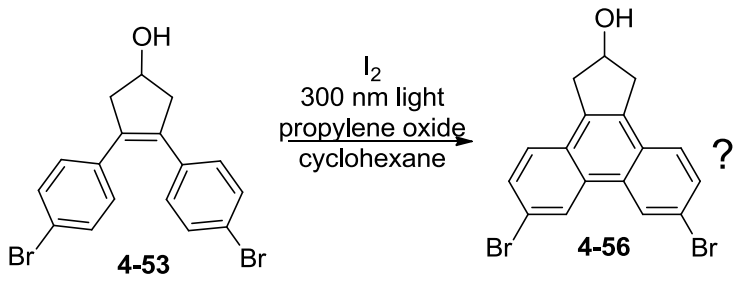

Scheme 4-20 – Photooxidation of alcohol **4-53** and its possible product

With this roadblock of poor solubility in the route to the *para* subunit **4-38,** the route to the *ortho* subunit **4-1** was continued. The demethylation step was performed on stilbene **4-25**, proceeding in excellent yield, with no evidence of loss of the alcohol (Scheme 4-21). It is not clear why the reaction proceeds so much better with the *ortho* substituted stilbene. Photocyclization gave a mix of the dichloro and mono chlorophenantherenes, **4-58** and **4-59**, respectively. The two compounds could be separated by column chromatography, using 5 % ethyl acetate in toluene as the solvent.

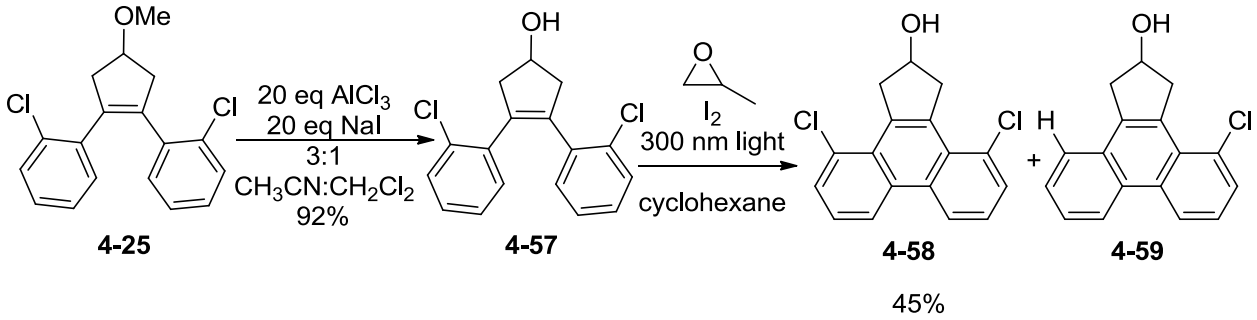

Scheme 4-21 – Demethylation and photocyclization of methyl cyclopentyl ether **4-25**

With the isolation of dichlorophenanthrene **4-58** completed, only two steps remained on the route to subunit **4-1**. The next step was cyanation of the chlorides, which had previously

been worked out for compound **4-47**. The same reaction conditions were used, i.e., palladium with the S-Phos ligand and zinc cyanide (Scheme 4-22).[10] The reaction returned a solid that was only sparingly soluble in organic solvents. Characterization of this compound by NMR was not possible, as no peaks were seen. Thinking that the reaction conditions might be the problem, an alternative procedure was found using 1,10-bis(diphenylphosphino)ferrocene (dppf) as a ligand for the palladium.[18] The new procedure does not seem as oxygen-sensitive as the reaction using S-Phos, so freeze-pump-thaw cycles were not used. Unfortunately this reaction gave the same results, an insoluble white solid. The solid dissolves in boiling toluene, but then precipitates upon cooling. The change in solubility of the product has led to the hypothesis that the desired compound has been formed, but it is not very soluble.

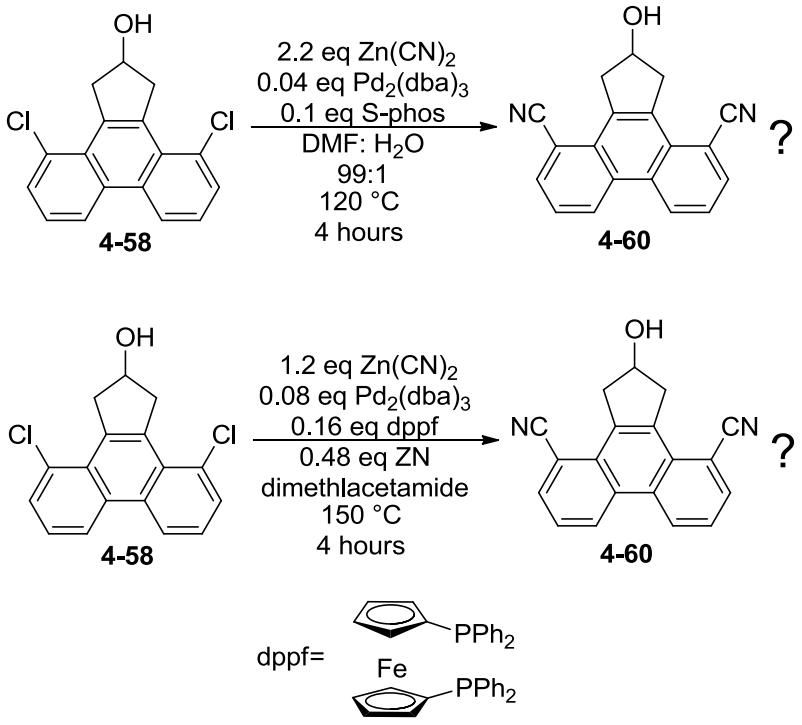

Scheme 4-22 – The attempted cyantions of dichlorophenanthrene **4-58**

4-4 Future Work

One possible way to fix to the solubility problem is to protect the alcohol group as something that is relatively simple to cleave, but that adds solubility.. The free alcohol on dichlorophenanthrene **4-58** can be protected and then the chlorines can be converted to aldehydes in two steps.(Scheme 4-23). Removal of the protecting group will give the target molecule **4-1**. Hopefully subunit **4-1** is more soluble then the dinitrile phenanthrene **4-60**.

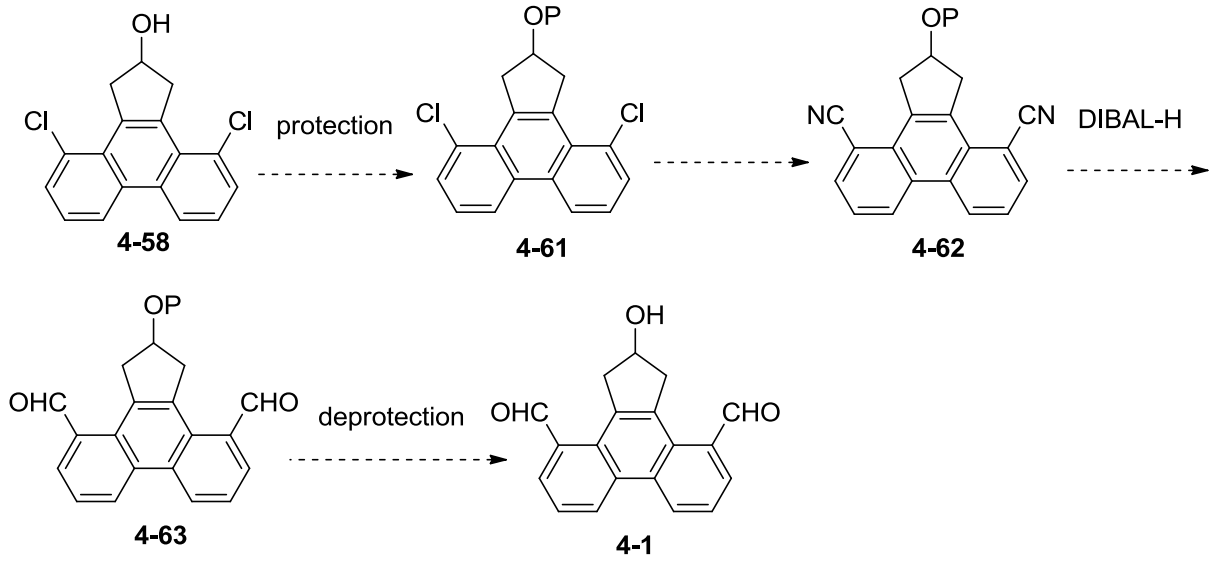

Scheme 4-23 – The use of protecting groups to add solubility in the route to **4-1**

4-5 Experimental

Trimethyl[(1-phenylethenyl)oxy]silane **4-7**

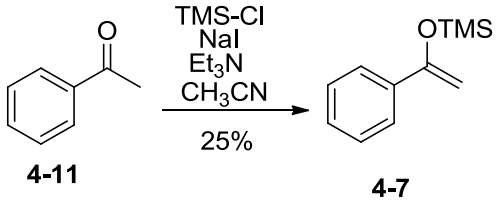

Acetophenone (2.00 g, 17.0 mmol), chlorotrimethylsilane (2.0 g, 18 mmol), and triethylamine (1.85 g, 18 mmol) were placed in a round bottom flask with 40 mL acetonitrile. Sodium iodide

(2.75 g, 18 mmol) in 20 mL acetonitrile was added dropwise, and the reaction mixture was stirred for 1 h. The reaction mixture was diluted with hexanes and washed with water. The organic layer was dried over $MgSO_4$, filtered and concentrated *in vacuo*. The resulting material was purified by column chromatography (SiO_2, hexanes) to give silyl enol ether **4-7** (0.432 g, 25% yield) as a colorless liquid. ^{1}H NMR (300 MHz, $CDCl_3$) δ 7.6 (m, 2H), 7.32 (m, 3 H), 4.92 (d, J=1.8 Hz, 1 H), 4.43 (d, *J*=1.8 Hz, 1 H), 0.28 (s, 9 H). ^{1}H NMR matches the reported spectrum.[19]

3-Methoxy-1,5-diphenylpentane-1,5-dione **4-10**

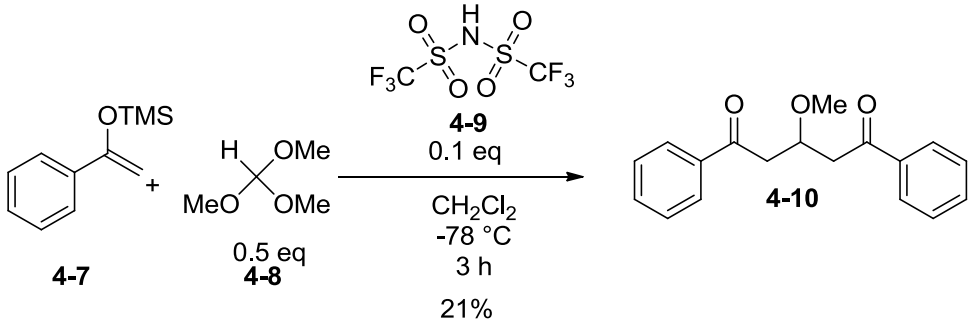

Silyl enol ether **4-7** (2.6 g, 13.5 mmol) was dissolved in 10 mL dichloromethane in a 50 mL round bottomed flask. Trimethyl orthoformate (0.72 g, 6.7 mmol,) was added. The reaction flask was cooled to -78 °C and bistrifluoromethanesulfonimide (0.095 g, 0.34 mmol) was added in dichloromethane (1 mL). The reaction mixture was stirred at -78 °C for three hours. The reaction mixture was then poured into saturated $NaHCO_3$ (aq). The mixture was extracted with ether (3 x 50 mL), the organic layers were dried over $MgSO_4$ and filtered, and the solvent was evaporated *in vacuo*. The reaction mixture was purified by column chromatography (SiO_2, 9:1 hexanes:ethyl acetate) to give **4-10** (0.406 g, 21% yield) as a colorless oil. ^{1}H NMR (300 MHz, $CDCl_3$) δ 8.06 (m, 2 H) 7.64 (m, 1 H), 7.54 (m, 2 H) 4.58 (m, 1 H) 3. 45 (s, 3H), 3.40 (m, 4H). ^{13}C NMR (100 MHz, $CDCl_3$) δ 198.2, 137.0, 133.2,128.6, 128.2, 74.3, 57.6, 43.3.

4-Methyoxy-1,2-diphenylcyclopent-1-ene **4-11**

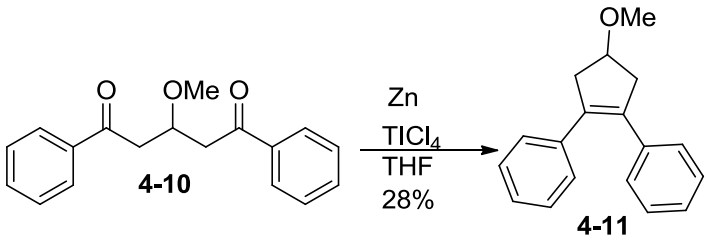

In an oven-dried flask, dry THF (3 mL) was added to zinc dust (0.090 g, 1.42 mmol). The flask was cooled in an ice bath, and titanium tetrachloride (0.135 g, 0.71 mmol) was added dropwise. The solution was stirred for 15 min and became blue. A solution of **4-10** (0.060 g, 0.21 mmol) in 3 mL THF was added to the reaction mixture. The reaction mixture was then heated to reflux for three h. Then, 10 mL water was added and the mixture was extracted with ether (3 x 35 mL). The organic layers were combined, dried over $MgSO_4$, filtered and the solvent was removed *in vacuo*. The resulting brown oil was purified by column chromatography (SiO_2, 9:1 hexanes:ethyl acetate) to give **4-11** (0.015 g, 28 % yield) as a colorless oil. ^{1}H NMR (300 MHz, $CDCl_3$) δ 7.21 (m, 10 H), 4.24 (m, 1 H), 3.41 (s, 3 H), 3.19 (m, 2 H), 2.95 (m, 2H). ^{13}C NMR (100 MHz, $CDCl_3$) δ 137.7, 134.8, 128.2, 128.1, 126.8, 78.6, 56.4, 44.9.

9,10-(2-Methoxycyclopentyl)phenanthrene **4-12**

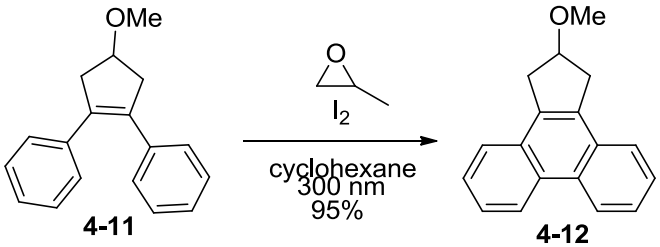

In a quartz photochemical reaction vessel were placed **4-11** (0.015 g, 0.06 mmol) and iodine (0.015 g, 0.06 mmol). Then 100 mL cyclohexane was added and the purple solution was degassed by bubbling Ar through the solution for 15 min. Propylene oxide (0.8 mL, 12 mmol) was added, and the vessel was placed in a Rayonet photoreactor with 12 RPR 300 lamps, fitted with a water cooler, and was irradiated

for 1 h. The solvent was removed *in vacuo* to give **4-12** (0.013 g, 95%) as a brown solid. ^{1}H NMR (300 MHz, $CDCl_3$) δ 8.68-8.74 (m, 2H), 7.82-7.88 (m, 2H), 7.60-7.66 (m, 4H), 4.52-4.60 (m, 1H), 3.61 (dd, *J*=16, 7 Hz, 2H), 3.51 (s, 3H), 3.40 (dd, *J*=16, 4 Hz, 2H)

{[1-(2-Bromophenyl)ethenyl]oxy}trimethylsilane **4-14**

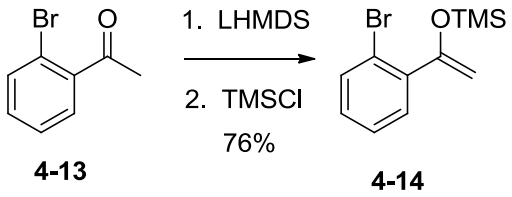

4-13 **4-14**

In a 100-mL oven-dried flask, lithium hexamethyl disilazide (23 mL, 10% solution in THF/ethylbenzene) was added to 25 mL dry THF and then the solution was cooled to -78 °C. Acetophenone **4-13** (2.7 mL, 21.1 mmol) was added dropwise to the solution and was stirred for 1 h. Chlorotrimethylsilane (3.0 mL, 23.2 mmol) was added, and the solution was stirred for an additional 1 h. The solvent was removed *in vacuo*, and the resulting slurry was purified by a plug of silica gel with hexane as the eluent. The solvent was removed *in vacuo*, and the resulting yellow liquid was vacuum distilled to give **4-14** (4.05 g, 76%) as a colorless liquid. ^{1}H NMR (300 MHz, $CDCl_3$) δ 7.56 (dd, *J*= 7.8 ,1.5 Hz 1H), 7.39 (dd, *J*=7.8, 1.5 Hz, 1H), 7.24-7.30 (m, 1H), 7.11-7.14 (m, 1H), 4.60 (d, *J*=1.2 Hz, 1H), 4.53 (d, *J*=1.5 Hz, 1H), 0.22 (s, 9H) ^{1}H NMR matches the reported spectrum.[20]

1,5-Bis(2-bromophenyl)-3-methoxypentane-1,5-dione **4-15**

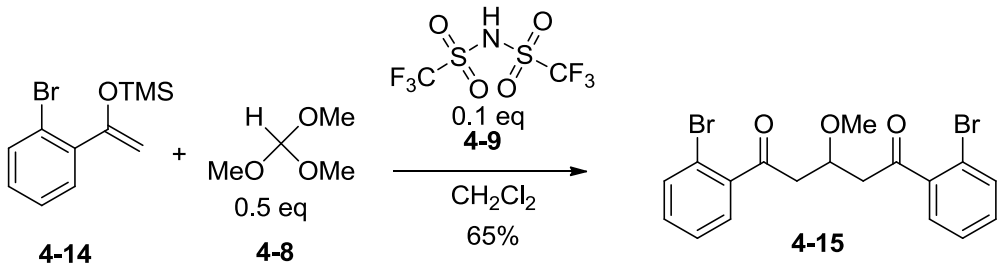

4-14 **4-8** **4-15**

Silyl enol ether **4-14** (1.0 g, 3.7 mmol) was dissolved in 5 mL dichloromethane in a 25 mL round bottom flask. Trimethyl orthoformate (0.18 mL, 1.7 mmol) was added. The reaction flask was cooled to -78 °C, and a solution of bistrifluoromethanesulfonimide (0.026 g, 0.09 mmol) in 3 mL dichloromethane was added. The reaction mixture was stirred at -78 °C for 3 h. The reaction mixture was then poured into a saturated $NaHCO_3$ (aq) solution. The mixture was then extracted with ether (3 x 25 mL). The organic layers were combined, dried over $MgSO_4$, filtered and the solvent was evaporated *in vacuo*. The resulting brown oil was purified by column chromatography (SiO_2, 9:1 hexanes:ethyl acetate) to give **4-15** (0.437 g, 61% yield) as a colorless oil. ^{1}H NMR (300 MHz, $CDCl_3$) δ 7.47-7.48 (m, 1H), 7.45 (m, 1H),7.03-7.08 (m, 4H), 6.96-7.02 (m, 2H), 4.31-4.39 (m, 1H), 3.42 (s, 3H), 3.18 (dd, *J*=15, 7 Hz, 2H), 2.95 (dd, *J*=15, 4 Hz). ^{13}C NMR (100 MHz, $CDCl_3$) δ 201.8, 141.5, 133.7, 131.7, 128.7, 127.5, 118.7, 74.0, 57.6, 47.0.

2,2'-(4-Methoxycyclopent-1-ene-1,2-diyl)bis(bromobenzene) **4-16**

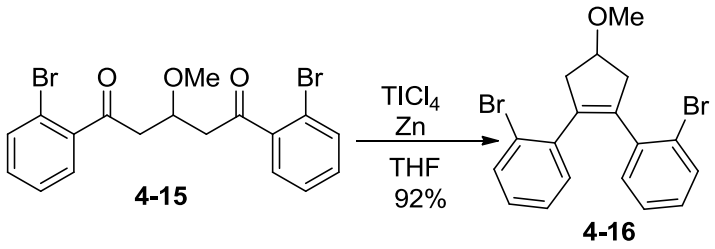

In an oven dried flask, 10 mL dry THF was added to zinc dust (0.289 g, 4.6 mmol). The flask was cooled in an ice bath and titanium tetrachloride (0.25 mL, 2.3 mmol) was added dropwise. The solution was stirred for 30 min, and then a solution of **4-15** (0.245 g, 0.57 mmol) in 8 mL THF was added to the reaction mixture via cannula. The reaction mixture was heated to reflux for 2 h. Then 20 mL water was added, and the mixture was extracted with ether (3 x 50 mL). The organic layers were combined, dried over $MgSO_4$, filtered and the solvent was removed *in vacuo*. The reaction mixture was purified with column chromatography (SiO_2, 9:1 hexanes:ethyl

acetate) to give **4-16** (0.208 g, 92 % yield). ^{1}H NMR (300 MHz, $CDCl_3$) δ 7.46 (m, 2H), 7.0-7.1 (m, 6H), 4.35 (m, 1H), 3.42 (s, 3 H), 3.17 (m, 2 H), 2.95 (m, 2H). ^{13}C NMR (75 MHz, $CDCl_3$) δ 138.7, 132.4, 130.7, 128.5, 127.0, 122.8, 79.9, 56.5, 43.3.

4,11-Dibromo-2-methoxy-2,3-dihydro-1H-cyclopenta[l]phenanthrene (**4-17)**

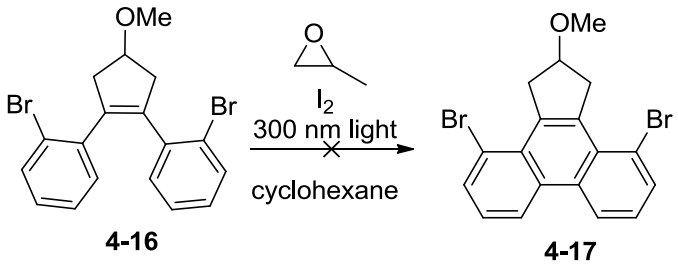

4-16 **4-17**

In a quartz photochemical reaction vessel was placed **4-16** (0.042 g, 0.11 mmol) and iodine (0.027 g, 0.11 mmol). Cyclohexane (200 mL) was added and the purple solution was degassed by bubbling argon through the solution for 15 min. Propylene oxide (1.5 mL, 21 mmol) was added and the vessel was placed in a rayonet photoreactor with 12 RPR 300 lamps, fitted with a water cooler and was irradiated for 24 hours. The purple color was still present so the solution was washed with 10% sodium thiosulfate, dried over $MgSO_4$ and the solvent was removed *in vacuo* to give 0.032 g of **4-16** as a brown oil. ^{1}H NMR showed only the starting material.

((1-(2-Chlorophenyl)vinyl)oxy)trimethylsilane **4-24**

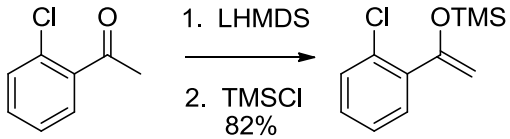

4-23 **4-24**

In a 100 mL oven dried flask, lithium hexamethyldisilazane (36 mL, 10% in THF/ethylbenzene was added to 30 mL dry THF and then the solution was cooled to -78 °C. Acetophenone **4-23** (4.2 mL, 32.3 mmol) was added dropwise to the solution and was stirred for one h. Chlorotrimethylsilane (4.6 mL, 35.6

mmol) was added and the solution was stirred for an additional h. The solvent was removed *in vacuo* and the resulting slurry was purified by a plug of silica gel with hexane as the eluent. The solvent was removed *in vacuo* to give **4-24** (6.05 g, 82% yield) as a colorless liquid. ^{1}H NMR (300 MHz, $CDCl_3$) δ 7.44-7.48 (m, 1H), 7.36-7.38 (m, 1H), 7.19-7.25 (m, 2H), 4.68 (d, *J*=1.8 Hz, 1H), 4.64 (d, *J*=1.5 Hz, 1H), 0.26 (s, 9H). ^{1}H matches the reported spectra.[21]

1,5-Bis(2-chlorophenyl)-3-methoxypentane-1,5-dione **4-25**

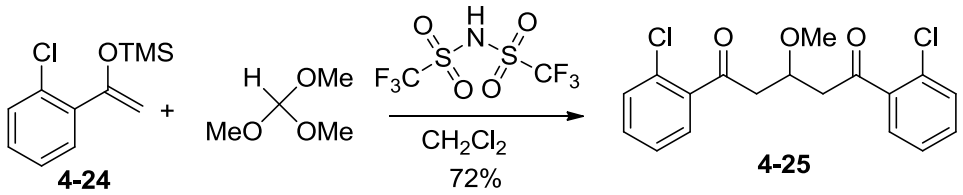

4-24 **4-25**

Silyl enol ether **4-24** (2.3 g, 10.2 mmol) was dissolved in 10 mL dichloromethane in a 25 mL flask. Trimethyl orthoformate (0.5 mL, 4.6 mmol) was added. The reaction flask was cooled to -78 °C and a solution of bistrifluoromethanesulfonimide (0.071 g, 0.09 mmol) in 3 mL dichloromethane was added. The reaction mixture was stirred at -78 °C for three h. The reaction mixture was then poured into 50 mL $NaCO_3$ (aq, sat.). The mixture was extracted with ether (3 x 25 mL), the organic layers were dried over $MgSO_4$, filtered and the solvent was removed *in vacuo*. The reaction mixture was purified by column chromatography (SiO_2, 9:1 hexanes:ethyl acetate) to give **4-25** (0.43 g, 72% yield) as a yellow oil. ^{1}H NMR (400 MHz, $CDCl_3$) δ 7.47-7.49 (m, 2H), 7.31-7.39 (m, 6H), 4.32 (m, 1H), 3.16-3.32 (m, 7H), ^{13}C NMR (100 MHz, $CDCl_3$) δ 200.9, 139.1, 131.8, 130.8, 130.7, 129.0, 126.9, 74.0, 47.2. HRMS (EI) calcd. for $C_{18}H_{16}O_3Cl_2$ 350.04766 found 350.04741.

2,2'-(4-Methoxycyclopent-1-ene-1,2-diyl)bis(chlorobenzene) **4-26**

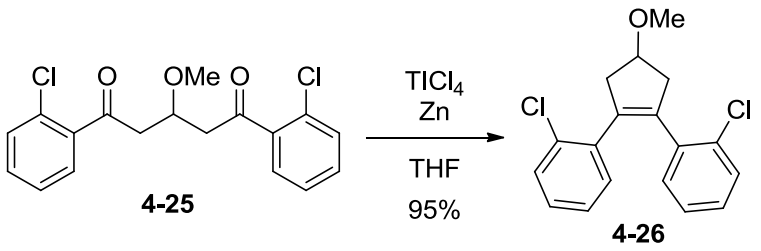

In an oven-dried flask, 45 mL dry THF was added to zinc dust (2.80 g, 43 mmol). The flask was cooled in an ice bath and titanium tetrachloride (2.4 mL, 21.5 mmol) was added dropwise. The solution was stirred for 30 min and became blue. A solution of **4-25** (1.88 g, 5.4 mmol) in 8 mL THF was added to the reaction mixture via cannula. The reaction mixture was then heated to reflux for 2 h. Then 20 mL water was added, and the mixture was extracted with ether (3 x 50 mL). The organic layers were combined, dried over $MgSO_4$, filtered and the solvent was removed *in vacuo*. The reaction mixture was purified by column chromatography (SiO_2, 9:1 hexanes:ethyl acetate) to give **4-26** (1.60 g, 92 % yield). ^{1}H NMR (300 MHz, $CDCl_3$) δ 7.28 (d, *J*=8 Hz, 2H), 7.0-7.1 (m, 4H), 4.35 (m, 1H), 3.42 (s, 3 H), 3.18 (m, 2 H), 2.95 (m, 2H) ^{13}C NMR (75 MHz, $CDCl_3$) δ 137.2, 136.7, 133.0, 130.7, 129.3, 126.4, 79.9, 56.4, 43.3. HRMS (EI) calcd. for $C_{18}H_{16}OCl_2$ 318.05783 found 318.05845.

4,11-Dichloro-2-methoxy-2,3-dihydro-1H-cyclopenta[l]phenanthrene **4-27**

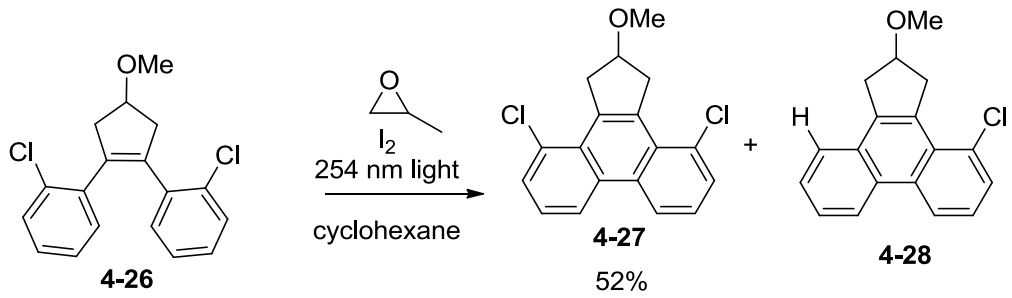

In a quartz photochemical reaction vessel were placed **4-26** (0.040 g, 0.13 mmol) and iodine (0.032 g, 0.13 mmol). Then 100 mL of cyclohexane was added, and the purple solution was degassed by bubbling

Ar through the solution for 15 min. Propylene oxide (1.8 mL, 25 mmol) was added, and the vessel was placed in a Rayonet photoreactor with 12 RPR 300 lamps, fitted with a water cooler and irradiated. After 24 h, the purple color was no longer present, so the solvent was removed *in vacuo*, and the brown oil was purified by column chromatography (SiO_2, 19:1 hexanes:ethyl acetate) to give **4-27** (0.021 g, 52%) as a white solid. ^{1}H NMR (300 MHz, $CDCl_3$) δ 8.57 (dd, *J*=5.4, 1.8 Hz, 2H), 7.65 (dd, *J*=8, 1.2 Hz. 2H), 7.46 (t, *J*=8 Hz, 2H), 4.27 (m, 1H), 3.95 (m, 4H), 3.24 (s, 3H). ^{13}C NMR (100 MHz, $CDCl_3$) δ 42.7, 56.3, 80.2, 122.6, 126.0, 128.3, 129.9, 131.6, 132.9, 136.2. 0.005 grams of pure **4-28** was also isolated: ^{1}H NMR (300 MHz, $CDCl_3$) δ 8.62-8.66 (m, 2H), 7.83-7.87 (m, 1H), 7.60-7.67 (m, 3H), 7.457 (t, *J*=7.8 Hz, 1H) ^{13}C NMR (100 MHz, $CDCl_3$) δ 37.9, 44.0, 56.5, 80.4, 122.3, 123.4, 124.8, 125.5, 126.3, 127.3, 128.2, 129.2, 129.6, 130.1, 131.8, 133.1, 133.2, 137.7.

2-Methoxy-2,3-dihydro-1H-cyclopenta[l]phenanthrene-4,11-dicarbonitrile **4-33**.

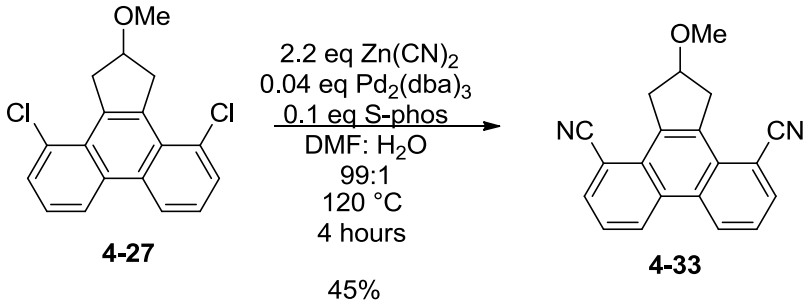

In a 5 mL flask with a stir bar were placed dichloride **4-27** (0.092 grams, 0.29 mmol), zinc cyanide (0.075 grams, 0.64 mmol), $Pd_2(dba)_3$ (0.027 grams, .029 mmol) and 2-dicyclohexylphosphino-2′,6′-dimethoxybiphenyl (0.024 grams, 0.058 mmol). Then 1.0 mL DMF was added along with 1 μL of water, and the solution was degassed with 3 freeze-pump-thaw cycles. The flask was put in an oil bath at 120 °C for 2 h. The reaction mixture was then cooled to room temperature and diluted with 25 mL ethyl acetate. The solution was then washed with NaOH (aq. 1 M). The layers were separated and the organic layer was dried over $MgSO_4$,

filtered and dried *in vacuo*. The resulting oil was then purified by column chromatrography (SiO_2, 10-50% ethyl acetate in hexanes) to give **4-33** (0.032 g, 45% yield) as a white powder. ^{1}H NMR (400 MHz $CDCl_3$) δ 8.86 (d *J*=8 Hz, 2 H) 8.05 (d *J*=7.2 Hz, 2H), 7.70 (t, *J*=8 Hz, 2 H), 4.469 (m, 1H), 4.1-3.9 (m, 4H) 3.48 (s, 3H) ^{13}C NMR (100 MHz $CDCl_{3\delta}$) 137.6, 136.0, 130.6, 130.0, 128.2, 125.8, 120.1, 108.8, 80.1, 56.6, 40.8. IR 2222 cm^{-1} (S)

((1-(4-Bromophenyl)vinyl)oxy)trimethylsilane **4-41**

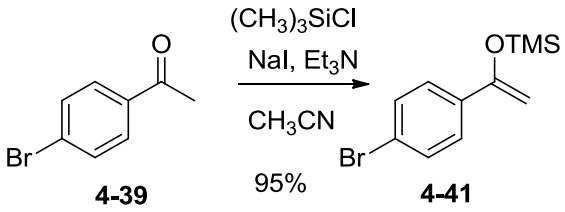

In a 10 mL flask fitted with a stir bar, 4'-bromoacetophenone (**4-39**, 3.00 g, 15.1 mmol) was dissolved in 30 mL acetonitrile. Triethylamine (2.87 mL, 22.6 mmol) was added, along with chlorotrimethylsilane (4.2 mL, 30.2 mmol). Sodium iodide (3.39 g, 22.6 mmol) was then dissolved in 10 mL acetonitrile and added via cannula to the reaction mixture. The mixture was stirred for 2 h, and then the solvent was removed *in vacuo*. The resulting brown slurry was purified with a plug of silica gel with hexanes as the eluent to give **4-41** (3.73 g, 95% yield) as a colorless liquid. ^{1}H NMR (400 MHz, $CDCl_3$) δ 7.46 (s, 4H), 4.89 (d, *J*=2Hz, 1H), 4.44 (d, *J*=2Hz, 1H), 0.27 (s, 9H). ^{1}H NMR matches the reported spectra.[22]

1,5-Bis(4-bromophenyl)-3-methoxypentane-1,5-dione **4-42**

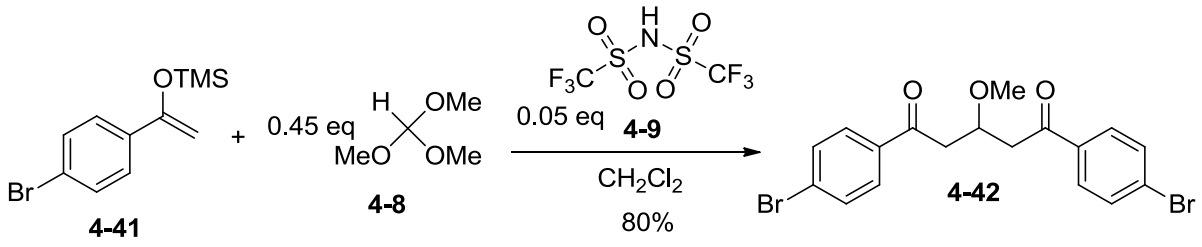

Silyl enol ether **4-41** (2.72 g, 10 mmol) was dissolved in 30 mL dichloromethane in a 50 mL round bottom flask. Trimethyl orthoformate (0.478 g, 4.5 mmol) was added. The reaction flask was cooled to -78 °C and a solution of bistrifluoromethanesulfonimide (0.141 g, 0.5 mmol) in 5 mL dichloromethane was added. The reaction mixture was stirred at -78 °C for 3 h, then poured into 50 mL $NaHCO_3$ (aq., sat.). The mixture was extracted with ether (3 x 50 mL), the organic layers were dried over $MgSO_4$, filtered and the solvent was evaporated *in vacuo*. The reaction mixture was purified by column chromatography (SiO_2, 9:1 hexanes:ethyl acetate) to give **4-42** (1.32 g, 80% yield) as a yellow oil. ^{1}H NMR (300 MHz, $CDCl_3$) δ 7.85 (d, *J*=9 Hz, 4H), 7.61 (d, *J*=9Hz, 4H), 4.41 (m, 1H), 3.35 (s, 3H), 3.1-3.3(m, 4H) ^{13}C NMR (100 MHz, $CDCl_3$) δ 197.1, 135.6, 131.8, 129.6, 128.4, 74.1, 57.6, 43.0. HRMS (EI) calcd. for $C_{18}H_{16}O_3Br_2$ 437.94665 found 437.94758.

4,4'-(4-Methoxycyclopent-1-ene-1,2-diyl)bis(bromobenzene) **4-43**

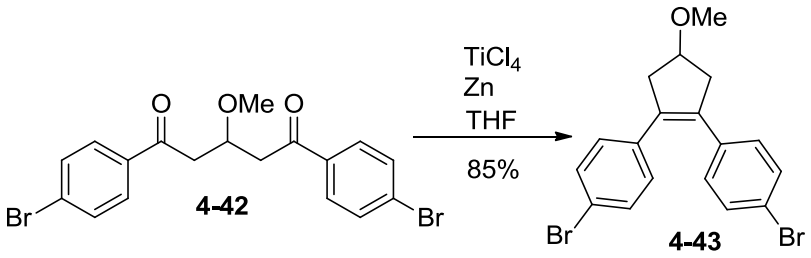

To an oven-dried 2-necked flask under Ar, zinc dust (2.20 g, 33.8 mmol) was added. Then 30 mL dry THF was injected into the flask, and the mixture was stirred. The flask was cooled in an ice water bath and $TiCl_4$ (1.9 mL, 3.22g, 17 mmol) was added dropwise. A yellow cloud formed, and the solution turned dark blue. The mixture was stirred for 15 min, then diketone **4-42** (1.85 g, 4.2mmol) in 5 mL dry THF was added dropwise. After the addition, the solution was heated to reflux for 3 h. Then, 20 mL water was added and the solution bubbled. The reaction mixture was extracted with ethyl acetate (3 x 50 mL), the organic layers were combined, dried

over MgSO4, and filtered, and the solvent was removed *in vacuo* to give **4-43** (1.16 grams, 85%) as a colorless oil. ^{1}H NMR (400 MHz, $CDCl_3$)δ 7.32-7.36(m, 4H), 7.01-7.05(m, 4H), 4.19(m, 1H), 3.38 (s, 3H), 3.11 (dd, *J*= 16, 7Hz, 2H), 2.90 (dd, *J*=16, 3.2 Hz, 2H) ^{13}C NMR ($CDCl_3$) δ 136.2, 134.5, 131.4, 129.8, 120.9, 78.3, 56.4, 44.8.

6,9-Dibromo-2-methoxy-2,3-dihydro-1H-cyclopenta[l]phenanthrene **4-44**

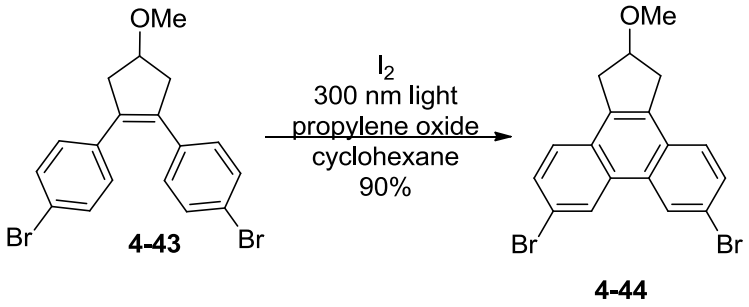

Stilbene **4-43** (0.116 g, 0.32 mmol) was dissolved in 200 mL hexanes in a quartz photochemical reaction vessel. Iodine (0.08 g, 0.32 mmol) was added, and Ar was bubbled through the solution for 30 min. Propylene oxide (4.4 mL, 63.4 mmol) was added and the solution was put in the Rayonet and irradiated with 300-nm light. After the disappearance of the iodine color (~48 h) the solution was transferred to a flask and the solvent was removed *in vacuo*. The resulting white solid was purified by column chromatography (SiO_2, 19:1 hexanes:ethyl acetate) to give **4-44** (0.103 g, 90% yield) as a white solid.^{1}H NMR (400 MHz, $CDCl_3$) δ 8.61(d, *J*=2 Hz, 2H), 7.68(dd, *J*= 8, 2 Hz, 2H), 7.62 (d, *J*= 8 Hz, 2H), 4.52 (m, 1H), 3.46-3.52 (m, 2H) 3.49 (s, 3H), 3.31 (dd, *J*= 3.6, 16 Hz, 2H). ^{13}C NMR ($CDCl_3$) δ 134.9, 130.6, 130.3, 128.5, 126.4, 125.9, 120.2, 80.6, 56.7, 38.6. HRMS (EI) calcd. for $C_{18}H_{14}OBr_2$ 403.94117 found 403.94092.

2-Methoxy-2,3-dihydro-1H-cyclopenta[l]phenanthrene-6,9-dicarbaldehyde **4-45**

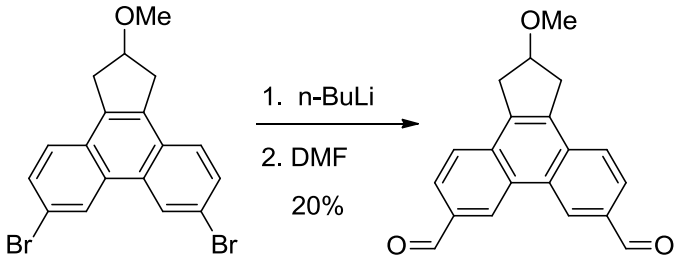

4-44 **4-45**

Phenanthrene **4-44** (0.150 g, 0.37 mmol) was dissolved in 10 mL dry THF. The solution was cooled to -78 °C and a 1.6 M solution of n-BuLi in hexanes (0.93 mL, 1.5 mmol) was added dropwise. The solution was allowed to stir under argon for 1 h. DMF (0.26 mL, 3.0 mmol) was then added dropwise, and the solution was allowed to warm to room temperature. After 1 h, 15 mL 1 M phosphoric acid was added, and the solution was stirred for 5 min. The solution was then diluted with 50 mL ethyl acetate and the layers were seperated. The organic layer was washed with 25 mL HCl (2 M, aq.) and then 50 mL water. The organic layer was dried over $MgSO_4$, filtered and the solvent removed *in vacuo* to give a black oil. The black oil was purified by column chromatography (SiO_2, 19:1 hexanes:ethyl acetate) to give **4-45** (0.023 g, 20% yield) as a white solid. ^{1}H NMR 300 MHz ($CDCl_3$) δ 10.29 (s, 2H), 9.23 (d, *J*=1.2 Hz), 8.15 (dd, *J*=8.4, 1.2 Hz, 2H), 7.99 (d, *J*=8.4 Hz, 2H), 4.59 (m, 1H), 3.65 (dd, *J*=16, 6.6 Hz, 2H), 3.51 (s, 3H), 3.44-3.50 (m, 2H) ^{13}C NMR (125 MHz, $CDCl_3$) δ 192.1, 138.5, 134.1, 133.8, 130.3, 127.2, 126.2, 126.1, 80.4, 56.7, 39.0.

2-Methoxy-2,3-dihydro-1H-indene **4-47**

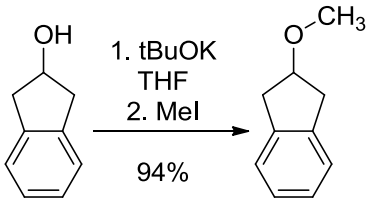

4-46 **4-47**

To a solution of **4-46** (2.05 g ,15.3 mmol) in 30 ml THF, was added potassium *tert*-butoxide (2.010 g 18.0 mmol). The mixture was stirred at 0 °C for 10 min under Ar. Methyl iodide (1.1 ml, 17.35 mmol) was added, and the mixture stirred for 3 h at room temperature. THF was removed *in vacuo*, and the residue was poured into a separatory funnel charged with water (50 mL) and ether (50 mL). The layers were separated, and the aqueous layer was extracted with ether (3 x 25 mL). The combined organic layers were then washed with brine and dried over $MgSO_4$. The solution was concentrated *in vacuo* to give **4-47** (2.12 g, 94%) as a yellow oil: ^{1}H NMR ($CDCl_3$) δ 7.16-7.24 (m, 4H), 4.32 (1H, m), 3.40 (3H, s), 3.24 (dd, *J*= 16, 6 Hz), 3.07 (dd, *J*=16, 4 Hz, 2H), ^{13}C NMR (100 MHz, $CDCl_3$) δ 140.7, 126.5, 124.6, 81.8, 56.5, 38.9. Spectra match the reported values.[23]

2,3-Dihydro-1H-inden-2-ol **4-46**

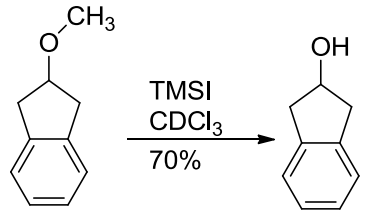

4-47 **4-46**

Methyl ether **4-47** (0.158 g, 1.1 mmol) was dissolved in 1 mL $CDCl_3$ and placed in an NMR tube. Iodotrimethylsilane (0.20 mL, 1.4 mmol) was added, and the mixture darkened. The reaction was monitored by ^{1}H NMR, and after 24 h there was a disappearance of the signal for the methyl group (singlet at 3.40 ppm). The solution was then poured into 5 mL methanol, and the solvent was removed *in vacuo* to give a brown oil. The oil was dissolved in 25 mL ethyl acetate and washed with 25 mL sodium thiosulfate (5 %, aq.) and then 25 mL water. The organic layer was then dried over $MgSO_4$, filtered, and the solvent removed *in vacuo* to give **4-46** (0.103 g, 70% yield) as a brown solid. ^{1}H NMR ($CDCl_3$, 300 MHz): 7.18-7.32 (m, 4H), 4.73 (m, 1H), 3.25 (dd, *J*= 16., 5.8 Hz, 2H), 2.94 (dd, 2H, *J* = 16, 3.3 Hz, 2H). Peaks match the reported spectrum.[24]

Tribenzylorthoformate **4-52**

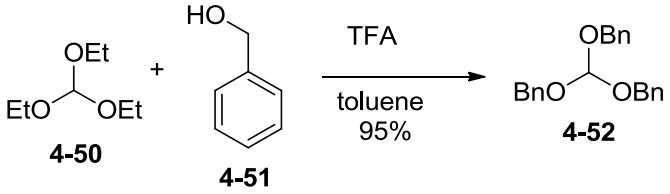

Benzyl alcohol **4.51** (30 mL, 290 mmol, 4 eq) was dissolved in 25 mL toluene. Triethyl orthoformate **4.50** (12.1 mL, 73 mmol, 1 eq) and trifluoroacetic acid (0.54 mL, 7 mmol, 0.1 eq) were added and the solution was stirred at room temperature for 30 min. The reaction mixture was then put under vacuum (water aspirator) and slowly distilled. After raising the temperature to 60 °C there were no longer any volatiles left, so the excess benzyl alcohol was then distilled under vacuum (mechanical pump, b.p. 75-85 °C), leaving tribenzylorthoformate **4-52** (22.83 g, 95% yield) in the reaction flask as a colorless liquid. ^{1}H NMR (400 MHz, $CDCl_3$) δ 7.28-7.38

(m, 15H), 5.45 (s, 1H), 4.68 (s, 6H) ^{13}C NMR (100 MHz, $CDCl_3$) δ 137.4, 128.4, 127.9, 127.7, 111.4, 66.5. NMR spectra match the reported values.[14]

6,9-Dibromo-2,3-dihydro-1H-cyclopenta[l]phenanthren-2-ol **4-54**

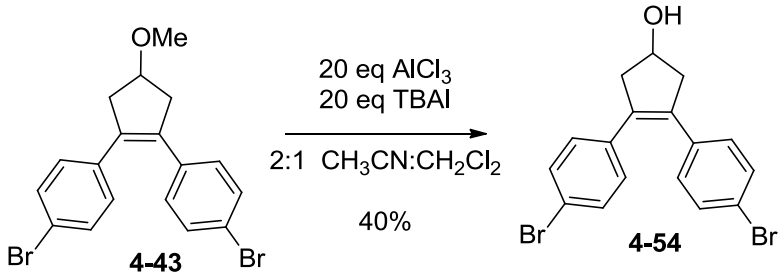

Stilbene **4-43** (0.116g, 0.3 mmol) was dissolved in 12 mL CH_2Cl_2 and 22 mL acetronitrile in a flask. Tetrabutylammonium iodide (2.73 g, 7.4 mmol) was added and the solution was cooled to 0 °C. Aluminum trichloride (0.98 g, 7.4 mmol) was added, the solution darkened, and was stirred at 0 °C for 6 h. Then, 15 mL water was added, and a precipitate formed. The mixture was diluted with CH_2Cl_2, and the solid dissolved. The layers were separated and the aqueous layer was extracted with 25 mL CH_2Cl_2. The organic layers were combined and washed with 25 mL sodium thiosulfate (5 %, aq.). The organic layer was then dried over $MgSO_4$, filtered, and the solvent removed *in vacuo* to give a white solid. The solid was subjected to sonication for 1 h in 50 mL ethyl acetate and then filtered. The filtrate was purified by column chromatography (SiO_2, 3:1 hexanes:ethyl acetate) to give **4-54** (0.040 g, 40% yield) as a white solid. ^{1}H NMR (400 MHz, $CDCl_3$) δ 7.33-7.36 (m, 4H), 7.01-7.05 (m, 4H), 4.64 (m, 1H), 3.22 (m, 2H), 2.82 (m, 2H). ^{13}C NMR (100 MHz, $CDCl_3$) δ 136.1, 134.4, 131.4, 129.8, 121.0, 69.6, 48.4. HRMS (EI) calcd. for $C_{18}H_{16}OBr_2$ 391.94117 found 391.94078.

3,4-Bis(2-chlorophenyl)cyclopent-3-enol **4-57**

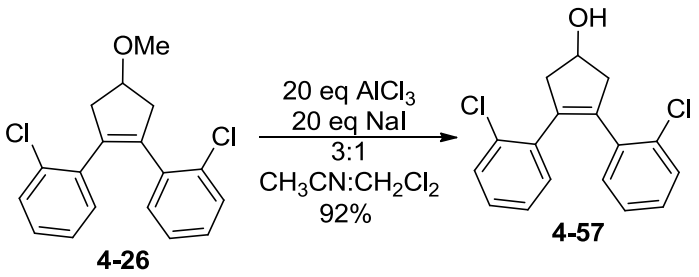

4-26 **4-57**

Chlorostilbene **4-26** (1.15 g, 3.6 mmol) was dissolved in 23 mL of CH_2Cl_2 and 69 mL of acetonitrile in flask. Sodium iodide (10.84 g, 72 mmol) was added and the solution was cooled to 0 °C. Aluminum trichloride (9.61 g, 72 mmol) was added and the solution darkened and was stirred at 0 °C for 6 h. Then, 50 mL water was added and a precipitate formed. The mixture was diluted with 100 mL CH_2Cl_2, and the solid dissolved. The layers were separated, and the aqueous layer was extracted with 75 mL CH_2Cl_2. The organic layers were combined and washed with sodium thiosulfate (5 %, aq.). The organic layer was then dried over $MgSO_4$, filtered and the solvent was removed *in vacuo* to give a brown solid. The solid was purified by column chromatography (SiO_2, 3:1 hexanes:ethyl acetate) to give **4-54** (1.01 g, 92% yield). ^{1}H NMR (400 MHz $CDCl_3$) δ 7.28 (dd, *J*=7.6, 0.8 Hz, 2H), 7.04-7.11 (m, 2H), 7.0-7.03 (m, 4H), 4.69 (m, 1H), 3.26 (dd, *J*=16, 6.0 Hz, 2H), 2.86 (dd, *J*=16, 2 Hz, 2H). ^{13}C NMR (100 MHz $CDCl_3$) δ 137.3, 136.5, 133.1, 130.6, 129.3, 128.4, 126.5, 71.6, 47.2.

4,11-Dichloro-2,3-dihydro-1H-cyclopenta[l]phenanthren-2-ol **4-58**

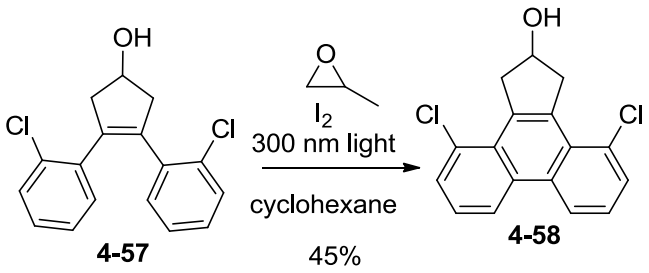

Stilbene **4-57** (0.313 g, 1.03 mmol) was dissolved in 250 mL cyclohexane in a quartz photochemical reaction vessel. Iodine (0.261 g, 1.03 mmol) was added and Ar was bubbled through the solution for 30 min. Propylene oxide (14.4 mL, 206 mmol) was added and the solution was irradiated with 300-nm light. After 4 h, an aliquot was removed and the solvent was removed by rotary evaporation. ^{1}H NMR of this aliquot showed the disappearance of the starting material. The solution was washed with 50 mL sodium thiosulfate (5 %, aq), dried over $MgSO_4$, filtered and the solvent removed *in vacuo*. The resulting brown solid was purified by column chromatography (SiO_2, 19:1 hexanes:ethyl acetate) to give **4-58** (0.141 g, 45 % yield). ^{1}H NMR (400 MHz, $CDCl_3$) δ 8.54 (dd, *J*=8.4, 0.8 Hz, 2H), 7.64 (dd, *J*=7.6, 0.8 Hz, 2H), 7.45 (t, *J*=8 Hz, 2H). 4.73 (bs, 1H), 3.99 (dd, *J*=16, 6.0 Hz, 2H), 3.88 (dd, *J*=16, 2.4 Hz, 2H). ^{13}C NMR ($CDCl_3$) δ 135.9, 132.9, 131.6, 129.9, 128.3, 126.1, 122.6, 71.3, 46.3. HRMS (EI) $C_{17}H_{12}OCl_2$ calcd. 302.02653 found 302.02576.

4-6 References

1. Cossy, J.; Lutz, F.; Alauze, V.; Meyer, C., Carbon-carbon bond forming reactions by using bistrifluoromethanesulfonimide. *Synlett* **2002**, 45–48.
2. Cazeau, P.; Duboudin, F.; Moulines, F.; Babot, O.; Dunogues, J., A new practical synthesis of silyl enol ethers : Part.I. From simple aldehydes and ketones. *Tetrahedron* **1987,** *43* (9), 2075-2088.

3. Liu, L.; Yang, B.; Katz, T. J.; Poindexter, M. K., Improved methodology for photocyclization reactions. *J. Org. Chem.* **1991,** *56* (12), 3769-75.
4. Wiles, C.; Watts, P.; Haswell, S. J.; Pombo-Villar, E., The regioselective preparation of 1,3-diketones. *Tetrahedron Lett.* **2002,** *43* (16), 2945-2948.
5. Mallory, F. B.; Mallory, C. W., Photocyclization of stilbenes and related molecules. *Org. Reactions* **1984,** *30*, 1-456.
6. Mallory, F. B.; Mallory, C. W., personal communication. 2010.
7. Purushothaman, E.; Pillai, V. N. R., Photoreactions of 4,5-diarylimidazoles - singlet oxygenation and cyclodehydrogenation. *Indian J. Chem. Sect B-Org. Chem. Incl. Med. Chem.* **1989,** *28* (4), 290-293.
8. Pétrier, C.; L. Gemal, A.; Luche, J.-L., Ultrasounds in organic synthesis 31. A simple, high yield modification of the bouveault reaction. *Tetrahedron Lett.* **1982,** *23* (33), 3361-3364.
9. Littke, A. F.; Schwarz, L.; Fu, G. C., Pd/P(t-Bu)3: A mild and general catalyst for Stille reactions of aryl chlorides and aryl bromides. *J. Am. Chem. Soc.* **2002,** *124* (22), 6343-6348.
10. Chobanian, H. R.; Fors, B. P.; Lin, L. S., A facile microwave-assisted palladium-catalyzed cyanation of aryl chlorides. *Tetrahedron* **2006,** *47*, 3303–3305.
11. Yin, J. J.; Rainka, M. P.; Zhang, X. X.; Buchwald, S. L., A highly active Suzuki catalyst for the synthesis of sterically hindered biaryls: Novel ligand coordination. *J. Am. Chem. Soc.* **2002,** *124* (7), 1162-1163.
12. Jung, M. E.; Lyster, M. A., Quantitative dealkylation of alkyl ethers via treatment with trimethylsilyl iodide. A new method for ether hydrolysis. *J. Org. Chem* **1977,** *42* (23), 3761-3764.
13. Park, J.; Lang, K.; Abboud, K. A.; Hong, S., Self-Assembled Dinuclear Cobalt(II)-Salen Catalyst Through Hydrogen-Bonding and Its Application to Enantioselective Nitro-Aldol (Henry) Reaction. *J. Am. Chem. Soc.* **2008,** *130* (49), 16484-16485.
14. Gil, L.; Han, Y.; Opas, E. E.; Rodan, G. A.; Ruel, R.; Seedor, J. G.; Tyler, P. C.; Young, R. N., Prostaglandin E2-bisphosphonate conjugates: potential agents for treatment of osteoporosis. *Bioorg. Med. Chem.* **1999,** *7* (5), 901-919.
15. Akiyama, T.; Shima, H.; Ozaki, S., A concise synthesis of (−)-conduritol F from l-quebrachitol via AlCl3-n-Bu4NI mediated demethylation. *Tetrahedron Lett.* **1991,** *32* (40), 5593-5596.
16. Node, M.; Ohta, K.; Kajimoto, T.; Nishide, K.; Fujita, E.; Fuji, K., Selective demtyhlation of aliphatic methyl ether in the presence of aromatic methyl ether with the aluminum chloride-sodium iodide-acetonitrile system. *Chem. Pharm. Bul.* **1983,** *31* (11), 4178-4180.
17. Grieco, P. A.; Speake, J. D., Synthetic Studies on Quassinoids: Total Synthesis and Biological Evaluation of (+)-Des-d-chaparrinone. *J. Org. Chem.* **1998,** *63* (17), 5929-5936.
18. Jin, F.; Confalone, P. N., Palladium-catalyzed cyanation reactions of aryl chlorides. *Tetrahedron Lett.* **2000,** *41* (18), 3271-3273.
19. Kerr, W. J.; Watson, A. J. B.; Hayes, D., In situ generation of Mes2Mg as a non-nucleophilic carbon-centred base reagent for the efficient one-pot conversion of ketones to silyl enol ethers. *Org. Biomol. Chem.* **2008,** *6* (7), 1238-1243.
20. Yamashita, M.; Yamada, K.-i.; Tomioka, K., Construction of Arene-Fused-Piperidine Motifs by Asymmetric Addition of 2-Trityloxymethylaryllithiums to Nitroalkenes: The Asymmetric Synthesis of a Dopamine D1 Full Agonist, A-86929. *J. Am. Chem. Soc.* **2004,** *126* (7), 1954-1955.

21. Saitoh, T.; Oyama, T.; Sakurai, K.; Niimura, Y.; Hinata, M.; Horiguchi, Y.; Toda, J.; Sano, T., Thermal Addition Reaction of Aroylketene with 1-Aryl-1-trimethylsilyloxyethylenes : Aromatic Substituent Effects of Aroylketene and Aryltrimethylsilyloxyethylene on Their Reactivity. *Chem. Pharm. Bull.* **1996,** *44* (5), 956-966.
22. Fuglseth, E.; Thvedt, T. H. K.; Møll, M. F.; Hoff, B. H., Electrophilic and nucleophilic side chain fluorination of para-substituted acetophenones. *Tetrahedron* **2008,** *64* (30–31), 7318-7323.
23. I. Bowers, N.; R. Boyd, D.; D. Sharma, N.; A. Goodrich, P.; R. Groocock, M.; John Blacker, A.; Goode, P.; Dalton, H., Stereoselective benzylic hydroxylation of 2-substituted indanes using toluene dioxygenase as biocatalyst. *J. Chem. Soc., Perkin Trans. 1* **1999,** (11), 1453-1462.
24. Arrowsmith, M.; Hadlington, T. J.; Hill, M. S.; Kociok-Kohn, G., Magnesium-catalysed hydroboration of aldehydes and ketones. *Chem. Commun.* **2012,** *48* (38), 4567-4569.

Chapter 5

5-1 Discussion and Synthesis of a Hexasubstituted Benzene Scaffold

The work described thus far has focused on the subunits, but the scaffold is an equally important part of the project. As discussed in Chapter 3, the chosen scaffold is a hexasubstituted benzene (**5-1**). Mislow and coworkers studied low temperature NMR spectra of **5-1**, where R=Cr(CO), and found that at room temperature the conformation shown predominates, but that it is mobile on the NMR timescale.[1] However, at room temperature, more than 99% of the molecules would be in the desired conformation (**5-1**).[1-2] This preference is beneficial for the construction of an aromatic belt because the subunits will be on the same face of the benzene ring, which should favor the intramolecular coupling.

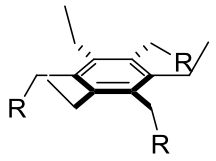

5-1

Figure 5-1 – The scaffold in the desired conformation

The synthesis of suitable scaffold precursors has been reported in the literature. [3] Scheme 5-1 shows the reaction that was carried out by Michelle Lacoske, a former undergraduate in the Goroff group, to synthesize the scaffold precursor. The reaction is a three-fold electrophilic

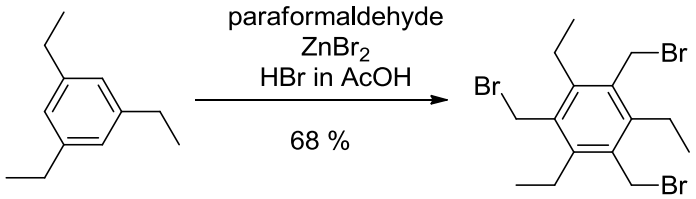

5-2 **5-3**

Scheme 5-1 – The synthesis of scaffold precursor **5-3**

aromatic substitution of 1,3,5-triethylbenzene (**5-2**), with paraformaldehyde as the electrophile and zinc bromide to activate it. The product (**5-3**) precipitates from the reaction mixture, so isolation is simply a filtration of the reaction mixture. Michelle Lacoske found the yield to be dependent on the scale of the reaction, with larger scale giving a better yield.

5-2 Stereoisomers in the Final Steps

Scheme 5-2 shows the final steps once the synthesis of a subunit is complete. The first

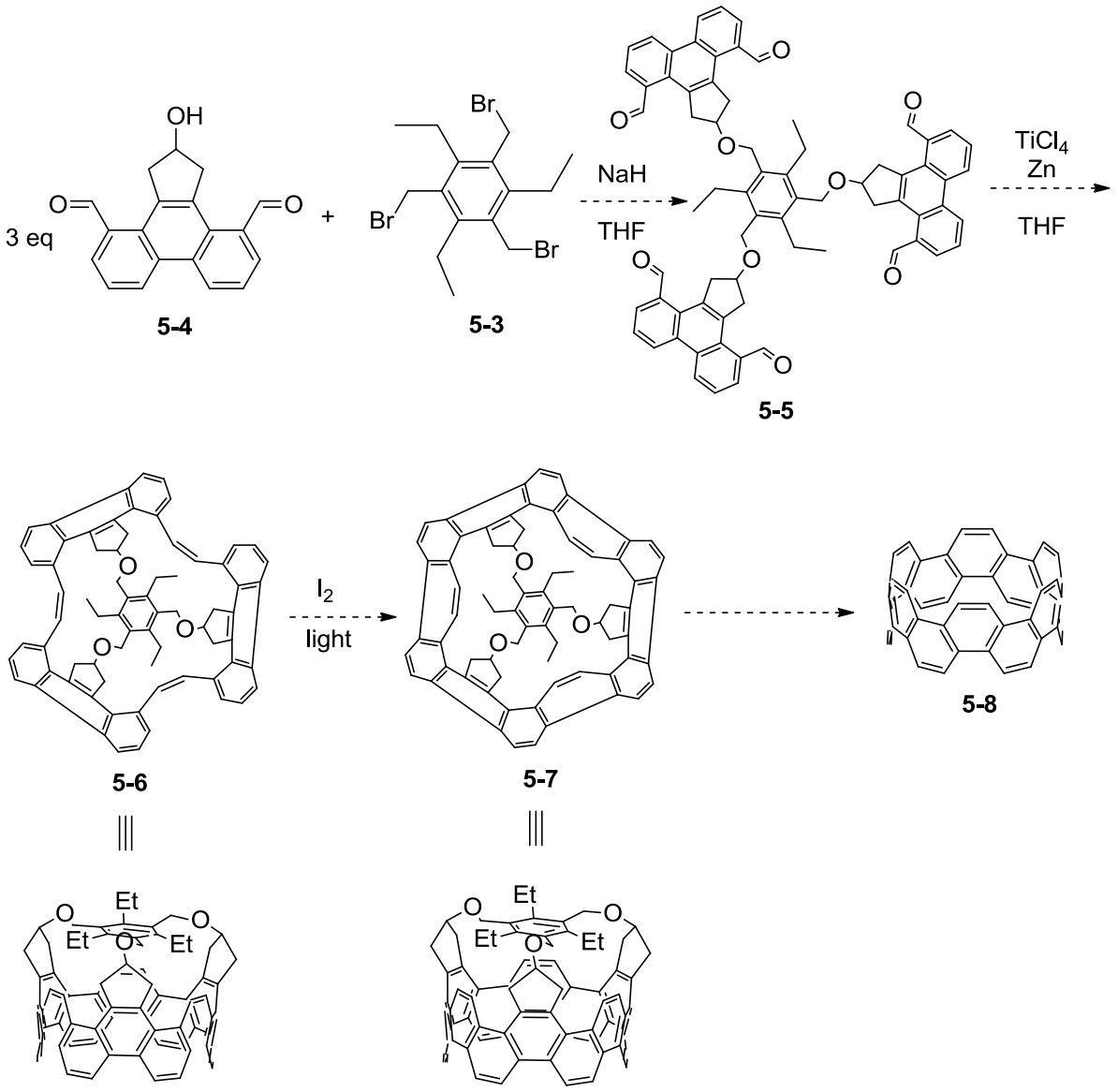

Scheme 5-2 – The final steps towards an aromatic belt

step is simply attachment of the subunits to the scaffold to give hexaldehyde **5-5**. The next step is the macrocyclization via McMurry coupling to give compound **5-6**. Macrocycle **5-6** will then be oxidized to give belt **5-7**. Finally removal of the scaffold would give [12]cyclophenacene (**5-8**).

There is one possible problem that has been considered: when macrocycle **5-6** is formed it has 3 stereogenic centers, which may complicate the synthetic plan (Figure 5-2). The connection point of the cyclopentene ring to the oxygen is a stereogenic center (marked with an asterisk), i.e., the hydrogen atom could face either toward, or away from the center of the assembly. Thus, compound **5-6** may form as a series of stereoisomers and this may complicate the next step because the stereoisomers may have different reactivities, so not every stereoisomer may oxidize to form the desired belt **5-7**.

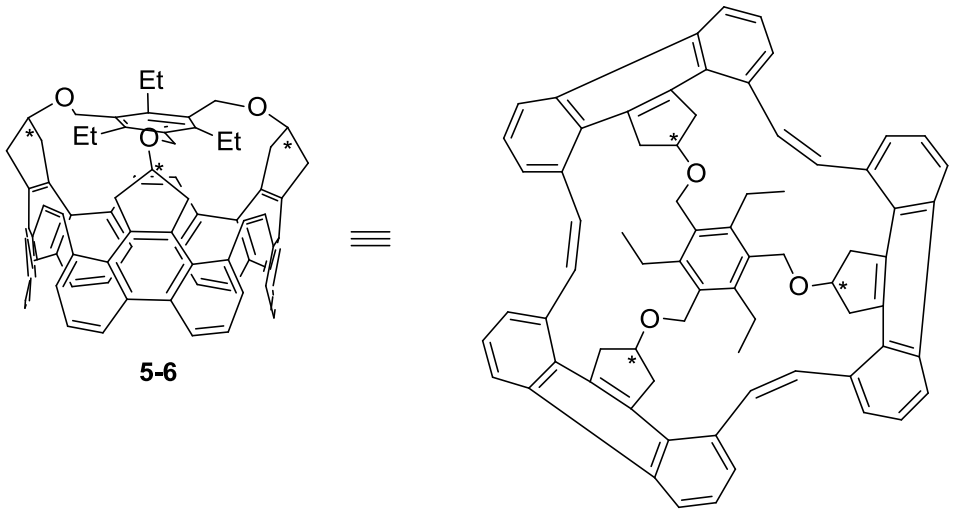

5-6 ≡ **5-6**

Figure 5-2 – The steroisomerism problem with compound **5-6**

One solution to this issue is to change the subunits so that the carbon that would form a stereocenter is now an amine. An amine was chosen because the barrier for inversion of an sp^3

nitrogen is low, so it has no fixed stereochemistry. A 3,6,9,10-substituted phenanthrene (Figure 5-2) was chosen because of the higher yields in the photocyclization.

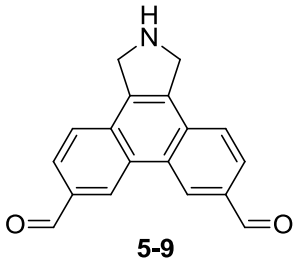

5-9

Figure 5-2 – The new amine subunit **5-9**

5-3 Progress Towards Amine Subunit 5-9

The first planned route to subunit **5-9** (Scheme 5-3) begins with a McMurry coupling of *p*- bromoacetophenone (**5-10**). Stilbene **5-11** is obtained as primarily the cis isomer, which undergoes the Mallory reaction to give phenanthrene **5-12**. Phenanthrene **5-12** is then subjected to radical bromination with NBS and benzoyl peroxide in carbon tetrachloride, but the product of this reaction is an insoluble white solid. The reaction was repeated a second time, but with the same outcome. The white solid gives the expected HRMS for phenanthrene **5-13**.

In order to circumvent the solubility problem, dibromophenanthrene **5-12** was allowed to react first with palladium acetate and potassium ferrocyanide to give dinitrile **5-16**. The benefit of using potassium ferrocyanide in this reaction is that it is a non-toxic source of cyanide. The radical bromination of phenanthrene **5-16** gave an insoluble white solid, which could not be characterized. It seems that adding bromines to the methyl groups causes a large drop in the solubility of these phenanthrenes.

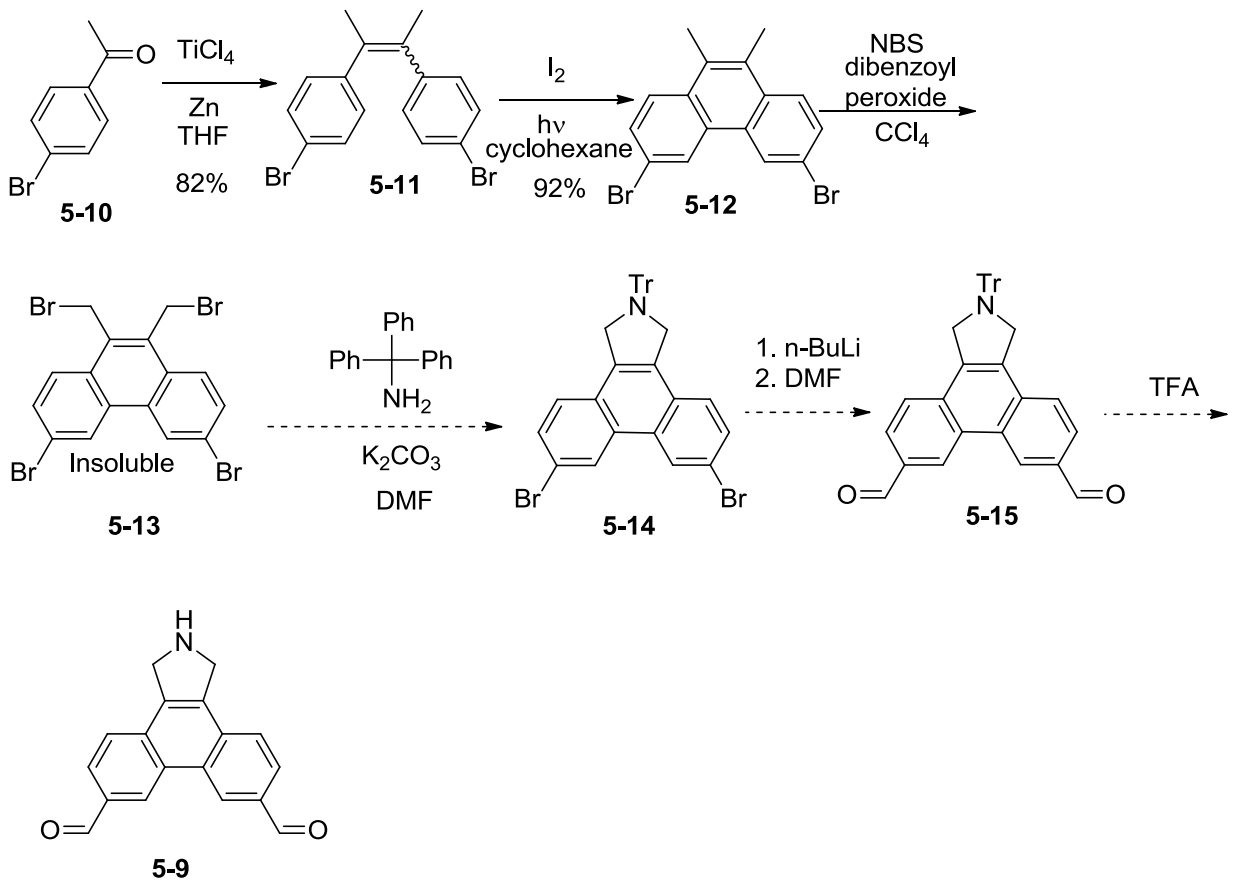

Scheme 5-3 – The first route to subunit **5-8**

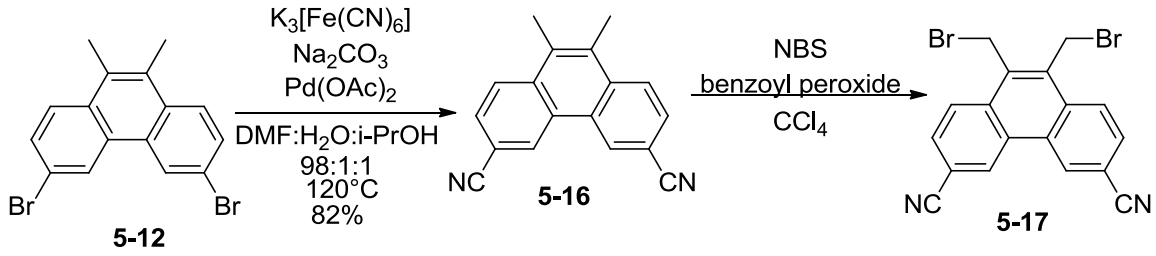

Scheme 5-4 – Functionalization of **5-12**

These earlier routes show that it may be better to attach the desired amine before forming a phenanthrene, with the hope that it increases the solubility (Scheme 5-5). Mizen and co-workers report the synthesis of diketone **5-19** from α-bromoacetophenone (**5-18**).[4] The reaction to form diketone **5-19** requires two equivalents of α-bromoacetophenone **5-18** to react with the benzyl amine. However, it also requires a second equivalent of benzylamine act as a base and

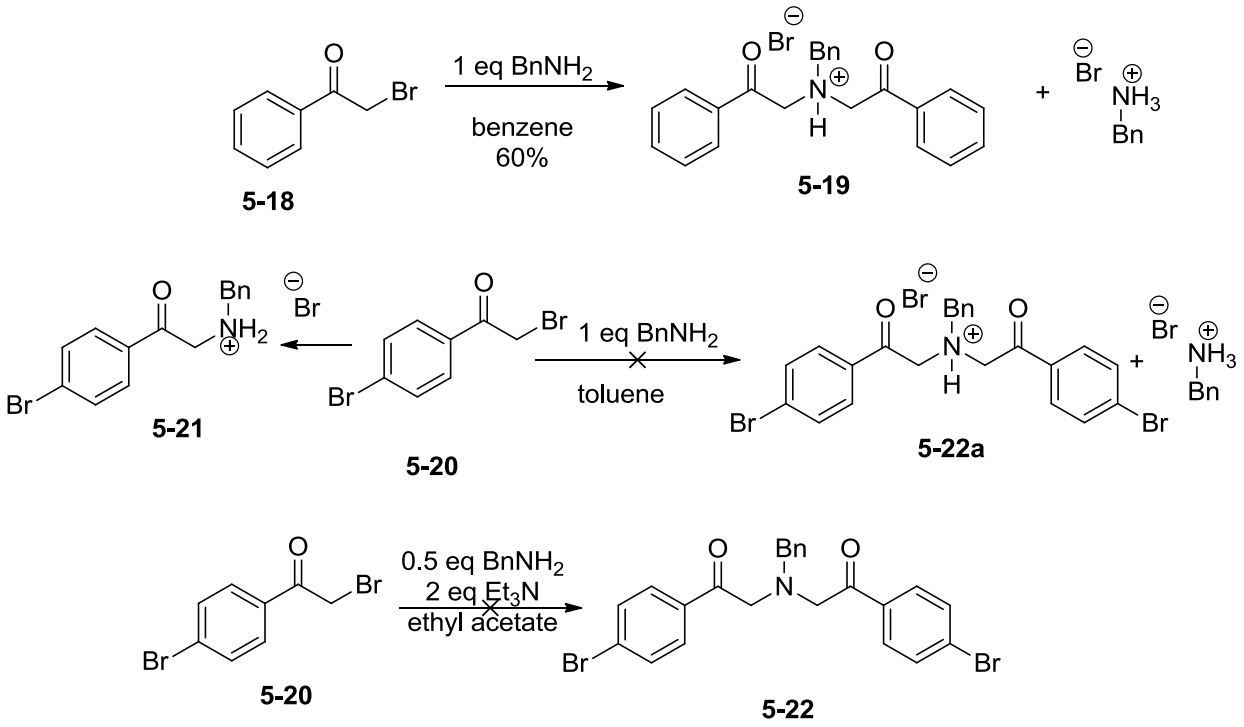

Scheme 5-5 – Using benzylamine to synthesize subunit **5-9**

remove a proton from the monsubstituted intermediate (not shown). Thus, the expected stoichiometry of reaction would be 1:1. Unfortunately when the reaction was performed with α-bromoacetophenone **5-20**, only the mono substituted product was isolated (**5-21)**. It is not clear why a para-substituted bromine so far away from the reacting atoms gives such a different result. Other variations of this reaction were attempted in which two equivalents of triethylamine were added and only one half equivalent of benzylamine, but this stoichiometry only gave a complicated mixture.[5]

Margarita Milton, an undergraduate in the Goroff group, is currently pursuing a new route to an amine subunit (Scheme 5-6). Benzenesulfonamide reacts with two equivalents of **5-17** in the presence of cesium carbonate to give the desired diketone **5-18**. A McMurry reaction then gives the desired product **5-19**, which is photocyclized to give phenanthrene **5-20**. All that

remains in the synthetic route is removal of the sulfonyl group and functionalization of the bromides to aldehydes.

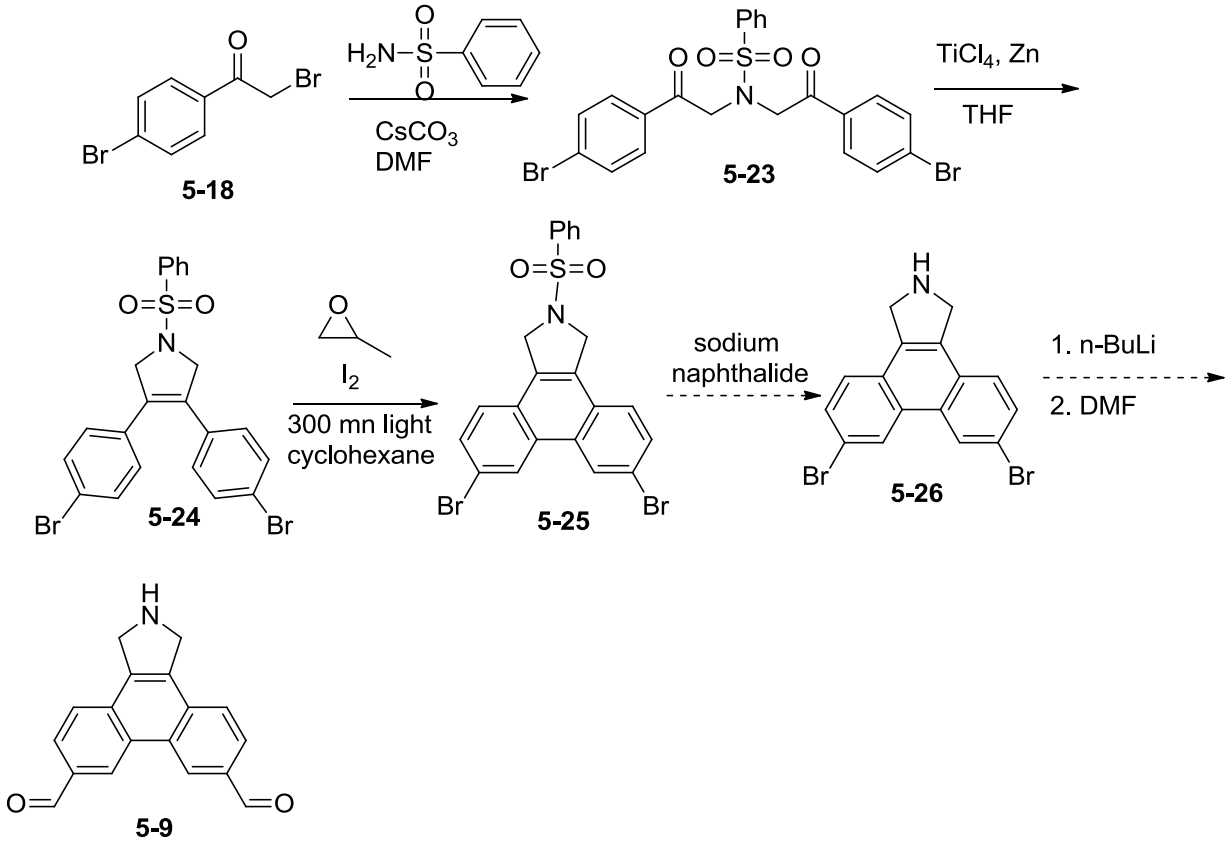

Scheme 5-6 – The route to subunit **5-**9 using benzenesulfonamide.

5-4 Summary and Conclusion

The use of a hexasubstituted benzene should aid in the formation of the initial macrocycle, because it puts the subunits closer in proximity. The McMurry reaction also improves the chance of obtaining a macrocycle, as the Scott group has previously synthesized the unscaffolded equivalent of **5-6** (compound **1-39**), using a McMurry coupling.[6] The use of phenanthrene-based subunits will block the self-cyclization that occurred in the earlier subunits, but it has introduced some solubility issues.

One of the many things that was developed during the course of this work was a synthetic route to phenanthrenes with substituents in the 1,8,9,10 and 3,6,9,10 positions. There were no routes found in the literature, but the developed route is scalable and allows for a range of functionality because of the halides used. If the halides are functionalized early in the synthetic route with the desired functionality, solubility may not be a problem. Unfortunately for this work, aldehydes are not compatible with the McMurry coupling early in the route and nitriles seem to make the solubility worse.

As of now, the synthesis of a subunit has not been completed, but is still underway. Unfortunately, the hypothesis that a scaffold can be used to construct an aromatic belt has yet to be fully tested. This synthesis of the subunits may only be a short time away, but until then the system cannot be tested. One thought to keep in mind about this approach is that all of the strain is built up in the last two steps, the macrocyclization and the oxidation.[7] However, no other group has isolated an aromatic belt, so the scaffold may be the key that was missing from the previous attempts. The scaffold can limit the side reactions and favor the desired couplings and oxidation.

One idea that has not been investigated synthetically, but that has been examined computationally, is the synthesis of [18]cyclophenacene. The strain energy of [18]cyclophenacene is only 59 kcal/mol, almost half the strain energy of [12]cyclophenacene (B3LYP/6-31G*). This means that it may be a much more viable synthetic target. The retrosynthetic analysis of [18]cyclophenacene is shown in Scheme 5-7. The subunit used to construct [18]cyclophenacene is a [5]phenacene **5-28**. [5]phenacene **5-28** could be synthesized from dinaphthyl indanol **5-29**. A Suzuki-Miyaura coupling between the previously reported

dibromoindanol **5-30** and a 1,5-substituted naphthalene **5-31** can be used to construct dinaphthyl indanol **5-29**.

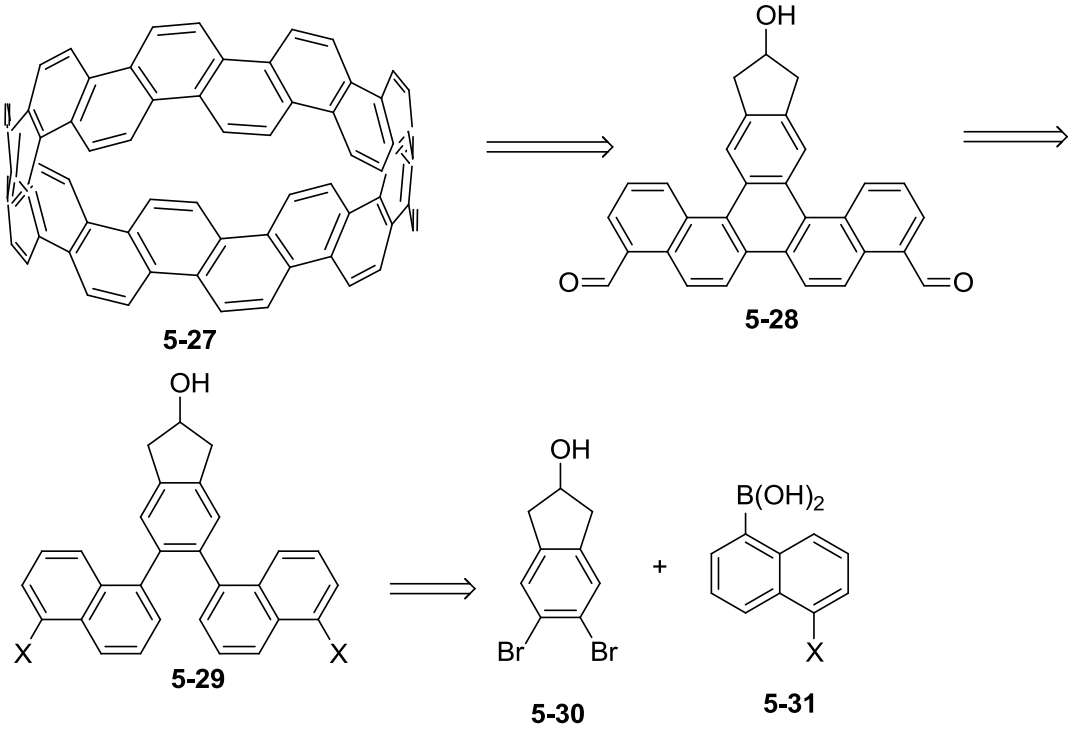

Scheme 5-7 – The retrosynthetic analysis of [18]cyclophenacene **(5-27)**

One of the main reasons that no synthetic effort has been put forth on this approach is that we can foresee a few potential issues. The first concern is that boronic acid **5-31** is not commercially available. A three-step route to compound **5-31** is shown in Scheme 5-8. 1,5-diaminonaphthalene (**5-32**) is commercially available and its conversion to 1,5-dibromonaphthalene (**5-33**) has been reported, but with only a 28% yield.[8] Lithiation followed by treatment with DMF would give bromoaldehyde **5-34**. The reaction of bromoaldehyde **5-34** with palladium and pinacol borate dimer would give naphthalene **5-35**, that could be coupled to bromoindanol **5-30**.

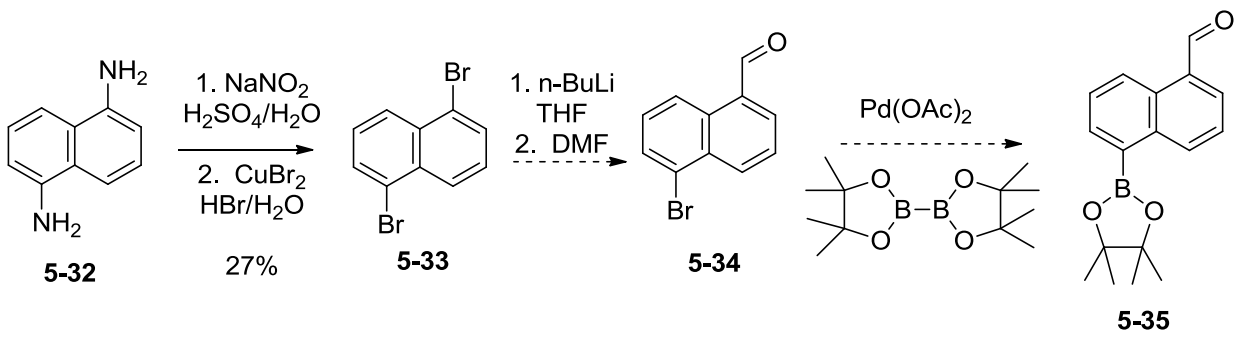

Scheme 5-8 – The proposed route to naphthyl boronate **5-35**

Previous attempts to perform Suzuki-Miyaura couplings on dibromoindanol **5-30** were problematic, but with the use of more active palladium catalyst this problem can be overcome. One possible solution is the use of the S-Phos ligand in the coupling, which has been shown to make very sterically hindered carbon-carbon bonds.[9] The oxidation of dinaphthyl **5-29** to [5]phenacene **5-28** does have literature precedent. Harvey and co-workers reported the photocyclization of dinaphthyl benzene **5-36** to give phenacene **5-37** in 98% yield(Scheme 5-10).[10]

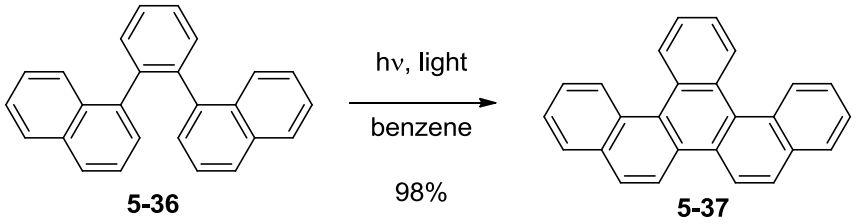

Scheme 5-9 – Literature precedent for the oxidation to a [5]phenacene[10]

One of the main reasons that this route has not been pursued has been a concern about solubility. Many phenanthrene derivatives have proven to be insoluble, and these larger aromatic systems are expected to have lower solubility. The incorporation of solubilizing groups on the naphthyl rings may solve this problem, but complicates the synthesis.

5-5 Experimental

1,3,5-Tris(bromomethyl)-2,4,6-triethylbenzene **5-3**

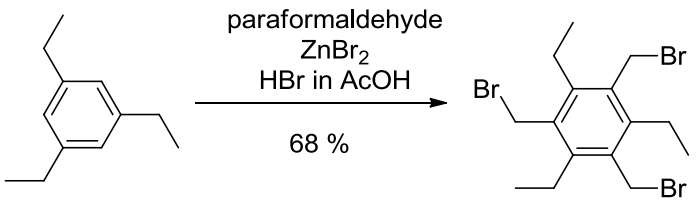

5-2 **5-3**

To a solution of 18 mL of 33% HBr in AcOH and paraformaldehyde (2.92 g, 98 mmol), triethylbenzene (1.7ml, 9.0 mmol) was added dropwise. $ZnBr_2$ (3.50 g, 16 mmol) was added slowly at room temperature under Ar. The mixture was then heated to 90 °C and stirred overnight. A white solid precipitated and this was filtered and washed with cold water. The solid was then dissolved in methylene chloride and washed with sodium thiosulfate followed by potassium carbonate. The organic layer was then dried over $MgSO_4$ and the solvent was removed *in vacuo*. Recrystallizatoin in methanol yielded compound **5-3** (2.92g, 72% yield) as a beige solid. ^{1}H NMR (300 MHz, $CDCl_3$) δ 4.58 (s, 6H), 2.94 (q, *J*=8 Hz, 6H), 1.34 (t, *J*=8 Hz, 9H). NMR matches the reported spectrum.[3]

4,4'-(But-2-ene-2,3-diyl)bis(bromobenzene) **5-11**

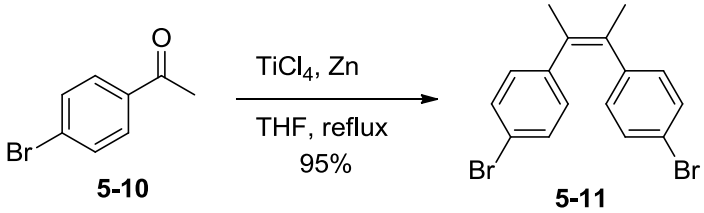

5-10 **5-11**

To a stirred oven-dried 2-necked flask under Ar, zinc dust (2.61 g, 40 mmol) was added. THF (30 mL, dried over sodium and benzophenone) was injected into the flask and the mixture was stirred. The flask was cooled in an ice water bath and $TiCl_4$ (2.2 mL, 20 mmol) was added dropwise. Yellow smoke was produced and the solution turned dark blue. The mixture was

stirred for 15 min, then 4'-bromoactophenone **5-10** (2.00 g, 10.0 mmol) was added dropwise as a solution in 5 mL THF. After the addition, the solution was heated to reflux for 3 h. Then, 20 mL water was added, and the solution bubbled. The reaction mixture was extracted with hexanes (3 x 50 mL). The organic layers were combined, dried over $MgSO_4$, filtered and the solvent was removed *in vacuo*. This gave **5-11** (1.72 g, 95%) as a white solid. ^{1}H NMR (400 MHz, $CDCl_3$) δ 8.07 (d, *J*=8 Hz, 2H), 7.51 (t, *J*=8 Hz, 2H), 2.74 (s, 6H).

3,6-Dibromo-9,10-dimethylphenanthrene **5-12**

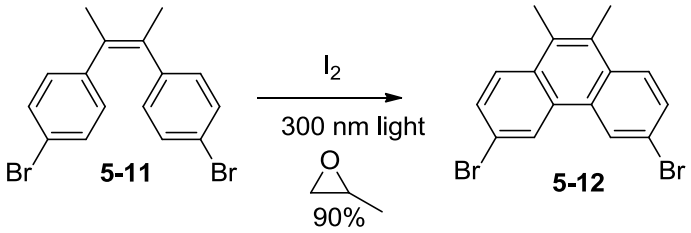

Stilbene **5-11** (0.116 g, 0.32 mmol) was dissolved in 200 mL hexanes in a quartz photochemical reaction vessel. Iodine (0.08 g, 0.32 mmol) was added, and Ar was bubbled through the solution for 30 min. Propylene oxide (4.4 mL, 63.4 mmol, 200 eq) was added and the solution was irradiated with 300-nm light. After the disappearance of the iodine color (~72 h) the solution was transferred to a round-bottomed flask and the solvent was removed *in vacuo*. The resulting white solid was run through a plug of silica with hexanes as the eluent to give **5-12** (0.103 g, 90%) as a white solid. ^{1}H NMR (400 MHz, $CDCl_3$) δ 8.68 (d, *J*=2 Hz, 2H) 7.94 (d, *J*=8.5 Hz, 2H) 7.70 (dd, *J*=8.5, 2 Hz, 2H), 2.67 (s, 6H) ^{13}C NMR (125 MHz, $CDCl_3$) δ 131.1, 130.2, 129.9, 129.6, 126.4, 125.5, 120.1, 15.9.

3,6-Dibromo-9,10-bis(bromomethyl)phenanthrene (**5-13**)

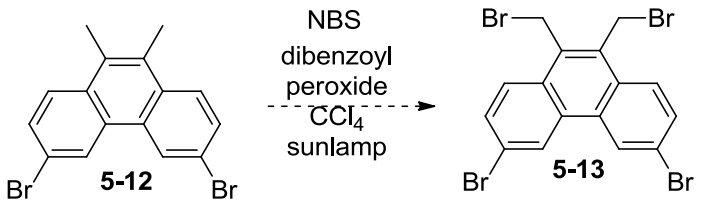

Phenanthrene **5-12** (0.070 g, 0.2 mmol) was dissolved in 5 mL CCl_4 in a 10 mL flask with a stir bar. N-Bromosuccinimide (0.068 g, 0.4 mmol) was added along with dibenzoyl peroxide (75%, 0.005 g, 0.02 mmol). The resulting mixture was heated to 80 °C and irradiated with a sun lamp for 4 h. The solution was cooled to room temperature diluted with 50 mL toluene and 50 mL water. The organic layer was removed and the aqueous layer was extracted with toluene (2 x 50 mL). The organic layers were combined, dried over $MgSO_4$ and the solvent was removed *in vacuo*. The resulting white powder (0.090 g) was insoluble in CH_2Cl_2, benzene, chloroform, hexanes, ethyl acetate, acetone and DMSO. It was slightly soluble in hot toluene, but an NMR has yet to be obtained. HRMS (EI) calculated 517.75155 found 517.75207

9,10-Dimethylphenanthrene-3,6-dicarbonitrile **(5-16)**

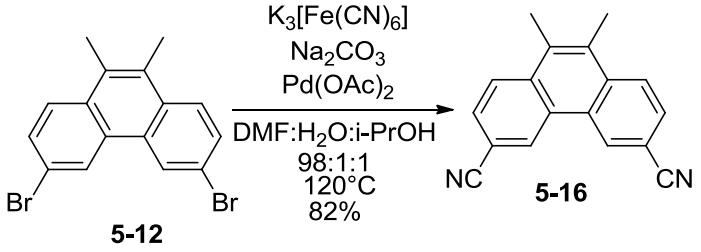

A solution of **5-12** (0.215 g, 0.6 mmol), sodium carbonate (0.063, 0.6 mmol) and palladium acetate (0.007 g, 0.03 mmol) in a mixture of DMF (2 mL), water (0.02 mL) and isopropanol (0.02 mL) was heated to 120 °C under Ar. Potassium ferrocyanide (0.100g, 0.2 mmol) was added and the solution was stirred at 120 °C for 4 h. The reaction mixture was cooled and the mixture was diluted with 50 mL of ethyl acetate and 50 mL water. The layers were separated

and the organic layer was washed with water (3 x 25 mL), dried over $MgSO_4$, filtered and concentrated *in vacuo*. The resulting brown solid was purified by column chromatography (SiO_2, 19:1 hexanes:ethyl acetate) to give **5-16** (0.122 g, 82 % yield) as a white solid. ^{1}H NMR (400 MHz, $CDCl_3$) δ 8.80 (bs, 2H) 8.15 (bs, 2H) 7.80 (bs, 2H), 2.67 (s, 6H); ^{13}C NMR (100 MHz, $CDCl_3$) δ 134.6, 132.8, 129.1, 128.1, 127.8, 125.9, 118.9, 109.9, 16.3.

2-(Benzylamino)-1-(4-bromophenyl)ethanone hydrobromide (**5-21**)

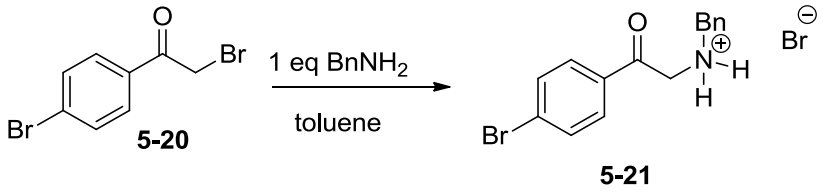

Acetophenone **5-20** (2.00 g, 7.2 mmol) was dissolved in 15 mL toluene. Benzylamine (0.79 mL, 7.2 mmol) was added and the solution was put under argon and a reflux condenser was attached. The solution was heated to 120 ºC for 48 h. A white precipitate was seen and the reaction was cooled and the white solid was filtered. The white solid was then placed in 10 mL of methanol and sonicated for 15 min then filtered. The resulting white solid was **5-21**. ^{1}H NMR (500 MHz, $CDCl_3$) δ 9.46 (bs, 2 H), 7.92 (m ,2 H), 7.84 (m, 2 H), 7.56 (m, 2H), 7.43 (m, 3 H), 4.83 (s, 2 H), 4.22 (s, 2 H).

5-6 References

1. Iverson, D. J.; Hunter, G.; Blount, J. F.; Damewood, J. R.; Mislow, K., Static and dynamic stereochemistry of hexaethylbenzene and of its tricarbonylchromium, tricarbonylmolybdenum, and dicarbonyl(triphenylphosphine)chromium complexes. *J. Am. Chem. Soc.* **1981,** *103* (20), 6073-6083.
2. Kilway, K. V.; Siegel, J. S., Control of functional group proximity and direction by conformational networks: synthesis and stereodynamics of persubstituted arenes. *Tetrahedron* **2001,** *57* (17), 3615-3627.
3. Vacca, A.; Nativi, C.; Cacciarini, M.; Pergoli, R.; Roelens, S., A new tripodal receptor for molecular recognition of monosaccharides. A paradigm for assessing glycoside binding

affinities and selectivities by ^{1}H NMR spectroscopy. *J. Am. Chem. Soc.* **2004,** *126* (50), 16456-16465.
4. Arduengo, A. J.; Stewart, C. A.; Davidson, F.; Dixon, D. A.; Becker, J. Y.; Culley, S. A.; Mizen, M. B., The synthesis, structure, and chemistry of 10-Pn-3 systems: tricoordinate hypervalent pnicogen compounds. *J. Am. Chem. Soc.* **1987,** *109* (3), 627-647.
5. Tang, G.; Ji, T.; Hu, A.-F.; Zhao, Y.-F., Novel N,S-Phenacyl Protecting Group and Its Application for Peptide -Synthesis. *Synlett* **2008,** *2008* (EFirst), 1907-1909.
6. (a) Brooks, M. A. 1,2-Shifts in Aryl Radicals and Synthetic Routes Toward Cyclo[12]phenacene: A Molecular Belt. Dissertation, Boston College, Chestnut Hill, MA, 1998; (b) St.Martin-Davis, H. M. Synthetic Routes Towards Cyclo[N]phenacenes and [8]Circulene: Molecular Belts and Saddles. Dissertation, Boston College, Chestnut Hill, MA, 2002.
7. Eisenberg, D.; Shenhar, R.; Rabinovitz, M., Synthetic approaches to aromatic belts: building up strain in macrocyclic polyarenes. *Chem. Soc. Rev.* **2010,** *39* (8), 2879-2890.
8. Chambers, R. R.; Collins, C. J.; Maxwell, B. E., Reductive debenzylation of 1-benzylnaphthalene by a sodium-potassium alloy. *J. Org. Chem.* **1985,** *50* (24), 4960-4963.
9. Wolfe, J. P.; Singer, R. A.; Yang, B. H.; Buchwald, S. L., Highly active palladium catalysts for Suzuki coupling reactions. *J. Am. Chem. Soc.* **1999,** *121* (41), 9550-9561.
10. Tang, X.-Q.; Harvey, R. G., A Convenient Synthesis of Benzo[s]picene. *J. Org. Chem.* **1995,** *60* (11), 3568-3568.

Chapter 6

6-1 π-π Stacking and the Hydrophobic Effect

This chapter describes a separate computational project independent of the belt synthesis. π-π stacking is a van der Waals interaction of two π systems. Chemists have focused more attention on π stacking than most other types of through-space interactions because it is found in such a wide range of systems.[1] There is debate if π-π stacking really is a special interaction between the π systems of aromatic groups or if it is simply a van der Waals interaction.[2] π-π stacking may just be a manifestation of the hydrophobic effect.[3]

The hydrophobic effect is a term used to describe the tendency for non-polar species to aggregate when placed into water. In order to minimize the disruption of the water's hydrogen bonding, the mixture equilibrates so that the solute takes up the smallest surface area.[4] This minimization of surface area plays a factor in π-π stacking, because an aromatic π-dimer has a smaller surface area than two separate aromatic molecules. Thus, the hydrophobic effect would favor aggregation of the molecules, and in dilute solutions dimers would form.

The Iverson group performed NMR titrations of the naphthalenes shown in Figure 6-1, to find the binding constants in different solutions.[5] The reason for using these naphthalenes in particular is that compound **6-1**, a dialkoxy naphthalene (DAN), is electron-rich, while compound **6-2**, naphthalene diimide (NDI), is electron poor. Figure 6-2 shows an electrostatic surface map of DAN and NDI. Red indicates greater electron density and blue means less electron density. By using naphthalenes with an electrostatic attraction, the Iverson group hoped to increase the binding constant for the dimer.

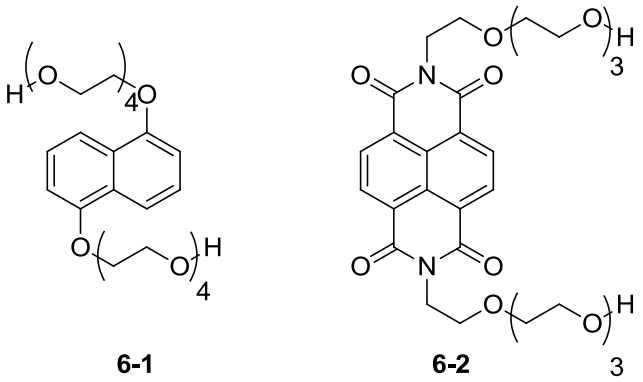

6-1 6-2

Figure 6-1 – The two naphthalenes used in the NMR titration

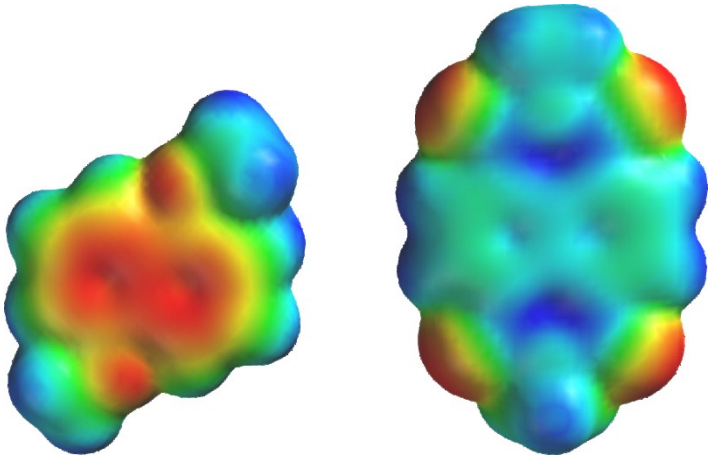

Figure 6-2 – An electrostatic surface mapping of DAN and NDI

The experimental data obtained by the Iverson group is shown in Table 6-1.[5] The data shows that the binding energy is largest in water and decreases with the polarity of the solvent. One would not expect the binding energy to increase with solvent polarity if the interaction were driven by the electrostatic attraction between the two molecules. As the polarity of the solvent increases it can shield the charge better and should decrease the interaction between the two molecules. Instead, the data suggest that the interaction is dominated by the hydrophobic effect; in an attempt to minimize disruption of the solvent-solvent interactions, the naphthalenes are pushed together.

Solvent	Free Energy
water	-4.5 kcal/mol
methanol	-2.0 kcal/mol
acetonitrile	-1.4 kcal/mol
acetone	-1.2 kcal/mol
DMSO	-0.7 kcal/mol
chloroform	-0.4 kcal/mol

Table 6-1 – The NMR binding data of the DAN:NDI dimer[5]

6-2 Computational Modeling of π-π Stacking with B3LYP

In collaboration with the Iverson group, the goal of the project described here was to use computational modeling to help understand what portion of the binding is driven by electrostatics and how much is driven by the hydrophobic effect. We began with density-functional theory (DFT) calculations using an implicit solvent model; because an implicit solvent model will not take solvent-solvent effects into account, the electrostatic portion of the interaction can be examined. All of the following calculations were performed with Spartan 08.[6] In order to reduce the computational time, the glycol chains on the naphthalenes are removed, since the binding we want to model is between the two π systems (Figure 6-3). To determine the interaction energy between naphthalenes **6-3** and **6-4**, three calculations need to be performed. The equilibrium geometries of compounds **6-3** and **6-4** are calculated separately, and then the equilibrium geometry of the dimer is modeled. The difference between the sum of the energies of compounds 6-3 and 6-4 and the energy of the dimer is the interaction energy.

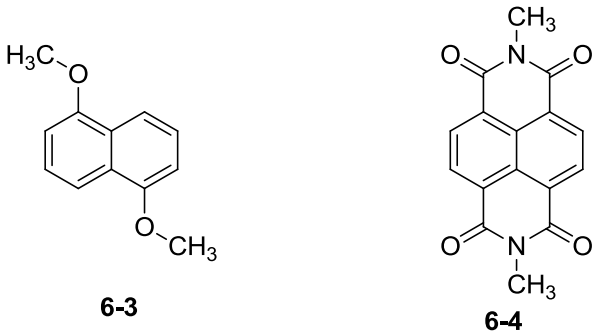

Figure 6-3 – The two naphthalenes being modeled

Initial calculations used the B3LYP functional and the 6-31G* basis set. The solvent model used was the SM8 solvent model,[7] an implicit, but sophisticated solvent model. It takes into account the surface area of the polar functional groups on the molecule and uses that as one of the many factors in determining the energy of solvation. One of the advantages of the SM8 model is that it adds a solvation term directly to the wavefunction. Thus, when a calculation is performed the solvation energy is taken into account during the minimization, rather than added on at the end like with many other solvent models. The equilibrium geometry obtained includes the solvation term, not just a vacuum geometry. The SM8 solvent model was developed and validated to reproduce experimental energies of solvation.[7] To the best of our knowledge, it has not been used to study the solvation of non-covalent dimers.

As an implicit solvent model, SM8 does not account for changes in solute-solvent interactions or solvent-solvent interactions, so these calculations do not reflect contributions from the hydrophobic effect. Instead only the electrostatic portion of the interaction is modeled. Thus, if the hydrophobic effect is a significant component of the interaction, these calculations will give smaller interaction energies than the experimental values, and changing solvent will give only minor differences in energy, compared to what has been observed experimentally.

In some of the calculations described below, a counterpoise (CP) correction is carried out in order to account for basis-set superposition error (BSSE).[8] BSSE arises when studying systems containing more than one molecule, if the chosen basis set is too small. The dimer can have apparent stabilization because the additional orbitals present in the dimer, compared to individual the monomers alone, provides added flexibility for the wavefunction. In order to decrease this error, a larger basis set can be used, but this leads to a longer calculation. Instead, the magnitude of the BSSE can be estimated, by performing a CP calculation, in which the energy of each monomer is calculated with the empty orbitals of the other monomer present. Unfortunately, the solvent model has not been implemented to handle the CP correction and gives an unrealistic energy of solvation if counterpoise is included.

The initial calculations show only a small interaction between the molecules with the specific solvent (implicit SM8 model) having only a very small effect on the interaction energy (Table 2). In vacuum, charge stabilization plays a greater role, leading to a much larger calculated interaction energy (4.0 kcal/mol). Any solvent helps to stabilize separation of charges, relative to vacuum, so the calculated dimer stabilization is smaller in solvent. The small calculated interaction energy is expected since the solvent model cannot describe the hydrophobic effect, but does take into account the electrostatics of the solvents.

Solvent	Experimental Data	CalculatedEnergy (kcal/mol)
water	-4.5 kcal/mol	-0.4
methanol	-2.0 kcal/mol	-0.4
acetonitrile	-1.4 kcal/mol	-0.6
acetone	-1.2 kcal/mol	-0.6
DMSO	-0.7 kcal/mol	-0.5
chloroform	-0.4 kcal/mol	-0.6
vacuum		-4.1 (-4.0 kcal/mol cp)

Table 6-2 – Interaction energies of DAN:NDI dimers (B3LYP/6-31G*, SM8 solvent model).

The orientation dependence of the interaction energy of the DAN:NDI dimer was also investigated. A variety of geometries were sampled, with different edges of one naphthalene positioned over the π–system of the other. Each orientation was given full freedom of movement during the geometry optimization. All of the calculations gave one of three minima, face-to-face, the edge of DAN pointing towards NDI, and the edge of NDI pointing towards DAN In water, the most stable DAN:NDI dimers were calculated to have the edge-to-face geometry, with only a 0.1 kcal/mol difference depending on which molecule is in the edge position.

To estimate the influence of the hydrophobic effect in this dimerization, we also examined the change in accessible surface area (ΔASA), i.e., the amount of surface area that is hidden when the molecules dimerize, for each of the DAN:NDI dimers.[9] The ΔASA provides a measure for the hydrophobic driving force for dimerization, depending on the dimer geometry. The edge-to-face geometries show similar ΔASA (~60 $Å^2$), but the face-to-face dimer has about 40 $Å^2$ more surface area that is hidden during dimerization (106 A^2 total).

As shown in Table 6-3 the different geometries of the homodimers were also investigated both in vacuum and with the SM8 solvent model in water. The DAN:DAN dimer shows the largest calculated interaction energy in water, -1.0 kcal/mol. The molecules are in an edge-to-

	Geometry	E_{calc} water (kcal/mol)	E_{calc} vacuum (kcal/mol)	ΔASA ($Å^2$)
DAN:NDI	face-face	-0.4	-4.0	106
	edge-face NDI on edge	-0.7		64
	edge-face DAN on edge	-0.8		60
DAN:DAN	slip face-face	-0.1	-1.9	79
	edge-face	-1	-2.3	56
NDI:NDI	face-face	0	-4.2	120
	edge-face	-0.1	-0.5	0
	slip face-face	-0.4	-4.2	113

Table 6-3 – The interaction energies of the DAN and NDI dimers (B3LYP/6-31G*/SM8)

face geometry similar to the one found in its crystal structure.[5] For the NDI:NDI dimer, the largest stabilization in water is in the slip-face-to-face geometry, which is the same geometry found in its crystal structure. The NDI:NDI face-to-face geometry also shows the largest ΔASA of any of the dimers. The NDI:NDI edge-to-face geometry shows only a small stabilization energy and no ΔASA because the molecules are not close together.

The calculated ΔASA values make it possible to estimate the contribution of the hydrophobic effect to overall free energies of interaction. Based on experimentally determined partition coefficients of mixtures of alkanes and water, Dill and coworkers have estimated a value of 40 cal/(mol*Å^2) for the energy of solvent-solvent interactions of water that are disrupted by a hydrophobic solute.[10] Multiplying the ΔASA by this value will give an approximate $E_{hydrophobic}$. Using this $E_{hydrophobic}$ term with the calculated interaction energy, the stabilization energy of the face-to-face dimer is 4.6 kcal/mol, and for both edge-to-face dimers, the stabilization energy is about 3.2 kcal/mol. In solution, both edge-to-face geometries have larger calculated interaction energies than the face-to-face dimer, but the face-to-face dimer is probably the predominant geometry, since it maximizes solvent-solvent interactions. If $E_{hydrophobic}$ is calculated for the homodimers, then the DAN:DAN dimer has a stabilization energy of 3.3 kcal/mol regardless of the geometry. For the NDI:NDI dimer, incorporating $E_{hydrophobic}$ gives stabilization energies of 4.7 kcal/mol for both the face-to-face and the slip-face-to-face geometry.

	Geometry	E_{calc} water (kcal/mol)	ΔASA (Å^2)	Estimated $E_{hdrophobic}$ (kcal/mol)	Estimated E_{total} (kcal/mol)
DAN:NDI	face-face	-0.4	106	-4.2	-4.6
	edge-face NDI on edge	-0.7	64	-2.6	-3.3
	edge-face DAN on edge	-0.8	60	-2.4	-3.2
DAN:DAN	slip face-face	-0.1	79	-3.2	-3.3
	edge-face	-1	56	-2.2	-3.2
NDI:NDI	face-face	0	120	-4.8	-4.8
	edge-face	-0.1	0	0	-0.1
	slip face-face	-0.4	113	-4.5	-4.9

Table 6-4 – The estimated E_{total} of the dimers

Comparing the different dimers shows that the NDI:NDI dimer and the DAN:NDI dimer have similar stabilization energies in solution of about 4.8 kcal/mol with $E_{hydrophobic}$, much larger than the experimentally determined value of 3.3 kcal/mol. The DAN:DAN has a smaller stabilization of only 3.3 kcal/mol, larger than the experimental value for the DAN:DAN dimer of 1.8 kcal/mol. These results indicate that the estimation of the hydrophobic effect does not reproduce all the experimental data and that further investigation is required.

It has been shown that B3LYP does not reproduce experimental values well for intermolecular interactions, such as hydrogen bonding.[11] Truhlar and coworkers have carried out a number of studies showing that most DFT functionals do not reproduce experimental intermolecular interactions well.[12] The Truhlar group has developed new functionals that attempt to model intermolecular interactions. These functionals were parameterized specifically to reproduce experimental data. A variety of new functionals have been reported, but the most promising are called M06 and M06-2X.[13] M06-2X is a functional that was specifically developed to model intermolecular interactions.

In order to evaluate the different functionals available, we chose the benzene dimer as the test case. The calculations on this small system should be very fast, and there is an agreed upon

value in the literature for the dimer stabilization energy (Table 6-5).[14] According to literature reports, the t-shape (**6-5**) and slip face-to-face (**6-6**) geometries of the benzene dimer were found to be lowest in energy (Figure 6-4).[14] The calculations that were performed on the benzene dimers with the B3LYP functional indicate almost no interaction energy, after including the counterpoise correction. The M06-2X functional gave the closest answer to the experimental value, but it still underestimated the interaction energy. In these calculations, the molecules adopt a geometry similar to a t-shaped dimer, but do not become totally orthogonal during the geometry optimizations. Although the M06 and M06-2X functionals underestimate the interaction energy, based on literature precedent[15] we decided to use them in place of B3LYP.

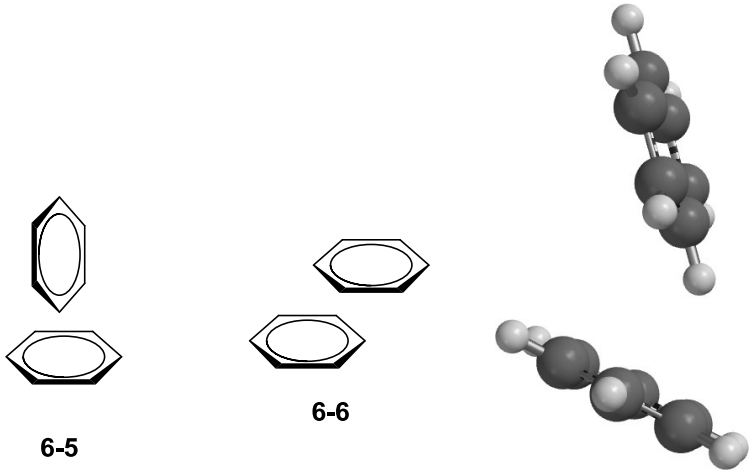

Figure 6-4 – The t-shaped and parallel displaced geometries and the minimum found in the M06-2X/6-31G* calculation.

Method	$E_{interaction}$ (kcal/mol)	CP corrected $E_{interaction}$ (kcal/mol)	Literature Value (kcal/mol)
B3LYP	-0.82	-0.03	-2.7
M06	-2.35	-1.47	
M06-2X	-3.17	-1.96	

Table 6-5 – Interaction energy of t-shaped benzene dimers in vacuum using the 6-31G* basis set

6-3 Modeling π-π Stacking with M06-2X

The previous computations on NDI and DAN dimers were repeated using the new functional (Table 6-6). Although M06-2X overestimates the interaction energy between the two molecules, the observed trend is similar to the experimental data, namely that the interaction energy increases with the polarity of the solvent. However, the calculated value in chloroform does not follow this trend.

Larger basis sets were also evaluated in vacuum calculations, but they give unexpected results. The largest basis set (6-311++G**) gives a larger BSSE than the medium level basis set (6-31+G**). The reason for the larger BSSE is unclear; perhaps the calculation did not reach a true energetic minima. The calculations with M06-2X and the SM8 solvent model show the naphthalenes 1 Å closer together than in the B3LYP calculations with SM8.

Solvent	$E_{interaction}$(kcal/mol)	$E_{cp\ correction}$(kcal/mol)
vacuum	-20.36	-15.34
water	-14.85	
methanol	-12.59	
acetonitrile	-12.49	
acetone	-11.77	
DMSO	-11.94	
chloroform	-13.06	
6-31+G**	-19.82	-18.24
6-311++G**	-21.6	-18.44

Table 6-6 – Interaction Energies of DAN:NDI dimer using M06-2X/6-31G* (unless otherwise noted)

The homodimers were also examined computationally (Table 6-7). The M06-2X functional again overestimate the interaction energy, and the calculations indicate very similar energies for dimers with very different geometries. These calculations were performed only in water and vacuum, to see if the results were worth pursuing in all of the solvents.

	Geometry	E_{calc} water(kcal/mol)	E_{calc} vacuum (kcal/mol)	E_{exp} (kcal/mol)
DAN:DAN	slip face-face	-8.1	-10.9	-1.8
	face-face	-8.6	-10.8	
NDI:NDI	face-face		-22.1	-3.3
	slip face-face		-23.6	

Table 6-7- The results of the homodimer studies using (M06-2X/6-31G*) and the SM8 solvent model.

Since the M06-2X/SM8 results overestimate the interaction energy, other solvent models were evaluated. Another solvent model that was used is Chipman's SS(V)PE (Surface Simulation of Volume Polarization for Electrostatics).[16] The model treats the solvent as a continuum, considering only the dielectric constant. The results (Table 6-8) indicate that as the dielectric constant decreases the interaction energy increases. The differences between solvents are minor, except for chloroform, which has the lowest dielectric constant and which is calculated to have the largest energy of interaction. These calculations were carried out using the M06-2X functional with the 6-31G* basis set.

Solvent	$E_{interaction}$ (kcal/mol)	Dielectric
water	-16.28	78.4
DMSO	-16.33	46.7
acetonitrile	-16.37	37.5
methanol	-16.39	32.7
acetone	-16.53	20.7
chloroform	-17.53	4.8

Table 6-8 – The interaction energy of DAN:NDI dimers (M06-2X/6-31G*) according to the SS(V)PE solvent model.

One thing to note about all of the previous calculations is that the interaction energy (enthalphy only) was compared to an experimentally obtained free energy. In order to get a free energy, a frequency calculation needs to be performed. After performing a frequency calculation, one can estimate the entropy using a rigid rotor approximation, and thereby obtain a free energy. The free energy of interaction for the DAN:NDI heterodimer was calculated in this

way. Using the M06-2X functional and 6-31G* basis set, this calculation gave a vacuum free energy of -5.3 kcal/mol. The free energy shows the importance of the entropy term since it reduces the interaction energy by 10 kcal/mol. Unfortunately, it is not practical to perform these calculations on a single computer: the frequency calculation on the DAN:NDI dimer took 300 hours to complete.

Wheeler, Houk and Swager found that the M06-2X functional overestimates the free energy in a study of Diels-Alder reactions.[17] They found that B3LYP reproduced the experimental values the best. This was presumed to be due to cancellation of errors.

6-4 Summary and Future Plans

A computational study of the dimerization of two napthalenes was investigated. The B3LYP functional gave the expected result, a small interaction energy that is similar in all the solvents. The M06-2X functional, which was developed for intermolecular interactions, gave very large interaction energies, but further calculations suggest that entropy plays a significant role in this system. Since the calculations performed are only able to model the electrostatic interaction and not the hydrophobic effect, it was decided to use explicit solvent to explore the hydrophobic effect.

In collaboration with Prof. Marivi Fernandez-Serra (SBU Physics) we plan to perform DFT calculations with explicit water molecules. Using explicit water will take into account the interaction between solvent and the π-system that is lost in a continuum model. Initial attempts will use molecular dynamics (MD) with the AMBER force field. These calculations use much less computational time, so a large variety of MD simulations can be performed, and those that seem promising can be performed at the DFT level.

6-5 Computational Methods

Calculations were performed with the program Spartan.[6] All calculations were optimized with the specific functional with the 6-31G* basis set, unless otherwise noted.

6-6 References

1. Meyer, E. A.; Castellano, R. K.; Diederich, F., Interactions with Aromatic Rings in Chemical and Biological Recognition. *Angewandte Chemie International Edition* **2003,** *42* (11), 1210-1250.
2. Grimme, S., Do Special Noncovalent π–π Stacking Interactions Really Exist? *Angewandte Chemie International Edition* **2008,** *47* (18), 3430-3434.
3. Martinez, C. R.; Iverson, B. L., Rethinking the term "pi-stacking". *Chemical Science* **2012,** *3* (7), 2191-2201.
4. Southall, N. T.; Dill, K. A.; Haymet, A. D. J., A View of the Hydrophobic Effect. *The Journal of Physical Chemistry B* **2001,** *106* (3), 521-533.
5. Cubberley, M. S.; Iverson, B. L., ^{1}H NMR investigation of solvent effects in aromatic stacking interactions. *J. Am. Chem. Soc.* **2001,** *123* (31), 7560-7563.
6. *Spartan '08*, 5.1; Wavefunction, Inc.: Irvine, CA.
7. Marenich, A. V.; Olson, R. M.; Kelly, C. P.; Cramer, C. J.; Truhlar, D. G., Self-Consistent Reaction Field Model for Aqueous and Nonaqueous Solutions Based on Accurate Polarized Partial Charges. *Journal of Chemical Theory and Computation* **2007,** *3* (6), 2011-2033.
8. Schwenke, D. W.; Truhlar, D. G., Systematic study of basis set superposition errors in the calculated interaction energy of two HF molecules. *J. Chem. Phys.* **1985,** *82* (5), 2418.
9. ΔASA is calculated with SPARTAN08 using a 1.4 angstrom solvent probe (the coulombic radii of water).
10. Brem, R.; Chan, H. S.; Dill, K. A., Extracting Microscopic Energies from Oil-Phase Solvation Experiments. *The Journal of Physical Chemistry B* **2000,** *104* (31), 7471-7482.
11. Del Bene, J. E.; Person, W. B.; Szczepaniak, K., Properties of Hydrogen-Bonded Complexes Obtained from the B3LYP Functional with 6-31G(d,p) and 6-31+G(d,p) Basis Sets: Comparison with MP2/6-31+G(d,p) Results and Experimental Data. *The Journal of Physical Chemistry* **1995,** *99* (27), 10705-10707.
12. Zhao, Y.; Schultz, N. E.; Truhlar, D. G., Design of Density Functionals by Combining the Method of Constraint Satisfaction with Parametrization for Thermochemistry, Thermochemical Kinetics, and Noncovalent Interactions. *Journal of Chemical Theory and Computation* **2006,** *2* (2), 364-382.
13. Zhao, Y.; Truhlar, D. G., Density Functionals with Broad Applicability in Chemistry. *Acc. Chem. Res.* **2008,** *41* (2), 157-167.
14. Sinnokrot, M. O.; Valeev, E. F.; Sherrill, C. D., Estimates of the Ab Initio Limit for π–π Interactions: The Benzene Dimer. *J. Am. Chem. Soc.* **2002,** *124* (36), 10887-10893.

15. Vura-Weis, J.; Ratner, M. A.; Wasielewski, M. R., Geometry and Electronic Coupling in Perylenediimide Stacks: Mapping Structure−Charge Transport Relationships. *J. Am. Chem. Soc.* **2010,** *132* (6), 1738-1739.
16. Chipman, D. M., Reaction field treatment of charge penetration. *J. Chem. Phys.* **2000,** *112*, 5558.
17. Wheeler, S. E.; McNeil, A. J.; Müller, P.; Swager, T. M.; Houk, K. N., Probing Substituent Effects in Aryl−Aryl Interactions Using Stereoselective Diels−Alder Cycloadditions. *J. Am. Chem. Soc.* **2010,** *132* (10), 3304-3311.

References

Chapter 1

1. Eisenberg, D.; Shenhar, R.; Rabinovitz, M., Synthetic approaches to aromatic belts: building up strain in macrocyclic polyarenes. *Chem. Soc. Rev.* **2010,** *39* (8), 2879-2890.
2. Neudorff, W. D.; Lentz, D.; Anibarro, M.; Schlüter, A. D., The Carbon Skeleton of the Belt Region of Fullerene C84 (D2). *Chem. Eur. J.* **2003,** *9* (12), 2745-2757.
3. Vögtle, F., Concluding remarks. *Top. Curr. Chem.* **1983,** *115*, 157-159.
4. Heilbronner, E., Molecular Orbitals in homologen Reihen mehrkerniger aromatischer Kohlenwasserstoffe: I. Die Eigenwerte yon LCAO-MO's in homologen Reihen. *Helv. Chim. Acta* **1954,** *37* (3), 921-935.
5. (a) Kroto, H. W.; Heath, J. R.; O'Brien, S. C.; Curl, R. F.; Smalley, R. E., C_{60}: Buckminsterfullerene. *Nature* **1985,** *318*, 162-164; (b) Iijima, S., Helical microtubules of graphitic carbon. *Nature* **1991,** *354* (6348), 56-58.
6. Scott, L. T., Conjugated belts and nanorings with radially oriented π orbitals. *Angew. Chem. Int. Ed.* **2003,** *42*, 4133-4135.
7. Kawase, T.; Kurata, H., Ball-, bowl-, and belt-shaped conjugated systems and their complexing abilities: Exploration of the concave-convex pi-pi interaction. *Chem. Rev.* **2006,** *106* (12), 5250-5273.
8. (a) Houk, K. N.; Lee, P. S.; Nendel, M., Polyacene and cyclacene geometries and electronic structures: Bond equalization, vanishing band gaps, and triplet ground states contrast with polyacetylene. *J. Org. Chem.* **2001,** *66* (16), 5517-5521; (b) Fokin, A. A.; Jiao, H.; Schleyer, P. v. R., From dodecahedrapentaene to the "[n]trannulenes". A new in-plane aromatic family. *J. Am. Chem. Soc.* **1998,** *120*, 9364-9365; (c) Choi, H. S.; Kim, K. S., Structures, Magnetic Properties, and Aromaticity of Cyclacenes. *Angew. Chem. Int. Ed.* **1999,** *38* (15), 2256-2258; (d) Turker, L.; Celebi, N., Some properties of cyclacenes and silacyclacenes. *Bull. Soc. Chim. Belg.* **1997,** *106* (4), 201-204; (e) Turker, L., AM1 treatment of cyclacene tubes. *Theochem* **1999,** *490*, 55-60; (f) Türker, L., Zigzag cyclopolyacenes: a theoretical study. *Theochem* **1999,** *491* (1–3), 275-280.
9. Aihara, J.-i., Aromaticity and superaromaticity in cyclopolyacenes. *J. Chem. Soc. Perk. Trans. 2* **1994,** (5), 971-974.
10. Baughman, R. H.; Zakhidov, A. A.; de Heer, W. A., Carbon Nanotubes--the Route Toward Applications. *Science* **2002,** *297* (5582), 787-792.
11. (a) Fort, E. H.; Donovan, P. M.; Scott, L. T., Diels−Alder Reactivity of Polycyclic Aromatic Hydrocarbon Bay Regions: Implications for Metal-Free Growth of Single-Chirality Carbon Nanotubes. *J. Am. Chem.Soc.* **2009,** *131* (44), 16006-16007; (b) Steinberg, B. D.; Scott, L. T., New Strategies for Synthesizing Short Sections of Carbon Nanotubes. *Angew. Chem. Int. Ed.* **2009,** *48* (30), 5400-5402; (c) Fort, E.; Scott, L., One-Step Conversion of Aromatic Hydrocarbon Bay Regions into Unsubstituted Benzene Rings: A Reagent for the Low-Temperature, Metal-Free Growth of Single-Chirality Carbon Nanotubes. *Angew. Chem. Int. Ed.* **2010,** *49* (37), 6626-6628; (d) Fort, E. H.; Scott, L. T., Carbon nanotubes from short hydrocarbon templates. Energy analysis of the Diels-Alder cycloaddition/rearomatization growth strategy. *J.*

Mat. Chem. **2011,** *21* (5), 1373-1381; (e) Fort, E. H.; Scott, L. T., Gas-phase Diels–Alder cycloaddition of benzyne to an aromatic hydrocarbon bay region: Groundwork for the selective solvent-free growth of armchair carbon nanotubes. *Tetrahedron Lett.* **2011,** *52* (17), 2051-2053.
12. Louie, S. G., Electronic properties, junctions, and defects of carbon nanotubes. *Carbon Nanotubes* **2001,** *80*, 113-145.
13. Vögtle, F.; Schröder, A.; Karbach, D., Strategy for the Synthesis of Tube-Shaped Molecules. *Angew. Chem. Int. Ed. Eng.* **1991,** *30* (5), 575-577.
14. Mitchell, R. H.; Boekelheide, V., Syntheses of [2.2]metacyclophane-1,9-diene and trans-15,16-dihydropyrene. *J. Am. Chem. Soc.* **1970,** *92* (11), 3510-3512.
15. (a) Ashton, P. R.; Brown, G. R.; Isaacs, N. S.; Giuffrida, D.; Kohnke, F. H.; Mathias, J. P.; Slawin, A. M. Z.; Smith, D. R.; Stoddart, J. F.; Williams, D. J., Molecular LEGO. 1. Substrate-directed synthesis via stereoregular Diels-Alder oligomerizations. *J. Am. Chem. Soc.* **1992,** *114* (16), 6330-6353; (b) Mathias, J. P.; Stoddart, J. F., Constructing a Molecular Lego Set. *Chem. Soc. Rev.* **1992,** *21* (4), 215-225; (c) Ashton, P. R.; Girreser, U.; Giuffrida, D.; Kohnke, F. H.; Mathias, J. P.; Raymo, F. M.; Slawin, A. M. Z.; Stoddart, J. F.; Williams, D. J., Molecular belts. 2. Substrate-directed syntheses of belt-type and cage-type structures. *J. Am. Chem. Soc.* **1993,** *115* (13), 5422-5429; (d) Kohnke, F. H.; Slawin, A. M. Z.; Stoddart, J. F.; Williams, D. J., Molecular Belts and Collars in the Making: A Hexaepoxyoctacosahydro[12]cyclacene Derivative. *Angew. Chem. Int. Ed. Eng.* **1987,** *26* (9), 892-894; (e) Ashton, P. R.; Isaacs, N. S.; Kohnke, F. H.; Slawin, A. M. Z.; Spencer, C. M.; Stoddart, J. F.; Williams, D. J., Towards the Making of [12]Collarene. *Angew. Chem. Int. Ed. Eng.* **1988,** *27* (7), 966-969.
16. (a) Cory, R. M.; McPhail, C. L., Transformations of a macrocyclic cyclophane belt into advanced [8]cyclacene and [8]cyclacene triquinone precursors. *Tetrahedron Lett.* **1996,** *37* (12), 1987-1990; (b) Cory, R. M.; McPhail, C. L.; Dikmans, A. J.; Vittal, J. J., Macrocyclic cyclophane belts via double diels-alder cycloadditions: Macroannulation of bisdienes by bisdienophiles. Synthesis of a key precursor to an [8]cyclacene. *Tetrahedron Lett.* **1996,** *37* (12), 1983-1986.
17. Kuwatani, Y.; Yoshida, T.; Kusaka, A.; Iyoda, M., All-Z-Tribenzo[12]-, tetrabenzo[16]- and pentabenzo[20]annulenes. *Tetrahedron Lett.* **2000,** *41* (3), 359-363.
18. Kuwatani, Y.; Yoshida, T.; Igarashi, J.-I.; Iyoda, M. In *Synthesis and properties of ALL-Z-pentabenzo[20]- and hexabenzo[24]annulenes*, 10th International Symposium on Novel Aromatics, San Diego, CA, August 4-8, 2001; San Diego, CA, 2001.
19. (a) Brooks, M. A. 1,2-Shifts in Aryl Radicals and Synthetic Routes Toward Cyclo[12]phenacene: A Molecular Belt. Dissertation, Boston College, Chestnut Hill, MA, 1998; (b) St.Martin-Davis, H. M. Synthetic Routes Towards Cyclo[N]phenacenes and [8]Circulene: Molecular Belts and Saddles. Dissertation, Boston College, Chestnut Hill, MA, 2002.
20. Scott, L. T.; Boorum, M. M.; McMahon, B. J.; Hagen, S.; Mack, J.; Blank, J.; Wegner, H.; de Meijere, A., A rational chemical synthesis of C_{60} *Science* **2002,** *295*, 1500-1503.
21. Kammermeier, S.; Jones, P. G.; Herges, R., Ring-Expanding Metathesis of Tetradehydro-anthracene—Synthesis and Structure of a Tubelike, Fully Conjugated Hydrocarbon. *Angew. Chem. Int. Ed. Eng.* **1996,** *35* (22), 2669-2671.
22. Viavattene, R. L.; Greene, F. D.; Cheung, L. D.; Majeste, R.; Trefonas, L. M., 9,9',10,10'-Tetradehydrodianthracene. Formation, protection, and regeneration of a strained double bond. *J. Am. Chem. Soc.* **1974,** *96* (13), 4342-4343.

23. Deichmann, M.; Näther, C.; Herges, R., Pyrolysis of a Tubular Aromatic Compound. *Org. Lett.* **2003,** *5* (8), 1269-1271.
24. Matsuo, Y.; Tahara, K.; Sawamura, M.; Nakamura, E., Creation of hoop- and bowl-shaped benzenoid systems by selective detraction of 60 fullerene conjugation. 10 cyclophenacene and fused corannulene derivatives. *J. Am. Chem. Soc.* **2004,** *126* (28), 8725-8734.
25. Gleiter, R.; Esser, B.; Kornmayer, S. C., Cyclacenes: Hoop-Shaped Systems Composed of Conjugated Rings. *Acc. Chem. Res.* **2009,** *42* (8), 1108-1116.
26. Esser, B.; Bandyopadhyay, A.; Rominger, F.; Gleiter, R., From Metacyclophanes to Cyclacenes: Synthesis and Properties of [6.8]3Cyclacene. *Chem. Eur. J.* **2009,** *15* (14), 3368-3379.
27. Kornmayer, S. C.; Esser, B.; Gleiter, R., DFT Calculations on Heterocyclacenes. *Org. Lett.* **2009,** *11* (3), 725-728.
28. Yao, T.; Yu, H.; Vermeij, R. J.; Bodwell, G. J., Nonplanar aromatic compounds. Part 10: A strategy for the synthesis of aromatic belts - all wrapped up or down the tubes? *Pure and Appl. Chem.* **2008,** *80*, 533-546.
29. Zhang, B.; Gregory P. Manning; Michał A. Dobrowolski; Cyranski, M. K.; Bodwell, G. J., Nonplanar aromatic compounds. 9. Synthesis, structure, and aromaticity of 1:2,13:14-dibenzo[2]paracyclo[2](2,7)-pyrenophane-1,13-diene. *Org. Lett.* **2008,** *10*, 273-376.
30. Bodwell, G., Personal Communication. 2009.
31. (a) Stuparu, M.; Lentz, D.; Rüegger, H.; Schlüter, A. D., Exploring the Chemistry of a Double-Stranded Cycle with the Carbon Skeleton of the Belt Region of the C84 Fullerene. *Eur. J. Org. Chem.* **2007,** *2007* (1), 88-100; (b) Denekamp, C.; Etinger, A.; Amrein, W.; Stanger, A.; Stuparu, M.; Schlüter, A. D., Towards a Fully Conjugated, Double-Stranded Cycle: A Mass Spectrometric and Theoretical Study. *Chem. Eur. J.* **2008,** *14* (5), 1628-1637; (c) Standera, M.; Hafliger, R.; Gershoni-Poranne, R.; Stanger, A.; Jeschke, G.; van Beek, J. D.; Bertschi, L.; Schluter, A. D., Evidence for Fully Conjugated Double-Stranded Cycles. *Chem. Eur. J.* **2011,** *17* (43), 12163-12174.

Chapter 2

1. Katsamanis, Z. E. Designing a Template-Directed Synthesis of Nonplanar Polycyclic Aromatic Belts. Stony Brook University, Stony Brook, NY, 2005.
2. Cui, L. Buckybelt Synthesis: Template Directed Approach Towards Cyclophenacene. Stony Brook University, Stony Brook, NY, 2006.
3. Zhou, L. Synthesis Different Tethered Compounds for Cylindrically Conjugated Organic Belts and Synthesis of Three-Dimensional Assemblies of Chromophores of FRET Studies. Stony Brook University, Stony Brook, NY, 2006.
4. Szejtli, J., Introduction and general overview of cyclodextrin chemistry. *Chem. Rev.* **1998,** *98* (5), 1743-1753.
5. Anderson, D. R.; Hickstein, D. D.; O'Leary, D. J.; Grubbs, R. H., Model Compounds of Ruthenium−Alkene Intermediates in Olefin Metathesis Reactions. *J. Am. Chem. Soc.* **2006,** *128* (26), 8386-8387.
6. Diederich, F.; Staab, H. A., Benzenoid versus Annulenoid Aromaticity: Synthesis and Properties of Kekulene. *Angewandte Chemie International Edition in English* **1978,** *17* (5), 372-374.
7. McMurry, J. E., Carbonyl-coupling reactions using low-valent titanium. *Chem. Rev.* **1989,** *89* (7), 1513-1524.
8. Höger, S.; Meckenstock, A.-D.; Pellen, H., High-yield macrocyclization via Glaser coupling of temporary covalent templated bisacetylenes. *J. Org. Chem.* **1997,** *62*, 4556-4557.
9. Trnka, T. M.; Grubbs, R. H., The development of $L_2X_2Ru{=}CHR$ olefin metathesis catalysts: An organometallic success story. *Acc. Chem. Res.* **2001,** *34* (1), 18-29.

Chapter 3

1. (a) Mallory, F. B.; Butler, K. E.; Evans, A. C.; Mallory, C. W., Phenacenes: A family of graphite ribbons. 1. Syntheses of some [7]phenacenes by stilbene-like photocyclizations. *Tetrahedron Lett.* **1996,** *37* (40), 7173-7176; (b) Mallory, F. B.; Butler, K. E.; Evans, A. C.; Brondyke, E. J.; Mallory, C. W.; Yang, C. Q.; Ellenstein, A., Phenacenes: A family of graphite ribbons. 2. Syntheses of some [7]phenacenes and an [11]phenacene by stilbene-like photocyclizations. *J. Am. Chem. Soc.* **1997,** *119* (9), 2119-2124; (c) Mallory, F. B.; Butler, K. E.; Berube, A.; Luzik, E. D.; Mallory, C. W.; Brondyke, E. J.; Hiremath, R.; Ngo, P.; Carroll, P. J., Phenacenes: a family of graphite ribbons. Part 3: Iterative strategies for the synthesis of large phenacenes. *Tetrahedron* **2001,** *57* (17), 3715-3724.
2. Beckhaus, H. D.; Verevkin, S.; Ruechardt, C.; Diederich, F.; Thilgen, C.; ter Meer, H. U.; Mohn, H.; Mueller, W., C70 is as stable as C60: experimental determination of the heat of formation of C70. *Angew. Chem., Int. Ed. Engl.* **1994,** *33* (9), 996-8.
3. Scott, L. T.; Boorum, M. M.; McMahon, B. J.; Hagen, S.; Mack, J.; Blank, J.; Wegner, H.; de Meijere, A., A rational chemical synthesis of C_{60} *Science* **2002,** *295*, 1500-1503.
4. Cui, L. Buckybelt Synthesis: Template Directed Approach Towards Cyclophenacene. Stony Brook University, Stony Brook, NY, 2006.
5. (a) Lerstrup, K.; Bailey, A.; McCullough, R.; Mays, M.; Cowan, D.; Kistenmacher, T., The synthesis and study of new selenium and tellurium heterocyclic w-donors. *Synth. Met.* **1987,** *19*, 647-652; (b) Bailey, A. B.; McCullough, R. D.; Mays, M. D.; Cowan, D. O.; Lerstrup, K. A., New organic π-donors: Analogues of HMTSF and HMTTeF. *Synth. Met.* **1988,** *27* (3-4), 425-430.
6. Huang, H.-C.; Reitz, D. R. Substituted cyclopentadienyl compounds for the treatment of inflammation. 5663180, 1997.
7. Süleyman, G.; Hasan, S., Concise syntheses of 2-aminoindans via indan-2-ol. *Tetrahedron* **2005,** *61* (28), 6801-6807.
8. Kantchev, E. A. B.; O'Brien, C. J.; Organ, M. G., Palladium Complexes of N-Heterocyclic Carbenes as Catalysts for Cross-Coupling Reactions—A Synthetic Chemist's Perspective. *Angew. Chem. Int. Ed.* **2007,** *46* (16), 2768-2813.
9. Yamazaki, S.; Yoshimura, T.; Yamabe, S.; Arai, T.; Tamura, H., Synthesis and unusual selenium extrusion reaction of a cyclic triselenide. *J. Org. Chem.* **1990,** *55* (1), 263-269.
10. McMurry, J. E., Titanium-induced dicarbonyl-coupling reactions. *Acc. Chem. Res.* **1983,** *16* (11), 405-411.
11. Kilway, K. V.; Siegel, J. S., Control of functional group proximity and direction by conformational networks: synthesis and stereodynamics of persubstituted arenes. *Tetrahedron* **2001,** *57* (17), 3615-3627.

Chapter 4

1. Cossy, J.; Lutz, F.; Alauze, V.; Meyer, C., Carbon-carbon bond forming reactions by using bistrifluoromethanesulfonimide. *Synlett* **2002**, 45–48.
2. Cazeau, P.; Duboudin, F.; Moulines, F.; Babot, O.; Dunogues, J., A new practical synthesis of silyl enol ethers : Part.I. From simple aldehydes and ketones. *Tetrahedron* **1987,** *43* (9), 2075-2088.
3. Liu, L.; Yang, B.; Katz, T. J.; Poindexter, M. K., Improved methodology for photocyclization reactions. *J. Org. Chem.* **1991,** *56* (12), 3769-75.
4. Wiles, C.; Watts, P.; Haswell, S. J.; Pombo-Villar, E., The regioselective preparation of 1,3-diketones. *Tetrahedron Lett.* **2002,** *43* (16), 2945-2948.
5. Mallory, F. B.; Mallory, C. W., Photocyclization of stilbenes and related molecules. *Org. Reactions* **1984,** *30*, 1-456.
6. Mallory, F. B.; Mallory, C. W., personal communication. 2010.
7. Purushothaman, E.; Pillai, V. N. R., Photoreactions of 4,5-diarylimidazoles - singlet oxygenation and cyclodehydrogenation. *Indian J. Chem. Sect B-Org. Chem. Incl. Med. Chem.* **1989,** *28* (4), 290-293.
8. Pétrier, C.; L. Gemal, A.; Luche, J.-L., Ultrasounds in organic synthesis 31. A simple, high yield modification of the bouveault reaction. *Tetrahedron Lett.* **1982,** *23* (33), 3361-3364.
9. Littke, A. F.; Schwarz, L.; Fu, G. C., Pd/P(t-Bu)3: A mild and general catalyst for Stille reactions of aryl chlorides and aryl bromides. *J. Am. Chem. Soc.* **2002,** *124* (22), 6343-6348.
10. Chobanian, H. R.; Fors, B. P.; Lin, L. S., A facile microwave-assisted palladium-catalyzed cyanation of aryl chlorides. *Tetrahedron* **2006,** *47*, 3303–3305.
11. Yin, J. J.; Rainka, M. P.; Zhang, X. X.; Buchwald, S. L., A highly active Suzuki catalyst for the synthesis of sterically hindered biaryls: Novel ligand coordination. *J. Am. Chem. Soc.* **2002,** *124* (7), 1162-1163.
12. Jung, M. E.; Lyster, M. A., Quantitative dealkylation of alkyl ethers via treatment with trimethylsilyl iodide. A new method for ether hydrolysis. *J. Org. Chem* **1977,** *42* (23), 3761-3764.
13. Park, J.; Lang, K.; Abboud, K. A.; Hong, S., Self-Assembled Dinuclear Cobalt(II)-Salen Catalyst Through Hydrogen-Bonding and Its Application to Enantioselective Nitro-Aldol (Henry) Reaction. *J. Am. Chem. Soc.* **2008,** *130* (49), 16484-16485.
14. Gil, L.; Han, Y.; Opas, E. E.; Rodan, G. A.; Ruel, R.; Seedor, J. G.; Tyler, P. C.; Young, R. N., Prostaglandin E2-bisphosphonate conjugates: potential agents for treatment of osteoporosis. *Bioorg. Med. Chem.* **1999,** *7* (5), 901-919.
15. Akiyama, T.; Shima, H.; Ozaki, S., A concise synthesis of (−)-conduritol F from l-quebrachitol via AlCl3-n-Bu4NI mediated demethylation. *Tetrahedron Lett.* **1991,** *32* (40), 5593-5596.
16. Node, M.; Ohta, K.; Kajimoto, T.; Nishide, K.; Fujita, E.; Fuji, K., Selective demtyhlation of aliphatic methyl ether in the presence of aromatic methyl ether with the aluminum chloride-sodium iodide-acetonitrile system. *Chem. Pharm. Bul.* **1983,** *31* (11), 4178-4180.
17. Grieco, P. A.; Speake, J. D., Synthetic Studies on Quassinoids: Total Synthesis and Biological Evaluation of (+)-Des-d-chaparrinone. *J. Org. Chem.* **1998,** *63* (17), 5929-5936.

18. Jin, F.; Confalone, P. N., Palladium-catalyzed cyanation reactions of aryl chlorides. *Tetrahedron Lett.* **2000,** *41* (18), 3271-3273.
19. Kerr, W. J.; Watson, A. J. B.; Hayes, D., In situ generation of Mes2Mg as a non-nucleophilic carbon-centred base reagent for the efficient one-pot conversion of ketones to silyl enol ethers. *Org. Biomol. Chem.* **2008,** *6* (7), 1238-1243.
20. Yamashita, M.; Yamada, K.-i.; Tomioka, K., Construction of Arene-Fused-Piperidine Motifs by Asymmetric Addition of 2-Trityloxymethylaryllithiums to Nitroalkenes: The Asymmetric Synthesis of a Dopamine D1 Full Agonist, A-86929. *J. Am. Chem. Soc.* **2004,** *126* (7), 1954-1955.
21. Saitoh, T.; Oyama, T.; Sakurai, K.; Niimura, Y.; Hinata, M.; Horiguchi, Y.; Toda, J.; Sano, T., Thermal Addition Reaction of Aroylketene with 1-Aryl-1-trimethylsilyloxyethylenes : Aromatic Substituent Effects of Aroylketene and Aryltrimethylsilyloxyethylene on Their Reactivity. *Chem. Pharm. Bull.* **1996,** *44* (5), 956-966.
22. Fuglseth, E.; Thvedt, T. H. K.; Møll, M. F.; Hoff, B. H., Electrophilic and nucleophilic side chain fluorination of para-substituted acetophenones. *Tetrahedron* **2008,** *64* (30–31), 7318-7323.
23. I. Bowers, N.; R. Boyd, D.; D. Sharma, N.; A. Goodrich, P.; R. Groocock, M.; John Blacker, A.; Goode, P.; Dalton, H., Stereoselective benzylic hydroxylation of 2-substituted indanes using toluene dioxygenase as biocatalyst. *J. Chem. Soc., Perkin Trans. 1* **1999,** (11), 1453-1462.
24. Arrowsmith, M.; Hadlington, T. J.; Hill, M. S.; Kociok-Kohn, G., Magnesium-catalysed hydroboration of aldehydes and ketones. *Chem. Commun.* **2012,** *48* (38), 4567-4569.

Chapter 5

1. Iverson, D. J.; Hunter, G.; Blount, J. F.; Damewood, J. R.; Mislow, K., Static and dynamic stereochemistry of hexaethylbenzene and of its tricarbonylchromium, tricarbonylmolybdenum, and dicarbonyl(triphenylphosphine)chromium complexes. *J. Am. Chem. Soc.* **1981,** *103* (20), 6073-6083.
2. Kilway, K. V.; Siegel, J. S., Control of functional group proximity and direction by conformational networks: synthesis and stereodynamics of persubstituted arenes. *Tetrahedron* **2001,** *57* (17), 3615-3627.
3. Vacca, A.; Nativi, C.; Cacciarini, M.; Pergoli, R.; Roelens, S., A new tripodal receptor for molecular recognition of monosaccharides. A paradigm for assessing glycoside binding affinities and selectivities by 1H NMR spectroscopy. *J. Am. Chem. Soc.* **2004,** *126* (50), 16456-16465.
4. Arduengo, A. J.; Stewart, C. A.; Davidson, F.; Dixon, D. A.; Becker, J. Y.; Culley, S. A.; Mizen, M. B., The synthesis, structure, and chemistry of 10-Pn-3 systems: tricoordinate hypervalent pnicogen compounds. *J. Am. Chem. Soc.* **1987,** *109* (3), 627-647.
5. Tang, G.; Ji, T.; Hu, A.-F.; Zhao, Y.-F., Novel N,S-Phenacyl Protecting Group and Its Application for Peptide -Synthesis. *Synlett* **2008,** *2008* (EFirst), 1907-1909.
6. (a) Brooks, M. A. 1,2-Shifts in Aryl Radicals and Synthetic Routes Toward Cyclo[12]phenacene: A Molecular Belt. Dissertation, Boston College, Chestnut Hill, MA, 1998; (b) St.Martin-Davis, H. M. Synthetic Routes Towards Cyclo[N]phenacenes and [8]Circulene: Molecular Belts and Saddles. Dissertation, Boston College, Chestnut Hill, MA, 2002.
7. Eisenberg, D.; Shenhar, R.; Rabinovitz, M., Synthetic approaches to aromatic belts: building up strain in macrocyclic polyarenes. *Chem. Soc. Rev.* **2010,** *39* (8), 2879-2890.
8. Chambers, R. R.; Collins, C. J.; Maxwell, B. E., Reductive debenzylation of 1-benzylnaphthalene by a sodium-potassium alloy. *J. Org. Chem.* **1985,** *50* (24), 4960-4963.
9. Wolfe, J. P.; Singer, R. A.; Yang, B. H.; Buchwald, S. L., Highly active palladium catalysts for Suzuki coupling reactions. *J. Am. Chem. Soc.* **1999,** *121* (41), 9550-9561.
10. Tang, X.-Q.; Harvey, R. G., A Convenient Synthesis of Benzo[s]picene. *J. Org. Chem.* **1995,** *60* (11), 3568-3568.

Chapter 6

1. Meyer, E. A.; Castellano, R. K.; Diederich, F., Interactions with Aromatic Rings in Chemical and Biological Recognition. *Angewandte Chemie International Edition* **2003,** *42* (11), 1210-1250.
2. Grimme, S., Do Special Noncovalent π–π Stacking Interactions Really Exist? *Angewandte Chemie International Edition* **2008,** *47* (18), 3430-3434.
3. Martinez, C. R.; Iverson, B. L., Rethinking the term "pi-stacking". *Chemical Science* **2012,** *3* (7), 2191-2201.
4. Southall, N. T.; Dill, K. A.; Haymet, A. D. J., A View of the Hydrophobic Effect. *The Journal of Physical Chemistry B* **2001,** *106* (3), 521-533.
5. Cubberley, M. S.; Iverson, B. L., ^{1}H NMR investigation of solvent effects in aromatic stacking interactions. *J. Am. Chem. Soc.* **2001,** *123* (31), 7560-7563.
6. *Spartan '08*, 5.1; Wavefunction, Inc.: Irvine, CA.
7. Marenich, A. V.; Olson, R. M.; Kelly, C. P.; Cramer, C. J.; Truhlar, D. G., Self-Consistent Reaction Field Model for Aqueous and Nonaqueous Solutions Based on Accurate Polarized Partial Charges. *Journal of Chemical Theory and Computation* **2007,** *3* (6), 2011-2033.
8. Schwenke, D. W.; Truhlar, D. G., Systematic study of basis set superposition errors in the calculated interaction energy of two HF molecules. *J. Chem. Phys.* **1985,** *82* (5), 2418.
9. ΔASA is calculated with SPARTAN08 using a 1.4 angstrom solvent probe (the coulombic radii of water).
10. Brem, R.; Chan, H. S.; Dill, K. A., Extracting Microscopic Energies from Oil-Phase Solvation Experiments. *The Journal of Physical Chemistry B* **2000,** *104* (31), 7471-7482.
11. Del Bene, J. E.; Person, W. B.; Szczepaniak, K., Properties of Hydrogen-Bonded Complexes Obtained from the B3LYP Functional with 6-31G(d,p) and 6-31+G(d,p) Basis Sets: Comparison with MP2/6-31+G(d,p) Results and Experimental Data. *The Journal of Physical Chemistry* **1995,** *99* (27), 10705-10707.
12. Zhao, Y.; Schultz, N. E.; Truhlar, D. G., Design of Density Functionals by Combining the Method of Constraint Satisfaction with Parametrization for Thermochemistry, Thermochemical Kinetics, and Noncovalent Interactions. *Journal of Chemical Theory and Computation* **2006,** *2* (2), 364-382.
13. Zhao, Y.; Truhlar, D. G., Density Functionals with Broad Applicability in Chemistry. *Acc. Chem. Res.* **2008,** *41* (2), 157-167.
14. Sinnokrot, M. O.; Valeev, E. F.; Sherrill, C. D., Estimates of the Ab Initio Limit for π–π Interactions: The Benzene Dimer. *J. Am. Chem. Soc.* **2002,** *124* (36), 10887-10893.
15. Vura-Weis, J.; Ratner, M. A.; Wasielewski, M. R., Geometry and Electronic Coupling in Perylenediimide Stacks: Mapping Structure−Charge Transport Relationships. *J. Am. Chem. Soc.* **2010,** *132* (6), 1738-1739.
16. Chipman, D. M., Reaction field treatment of charge penetration. *J. Chem. Phys.* **2000,** *112*, 5558.
17. Wheeler, S. E.; McNeil, A. J.; Müller, P.; Swager, T. M.; Houk, K. N., Probing Substituent Effects in Aryl−Aryl Interactions Using Stereoselective Diels−Alder Cycloadditions. *J. Am. Chem. Soc.* **2010,** *132* (10), 3304-3311.

Appendix

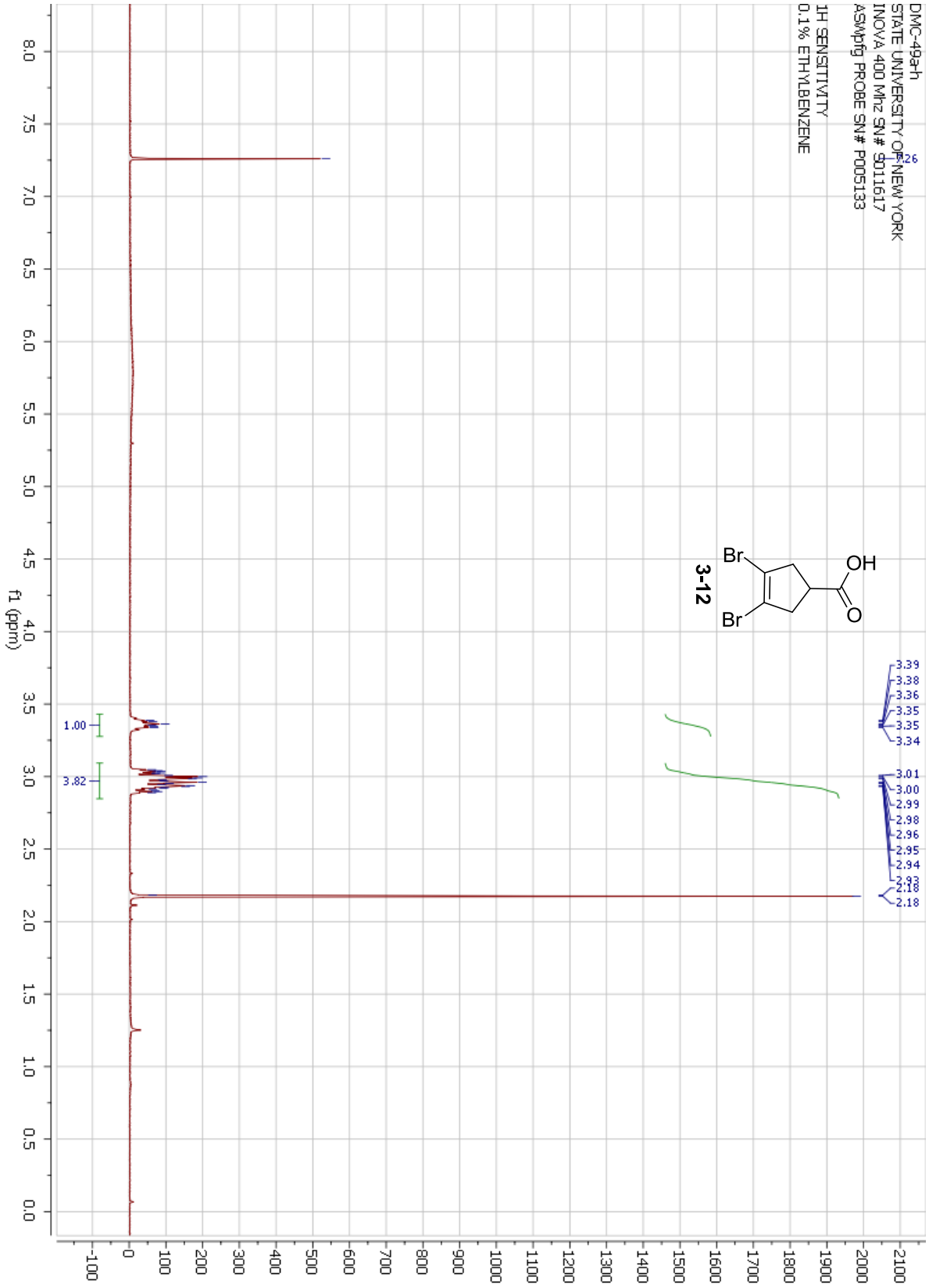
DMC-49a-h
STATE UNIVERSITY OF NEW YORK
INOVA 400 Mhz SN# 501617
ASMpfg PROBE SN# P005133
1H SENSITIVITY
0.1% ETHYLBENZENE
7.26
3-12
Br
Br
OH
O
3.39
3.38
3.36
3.35
3.35
3.34
3.01
3.00
2.99
2.98
2.96
2.95
2.94
2.18
2.18
1.00
3.82
f1 (ppm)

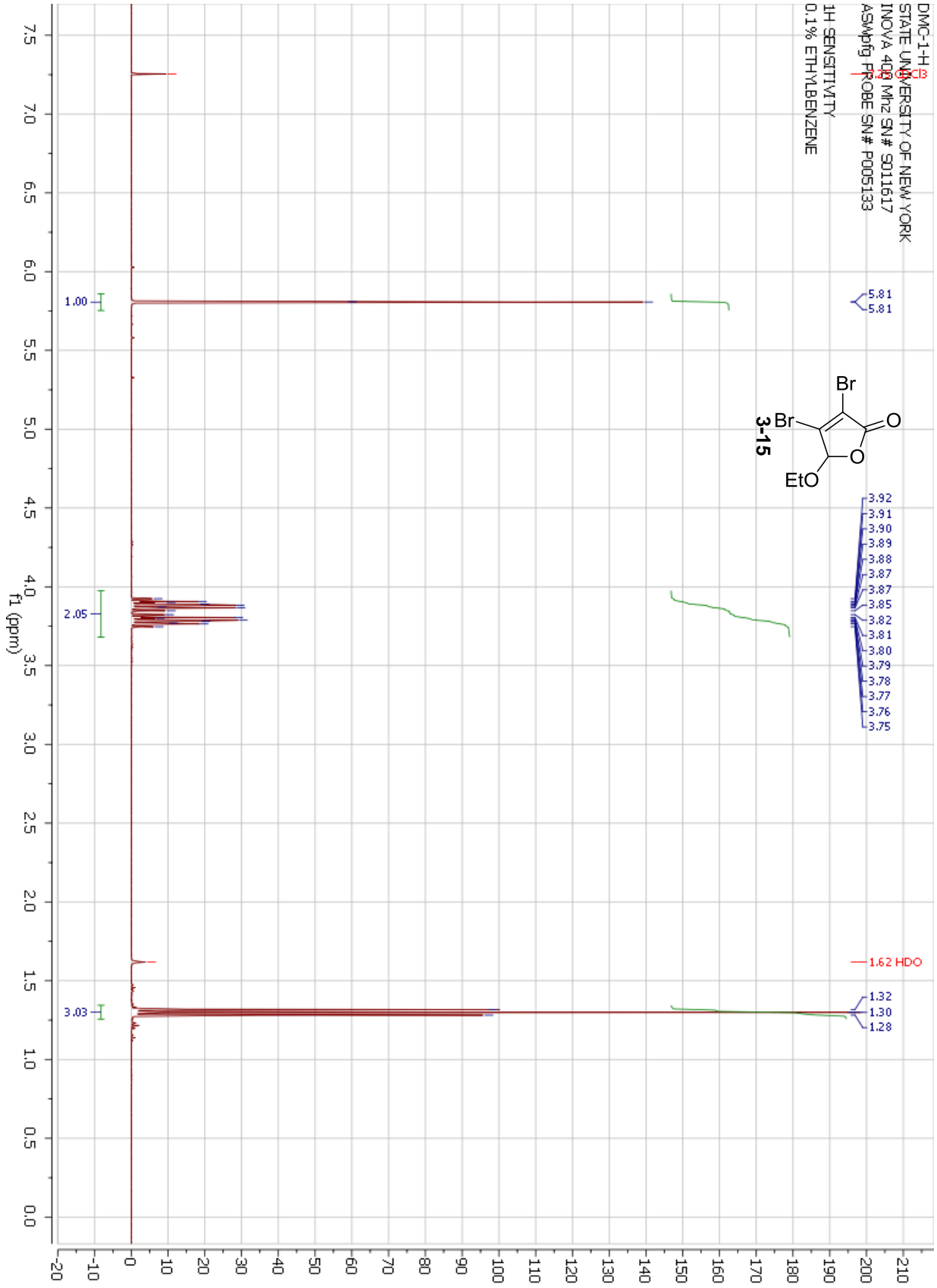
DMG-1-H
STATE UNIVERSITY OF NEW YORK
INOVA 400 MHz SN# 501617
ASMpfg PROBE SN# P005133
1H SENSITIVITY
0.1% ETHYLBENZENE
7.26 CHCl3
1.62 HDO
3-15
Br
Br
O
O
EtO
1.00
2.05
3.03
5.81
5.81
3.92
3.91
3.90
3.89
3.88
3.87
3.87
3.85
3.82
3.81
3.80
3.79
3.78
3.77
3.76
3.75
1.32
1.30
1.28
f1 (ppm)

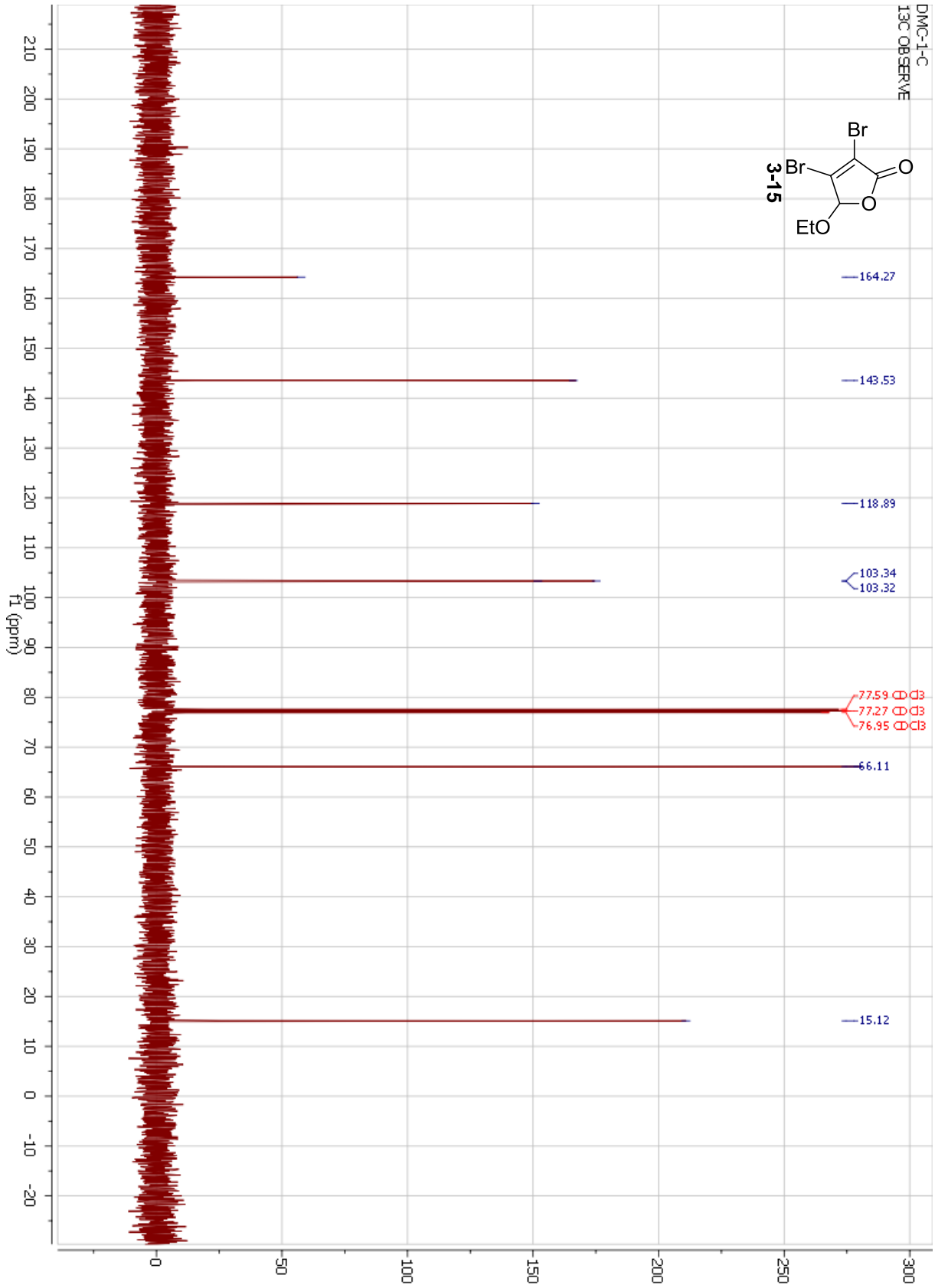
DMC-1-C
13C OBSERVE
Br
Br
O
O
EtO
3-15
164.27
143.53
118.89
103.34
103.32
77.59 CDCl3
77.27 CDCl3
76.95 CDCl3
66.11
15.12
f1 (ppm)

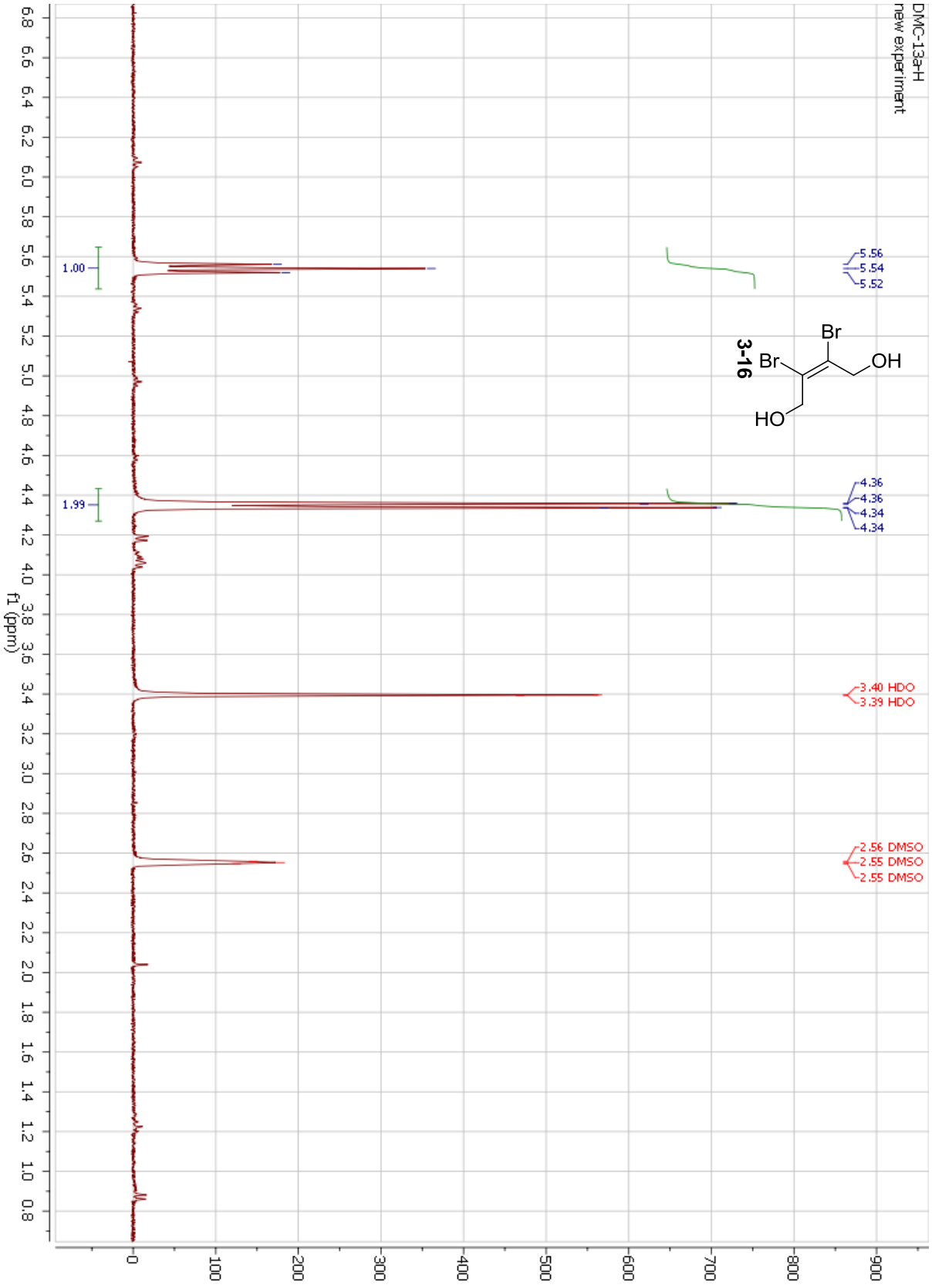
DMC-13a-H
new experiment
5.56
5.54
5.52
Br
3-16
Br
OH
HO
4.36
4.36
4.34
4.34
3.40 HDO
3.39 HDO
2.56 DMSO
2.55 DMSO
2.55 DMSO
1.00
1.99
f1 (ppm)

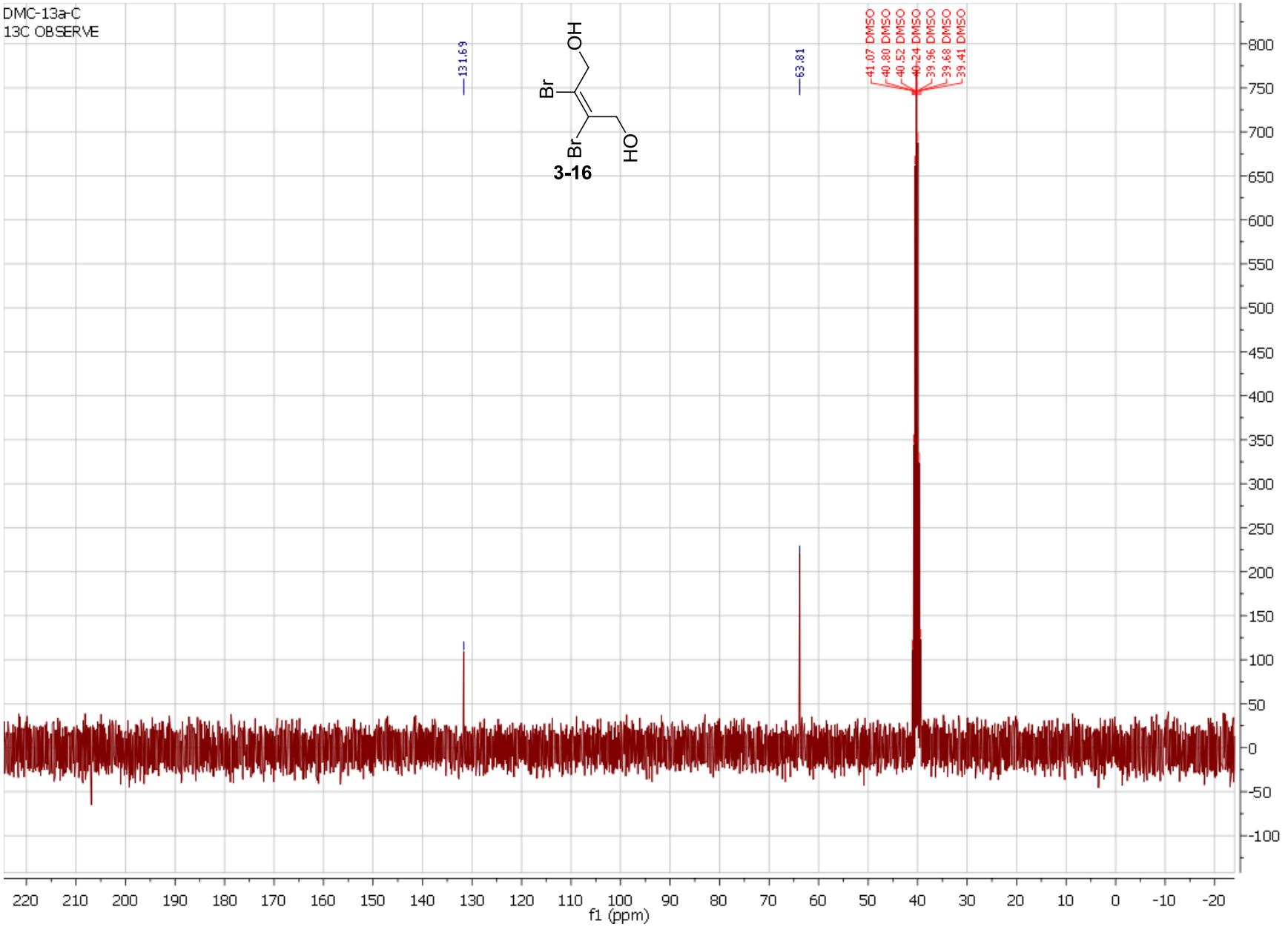
DMC-13a-C
13C OBSERVE
131.69
63.81
41.07 DMSO
40.80 DMSO
40.52 DMSO
40.24 DMSO
39.96 DMSO
39.68 DMSO
39.41 DMSO
OH
Br
Br
HO
3-16
f1 (ppm)

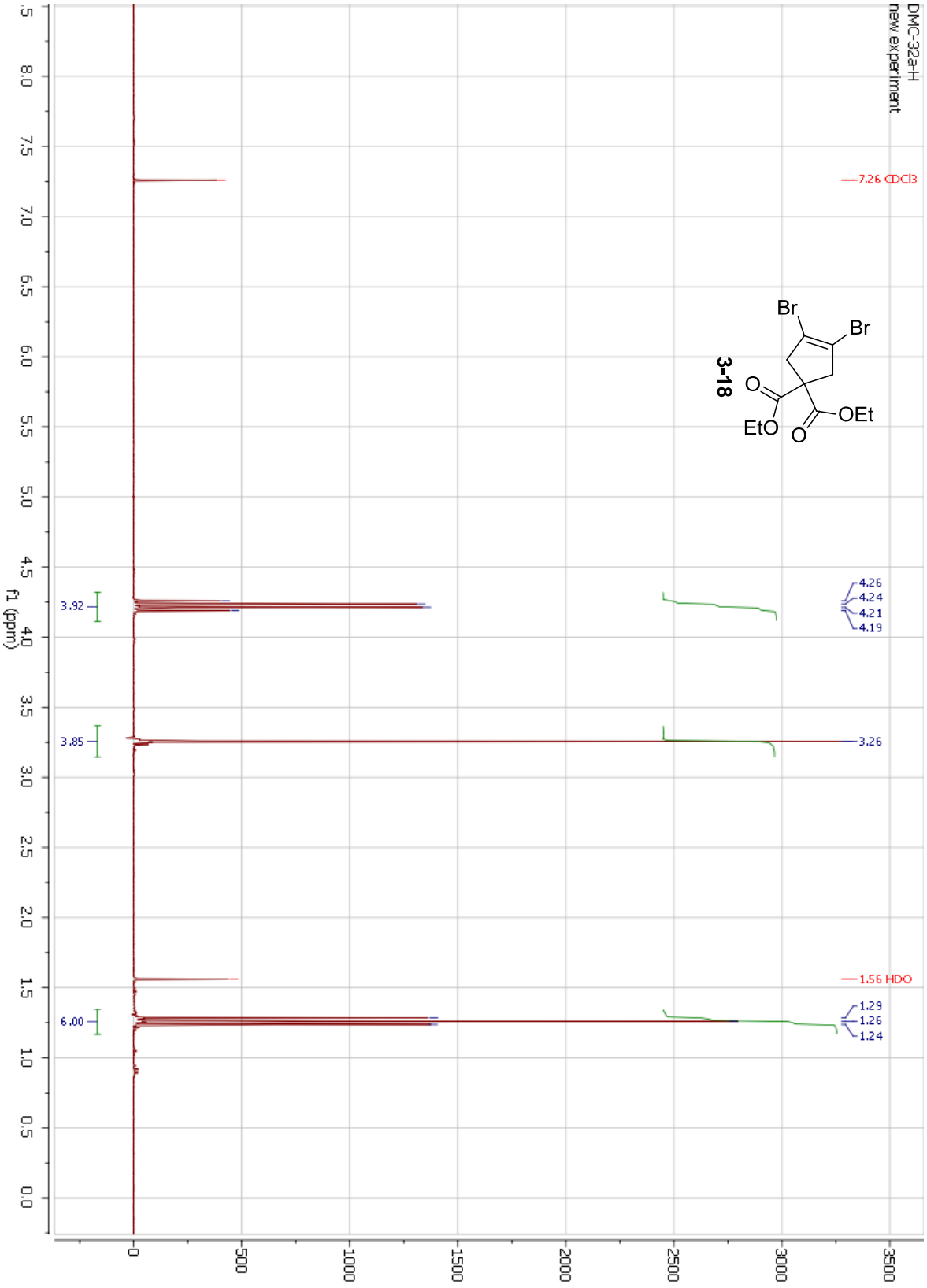
DMC-32a-H
new experiment
7.26 CDCl3
Br
Br
3-18
O
EtO
OEt
O
4.26
4.24
4.21
4.19
3.92
3.85
3.26
1.56 HDO
1.29
1.26
1.24
6.00
f1 (ppm)

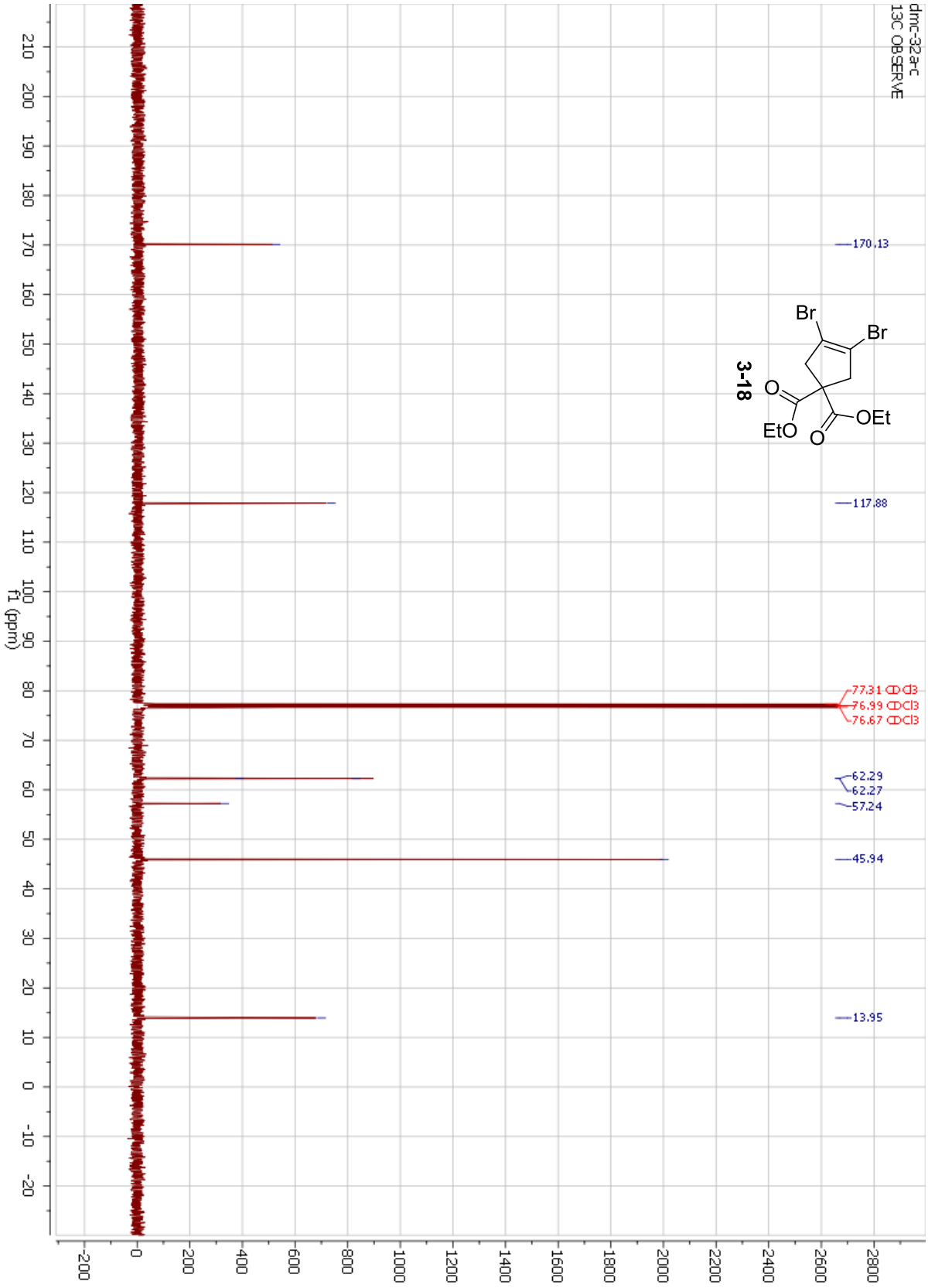
dmc-32a-c
13C OBSERVE
170.13
117.88
77.31 CDCl3
76.99 CDCl3
76.67 CDCl3
62.29
62.27
57.24
45.94
13.95
Br
Br
O
EtO
O
OEt
3-18
f1 (ppm)

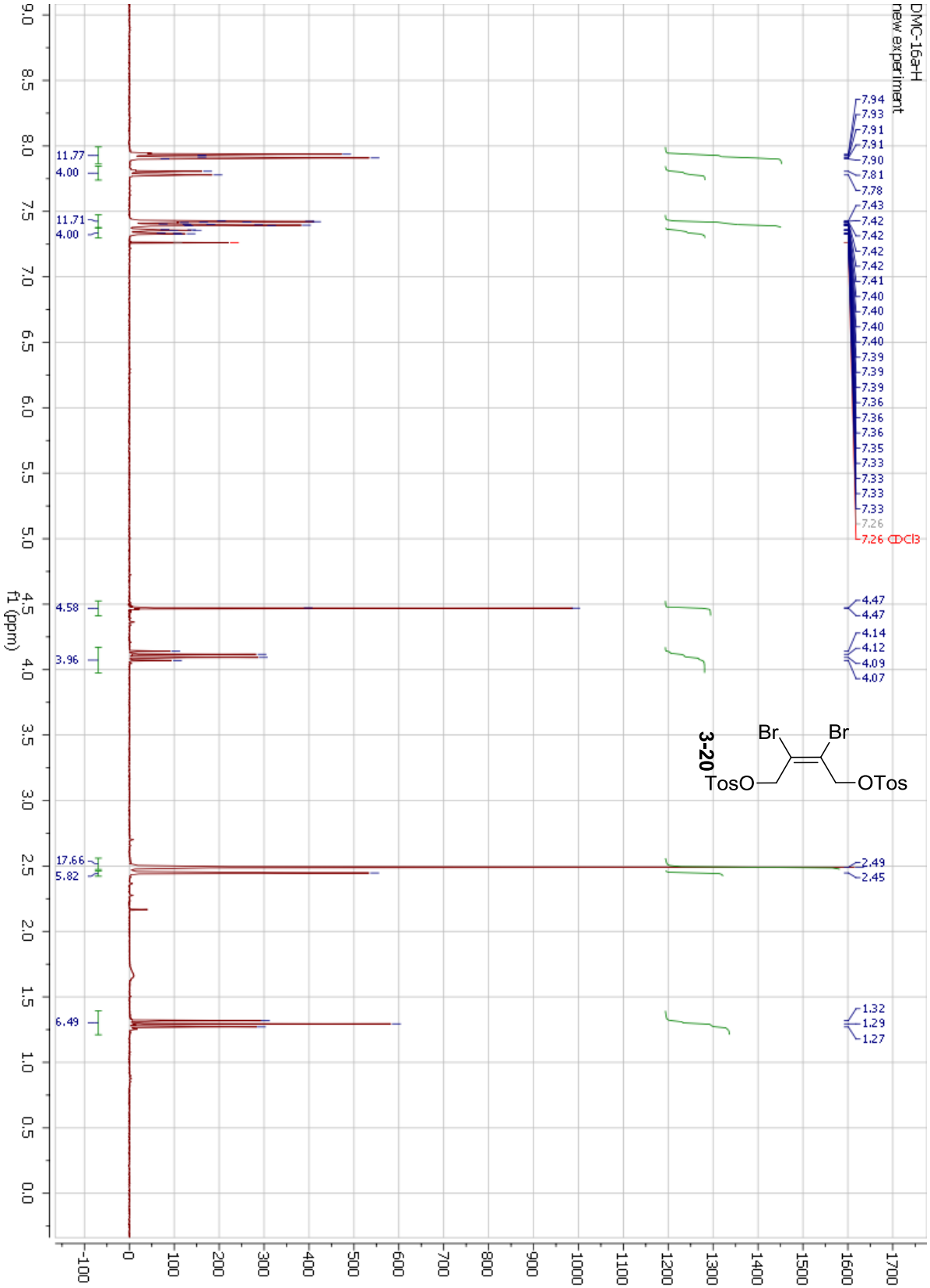
DMC-16a-H
new experiment
f1 (ppm)
11.77
4.00
11.71
4.00
4.58
3.96
17.66
5.82
6.49
7.94
7.93
7.91
7.91
7.90
7.81
7.78
7.43
7.42
7.42
7.42
7.42
7.41
7.40
7.40
7.40
7.40
7.39
7.39
7.39
7.36
7.36
7.36
7.35
7.33
7.33
7.33
7.33
7.26
7.26 CDCl3
4.47
4.47
4.14
4.12
4.09
4.07
2.49
2.45
1.32
1.29
1.27
3-20
Br
Br
TosO
OTos

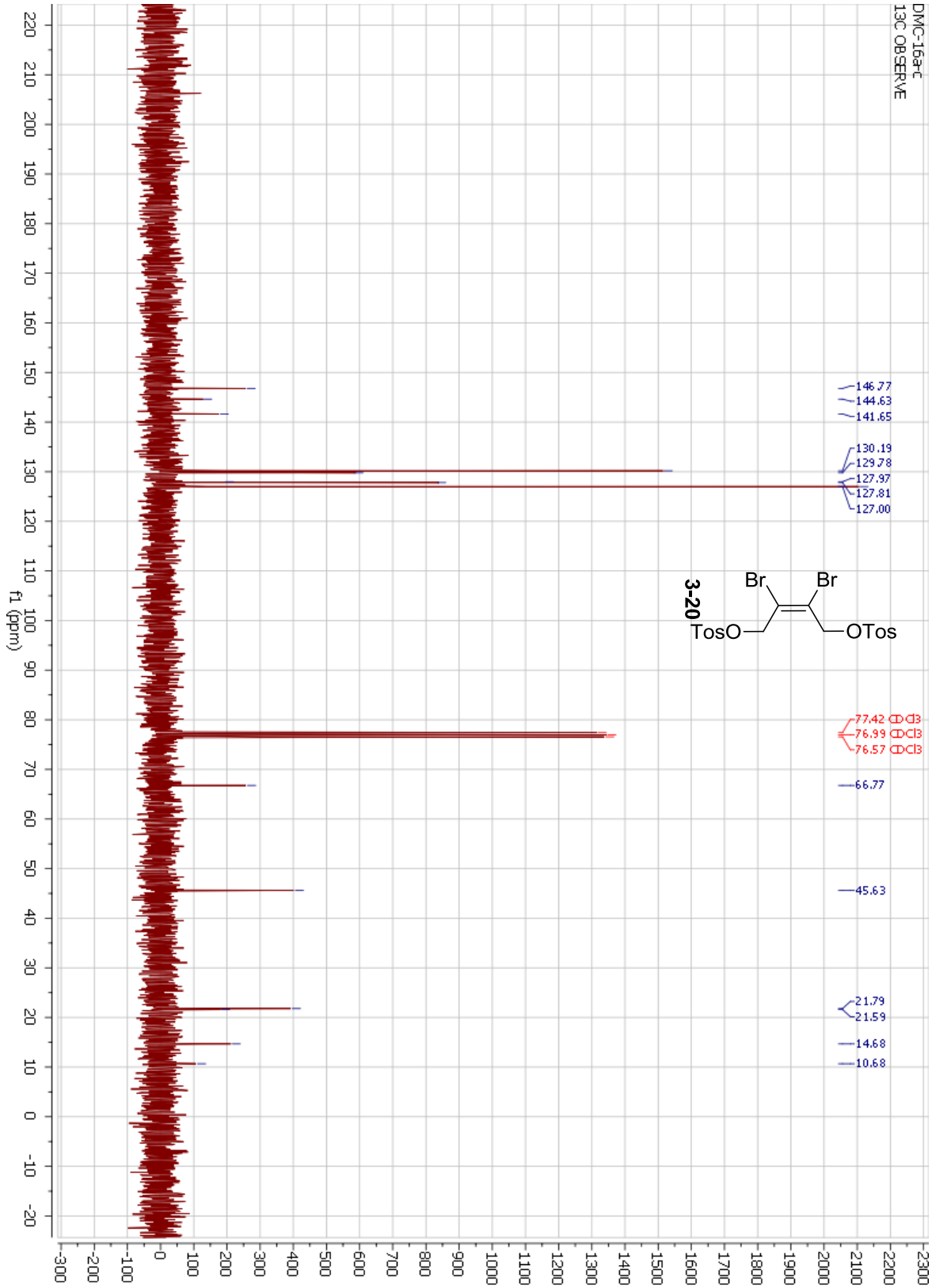
DMC-16a-c
13C OBSERVE
f1 (ppm)
146.77
144.63
141.65
130.19
129.78
127.97
127.81
127.00
77.42 CDCl3
76.99 CDCl3
76.57 CDCl3
66.77
45.63
21.79
21.59
14.68
10.68
3-20
Br
Br
TosO
OTos

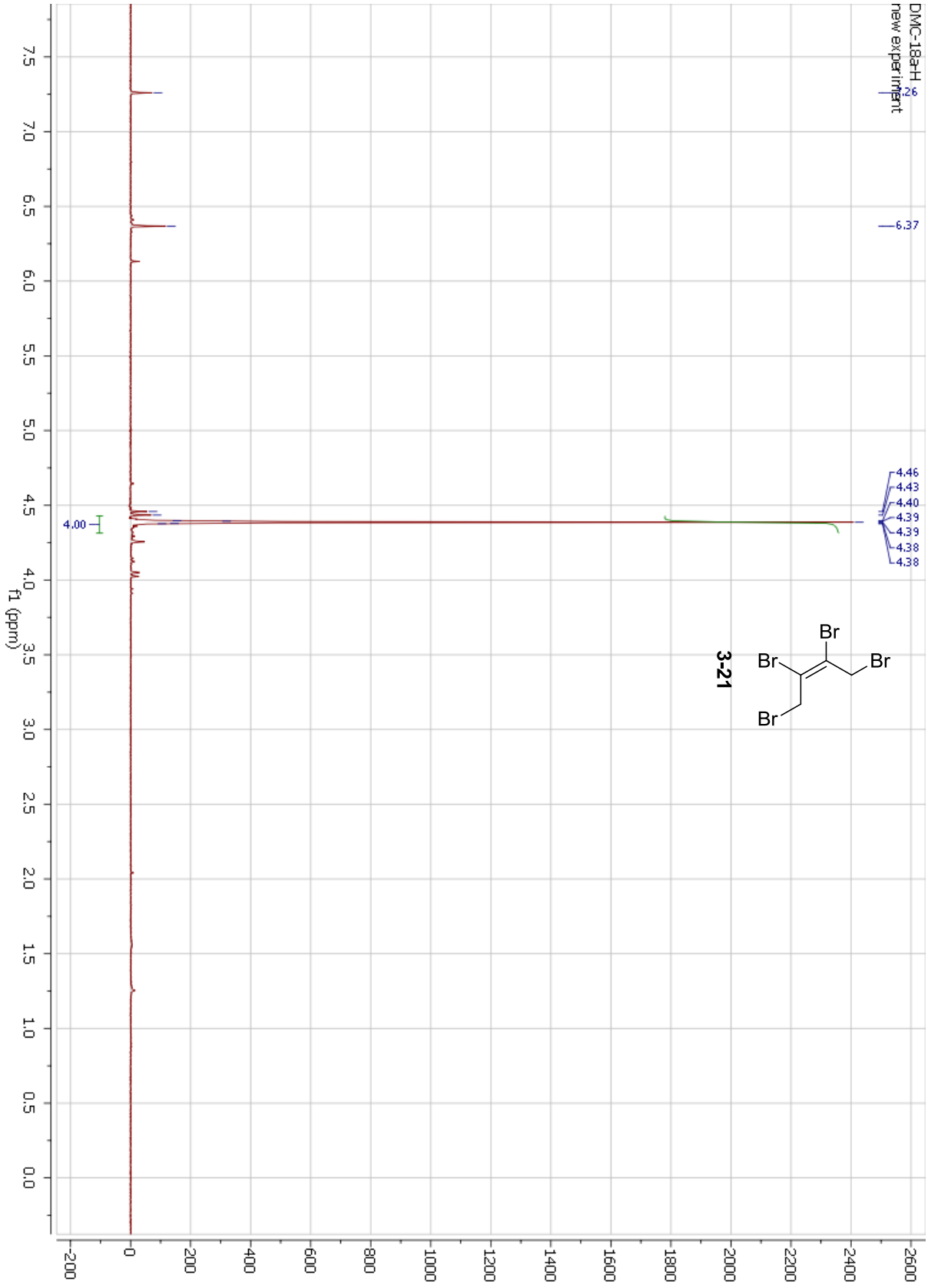
DMC-18a-H
new experiment
7.26
6.37
4.46
4.43
4.40
4.39
4.39
4.38
4.38
4.00
f1 (ppm)
3-21
Br
Br
Br
Br

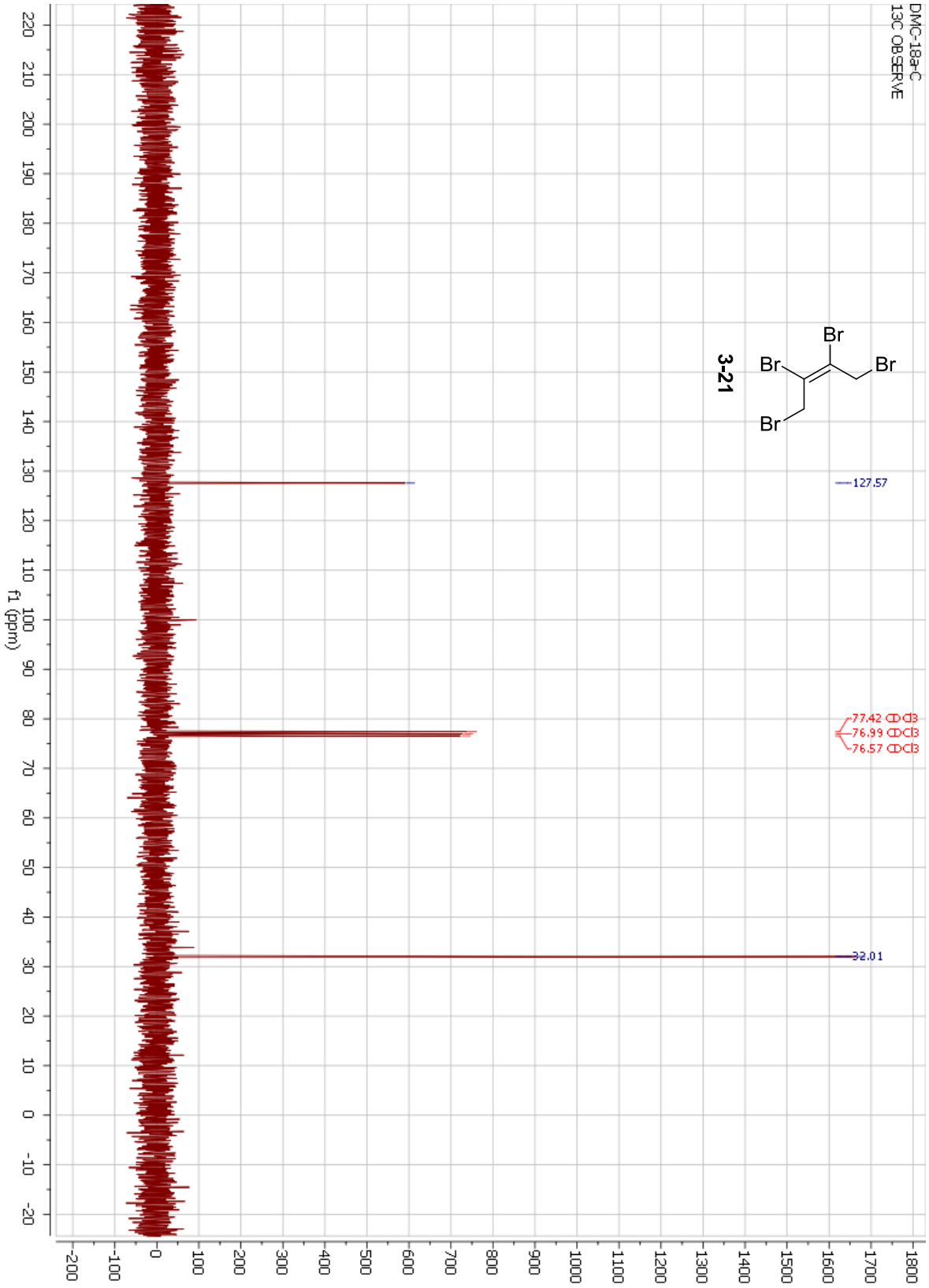
DMG-18a-C
13C OBSERVE
3-21
Br
Br
Br
Br
127.57
77.42 CDCl3
76.99 CDCl3
76.57 CDCl3
32.01
f1 (ppm)

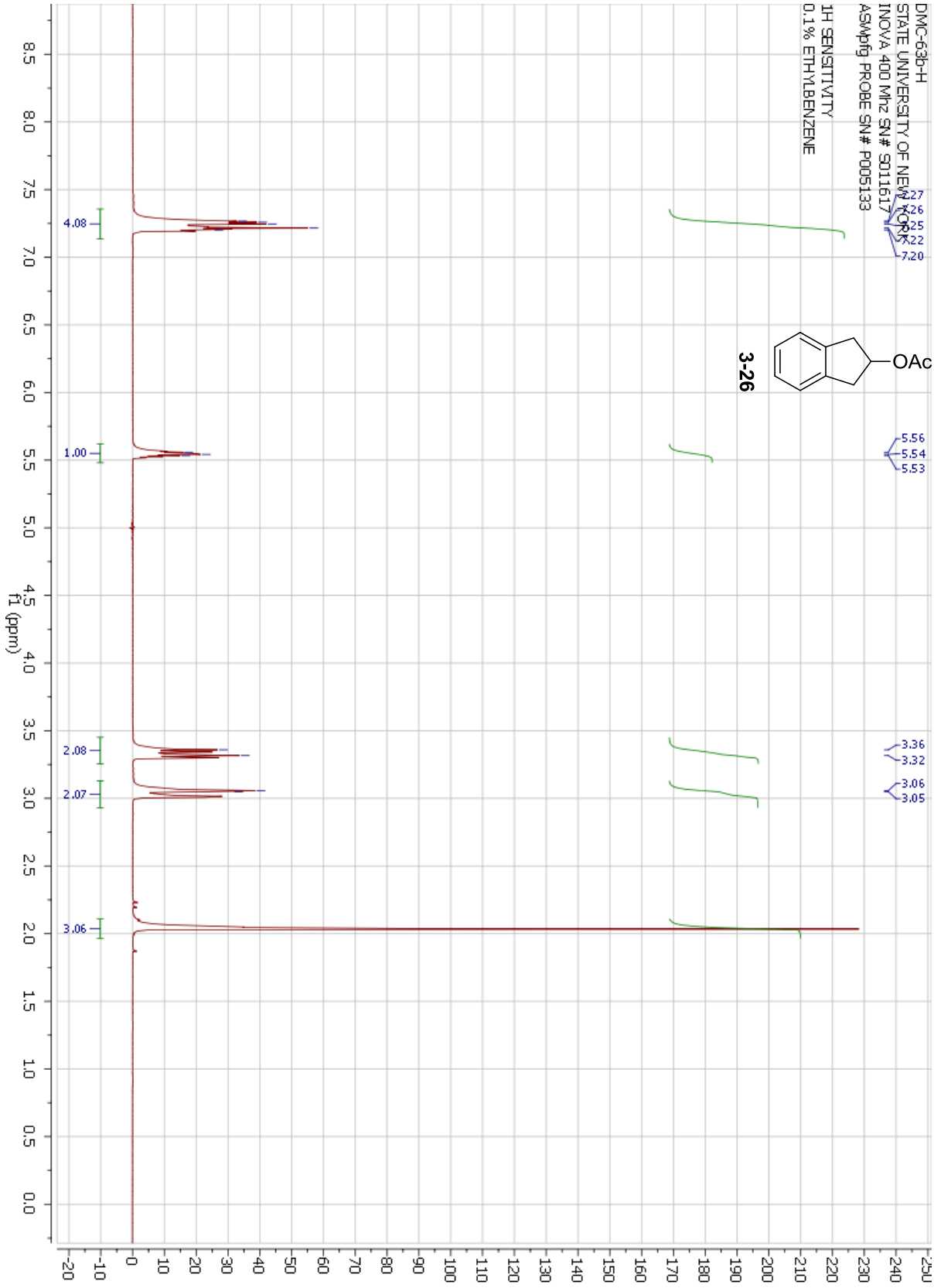
DMC-63b-H
STATE UNIVERSITY OF NEW YORK
INOVA 400 Mhz SN# 5011617
ASMpfg PROBE SN# P005133
1H SENSITIVITY
0.1% ETHYLBENZENE
3-26
OAc
7.27
7.26
7.25
7.22
7.20
5.56
5.54
5.53
3.36
3.32
3.06
3.05
4.08
1.00
2.08
2.07
3.06
f1 (ppm)

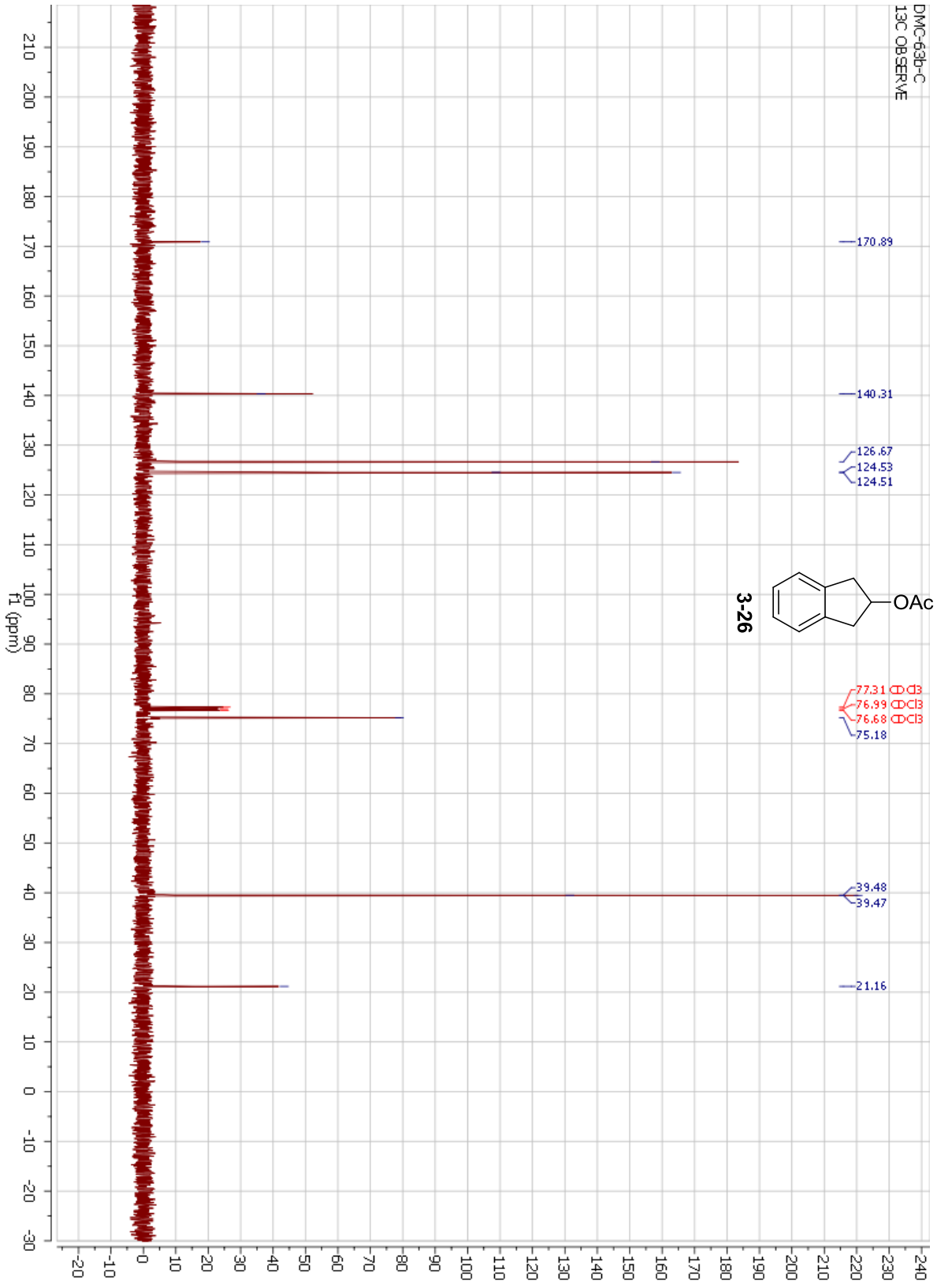
DMC-63b-C
13C OBSERVE
170.89
140.31
126.67
124.53
124.51
77.31 CDCl3
76.99 CDCl3
76.68 CDCl3
75.18
39.48
39.47
21.16
3-26
OAc
f1 (ppm)

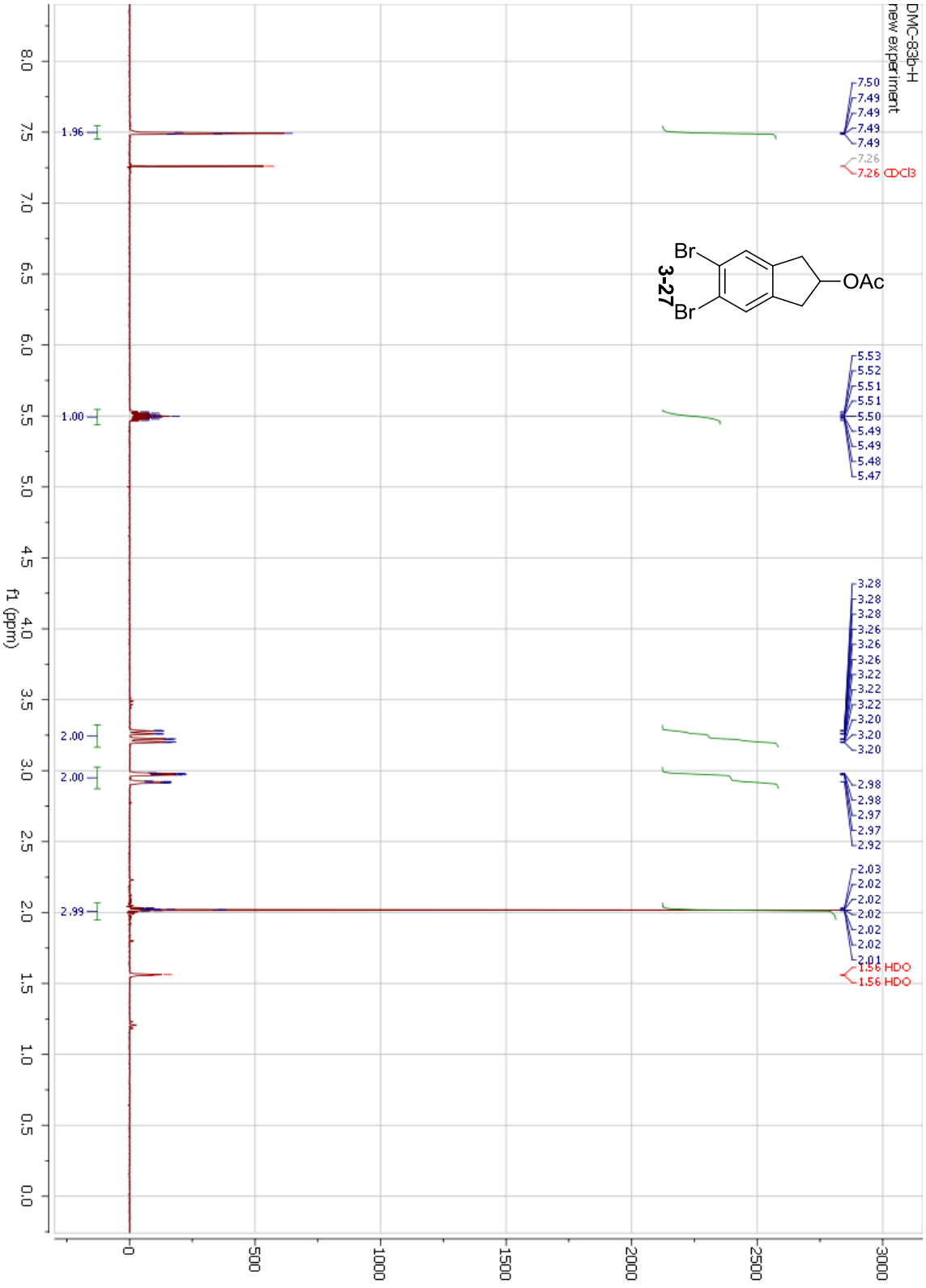
DMC-83b-H
new experiment
3-27
Br
Br
OAc
f1 (ppm)
1.96
1.00
2.00
2.00
2.99
7.50
7.49
7.49
7.49
7.49
7.26
7.26 CDCl3
5.53
5.52
5.51
5.51
5.50
5.49
5.49
5.48
5.47
3.28
3.28
3.28
3.26
3.26
3.26
3.22
3.22
3.22
3.20
3.20
3.20
2.98
2.98
2.97
2.97
2.92
2.03
2.02
2.02
2.02
2.02
2.02
2.01
1.56 HDO
1.56 HDO

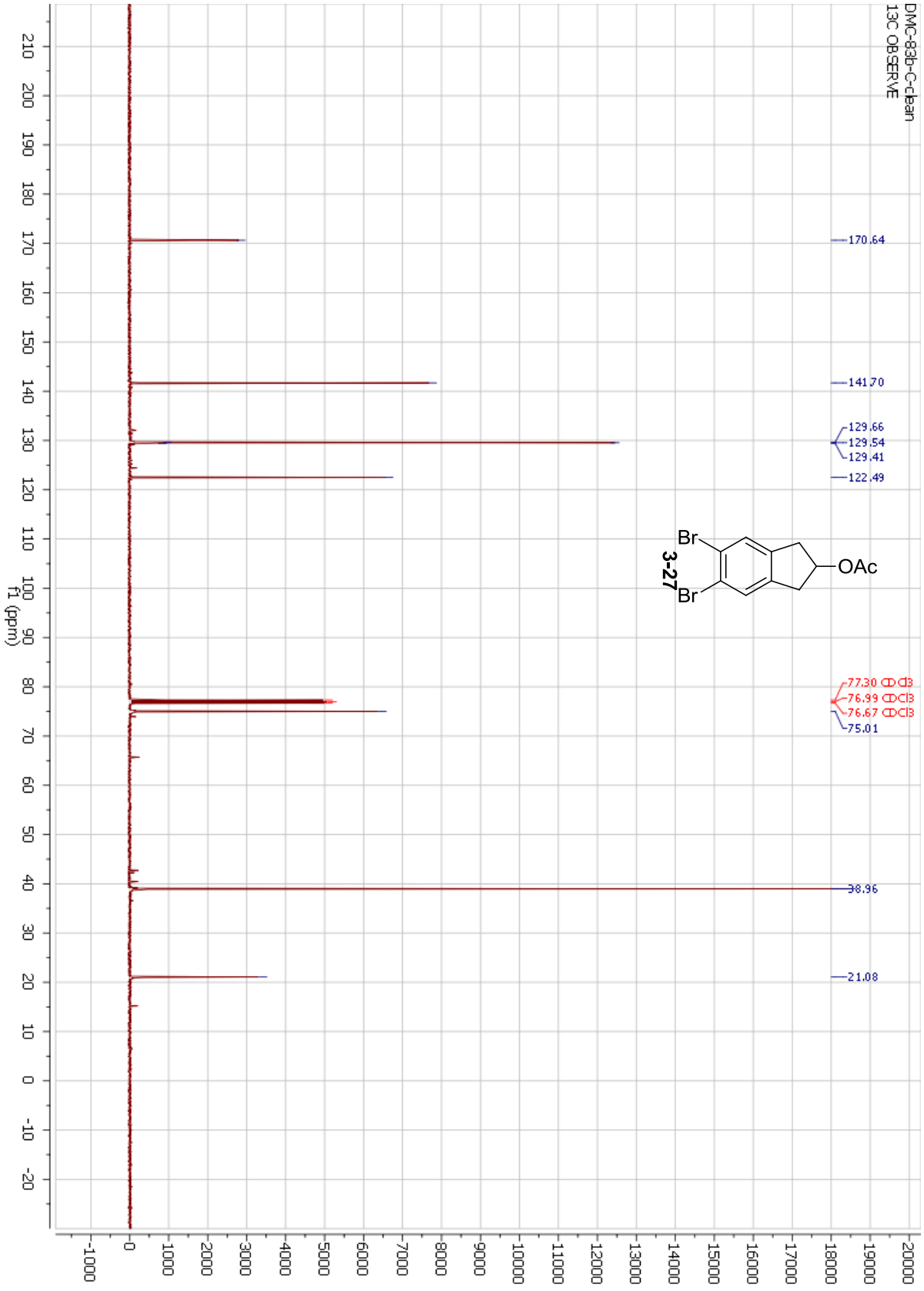
DMC-83b-C-clean
13C OBSERVE
170.64
141.70
129.66
129.54
129.41
122.49
77.30 CDCl3
76.99 CDCl3
76.67 CDCl3
75.01
38.96
21.08
Br
Br
OAc
3-27
f1 (ppm)

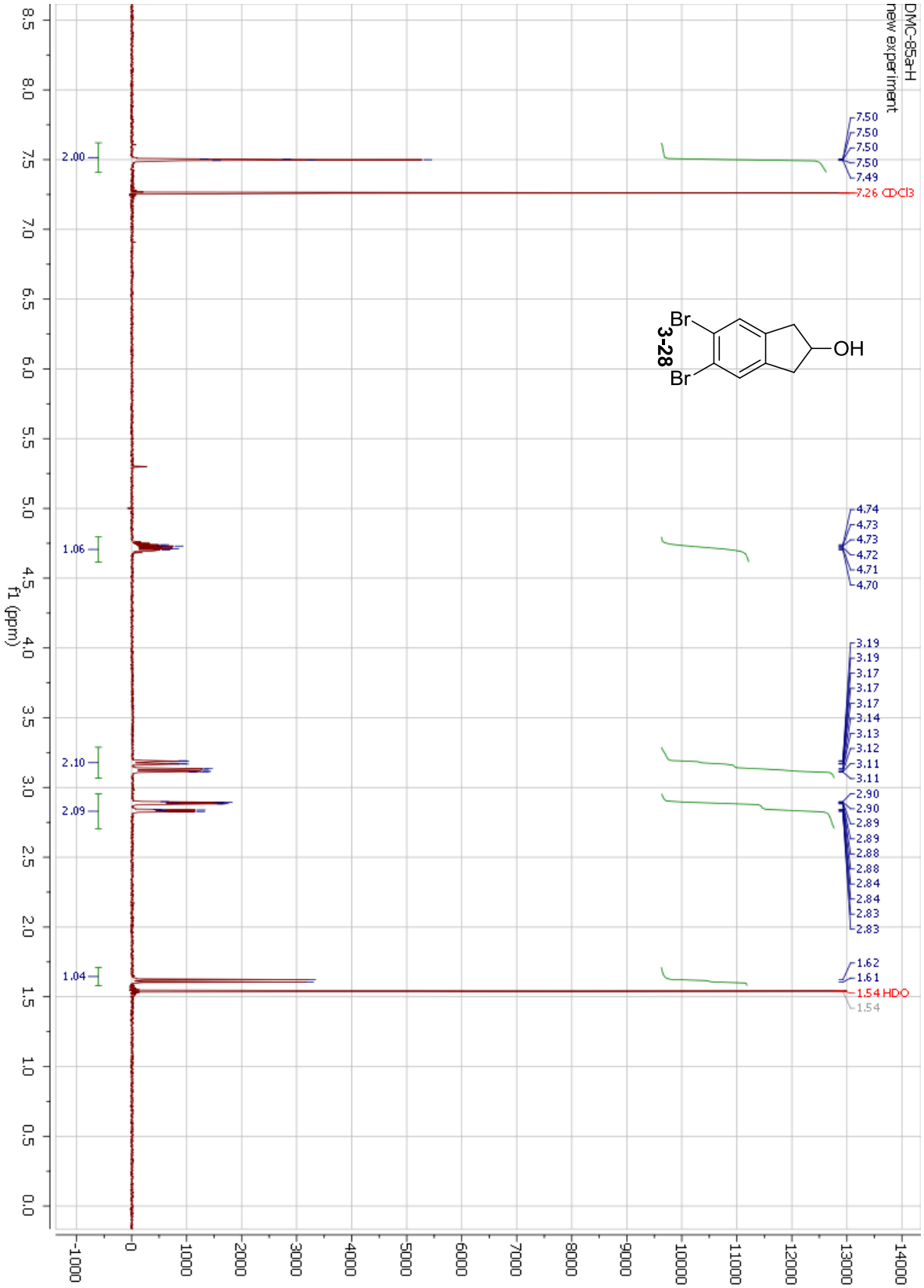
DMC-85a-H
new experiment
7.50
7.50
7.50
7.50
7.49
7.26 CDCl3
Br
Br
OH
3-28
4.74
4.73
4.73
4.72
4.71
4.70
3.19
3.19
3.17
3.17
3.17
3.14
3.13
3.12
3.11
3.11
2.90
2.90
2.89
2.89
2.88
2.88
2.84
2.84
2.83
2.83
1.62
1.61
1.54 HDO
1.54
2.00
1.06
2.10
2.09
1.04
f1 (ppm)

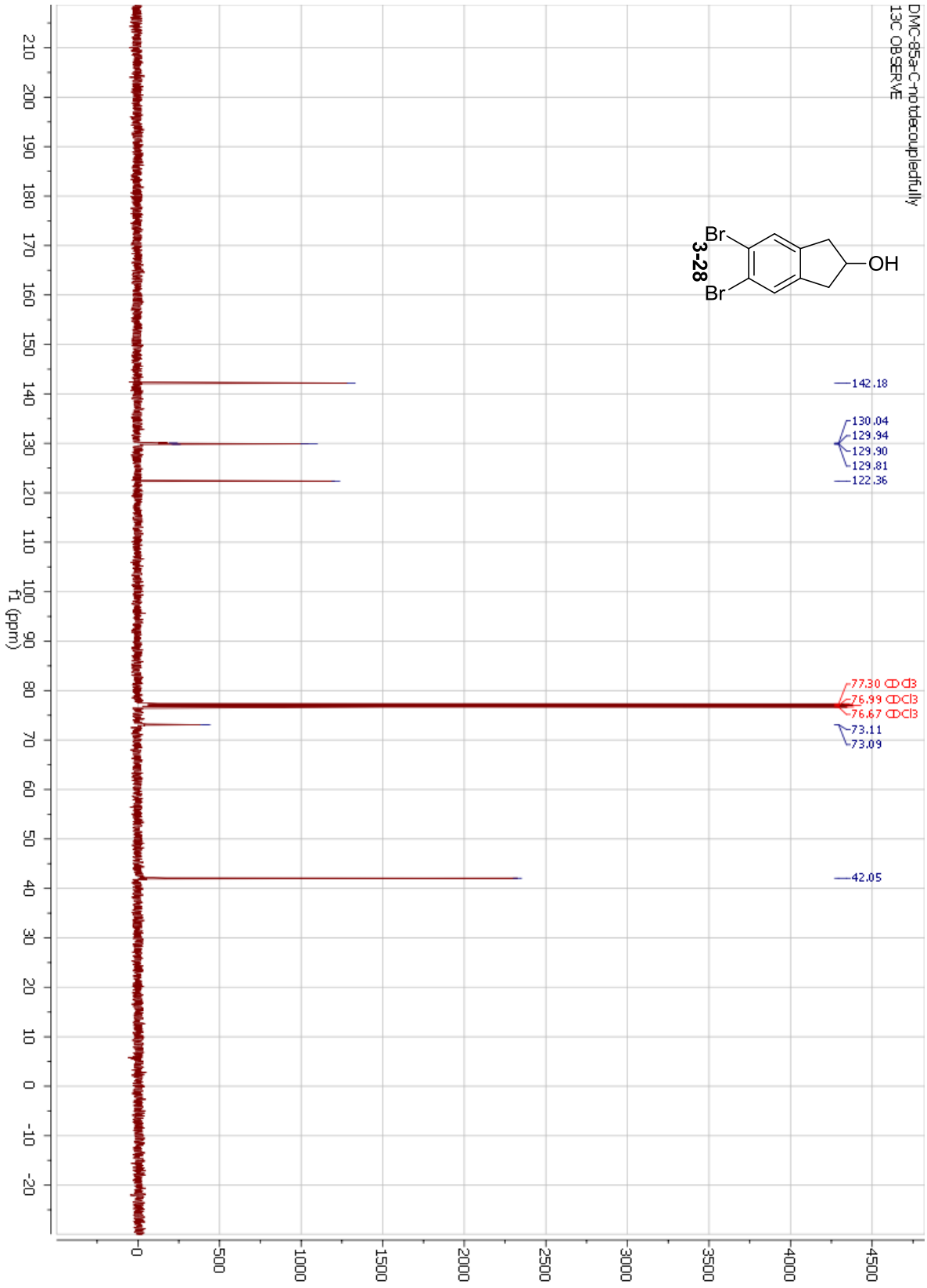
DMC-85a-C-nottdecoupledfully
13C OBSERVE
Br
Br
OH
3-28
142.18
130.04
129.94
129.90
129.81
122.36
77.30 CDCl3
76.99 CDCl3
76.67 CDCl3
73.11
73.09
42.05
f1 (ppm)

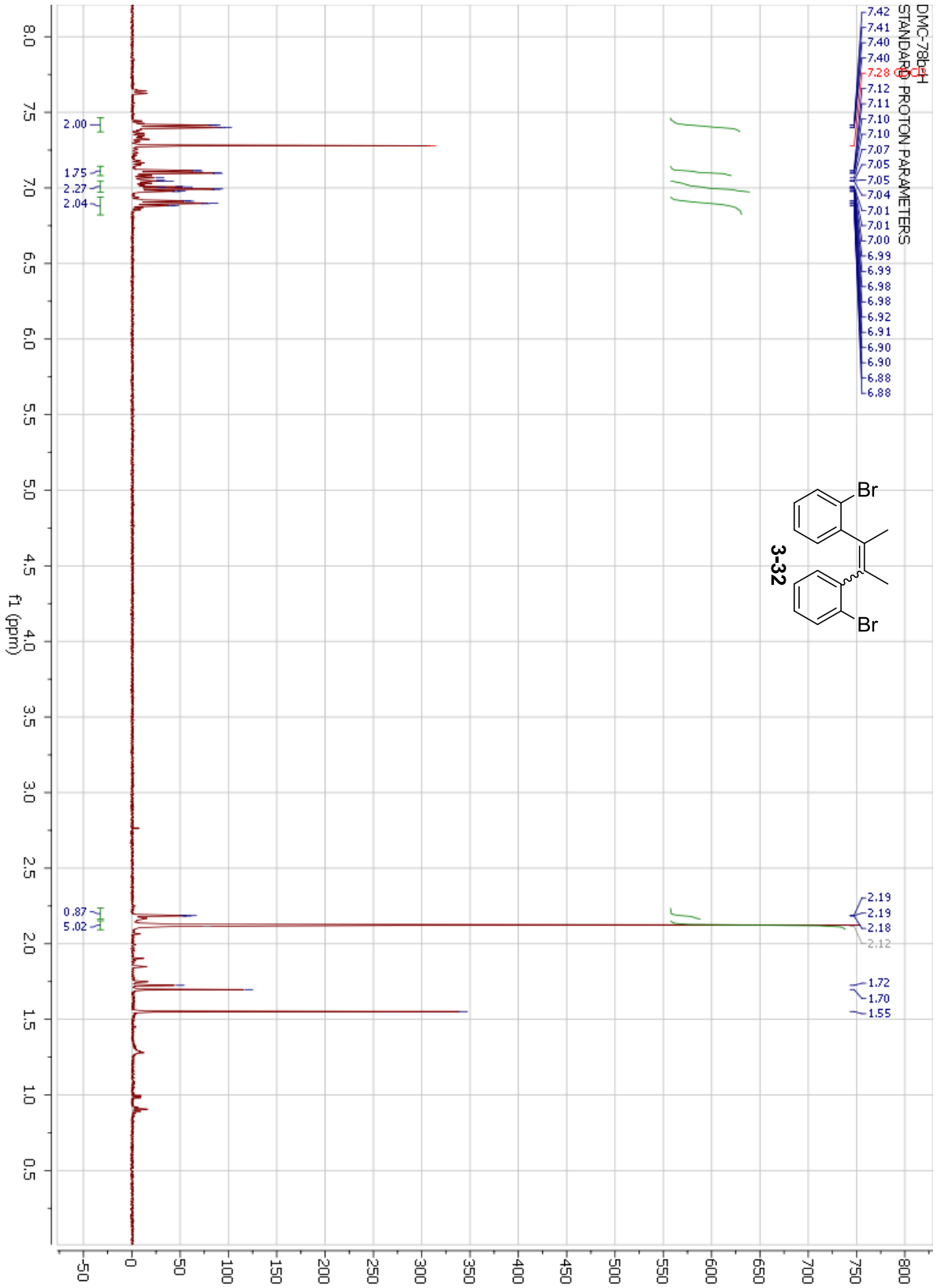
DMC-78bH
STANDARD PROTON PARAMETERS
7.42
7.41
7.40
7.40
7.28
7.12
7.11
7.10
7.10
7.07
7.05
7.05
7.04
7.01
7.01
7.00
6.99
6.99
6.98
6.98
6.92
6.91
6.90
6.90
6.88
6.88
2.00
1.75
2.27
2.04
0.87
5.02
2.19
2.19
2.18
2.12
1.72
1.70
1.55
Br
Br
3-32
f1 (ppm)

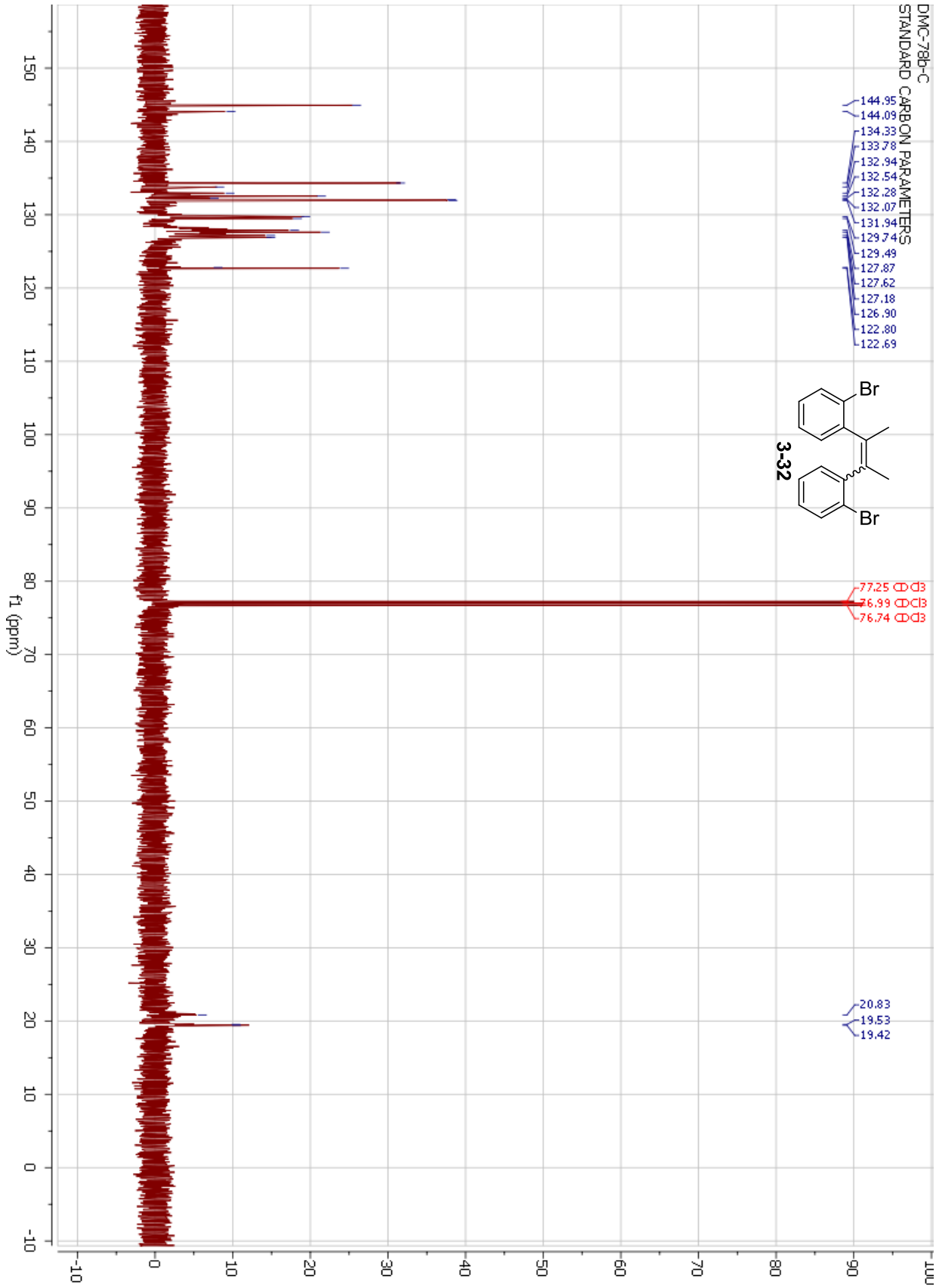
DMC-78b-C
STANDARD CARBON PARAMETERS
144.95
144.09
134.33
133.78
132.94
132.54
132.28
132.07
131.94
129.74
129.49
127.87
127.62
127.18
126.90
122.80
122.69
Br
Br
3-32
77.25 CDCl3
76.99 CDCl3
76.74 CDCl3
20.83
19.53
19.42
f1 (ppm)

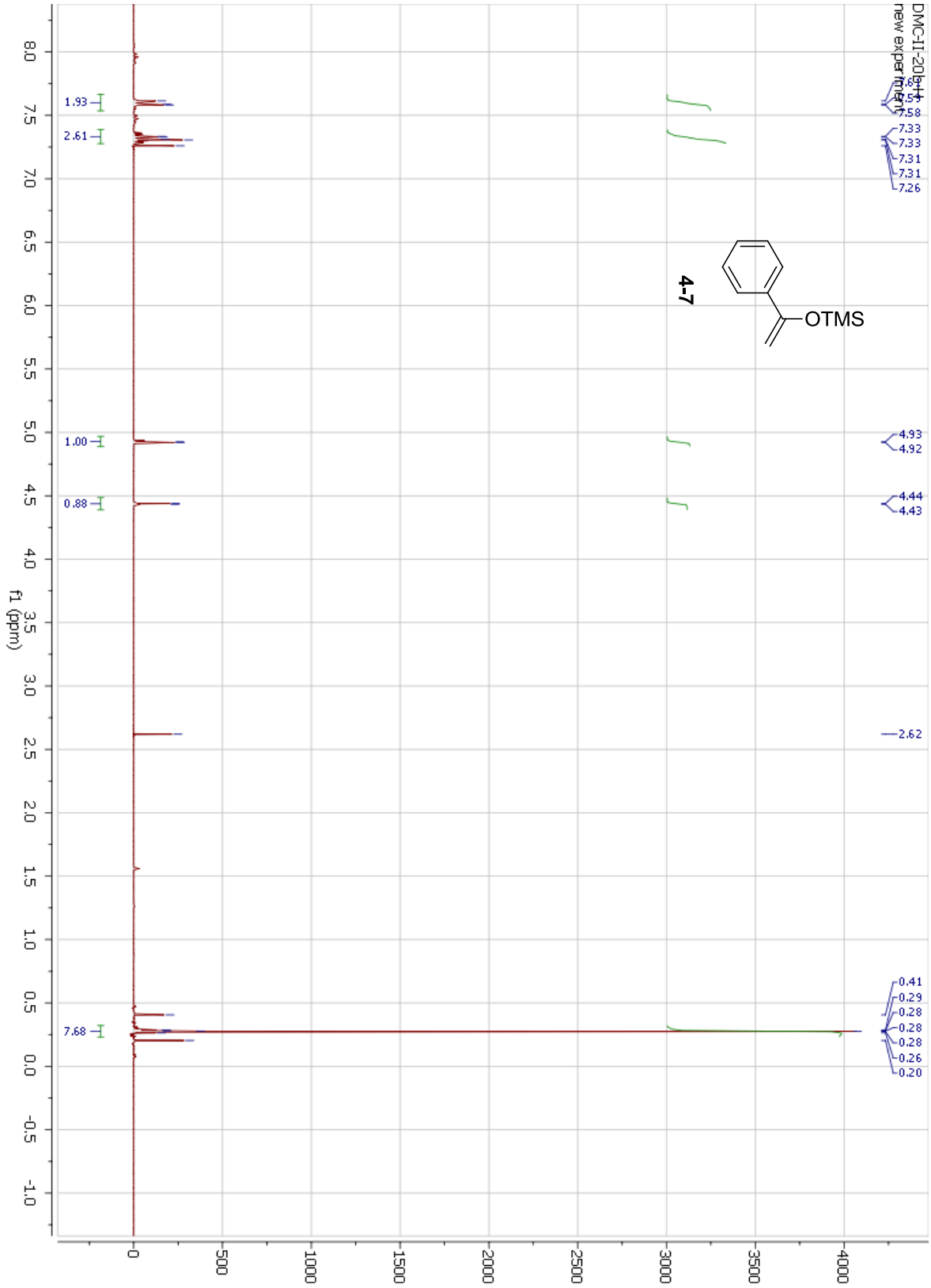
DMC-II-20-H-1
new experiment
4-7
OTMS
1.93
2.61
1.00
0.88
7.68
2.62
f1 (ppm)

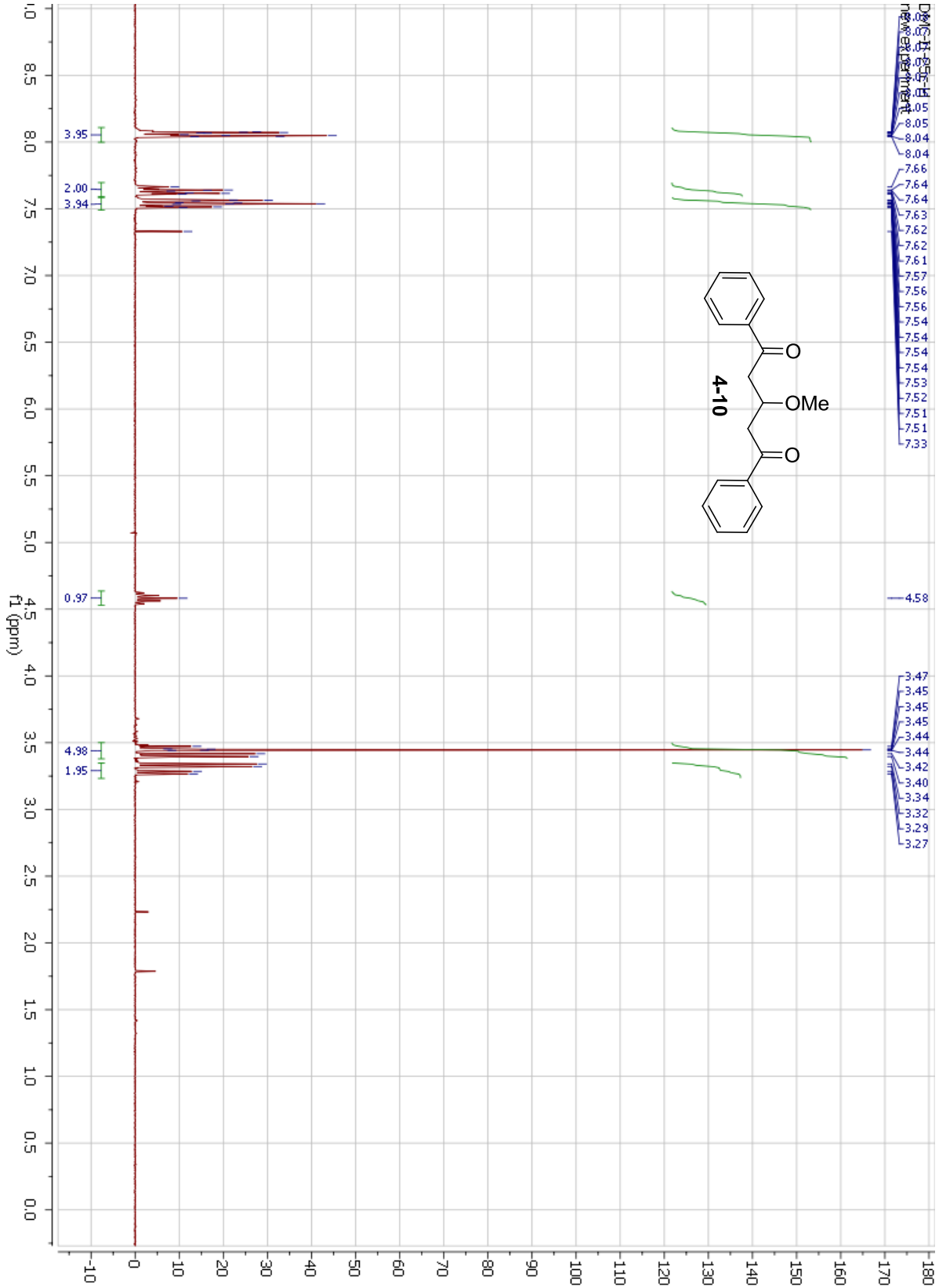
4-10
OMe
O
O
3.95
2.00
3.94
0.97
4.98
1.95
4.58
f1 (ppm)

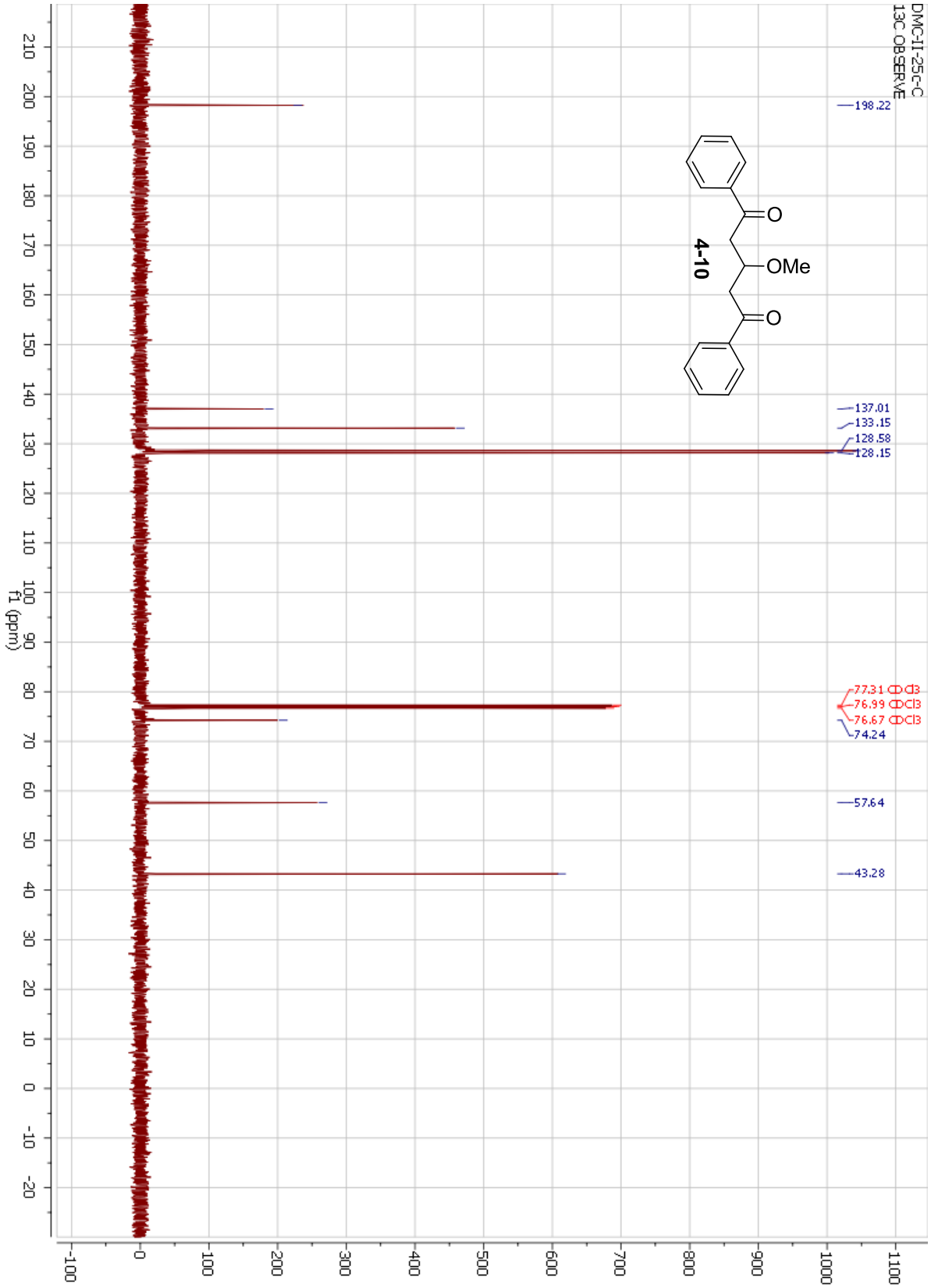
DMC-II-25c-C
13C OBSERVE
198.22
137.01
133.15
128.58
128.15
77.31 CDCl3
76.99 CDCl3
76.67 CDCl3
74.24
57.64
43.28
4-10
O
OMe
O
f1 (ppm)

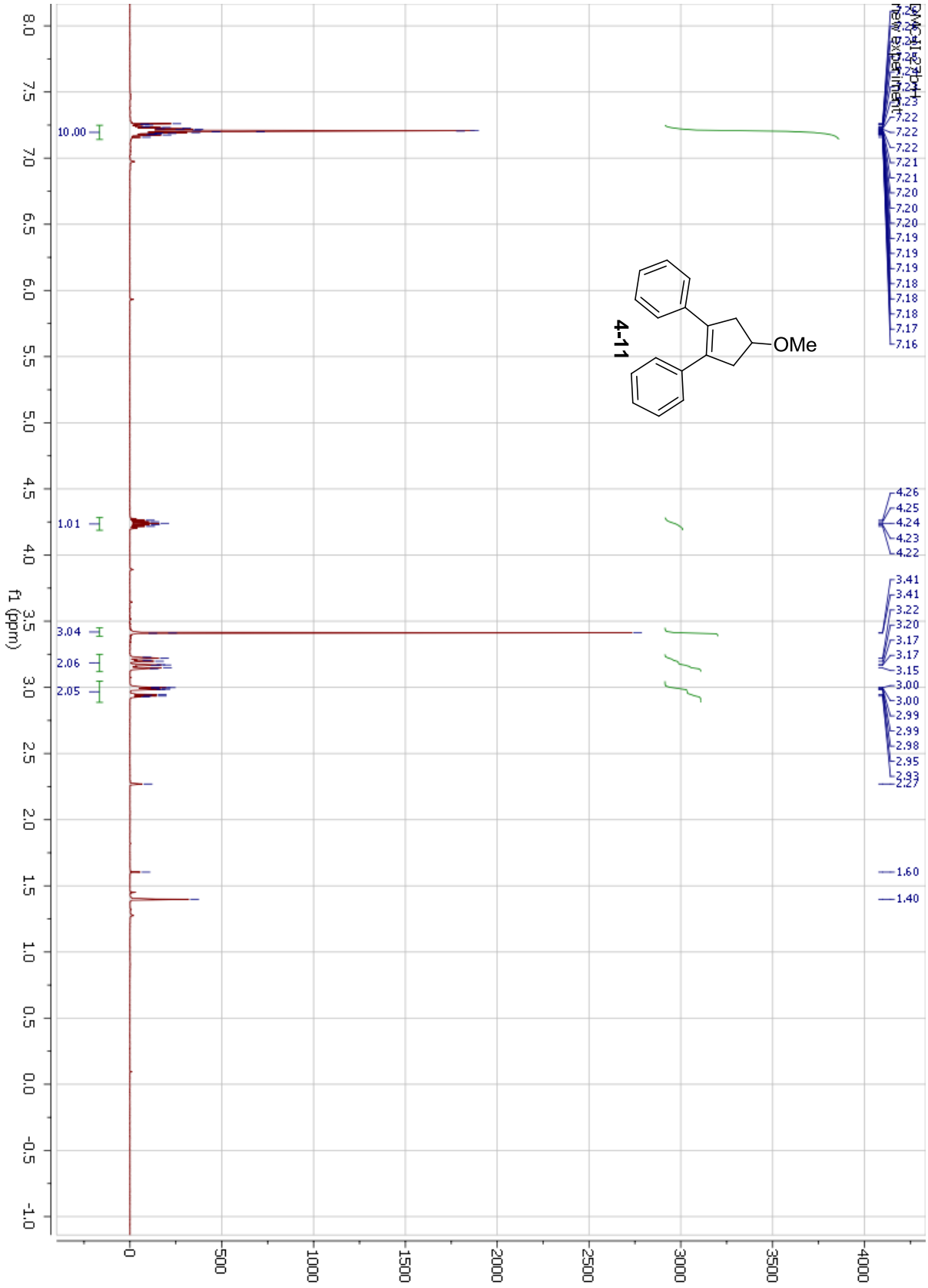
4-11
OMe
10.00
1.01
3.04
2.06
2.05
f1 (ppm)

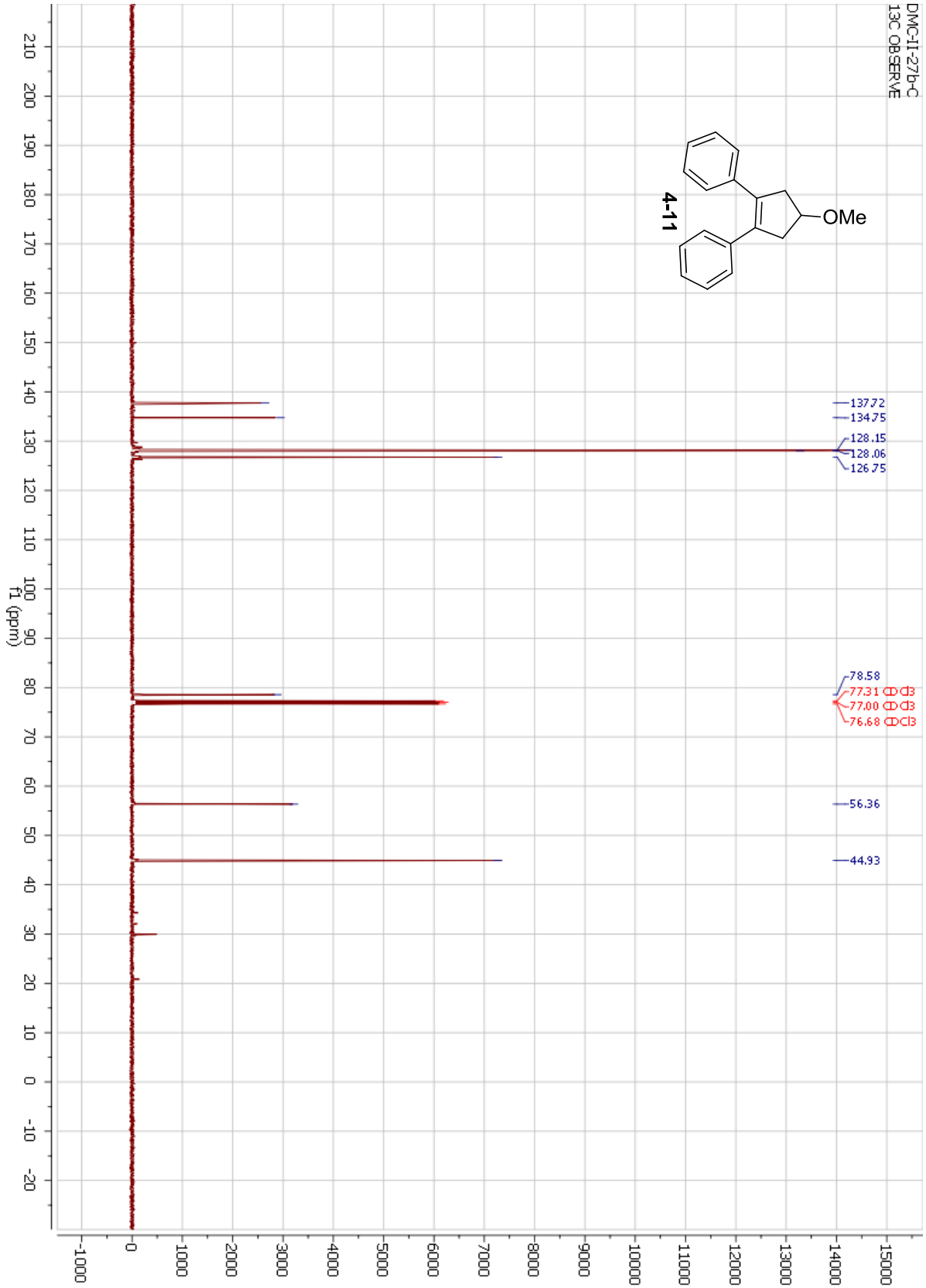
DMC-II-27b-C
13C OBSERVE
4-11
OMe
137.72
134.75
128.15
128.06
126.75
78.58
77.31 CDCl3
77.00 CDCl3
76.68 CDCl3
56.36
44.93
f1 (ppm)

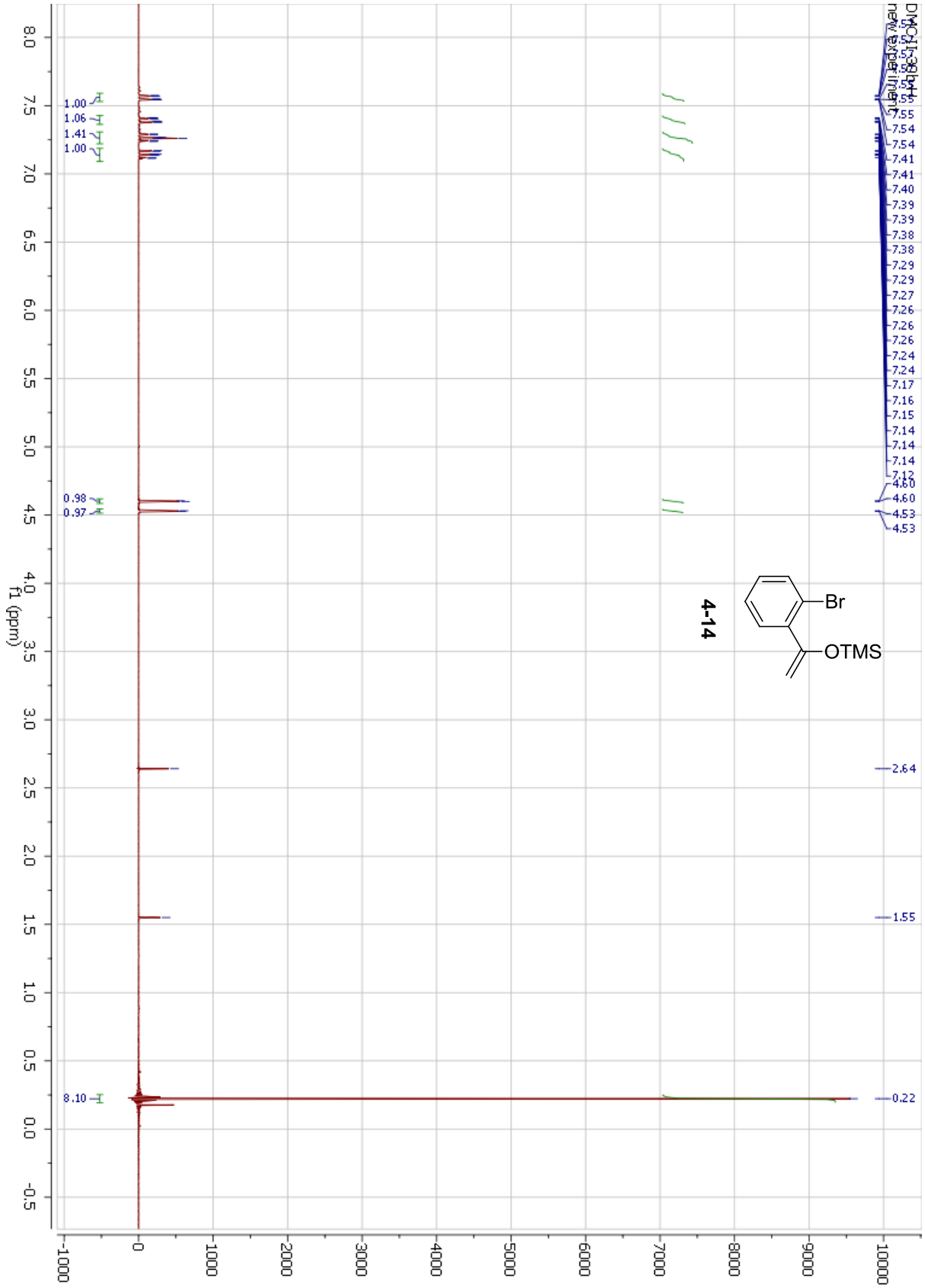
4-14
Br
OTMS
f1 (ppm)
1.00
1.06
1.41
1.00
0.98
0.97
8.10
2.64
1.55
0.22

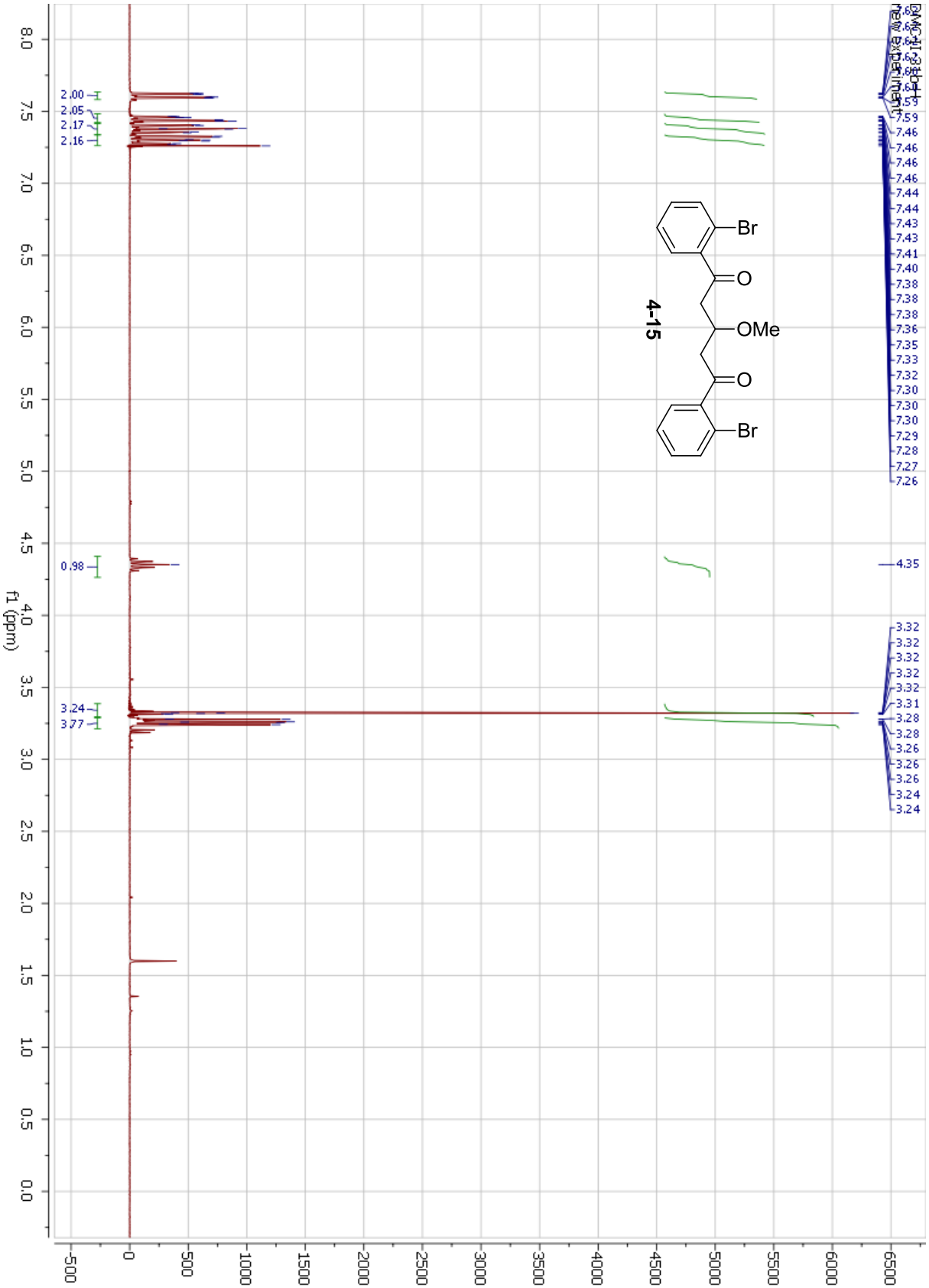
4-15
Br
O
OMe
O
Br
f1 (ppm)
2.00
2.05
2.17
2.16
0.98
3.24
3.77
4.35

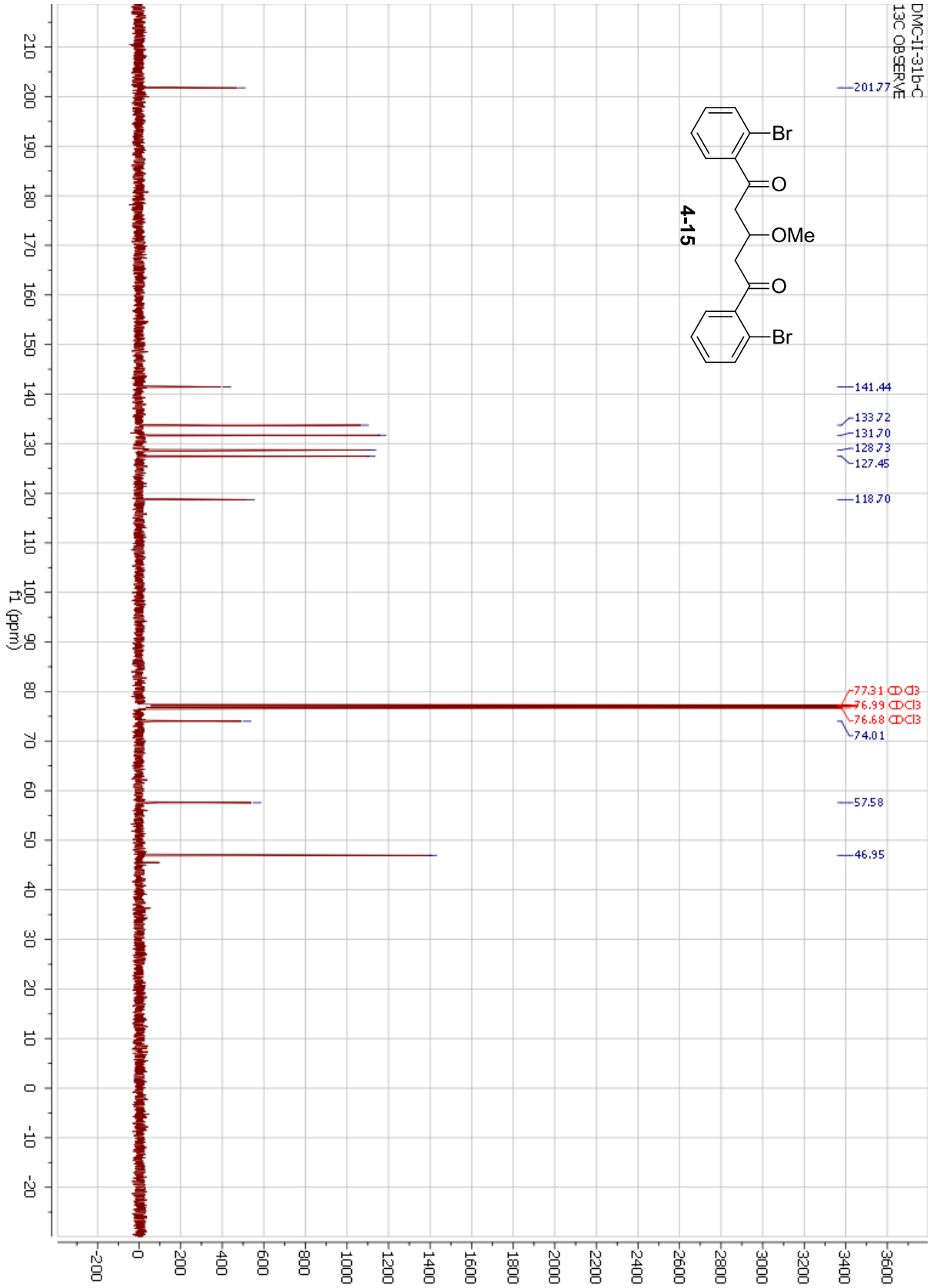
DMC-II-31b-C
13C OBSERVE
201.77
141.44
133.72
131.70
128.73
127.45
118.70
77.31 CDCl3
76.99 CDCl3
76.68 CDCl3
74.01
57.58
46.95
Br
O
OMe
O
Br
4-15
f1 (ppm)

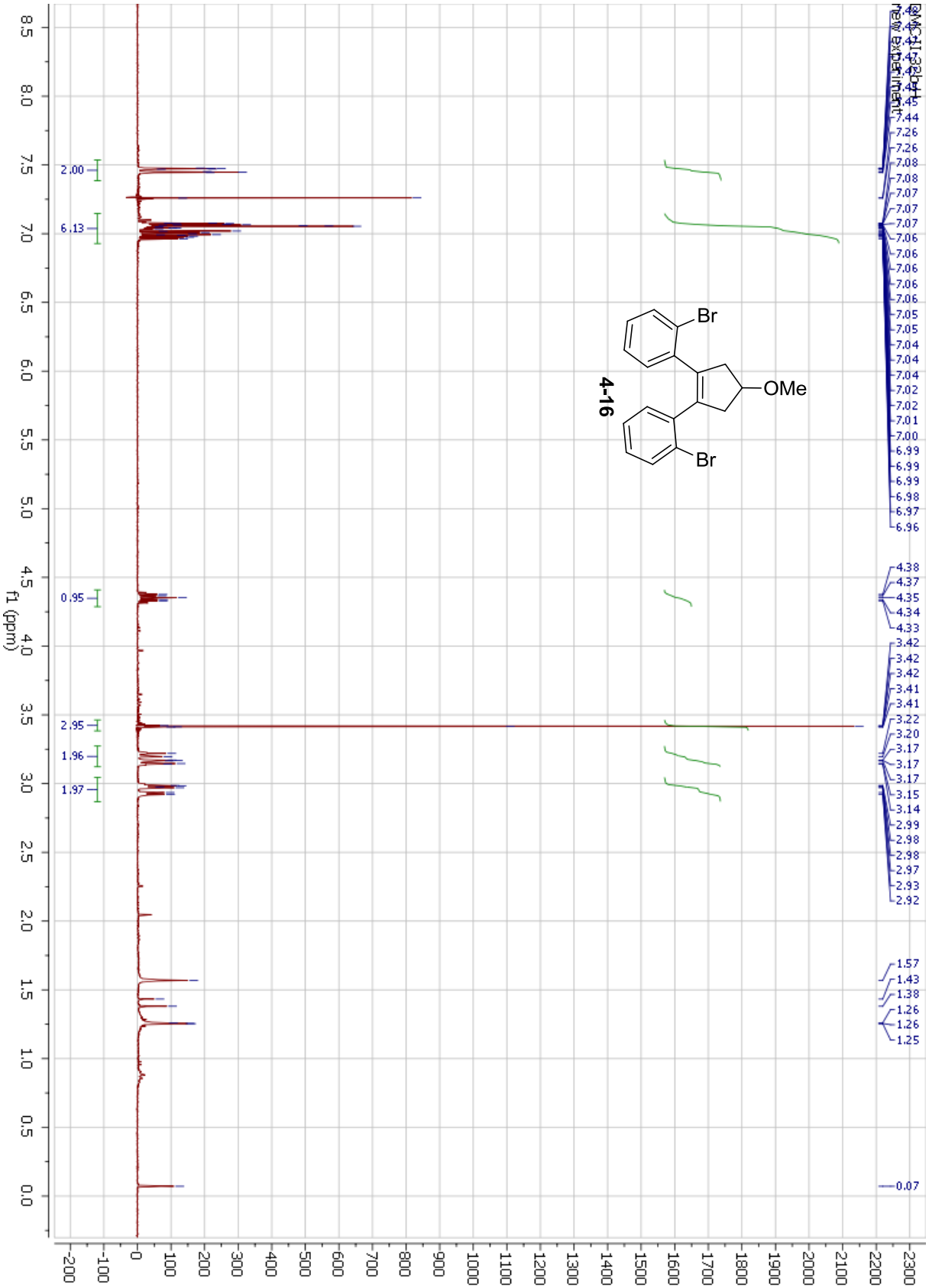
Br
OMe
Br
4-16
f1 (ppm)
2.00
6.13
0.95
2.95
1.96
1.97

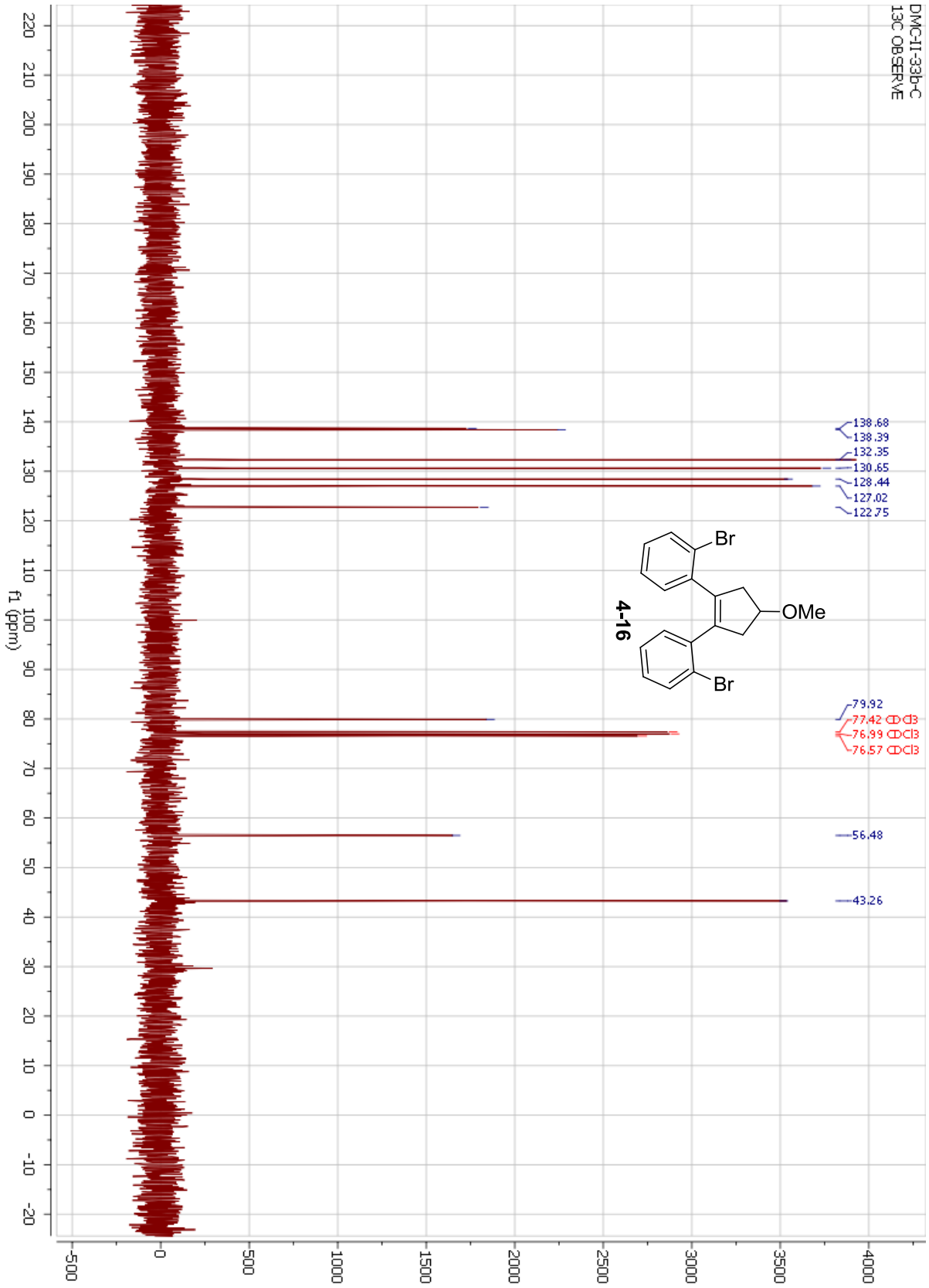
DMG-II-33b-C
13C OBSERVE
138.68
138.39
132.35
130.65
128.44
127.02
122.75
79.92
77.42 CDCl3
76.99 CDCl3
76.57 CDCl3
56.48
43.26
Br
OMe
Br
4-16
f1 (ppm)

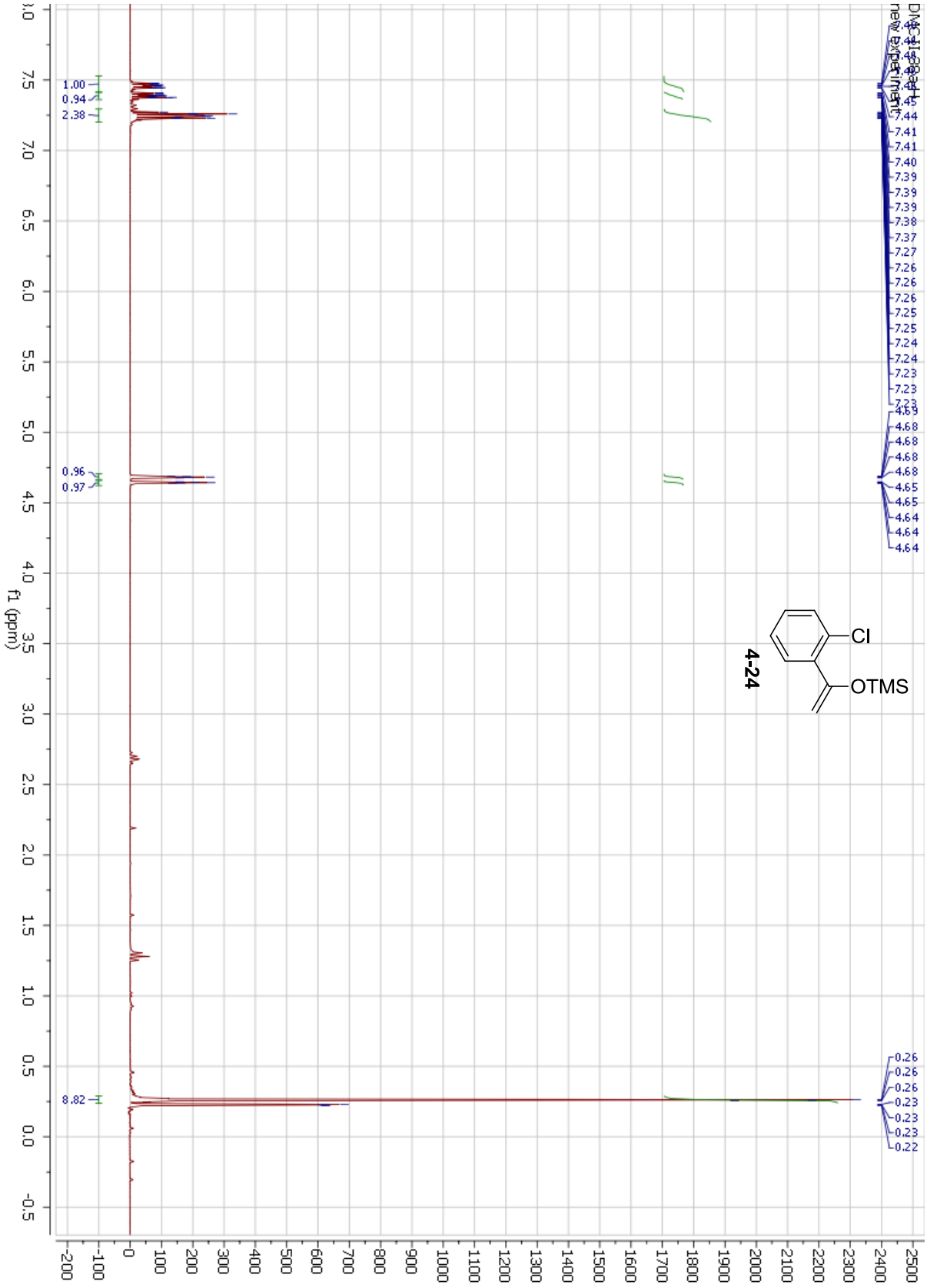
1.00
0.94
2.38
0.96
0.97
8.82
f1 (ppm)
4-24
Cl
OTMS

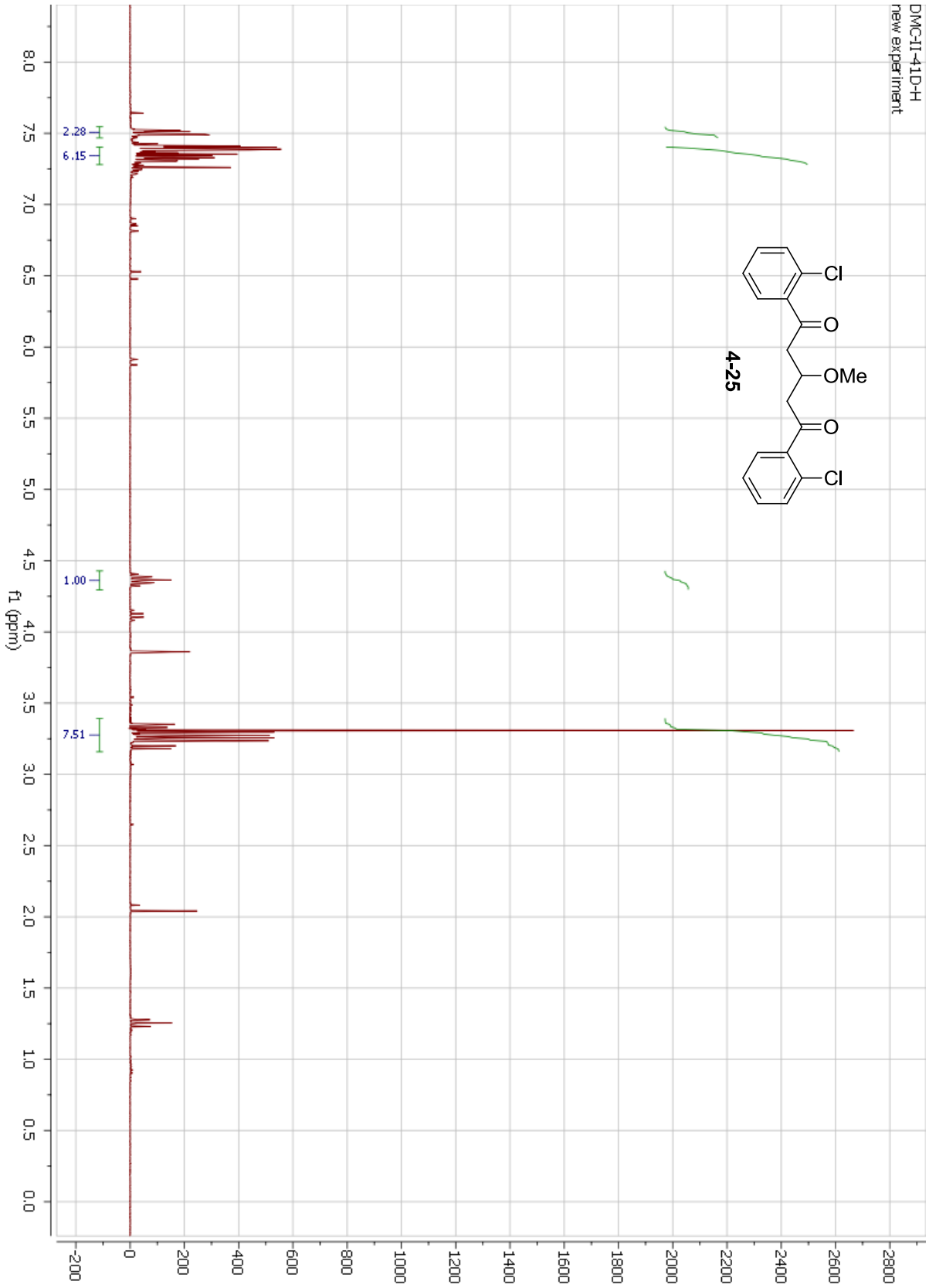
DMC-II-41D-H
new experiment
2.28
6.15
1.00
7.51
f1 (ppm)
Cl
O
OMe
O
Cl
4-25

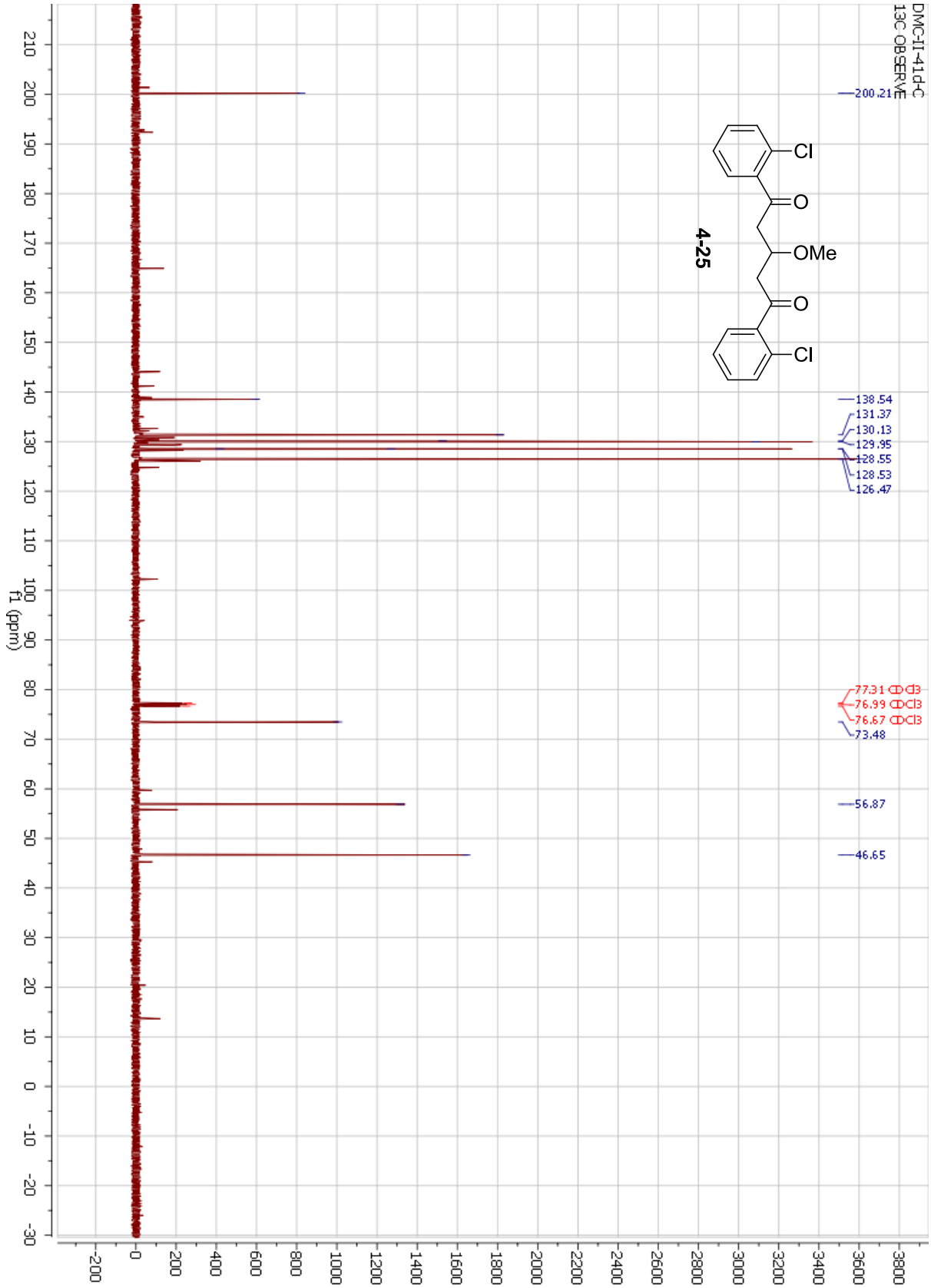
DMC-II-41d-C
13C OBSERVE
200.21
138.54
131.37
130.13
129.95
128.55
128.53
126.47
77.31 CDCl3
76.99 CDCl3
76.67 CDCl3
73.48
56.87
46.65
Cl
O
OMe
O
Cl
4-25
f1 (ppm)

University of Illinois SCS Mass Spectrometry Laboratory

File: 1118g
Sample: 1118g

Date Run: 09-14-2012 (Time Run: 11:10:48)

Ionization mode: EI+
Instrument: VG 70-VSE(B)

Scan: 37

Base: m/z 139; 52.4%FS

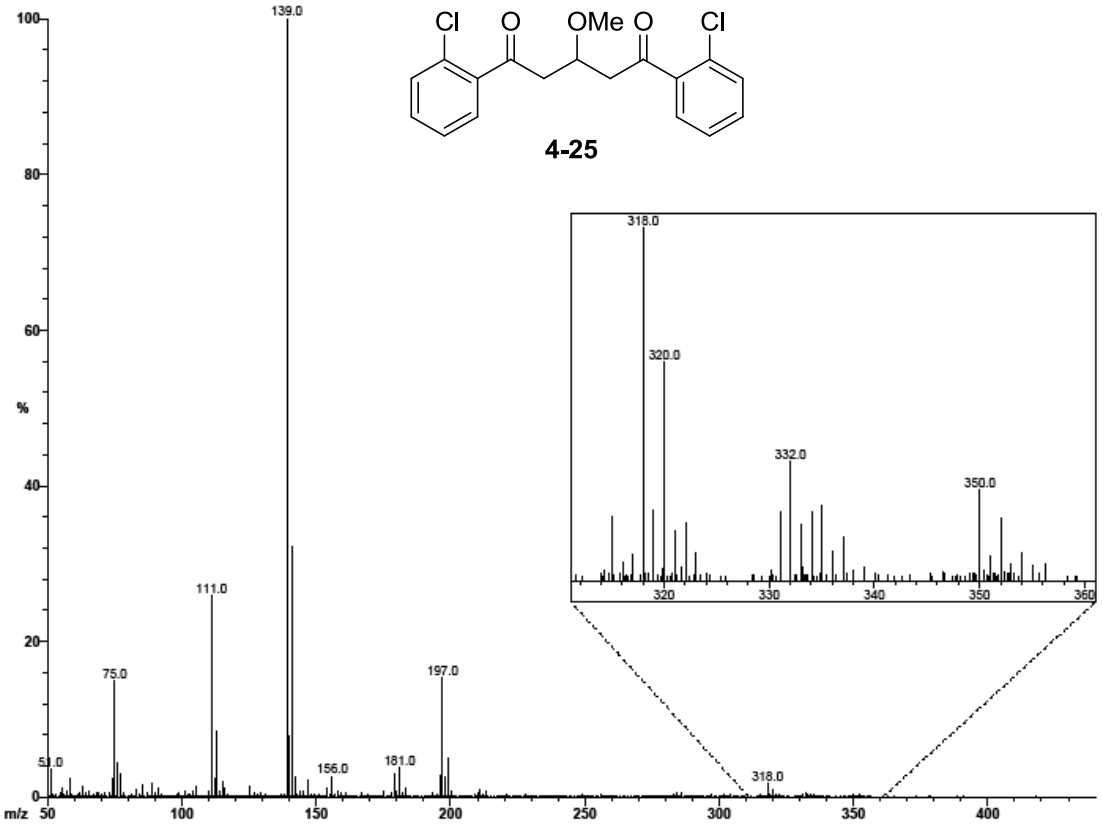

4-25

University of Illinois SCS Mass Spectrometry Laboratory

File: 1118ghr
Sample: 1118g

Date Run: 09-17-2012 (14:32:24)

Ionization mode: EI+

Instrument: 70-VSE(C)

Scan: 14

Base: m/z 350; 11.3%FS

Selected Isotopes : C H $O_{0-3}Cl_{0-2}$

Error Limit : 5 mmu

Unsaturation Limits : -.5 to 30

Measured Mass	*% Base*	*Formula*	*Calculated Mass*	*Error*	*Unsaturation*
350.04741	100.0%	$C_{24}H_{11}O\,Cl$	350.04985	-2.4	19.0
		$C_{18}H_{16}O_3Cl_2$	350.04766	-0.3	10.0

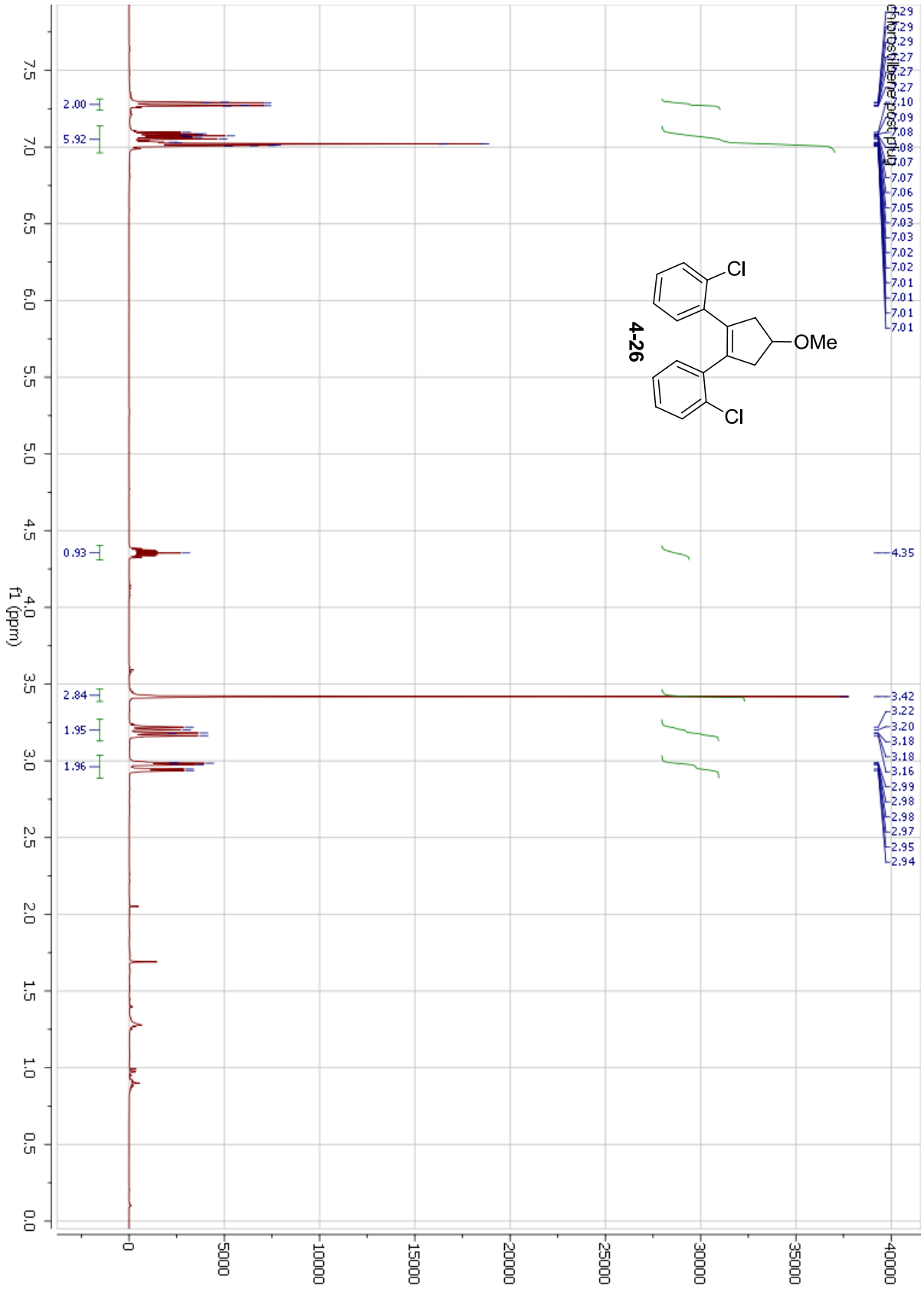
4-26
Cl
OMe
Cl
f1 (ppm)
2.00
5.92
0.93
2.84
1.95
1.96
4.35
3.42
3.22
3.20
3.18
3.18
3.16
2.99
2.98
2.98
2.97
2.95
2.94

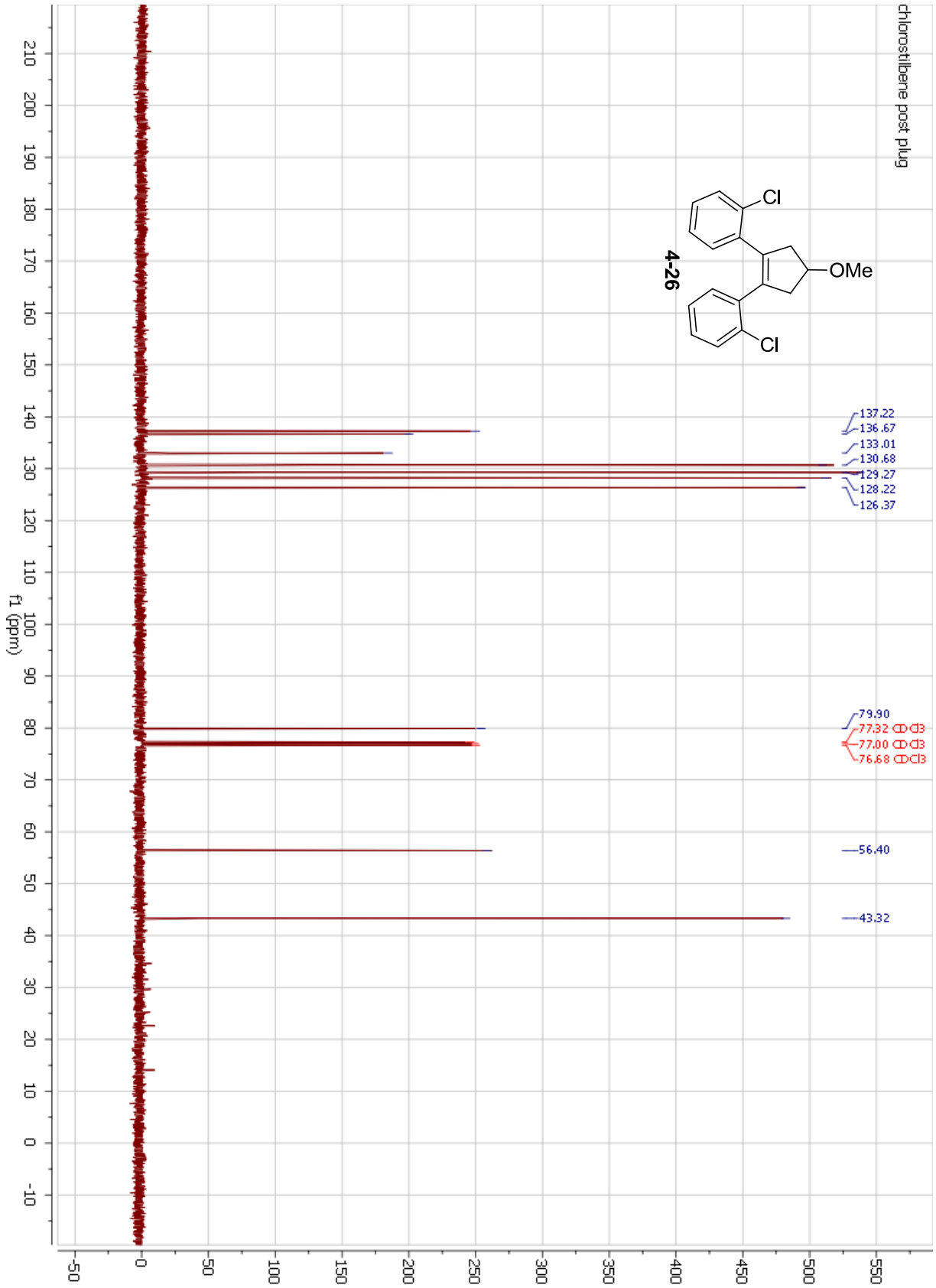
chlorostilbene post plug
Cl
OMe
Cl
4-26
137.22
136.67
133.01
130.68
129.27
128.22
126.37
79.90
77.32 CDCl3
77.00 CDCl3
76.68 CDCl3
56.40
43.32
f1 (ppm)

University of Illinois SCS Mass Spectrometry Laboratory

File: 1118h
Sample: 1118h

Date Run: 09-14-2012 (Time Run: 11:18:56)

Ionization mode: EI+
Instrument: VG 70-VSE(B)

Scan: 5

Base: m/z 318; 17.6%FS

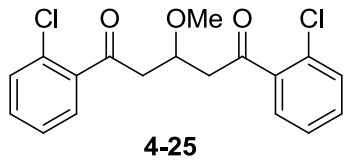

4-25

University of Illinois SCS Mass Spectrometry Laboratory

File: 1118hhr
Sample: 1118h

Date Run: 09-17-2012 (14:24:55)

Ionization mode: EI+

Instrument: 70-VSE(C)

Base: m/z 318; 32.8%FS

Scan: 24

Selected Isotopes : C H $O_{0-1}Cl_{0-2}$ **Error Limit : 5 mmu** **Unsaturation Limits : -.5 to 30**

Measured Mass	*% Base*	*Formula*	*Calculated Mass*	*Error*	*Unsaturation*
318.05845	100.0%	$C_{18}H_{16}O\,Cl_2$	318.05783	0.6	10.0

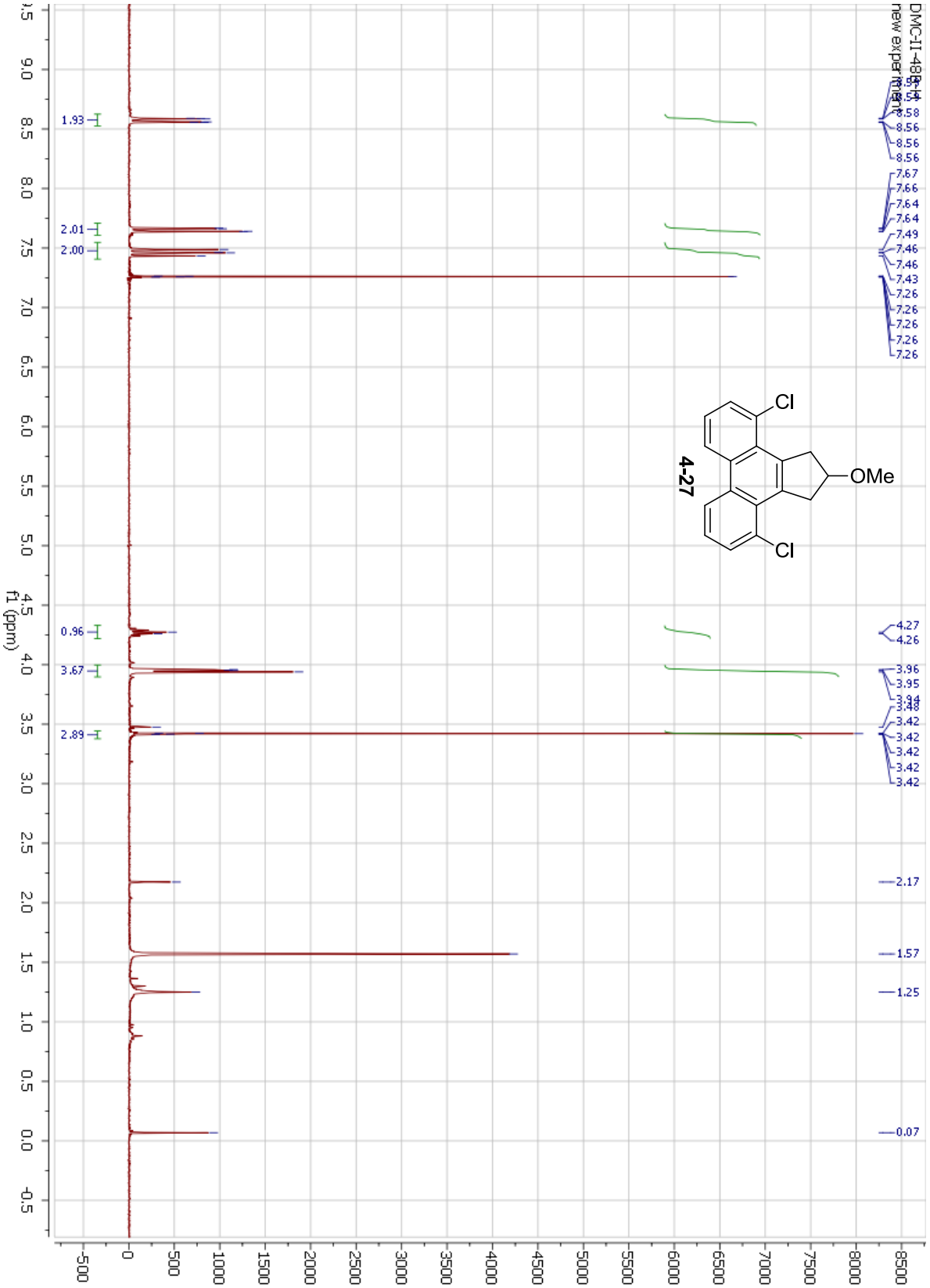
DMC-II-48-1-H
new experiment
1.93
2.01
2.00
0.96
3.67
2.89
8.58
8.56
8.56
8.56
7.67
7.66
7.64
7.64
7.49
7.46
7.46
7.43
7.26
7.26
7.26
7.26
7.26
4.27
4.26
3.96
3.95
3.94
3.48
3.42
3.42
3.42
3.42
3.42
2.17
1.57
1.25
0.07
Cl
OMe
Cl
4-27
f1 (ppm)

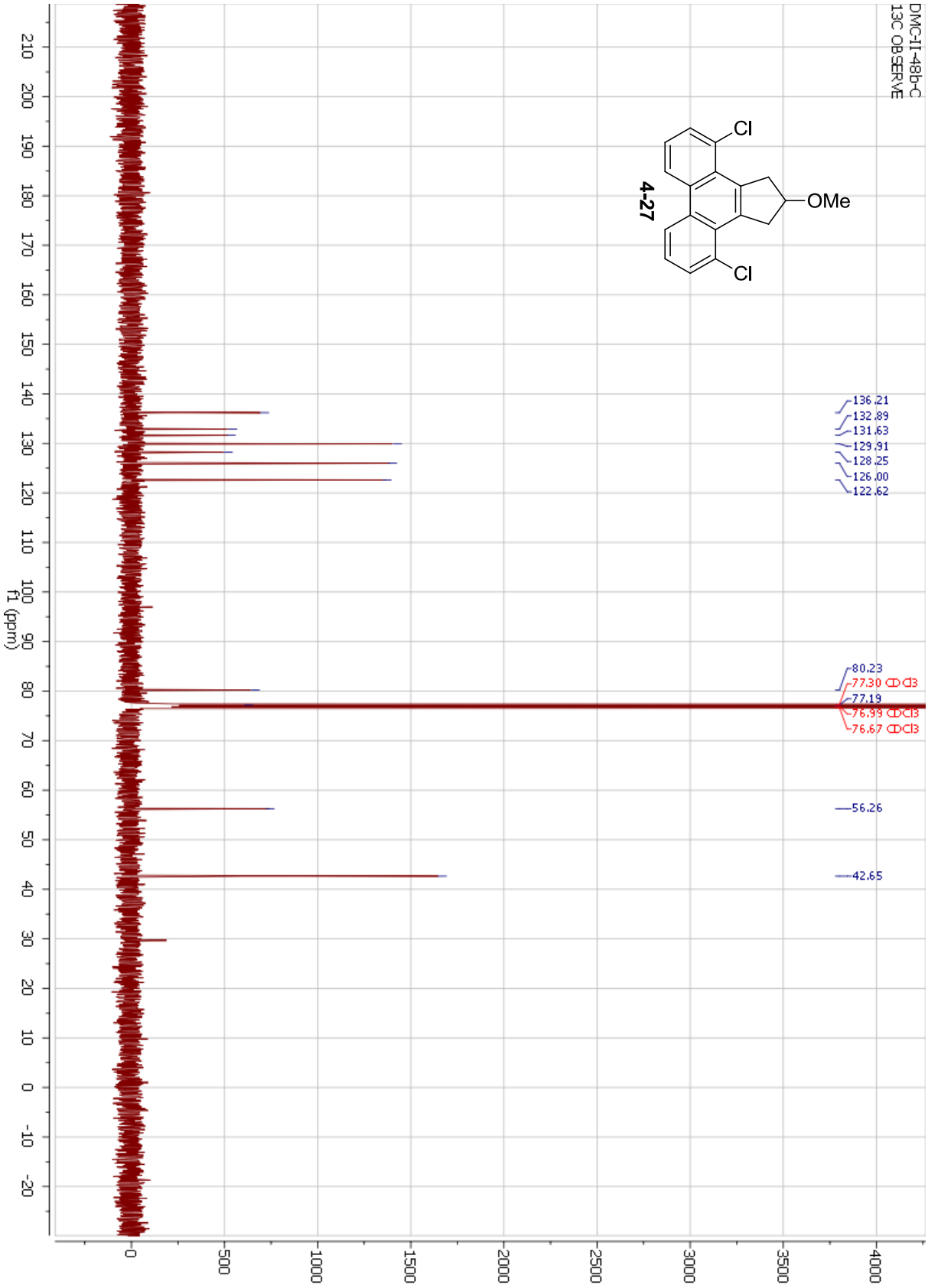
DMC-II-48b-C
13C OBSERVE
Cl
OMe
Cl
4-27
136.21
132.89
131.63
129.91
128.25
126.00
122.62
80.23
77.30 CDCl3
77.19
76.99 CDCl3
76.67 CDCl3
56.26
42.65
f1 (ppm)

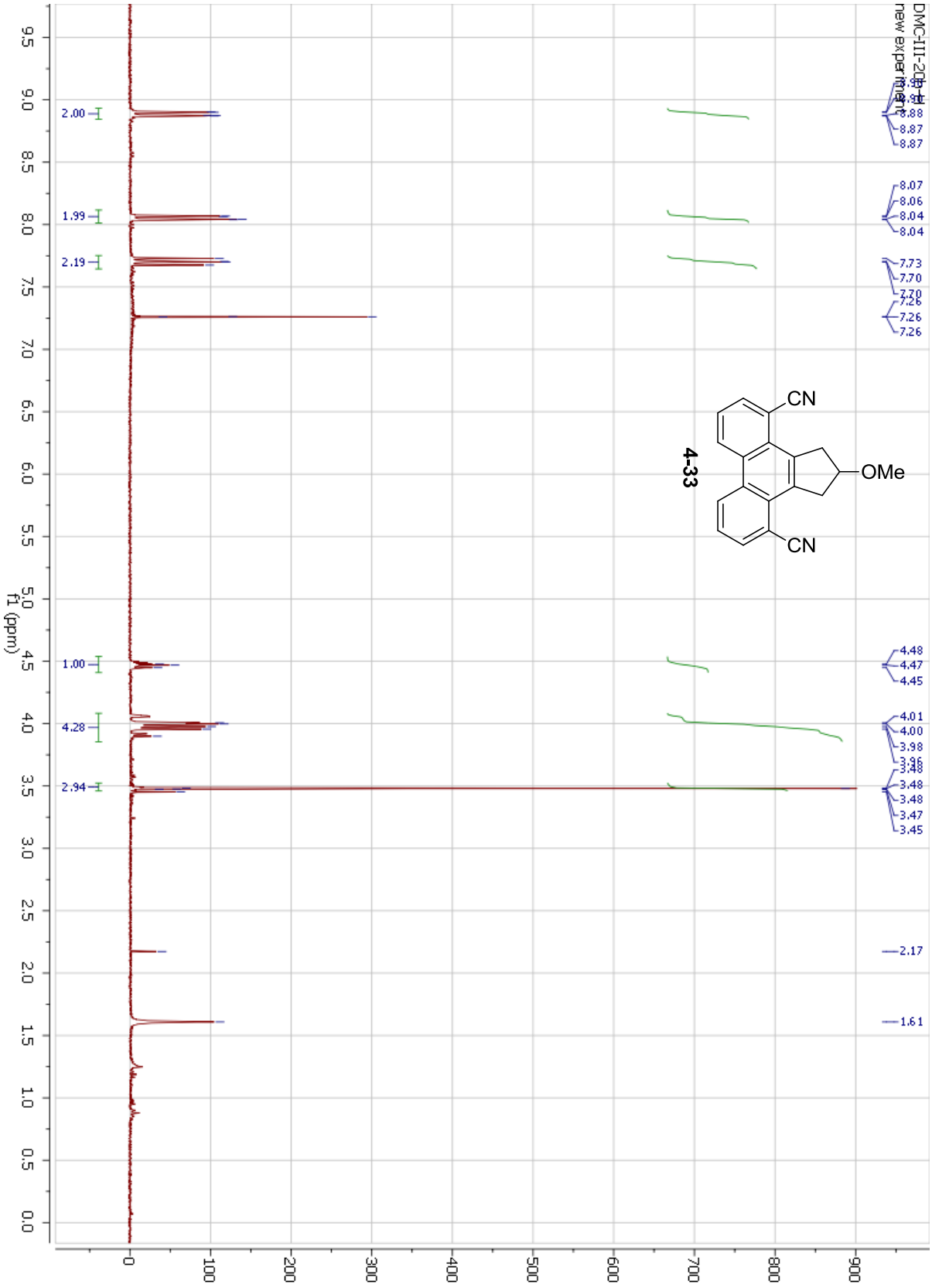
DMC-III-20a-H
new experiment
2.00
1.99
2.19
1.00
4.28
2.94
8.88
8.87
8.87
8.07
8.06
8.04
8.04
7.73
7.70
7.70
7.26
7.26
7.26
4.48
4.47
4.45
4.01
4.00
3.98
3.96
3.48
3.48
3.48
3.47
3.45
2.17
1.61
CN
OMe
CN
4-33
f1 (ppm)

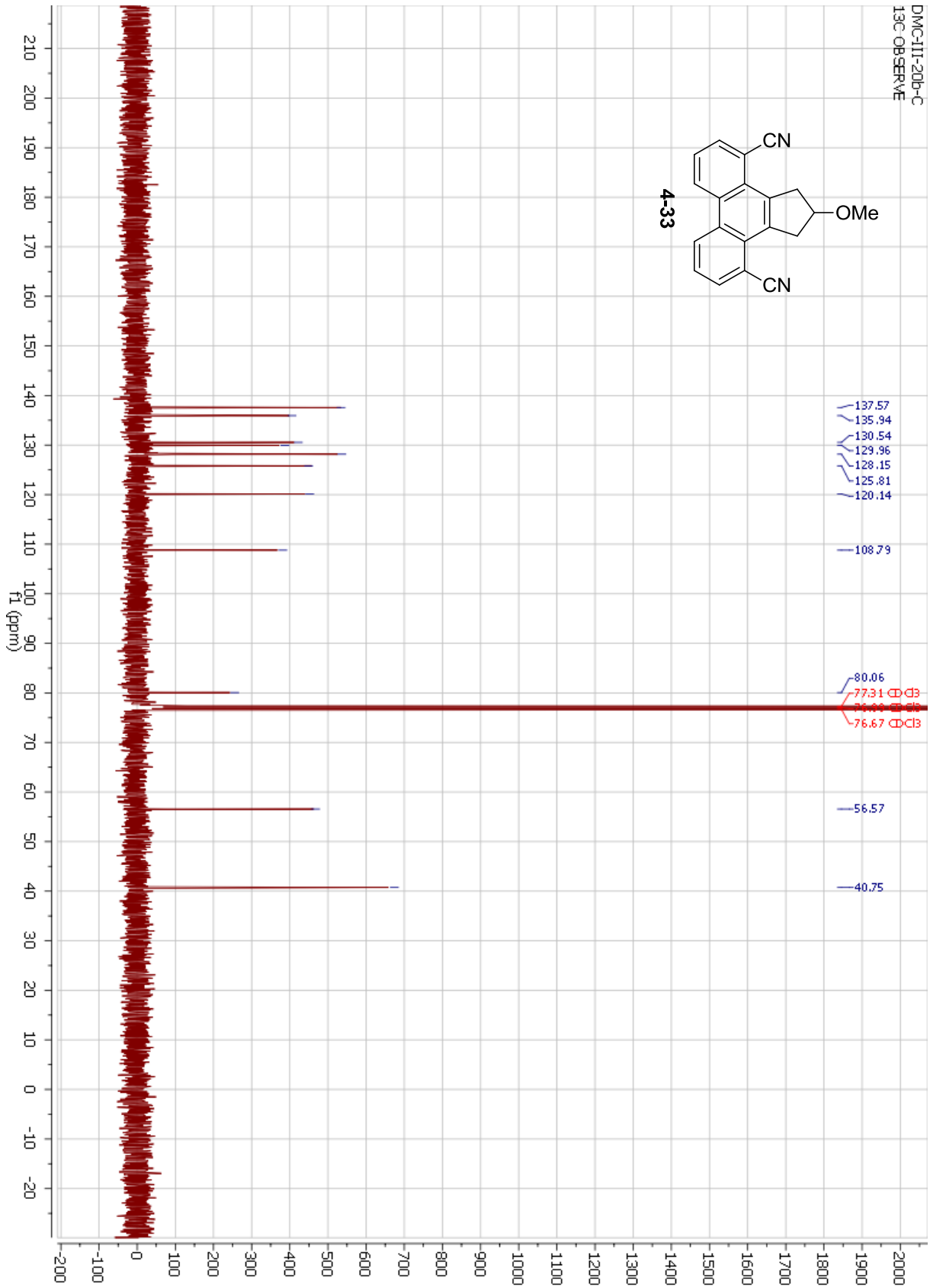
DMC-III-20b-C
13C OBSERVE
4-33
CN
OMe
CN
137.57
135.94
130.54
129.96
128.15
125.81
120.14
108.79
80.06
77.31 CDCl3
76.67 CDCl3
56.57
40.75
f1 (ppm)

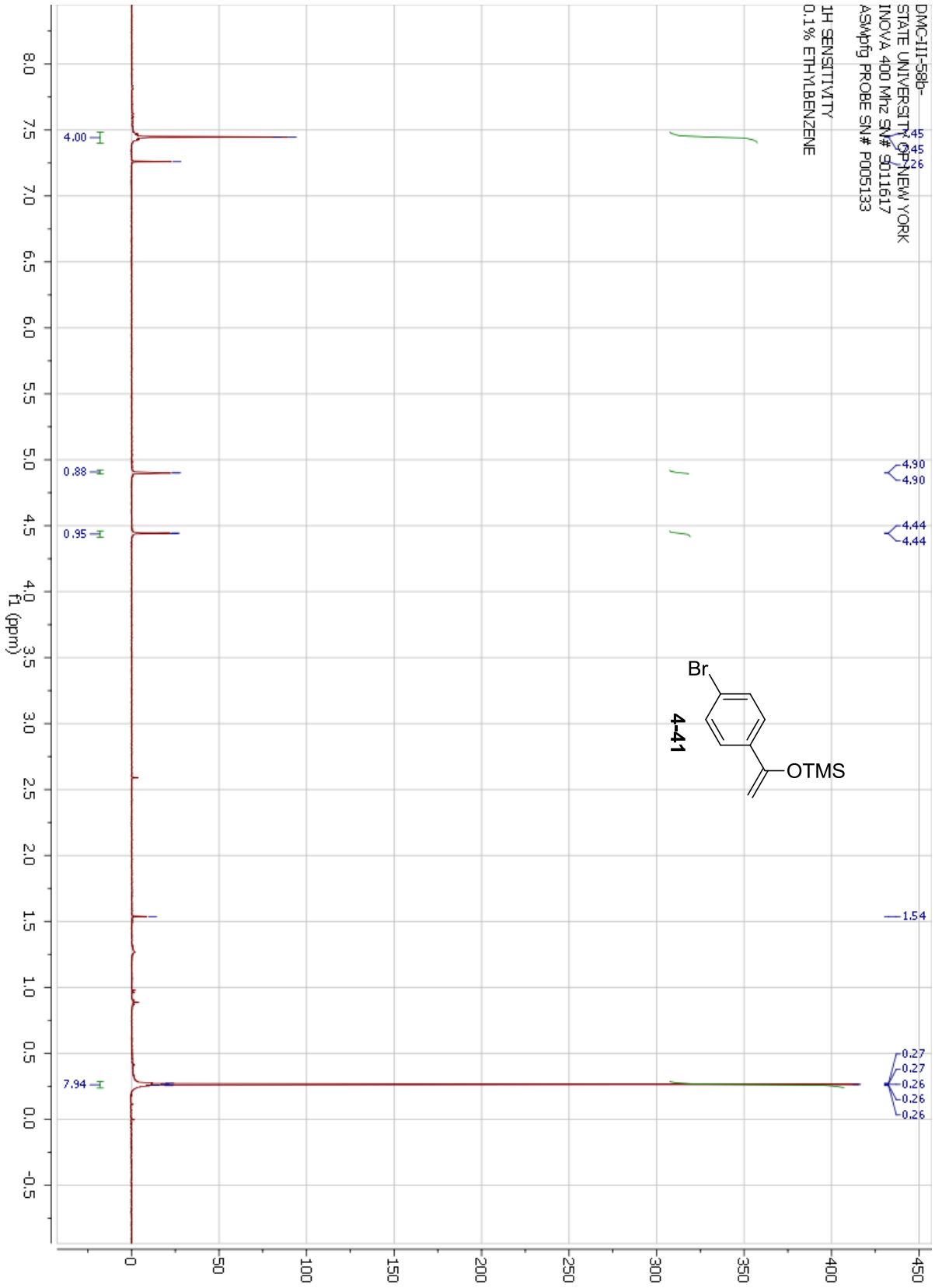
DMG-III-58b-
STATE UNIVERSITY OF NEW YORK
INOVA 400 MHz SN# 501617
ASMpfg PROBE SN# P005133
1H SENSITIVITY
0.1% ETHYLBENZENE
4.00
0.88
0.95
7.94
7.45
7.45
7.26
4.90
4.90
4.44
4.44
1.54
0.27
0.27
0.26
0.26
0.26
Br
OTMS
4-41
f1 (ppm)

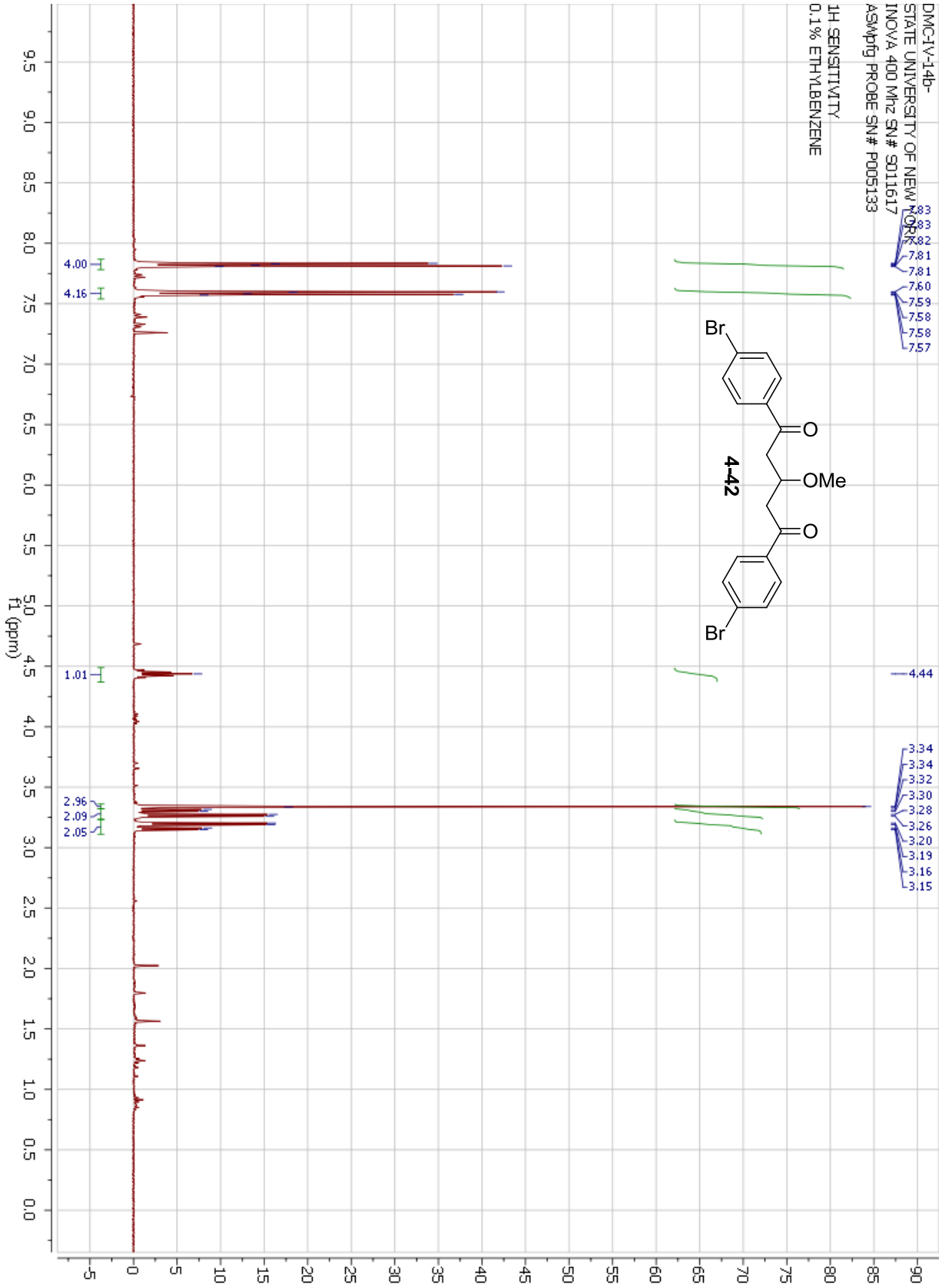
DMC-1V-14b-
STATE UNIVERSITY OF NEW YORK
INOVA 400 Mhz SN# S011617
ASWpfg PROBE SN# P005133
1H SENSITIVITY
0.1% ETHYLBENZENE
4-42
Br
O
OMe
O
Br
4.00
4.16
1.01
2.96
2.09
2.05
7.83
7.83
7.82
7.81
7.81
7.60
7.59
7.58
7.58
7.57
4.44
3.34
3.34
3.32
3.30
3.28
3.26
3.20
3.19
3.16
3.15
f1 (ppm)

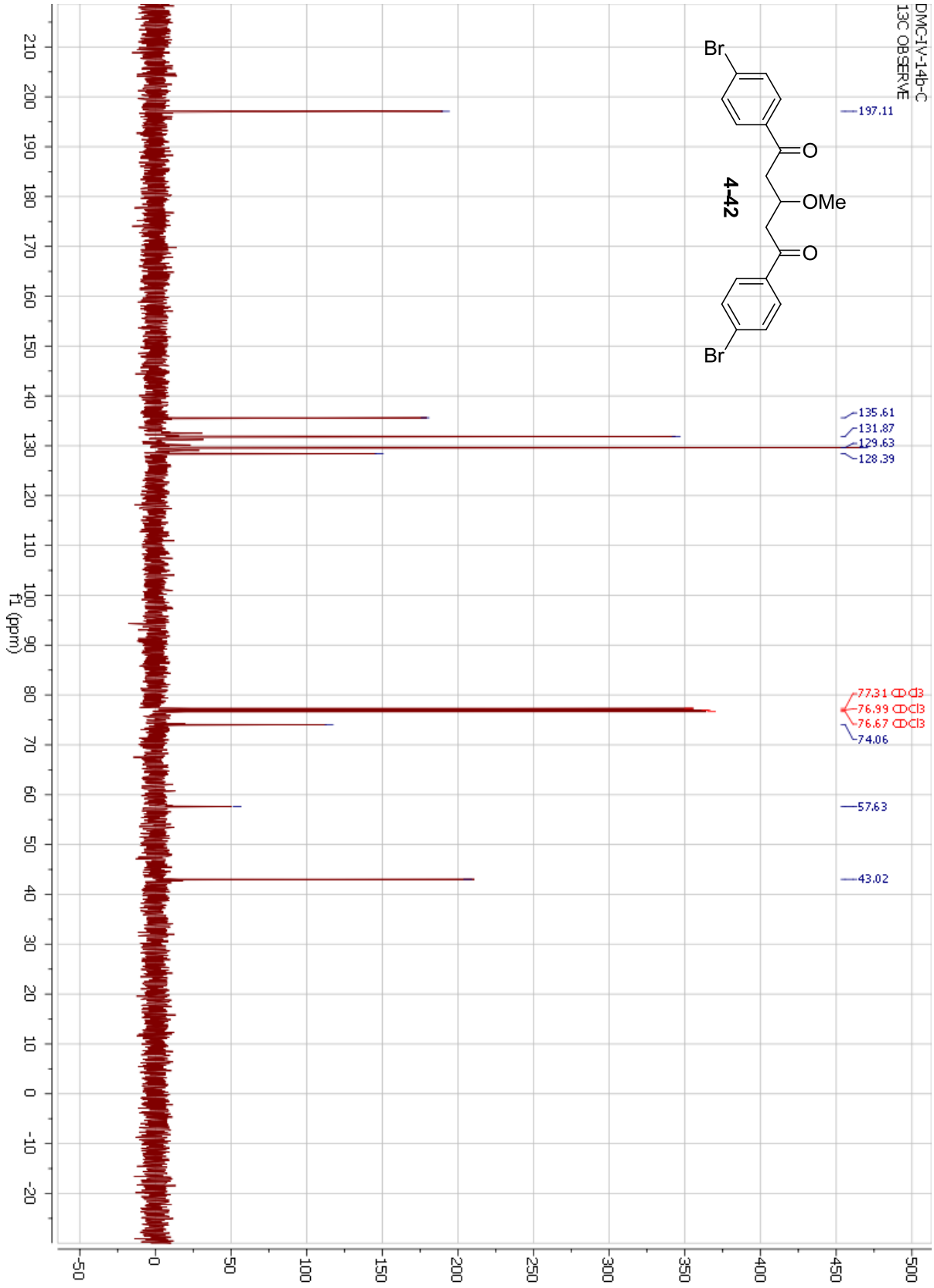
DMC-IV-14b-C
13C OBSERVE
Br
O
OMe
O
Br
4-42
197.11
135.61
131.87
129.63
128.39
77.31 CDCl3
76.99 CDCl3
76.67 CDCl3
74.06
57.63
43.02
f1 (ppm)

University of Illinois SCS Mass Spectrometry Laboratory

File: 1118c
Sample: 1118c

Date Run: 09-14-2012 (Time Run: 12:20:08)

Ionization mode: EI+
Instrument: VG 70-VSE(B)

Scan: 38
Peak at 446 is probably background oil.

Base: m/z 183; 96.6%FS

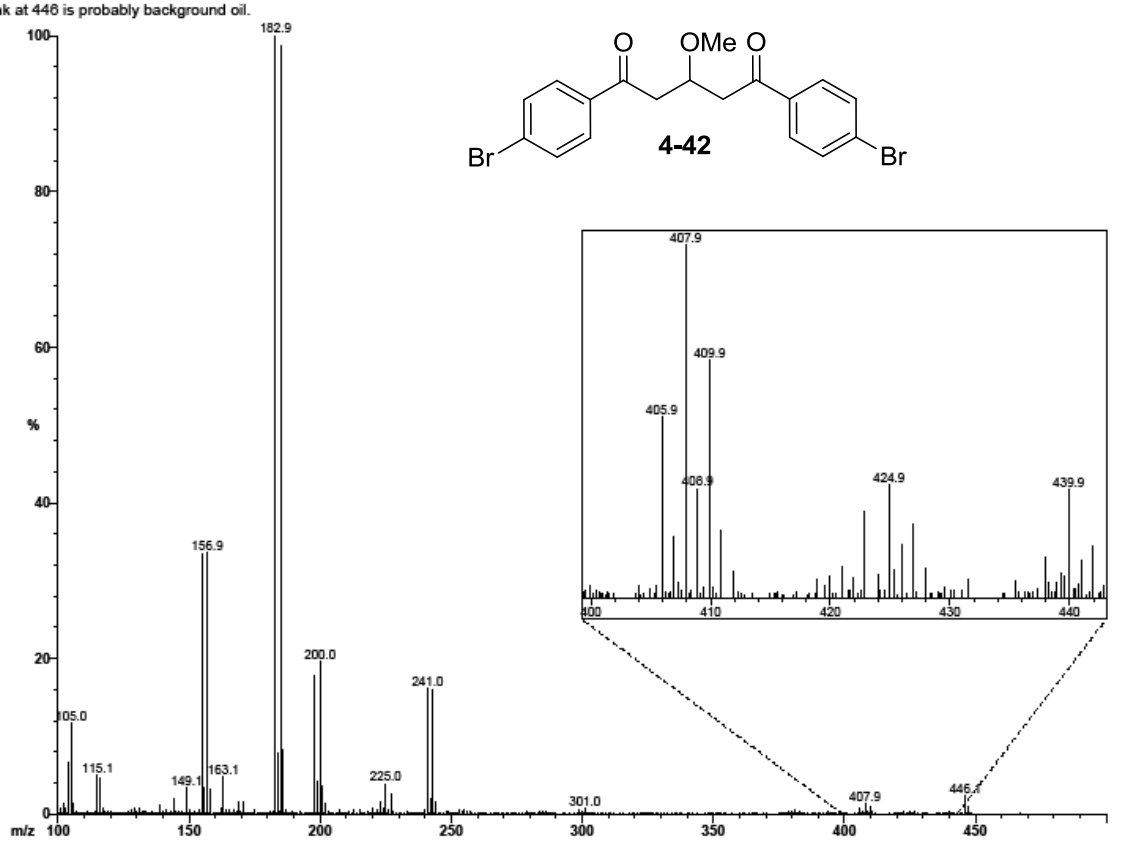

4-42

University of Illinois SCS Mass Spectrometry Laboratory

File: 1118chr
Sample: 1118c

Date Run: 09-17-2012 (17:04:35)

Ionization mode: EI+
Instrument: 70-VSE(C)

Base: m/z 425; 52.6%FS

Scan: 22

Selected Isotopes : C H $Br_{0-2}O_{0-4}$ **Error Limit : 5 mmu** **Unsaturation Limits : -.5 to 50**

Measured Mass	*% Base*	*Formula*	*Calculated Mass*	*Error*	*Unsaturation*
437.94758	10.5%	$C_{18}H_{16}Br_2O_3$	437.94665	0.9	10.0

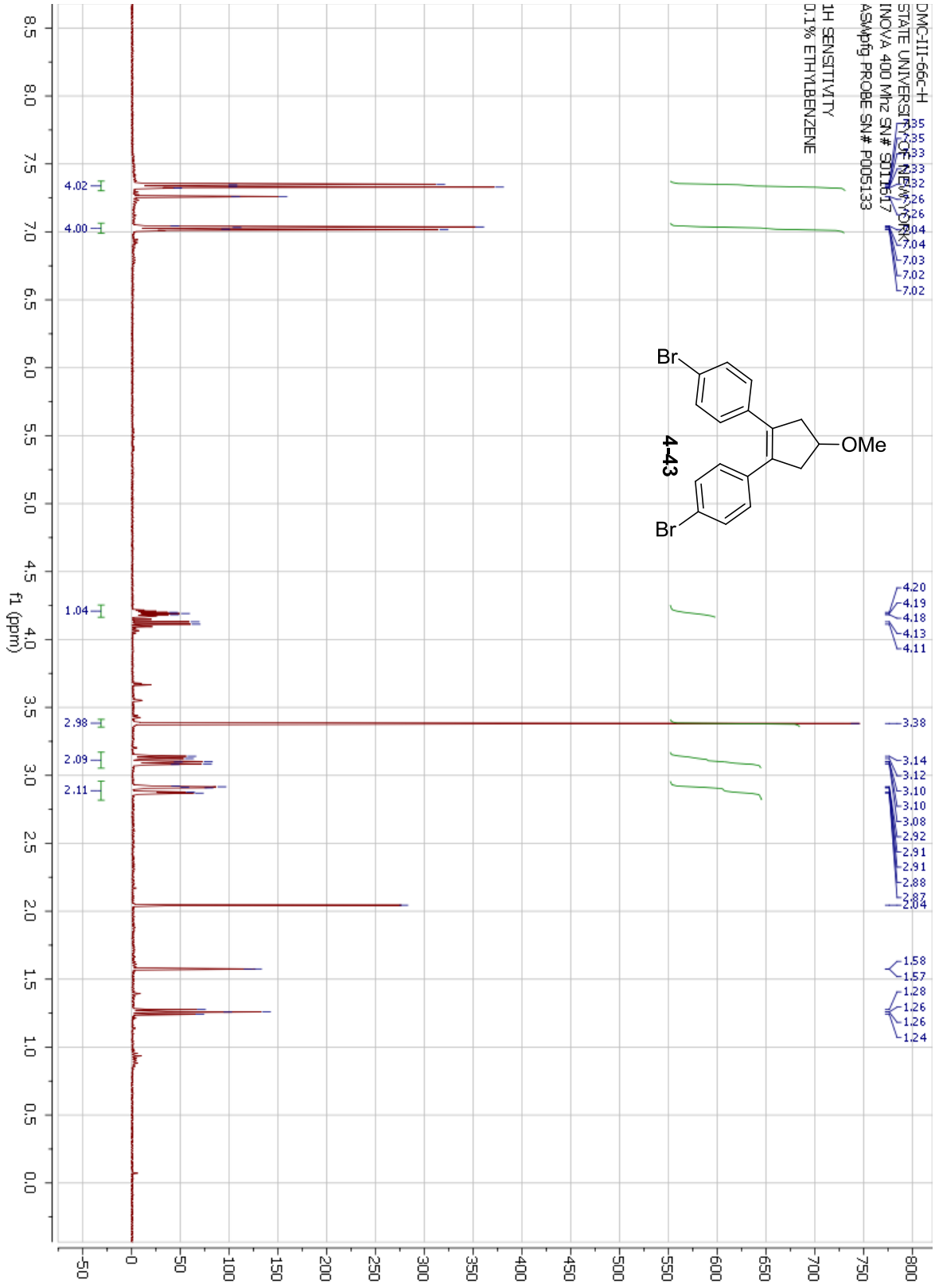
DMC-III-66c-H
STATE UNIVERSITY OF NEW YORK
INOVA 400 Mhz SN# 501617
ASMpfg PROBE SN# P005133
1H SENSITIVITY
0.1% ETHYLBENZENE
Br
OMe
Br
4-43
f1 (ppm)
4.02
4.00
1.04
2.98
2.09
2.11

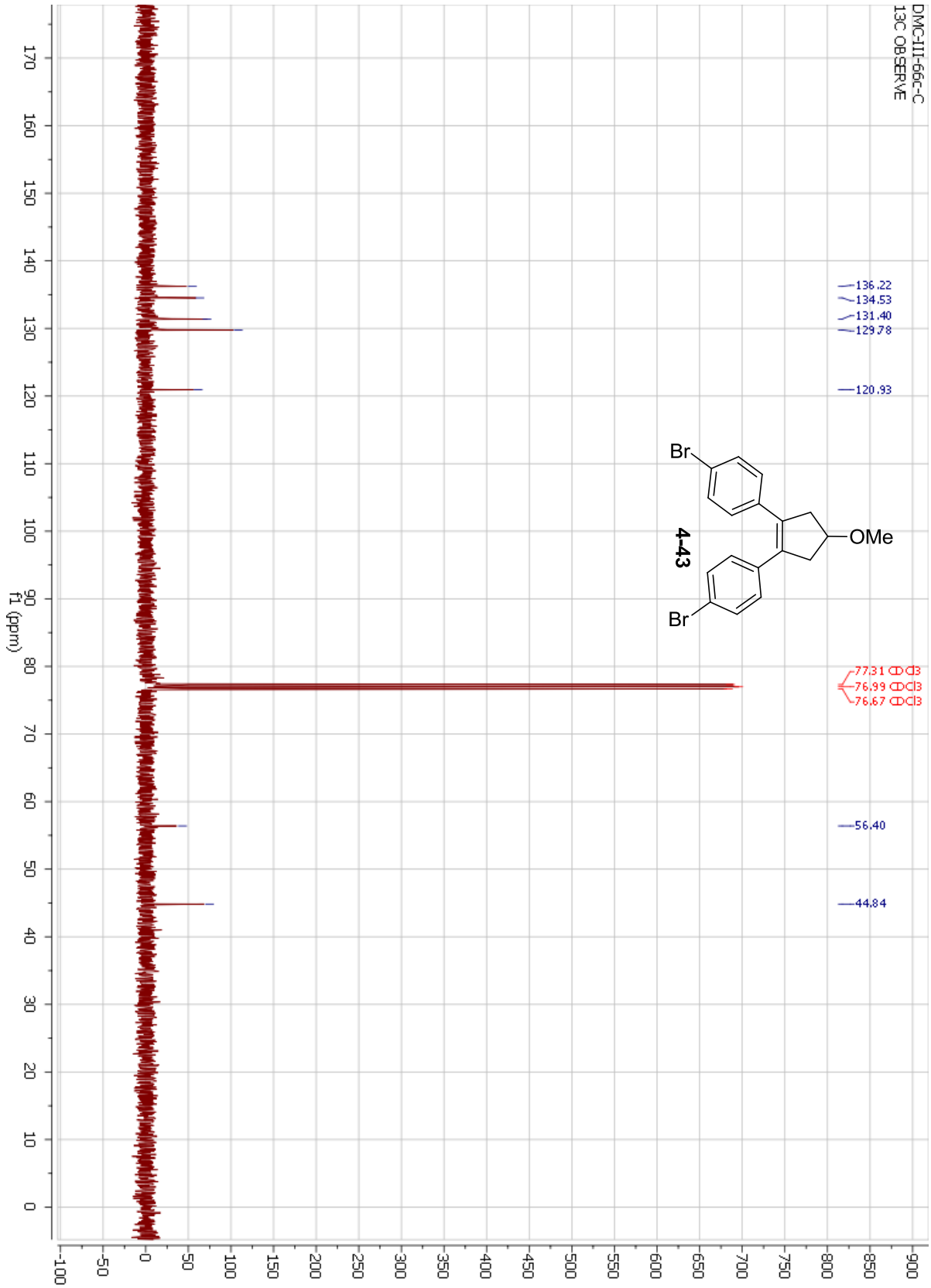
DMC-III-66c-C
13C OBSERVE
136.22
134.53
131.40
129.78
120.93
77.31 CDCl3
76.99 CDCl3
76.67 CDCl3
56.40
44.84
Br
OMe
Br
4-43
f1 (ppm)

University of Illinois SCS Mass Spectrometry Laboratory

File: 1118e
Sample: 1118e

Date Run: 09-14-2012 (Time Run: 11:54:25)

Ionization mode: EI+
Instrument: VG 70-VSE(B)

Scan: 28
Peak at 446 is probably background oil.

Base: m/z 394; 16.5%FS

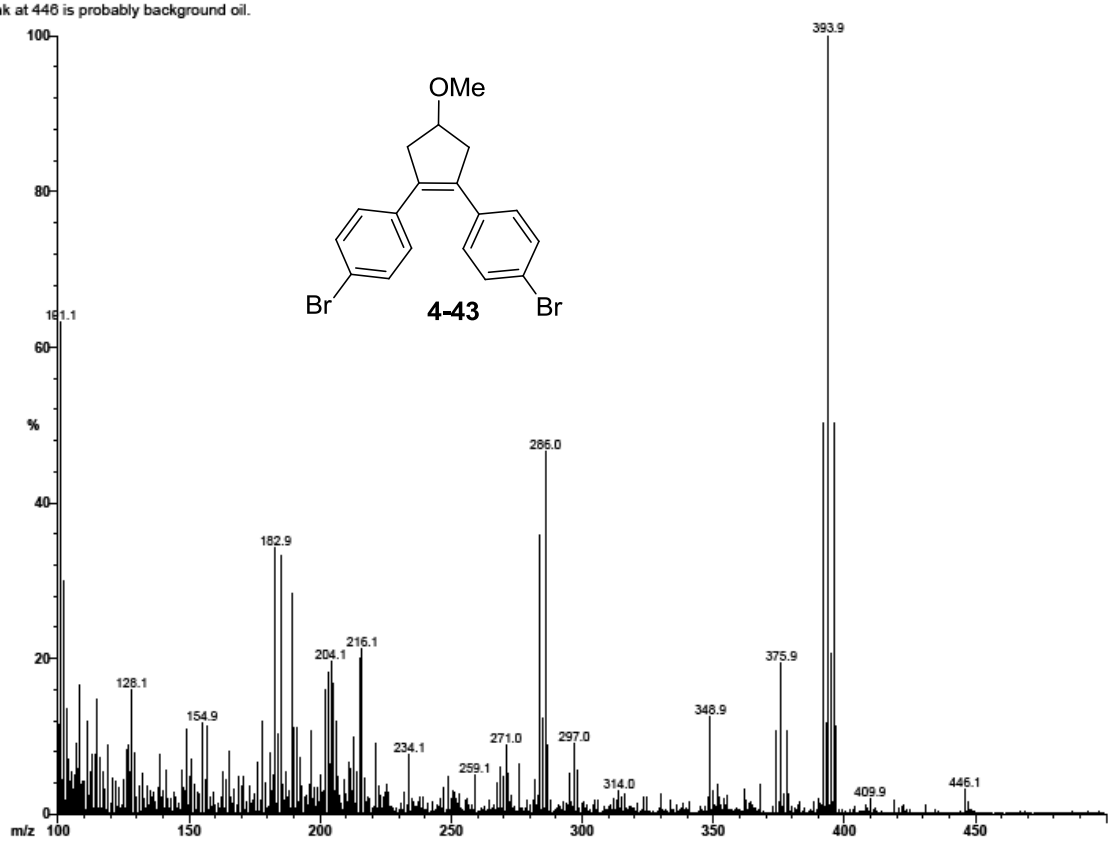

University of Illinois SCS Mass Spectrometry Laboratory

File: 1118ehr
Sample: 1118e

Date Run: 09-17-2012 (15:29:20)

Ionization mode: EI+

Instrument: 70-VSE(C)

Base: m/z 394; 35.3%FS

Scan: 42

Selected Isotopes : C H $O_{0-4}Br_{0-4}$ **Error Limit : 5 mmu** **Unsaturation Limits : -.5 to 30**

Measured Mass	*% Base*	*Formula*	*Calculated Mass*	*Error*	*Unsaturation*
391.94078	71.1%	$C_{17}H_{14}OBr_2$	391.94117	-0.4	10.0

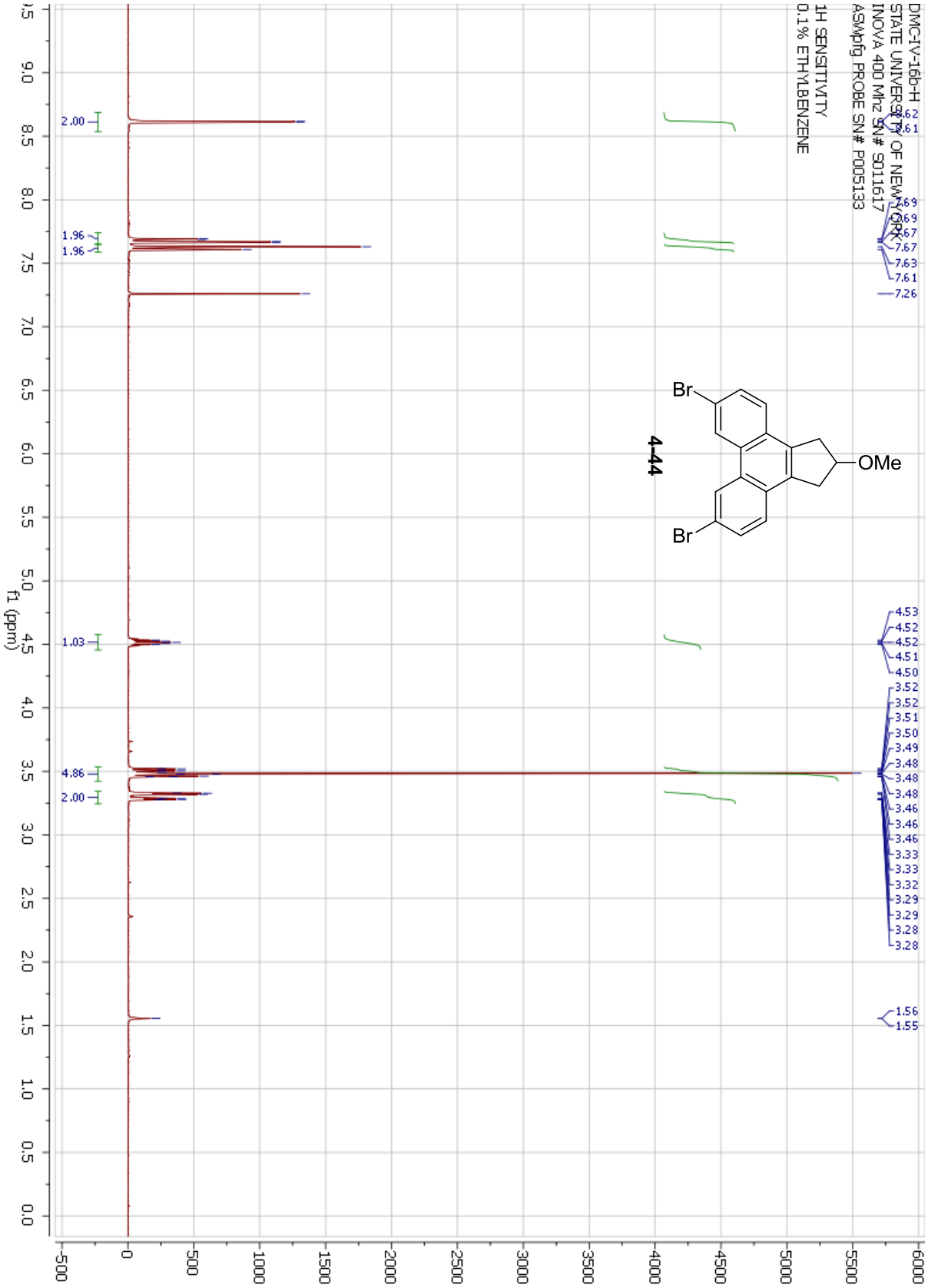
DMC-IV-16b-H
STATE UNIVERSITY OF NEW YORK
INOVA 400 Mhz SN# SD11617
ASWpfg PROBE SN# P005133
1H SENSITIVITY
0.1% ETHYLBENZENE
4-44
Br
Br
OMe
f1 (ppm)
2.00
1.96
1.96
1.03
4.86
2.00
7.62
7.61
7.69
7.69
7.67
7.67
7.63
7.61
7.26
4.53
4.52
4.52
4.51
4.50
3.52
3.52
3.51
3.50
3.49
3.48
3.48
3.48
3.46
3.46
3.46
3.33
3.33
3.32
3.29
3.29
3.28
3.28
1.56
1.55

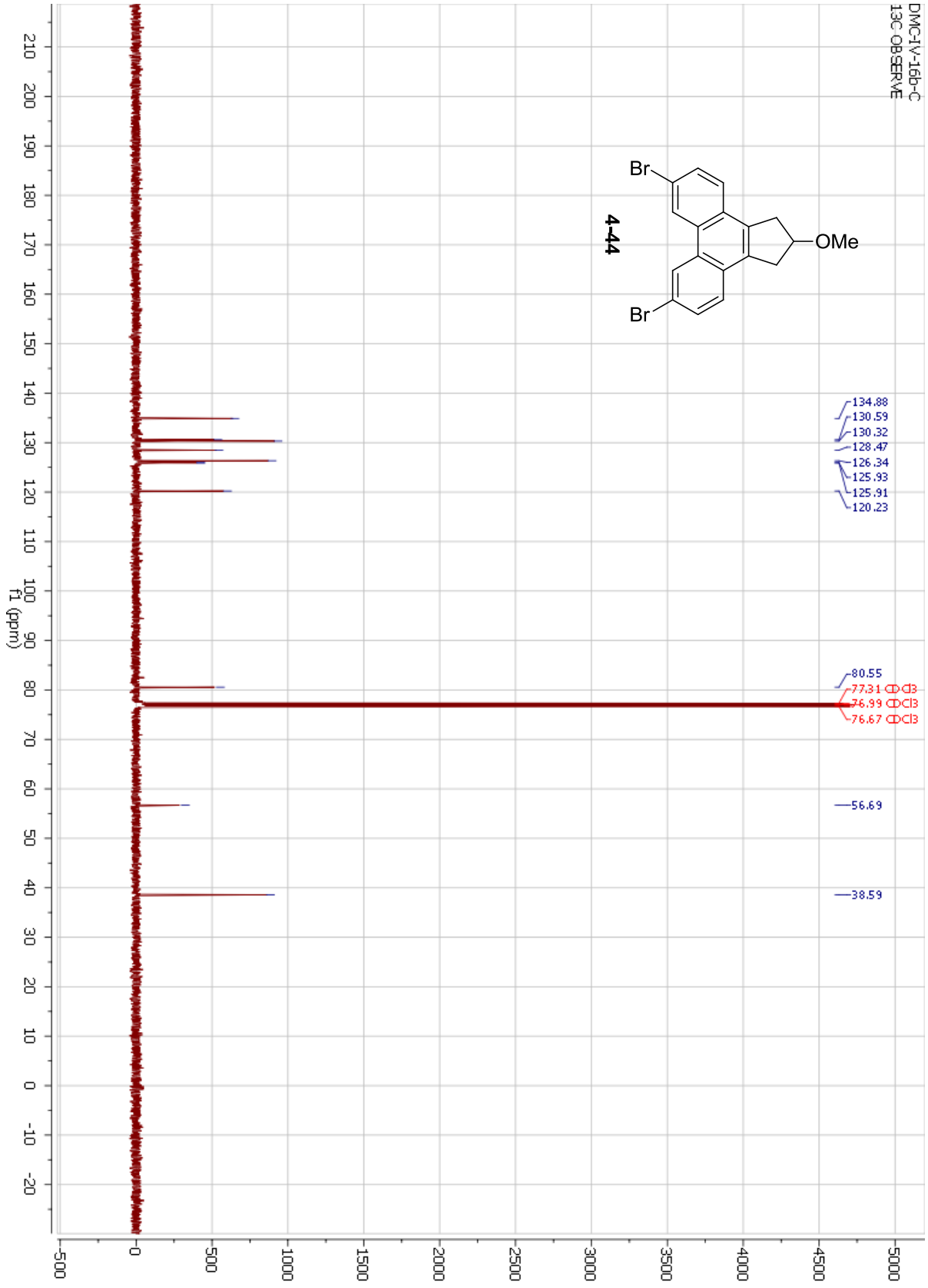
DMC-IV-16b-C
13C OBSERVE
4-44
Br
Br
OMe
134.88
130.59
130.32
128.47
126.34
125.93
125.91
120.23
80.55
77.31 CDCl3
76.99 CDCl3
76.67 CDCl3
56.69
38.59
f1 (ppm)

University of Illinois SCS Mass Spectrometry Laboratory

File: 1118f
Sample: 1118f

Date Run: 09-14-2012 (Time Run: 12:02:47)

Ionization mode: EI+
Instrument: VG 70-VSE(B)

Scan: 18
Peak at 446 is probably background oil.

Base: m/z 185; 7.7%FS

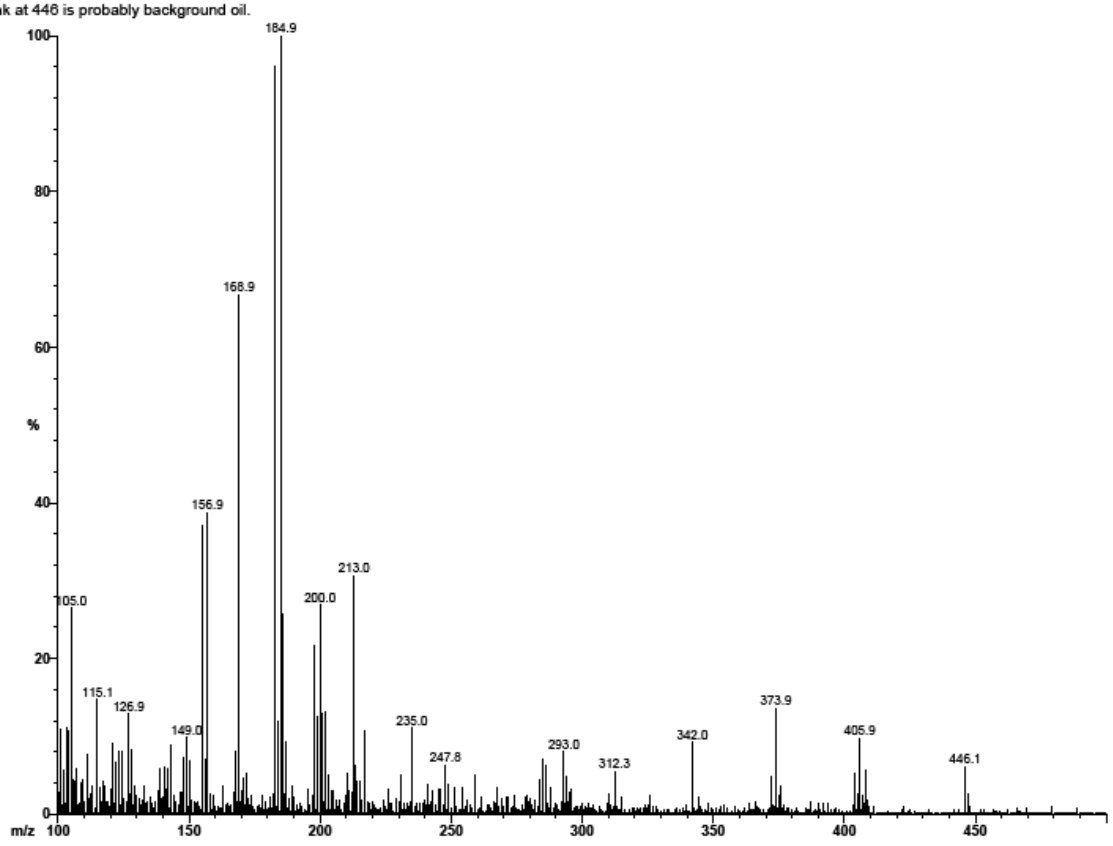

University of Illinois SCS Mass Spectrometry Laboratory

File: 1118fhr
Sample: 1118f

Date Run: 09-17-2012 (15:17:08)

Ionization mode: EI+
Instrument: 70-VSE(C)

Base: m/z 406; 21.4%FS

Scan: 36

Selected Isotopes : C H $Br_{0-2}O_{0-1}$ **Error Limit : 5 mmu** **Unsaturation Limits : -.5 to 50**

Measured Mass	*% Base*	*Formula*	*Calculated Mass*	*Error*	*Unsaturation*
403.94092	65.7%	$C_{18}H_{14}Br_2O$	403.94117	-0.3	11.0

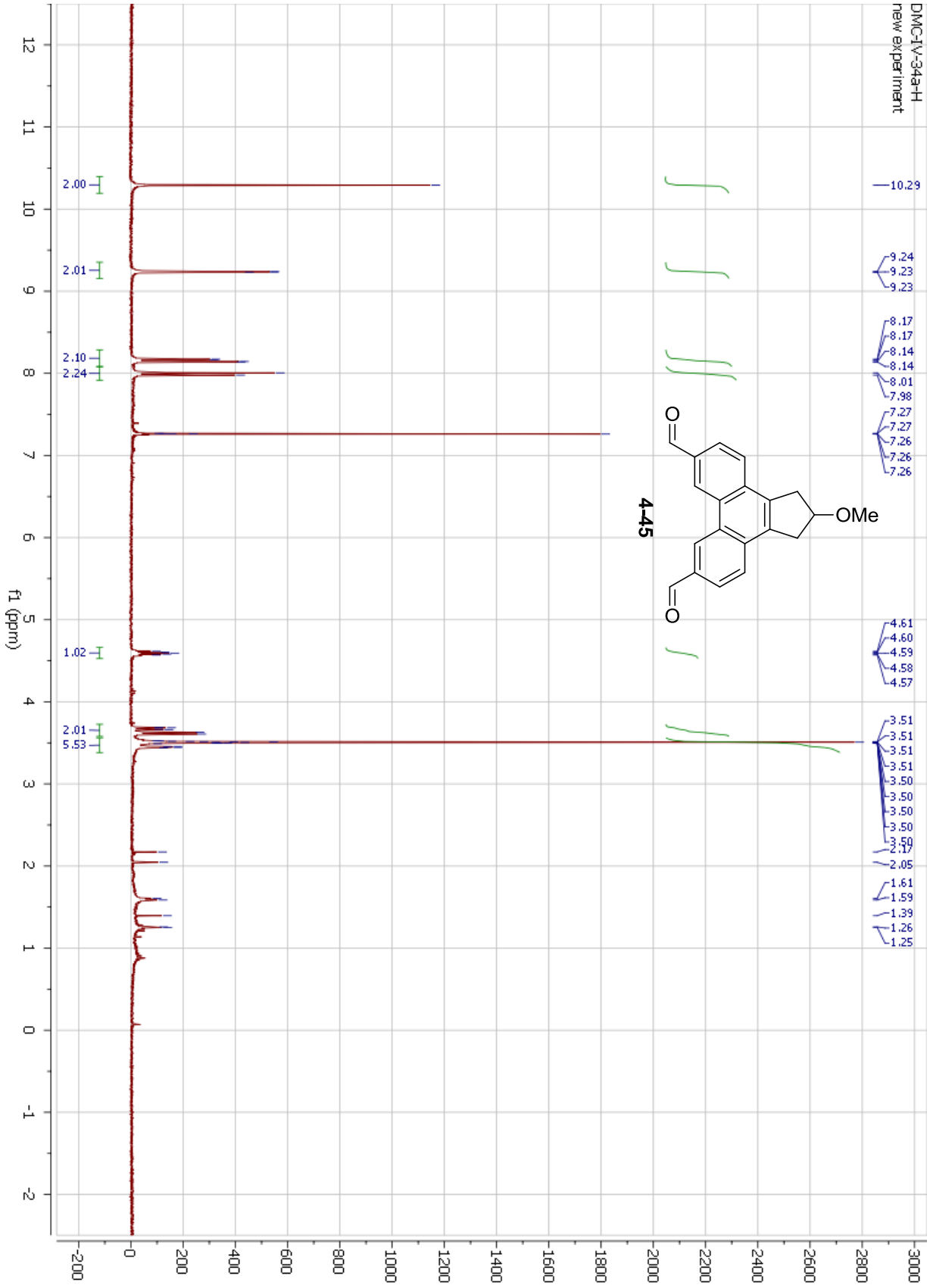
DMC-IV-34a-H
new experiment
4-45
OMe
O
O
f1 (ppm)
2.00
2.01
2.10
2.24
1.02
2.01
5.53
10.29
9.24
9.23
9.23
8.17
8.17
8.14
8.14
8.01
7.98
7.27
7.27
7.26
7.26
7.26
4.61
4.60
4.59
4.58
4.57
3.51
3.51
3.51
3.51
3.50
3.50
3.50
3.50
3.50
2.17
2.05
1.61
1.59
1.39
1.26
1.25

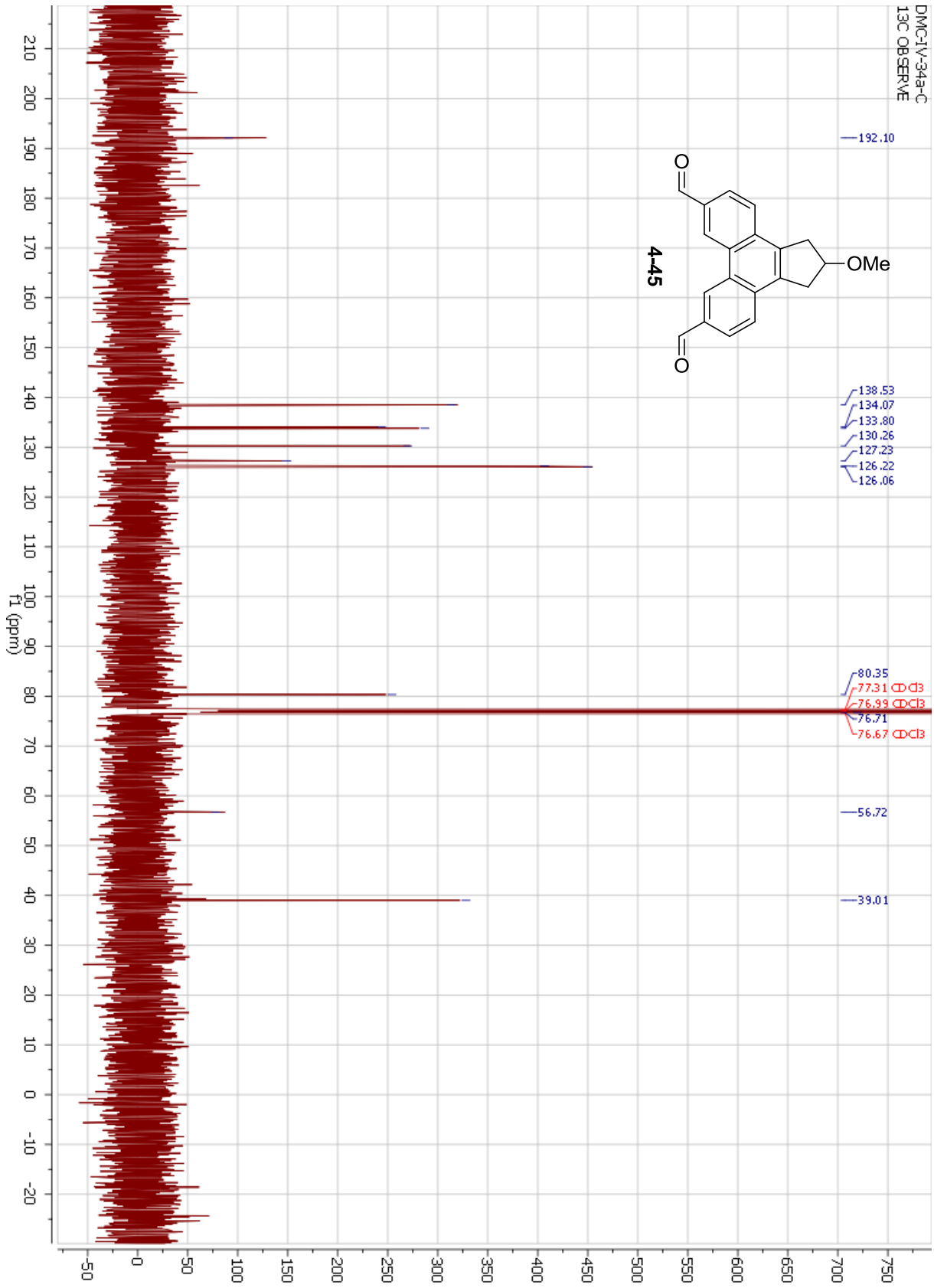
DMC-1V-34a-C
13C OBSERVE
192.10
138.53
134.07
133.80
130.26
127.23
126.22
126.06
80.35
77.31 CDCl3
76.99 CDCl3
76.71
76.67 CDCl3
56.72
39.01
OMe
4-45
f1 (ppm)

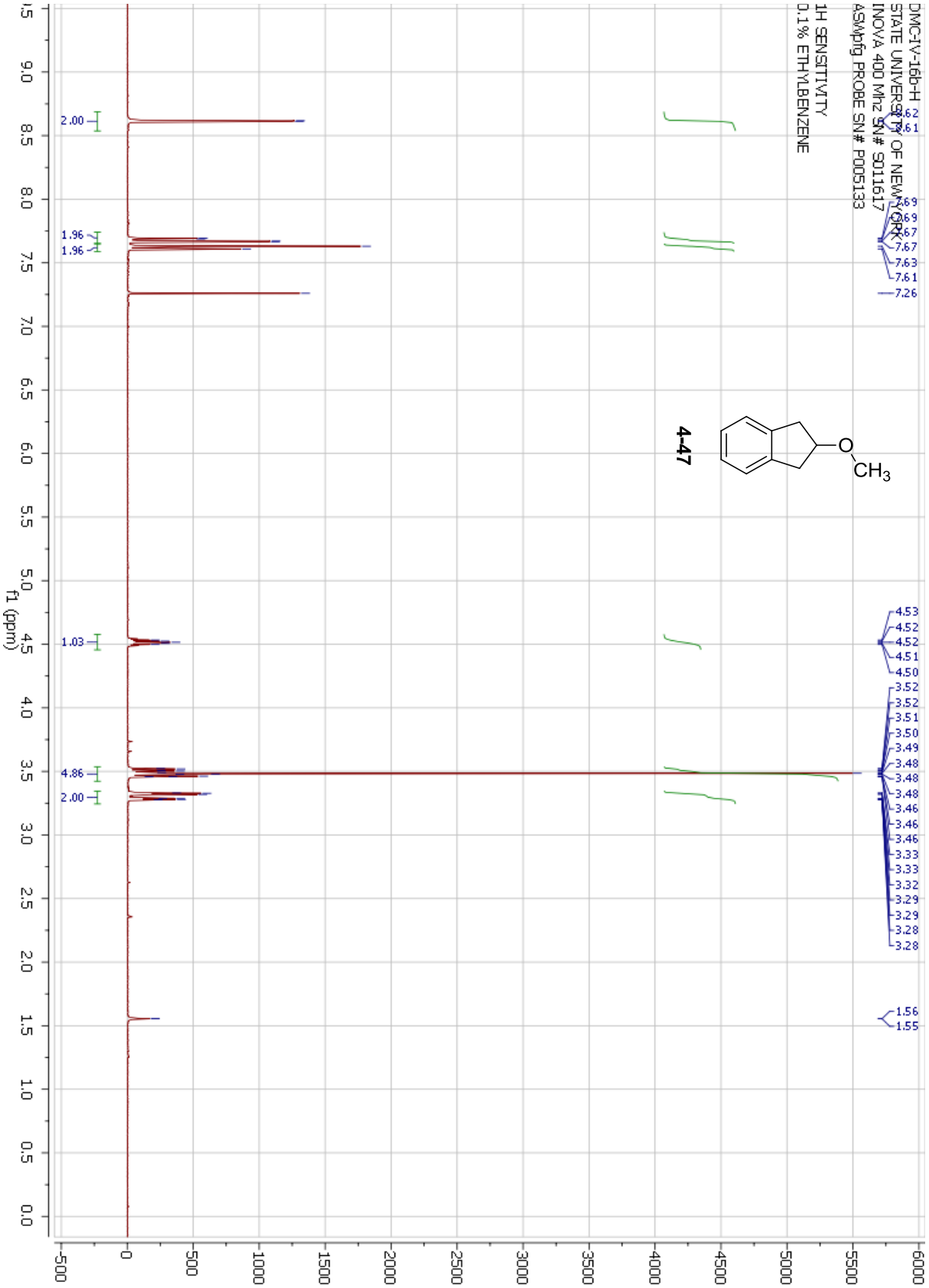
DMC-IV-16b-H
STATE UNIVERSITY OF NEW YORK
INOVA 400 MHz SN# SD11617
ASMpfg PROBE SN# P005133
1H SENSITIVITY
0.1% ETHYLBENZENE
4-47
O
CH3
f1 (ppm)
2.00
1.96
1.96
1.03
4.86
2.00
7.69
7.69
7.67
7.67
7.63
7.61
7.26
4.53
4.52
4.52
4.51
4.50
3.52
3.52
3.51
3.50
3.49
3.48
3.48
3.48
3.46
3.46
3.46
3.33
3.33
3.32
3.29
3.29
3.28
3.28
1.56
1.55

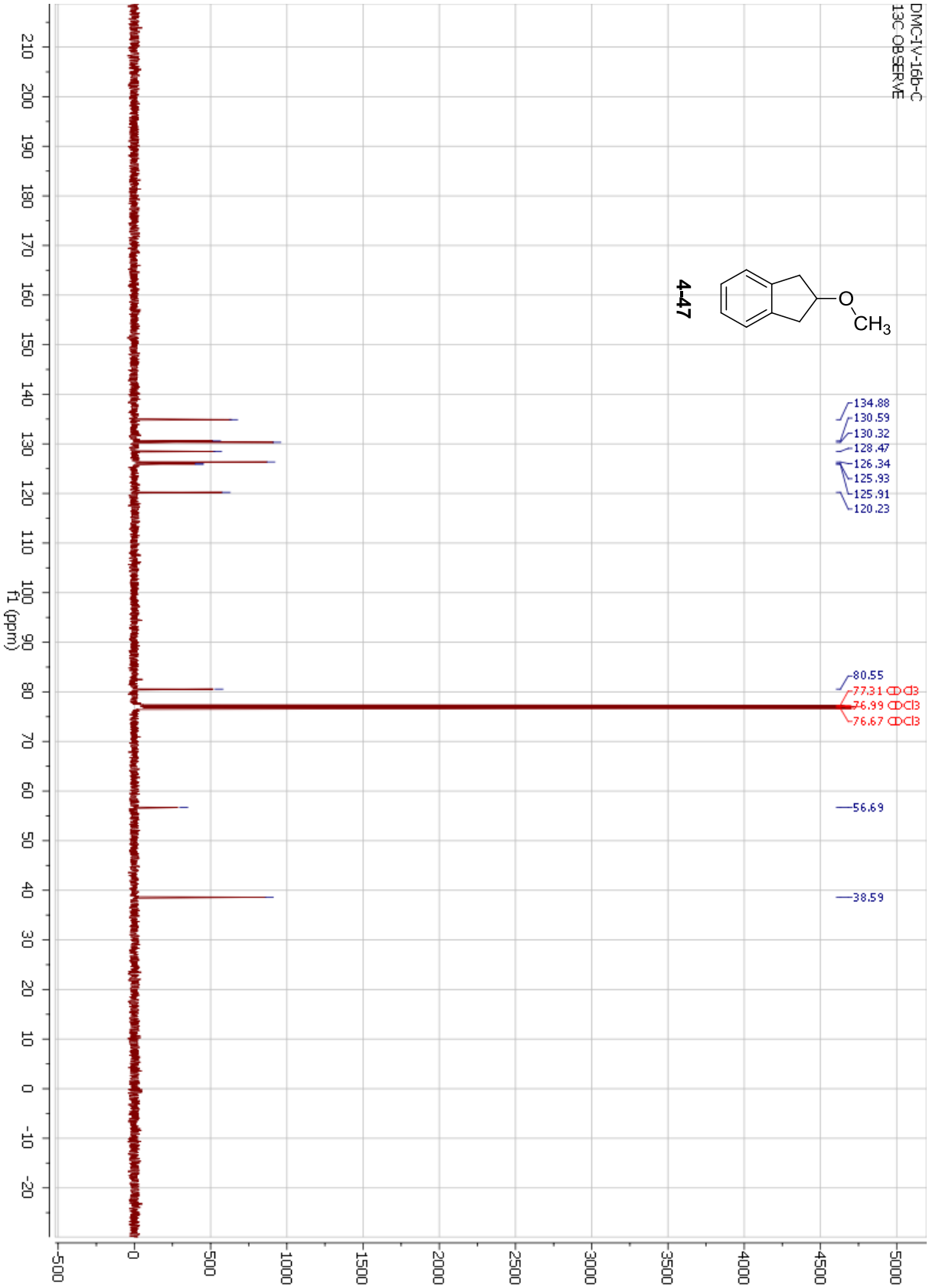
DMC-IV-16b-C
13C OBSERVE
4-47
O
CH3
134.88
130.59
130.32
128.47
126.34
125.93
125.91
120.23
80.55
77.31 CDCl3
76.99 CDCl3
76.67 CDCl3
56.69
38.59
f1 (ppm)

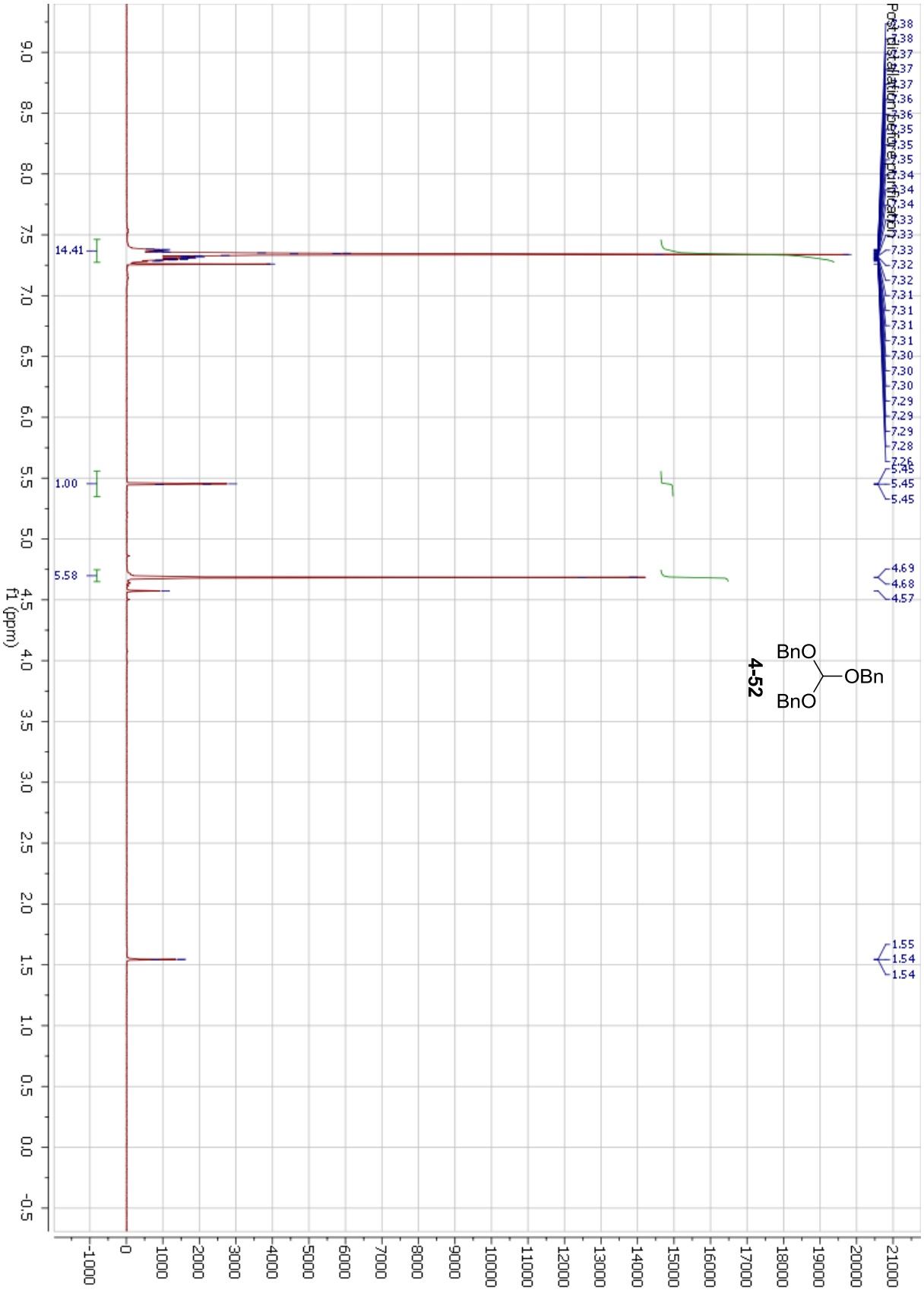
14.41
1.00
5.58
f1 (ppm)
4-52
BnO
OBn
BnO

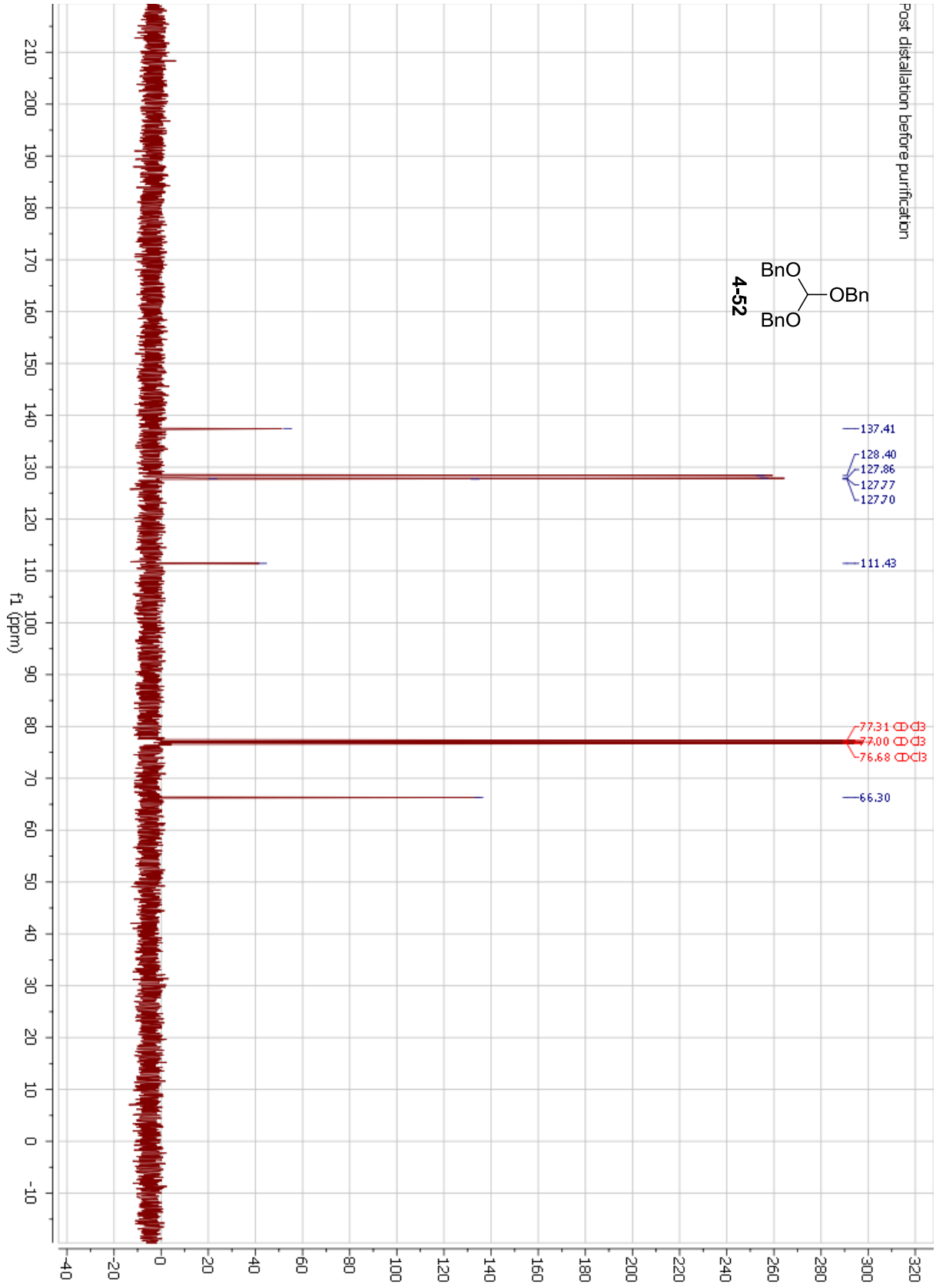
Post distallation before purification
4-52
BnO
OBn
BnO
137.41
128.40
127.86
127.77
127.70
111.43
77.31 CDCl3
77.00 CDCl3
76.68 CDCl3
66.30
f1 (ppm)

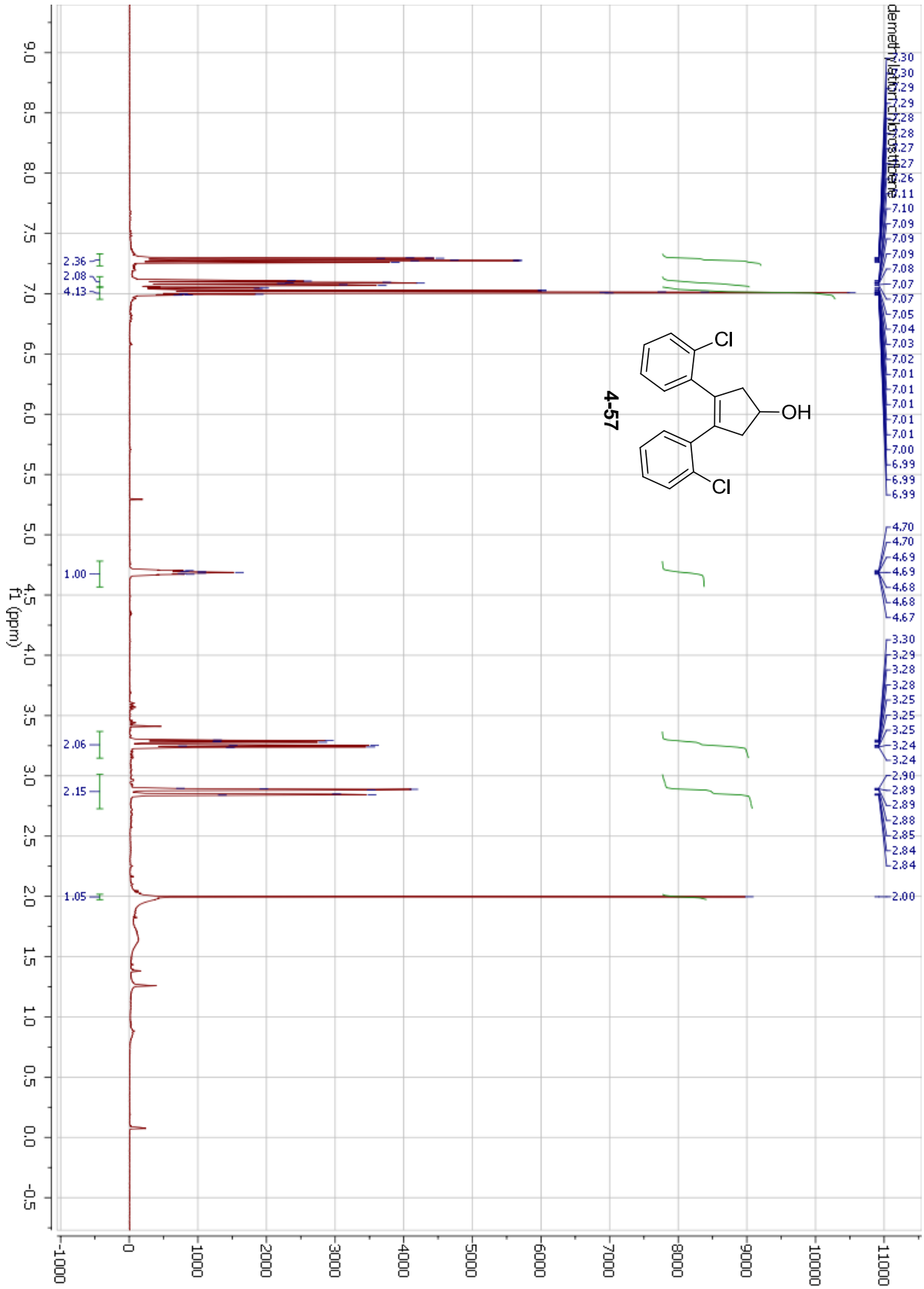
4-57
Cl
OH
Cl
2.36
2.08
4.13
1.00
2.06
2.15
1.05
f1 (ppm)

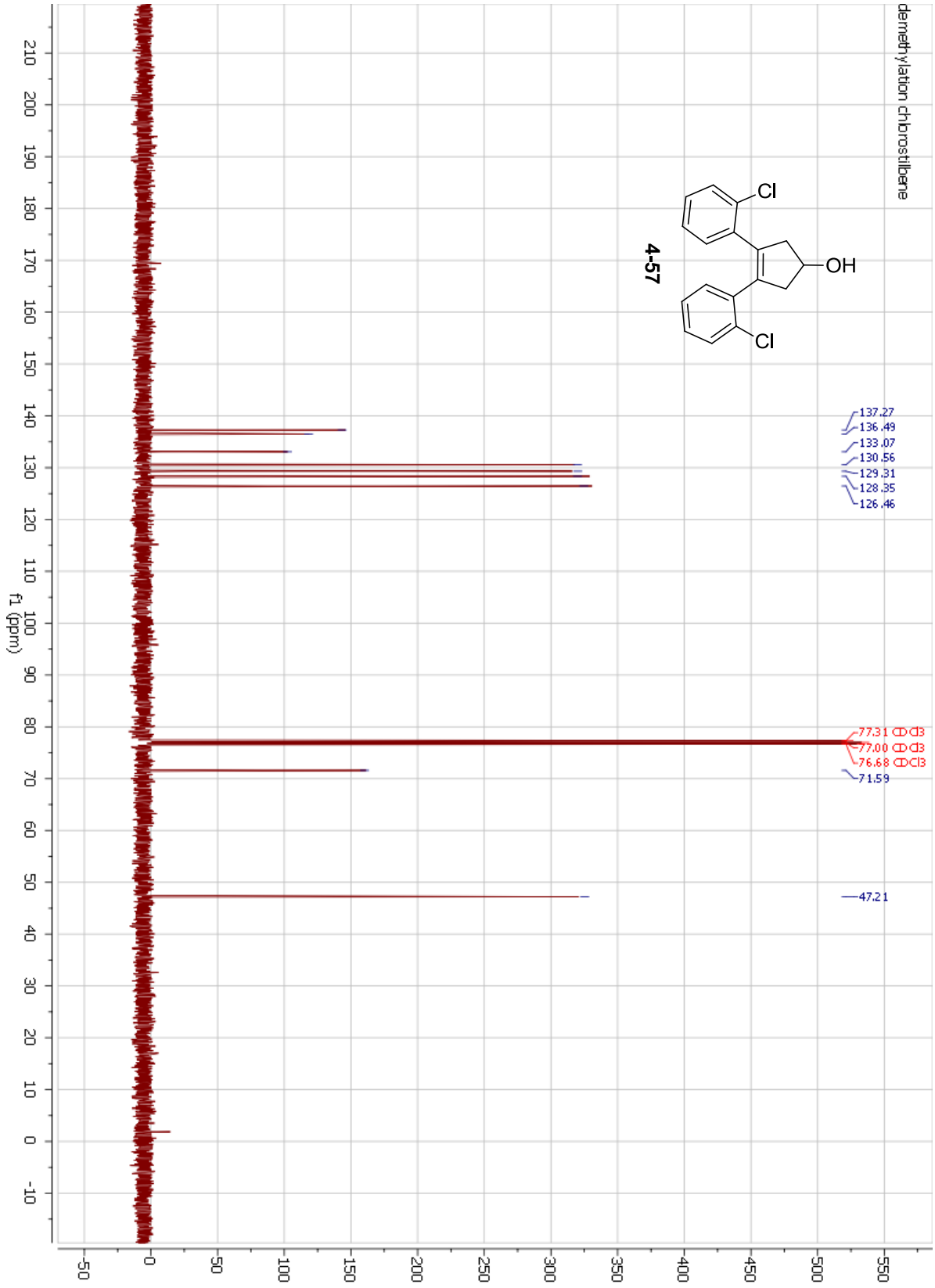
demethylation chlorostilbene
4-57
Cl
OH
Cl
137.27
136.49
133.07
130.56
129.31
128.35
126.46
77.31 CDCl3
77.00 CDCl3
76.68 CDCl3
71.59
47.21
f1 (ppm)

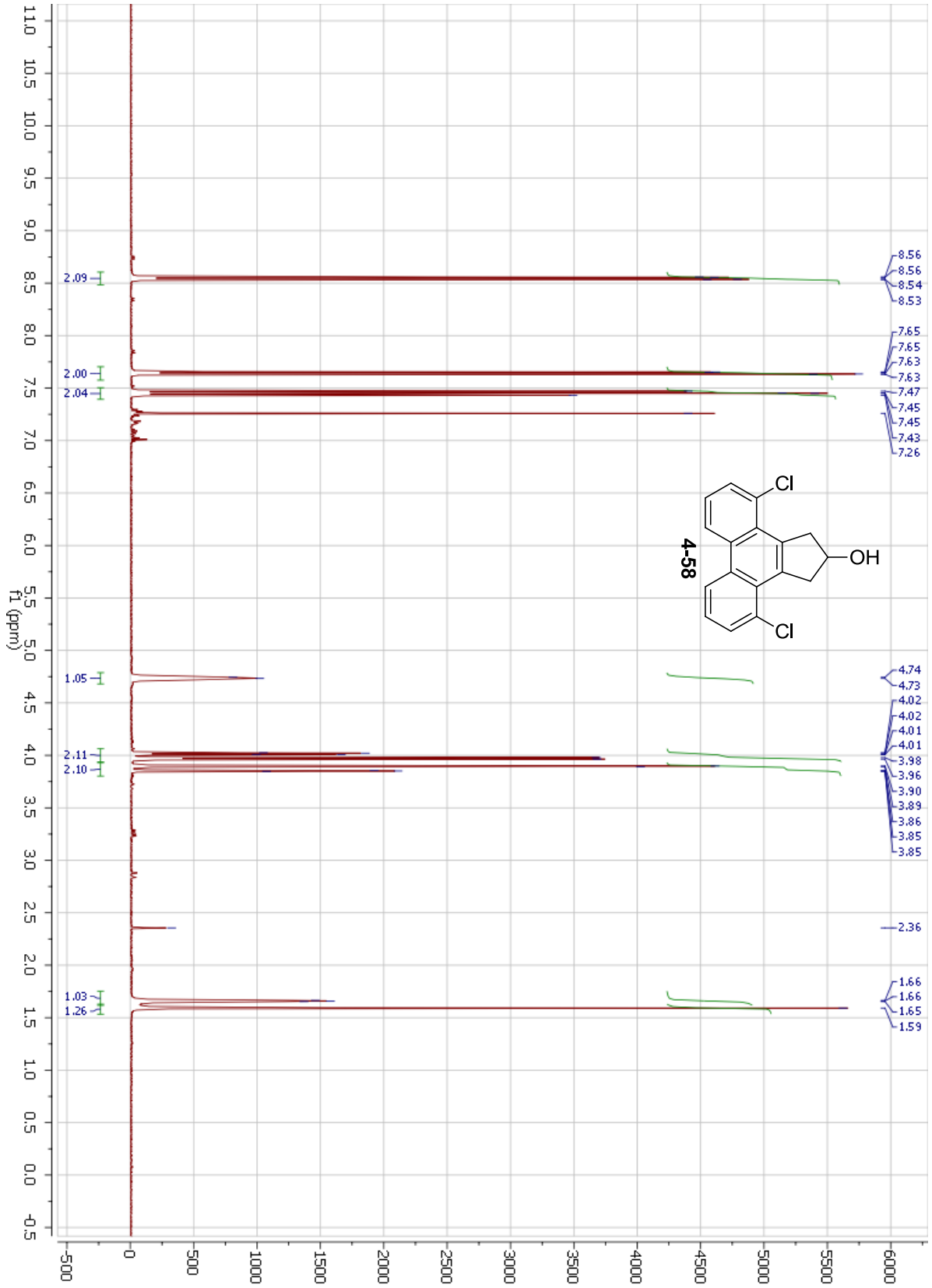
f1 (ppm)
11.0
10.5
10.0
9.5
9.0
8.5
8.0
7.5
7.0
6.5
6.0
5.5
5.0
4.5
4.0
3.5
3.0
2.5
2.0
1.5
1.0
0.5
0.0
-0.5
-500
0
500
1000
1500
2000
2500
3000
3500
4000
4500
5000
5500
6000
2.09
2.00
2.04
1.05
2.11
2.10
1.03
1.26
8.56
8.56
8.54
8.53
7.65
7.65
7.63
7.63
7.47
7.45
7.45
7.43
7.26
4.74
4.73
4.02
4.02
4.01
4.01
3.98
3.96
3.90
3.89
3.86
3.85
3.85
2.36
1.66
1.66
1.65
1.59
Cl
OH
Cl
4-58

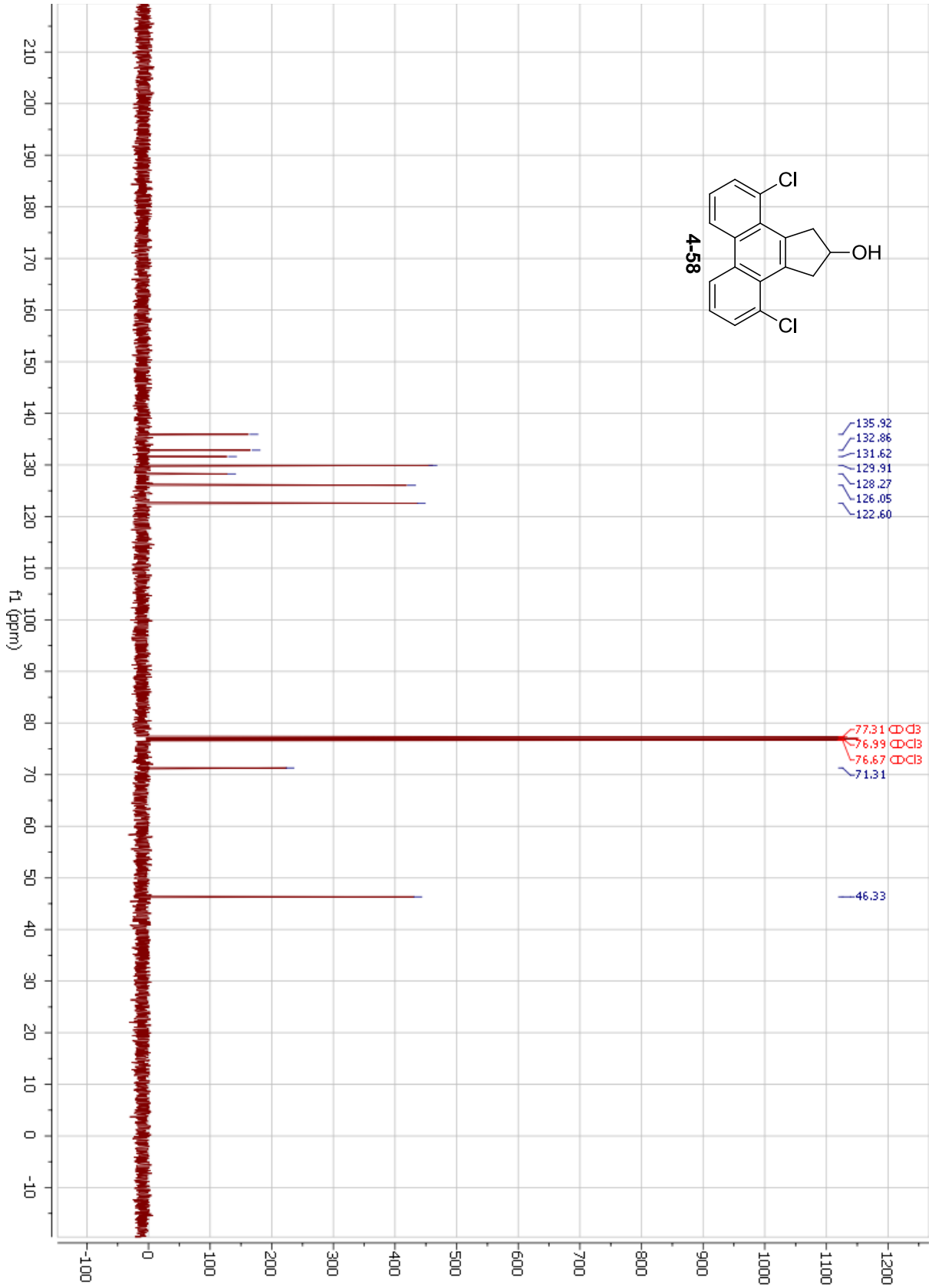
4-58
Cl
OH
Cl
135.92
132.86
131.62
129.91
128.27
126.05
122.60
77.31 CDCl3
76.99 CDCl3
76.67 CDCl3
71.31
46.33
f1 (ppm)

University of Illinois SCS Mass Spectrometry Laboratory

File: 1118k
Sample: 1118k

Date Run: 09-14-2012 (Time Run: 10:59:35)

Ionization mode: EI+
Instrument: VG 70-VSE(B)

Scan: 3

Base: m/z 302; 46.9%FS

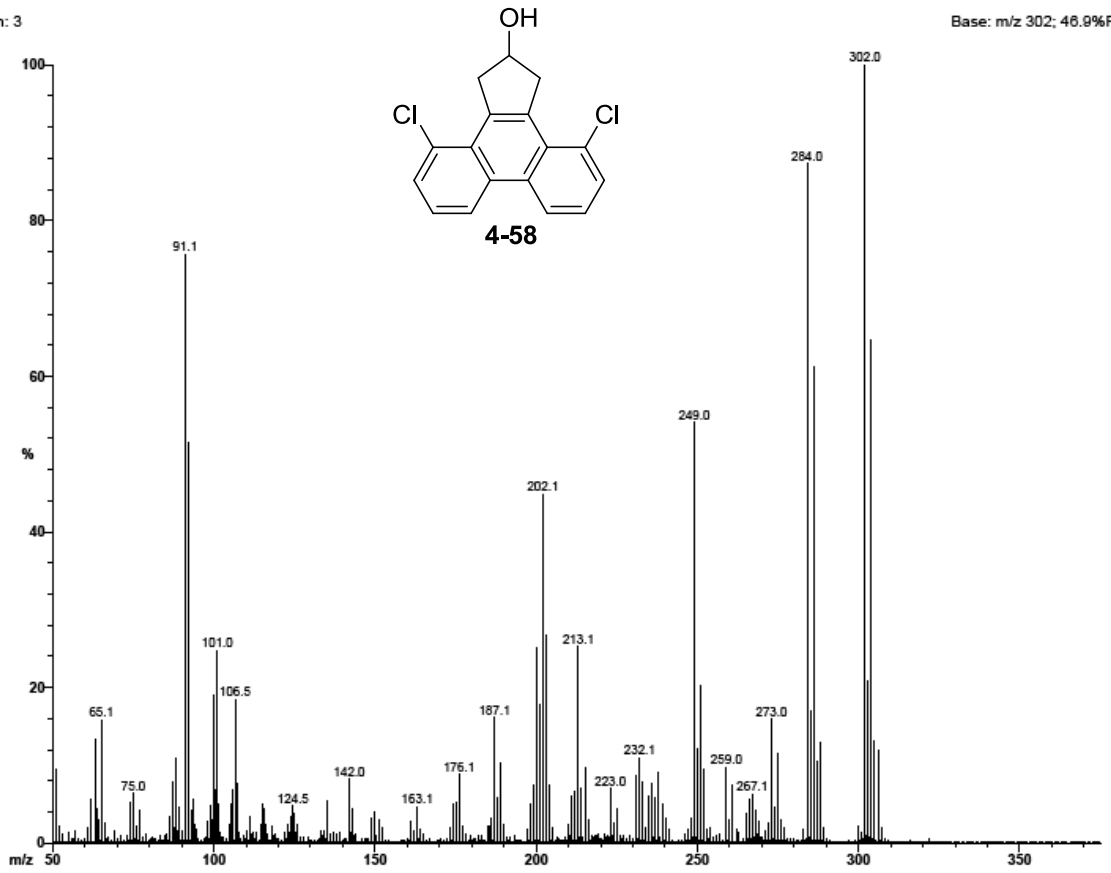

University of Illinois SCS Mass Spectrometry Laboratory

File: 1118khr
Sample: 1118k

Date Run: 09-17-2012 (14:16:54)

Ionization mode: EI+
Instrument: 70-VSE(C)

Base: m/z 293; 37.2%FS

Scan: 24

Selected Isotopes : C H $O_{0-1}Cl_{0-2}$ **Error Limit : 5 mmu** **Unsaturation Limits : -.5 to 30**

Measured Mass	*% Base*	*Formula*	*Calculated Mass*	*Error*	*Unsaturation*
302.02576	49.5%	$C_{17}H_{12}O\,Cl_2$	302.02653	-0.8	11.0

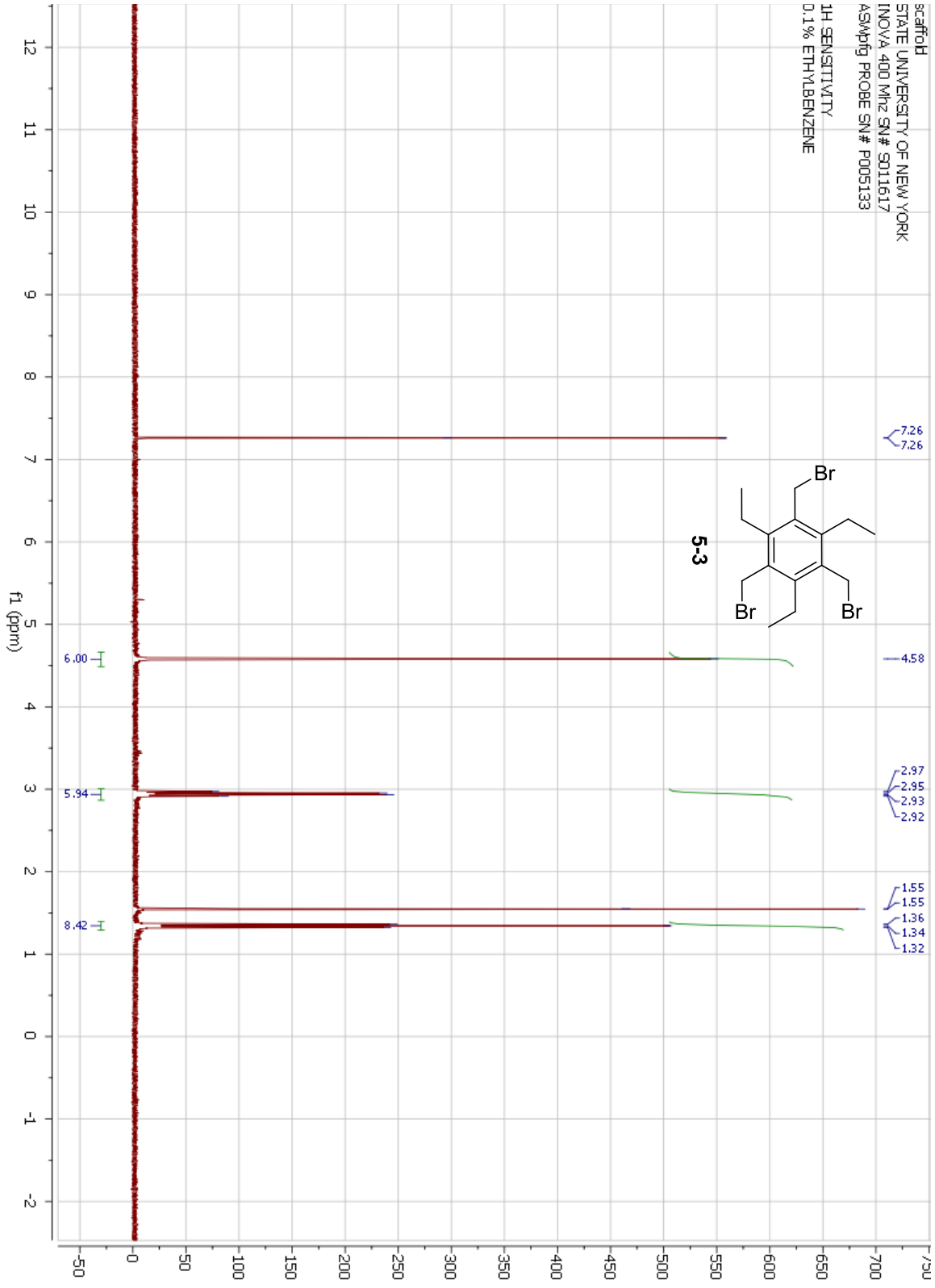
scaffold
STATE UNIVERSITY OF NEW YORK
INOVA 400 Mhz SN# 501617
ASMpfg PROBE SN# P005133
1H SENSITIVITY
0.1% ETHYLBENZENE
5-3
Br
Br
Br
7.26
7.26
4.58
2.97
2.95
2.93
2.92
1.55
1.55
1.36
1.34
1.32
6.00
5.94
8.42
f1 (ppm)

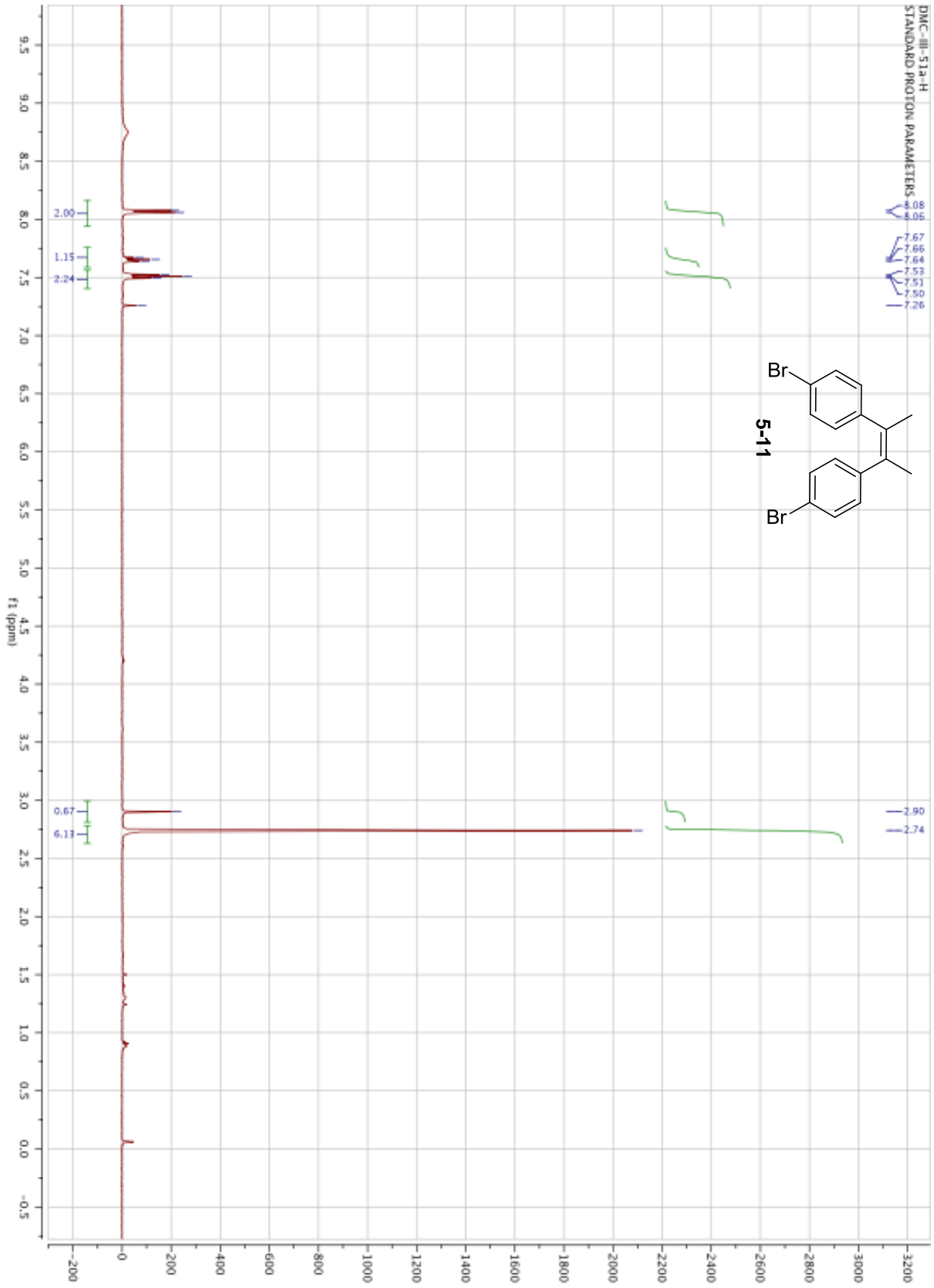
DMC-III-51a-H
STANDARD PROTON PARAMETERS
8.08
8.06
7.67
7.66
7.64
7.53
7.51
7.50
7.26
2.90
2.74
2.00
1.15
2.24
0.67
6.13
Br
Br
5-11
f1 (ppm)

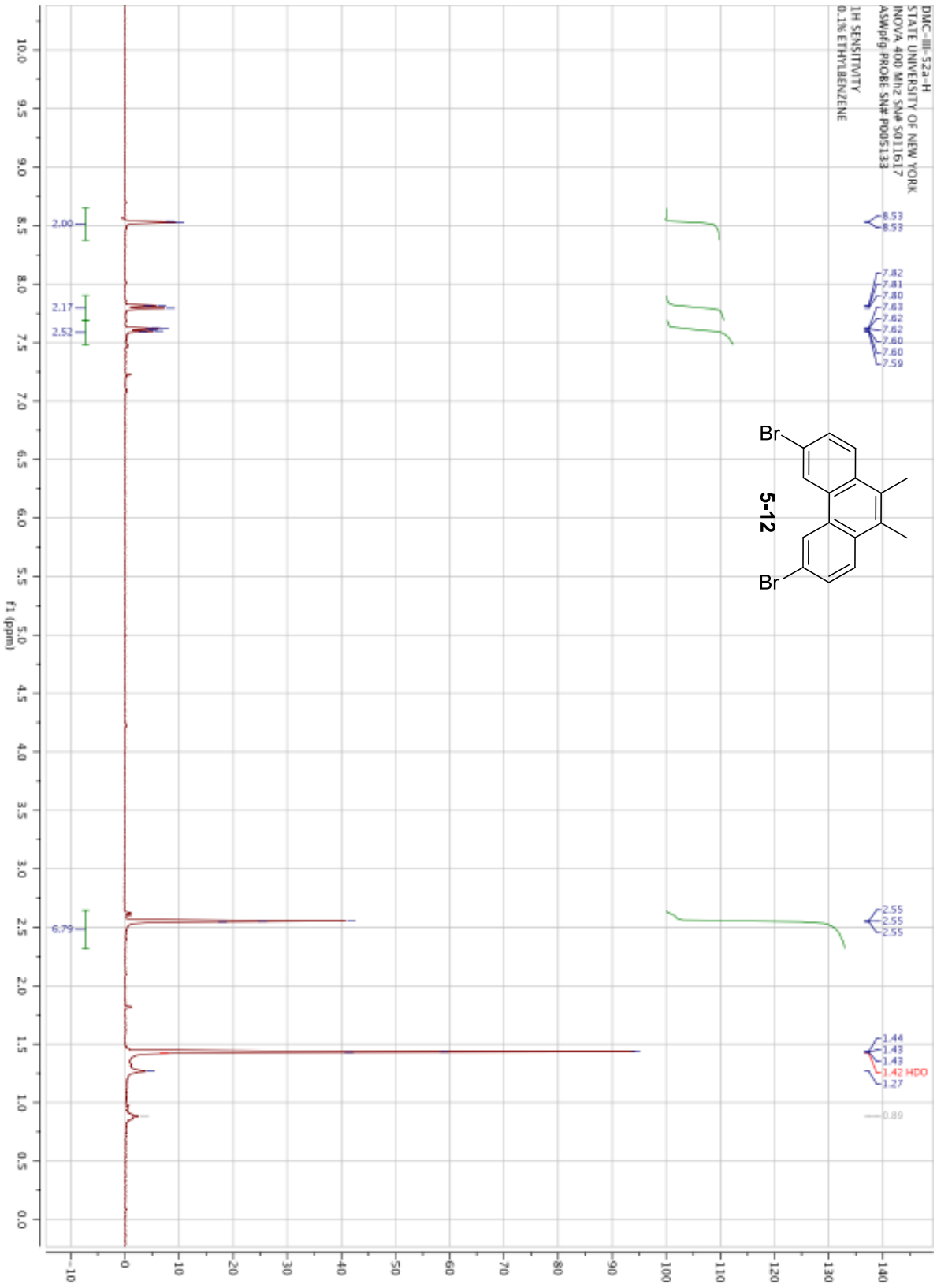
DMC-III-52a-H
STATE UNIVERSITY OF NEW YORK
INOVA 400 MHz SN# 501617
ASWpfg PROBE SN# P005133
1H SENSITIVITY
0.1% ETHYLBENZENE
8.53
8.53
7.82
7.81
7.80
7.63
7.62
7.62
7.60
7.60
7.59
2.55
2.55
2.55
1.44
1.43
1.43
1.42 HDO
1.27
0.89
2.00
2.17
2.52
6.79
Br
Br
5-12
f1 (ppm)

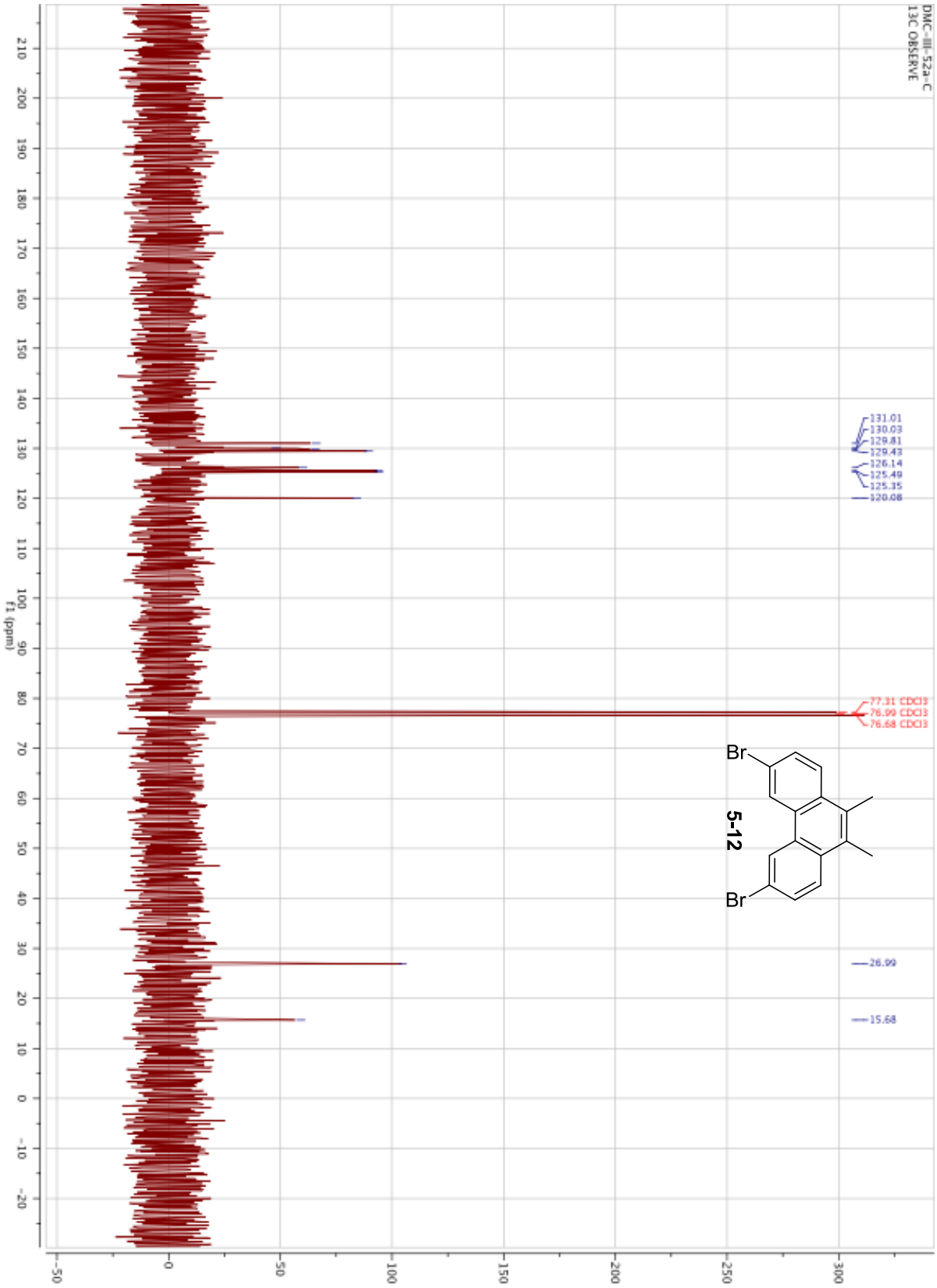
DMC-III-52a-C
13C OBSERVE
131.01
130.03
129.81
129.43
126.14
125.49
125.35
120.08
77.31 CDCl3
76.99 CDCl3
76.68 CDCl3
Br
5-12
Br
26.99
15.68
f1 (ppm)

University of Illinois SCS Mass Spectrometry Laboratory

File: 1118a
Sample: 1118a

Date Run: 09-14-2012 (Time Run: 11:47:42)

Ionization mode: EI+
Instrument: VG 70-VSE(B)

Scan: 15

Base: m/z 366; 11.3%FS

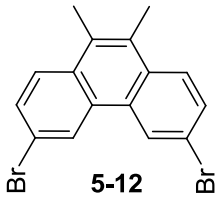

5-12

University of Illinois SCS Mass Spectrometry Laboratory

File: 1118b
Sample: 1118b

Date Run: 09-14-2012 (Time Run: 12:31:48)

Ionization mode: EI+
Instrument: VG 70-VSE(B)

Scan: 31

Base: m/z 204; 93.6%FS

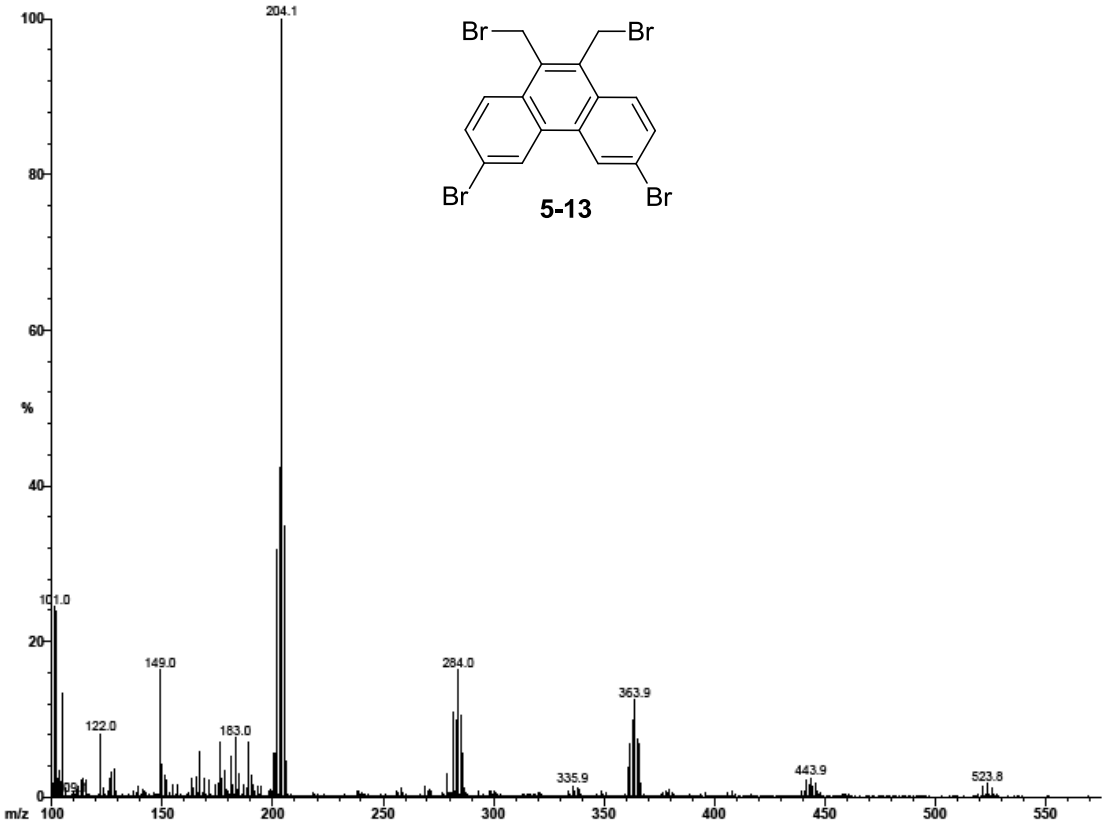

5-13

University of Illinois SCS Mass Spectrometry Laboratory

File: 1118bhr
Sample: 1118b

Date Run: 09-17-2012 (16:35:08)

Ionization mode: EI+

Instrument: 70-VSE(C)

Base: m/z 522; 18.2%FS

Scan: 44

Selected Isotopes : C H Br_{0-4} **Error Limit : 5 mmu** **Unsaturation Limits : -.5 to 50**

Measured Mass	*% Base*	*Formula*	*Calculated Mass*	*Error*	*Unsaturation*
517.75207	20.0%	$C_{16}H_{10}Br_4$	517.75155	0.5	10.0

Dimer of **6-3** and **6-4** (B3LYP/6-31G*)

Atom	X	Y	Z
H	-1.965369	1.497609	-2.810807
C	-1.220942	0.843638	-2.369990
C	-1.644601	-0.216374	-1.584954
C	1.097301	0.237908	-2.004991
C	-0.697424	-1.087693	-0.996868
C	0.151147	1.067927	-2.584019
C	0.687753	-0.851569	-1.200820
C	-1.106731	-2.185651	-0.203436
H	0.490585	1.897031	-3.195189
C	-0.160582	-3.019705	0.369893
H	-0.499790	-3.854239	0.974004
C	1.212560	-2.776114	0.181765
H	1.958452	-3.416278	0.640266
C	1.635862	-1.705968	-0.589615
C	3.085822	-1.438644	-0.759146
C	2.542371	0.500914	-2.227396
C	-2.552148	-2.439941	0.030152
C	-3.093027	-0.430490	-1.342689
O	2.938350	1.419987	-2.928256
O	3.949892	-2.109872	-0.207806
O	-2.947981	-3.373451	0.712094
O	-3.956276	0.319243	-1.782053
N	3.444133	-0.368099	-1.585711
C	4.881759	-0.130714	-1.758434
H	5.361785	-0.070230	-0.779885
H	5.000543	0.800429	-2.307494
H	5.333515	-0.957174	-2.313968
N	-3.452338	-1.545676	-0.577036
C	-4.888981	-1.744123	-0.355084
H	-5.297196	-0.903179	0.211925
H	-5.013967	-2.671046	0.199620
H	-5.404512	-1.793764	-1.316350
H	2.841422	3.231382	0.333902
C	2.104860	2.590837	0.811339
H	0.425515	3.687115	0.052668
C	0.764084	2.849246	0.649955
C	1.635301	0.671058	2.211324
C	-0.198028	2.008273	1.270192
C	2.553551	1.494946	1.587401
C	0.227638	0.904845	2.070504
C	-1.605976	2.230660	1.115393
H	3.617996	1.318881	1.691628
H	-0.394252	-0.766820	3.298265
C	-2.524081	1.402408	1.734173
H	-3.588605	1.571704	1.621273
C	-2.074741	0.319302	2.526934
H	-2.811032	-0.319652	3.007395
C	-0.733683	0.066564	2.695480

O	1.960693	-0.403954	2.984435
O	-1.934101	3.290686	0.323443
C	-3.310758	3.541387	0.068188
H	-3.783404	2.689784	-0.436049
H	-3.336013	4.414273	-0.586800
H	-3.853289	3.769473	0.994867
C	3.335711	-0.714586	3.170038
H	3.815406	-0.986434	2.222094
H	3.356440	-1.572973	3.843910
H	3.875379	0.122178	3.632197

Dimer of **6-3** and **6-4** in water (B3LYP/6-31G*) with SM8 solvent model

Atom	X	Y	Z
H	-2.009914	0.739044	-3.360908
C	-1.258114	0.217270	-2.780775
C	-1.662283	-0.660014	-1.786598
C	1.071938	-0.221088	-2.275416
C	-0.698990	-1.355259	-1.018055
C	0.109336	0.430479	-3.030445
C	0.681690	-1.123080	-1.256225
C	-1.089015	-2.269322	-0.009533
H	0.425080	1.113406	-3.810040
C	-0.126306	-2.927639	0.739371
H	-0.441973	-3.626088	1.505105
C	1.240543	-2.682489	0.518040
H	1.992034	-3.186411	1.114075
C	1.644599	-1.789834	-0.462226
C	3.083010	-1.511631	-0.668414
C	2.508734	0.030995	-2.531095
C	-2.525701	-2.516683	0.250945
C	-3.101769	-0.855693	-1.506254
O	2.893481	0.797231	-3.417349
O	3.965746	-2.010552	0.033741
O	-2.909769	-3.315771	1.108012
O	-3.986841	-0.232033	-2.097238
N	3.426992	-0.643018	-1.711293
C	4.864784	-0.397578	-1.908932
H	5.279220	0.116807	-1.039749
H	4.982370	0.216795	-2.796972
H	5.383872	-1.348585	-2.030418
N	-3.444768	-1.793363	-0.524785
C	-4.883476	-1.984106	-0.279731
H	-5.326545	-1.053752	0.079841
H	-4.997084	-2.766026	0.465728
H	-5.378905	-2.268206	-1.208616
H	2.873627	3.346942	0.103721
C	2.120719	2.816787	0.679287
H	0.470704	3.684438	-0.379341
C	0.786956	3.012321	0.408477
C	1.600854	1.244786	2.445089
C	-0.197416	2.320334	1.162957
C	2.540191	1.927528	1.696289
C	0.199300	1.426286	2.205989
C	-1.597896	2.474321	0.899170
H	3.599072	1.792063	1.878603
H	-0.470279	0.063649	3.749520
C	-2.537276	1.784886	1.641492
H	-3.595301	1.902134	1.442920
C	-2.118751	0.917610	2.677824
H	-2.871768	0.387550	3.253357
C	-0.785570	0.734069	2.959785
O	1.909315	0.357053	3.446550
O	-1.903243	3.332671	-0.128069
C	-3.272870	3.435481	-0.527779

H	-3.661534	2.465718	-0.859615
H	-3.282873	4.135818	-1.363527
H	-3.896466	3.831499	0.281402
C	3.286360	0.021520	3.638123
H	3.717432	-0.407587	2.726177
H	3.299397	-0.724997	4.432925
H	3.869946	0.893366	3.954316

Dimer of **6-3** and **6-4** edge to face **6-3** on edge (B3LYP/6-31G*)

Atom	X	Y	Z
H	5.291211	-1.616996	-1.053611
C	4.445005	-1.028738	-0.715053
C	3.289805	-1.688492	-0.324963
C	3.421807	1.116401	-0.237681
C	2.166614	-0.954616	0.124071
C	4.510809	0.375433	-0.671330
C	2.233086	0.464200	0.167943
C	0.976464	-1.609464	0.528034
H	5.409319	0.901552	-0.975293
C	-0.107219	-0.868455	0.970341
H	-1.011042	-1.383931	1.274836
C	-0.042793	0.538809	1.012184
C	1.107324	1.200329	0.613656
C	1.161034	2.684750	0.640048
C	3.508697	2.600500	-0.204146
C	0.883858	-3.092187	0.467118
C	3.230211	-3.171510	-0.378788
O	4.517572	3.200638	-0.544003
O	0.216562	3.378973	0.991693
O	-0.130454	-3.697865	0.785883
O	4.169559	-3.858198	-0.752951
N	2.363674	3.285007	0.239295
C	2.400464	4.751593	0.281526
H	1.661729	5.161988	-0.411806
H	3.402076	5.066848	-0.001162
H	2.156308	5.095359	1.288998
N	2.028275	-3.774445	0.021220
C	1.990085	-5.240316	-0.047115
H	2.175293	-5.566706	-1.073208
H	1.006675	-5.562631	0.286348
H	2.770058	-5.659444	0.592947
H	-3.768772	1.823648	3.041332
C	-3.657495	1.539303	1.998224
H	-3.899962	-0.560289	2.372745
C	-3.731641	0.214293	1.634080
C	-3.291392	2.221160	-0.296289
C	-3.582216	-0.150583	0.269178
C	-3.428129	2.553050	1.038817
C	-3.377431	0.855638	-0.723549
C	-3.598508	-1.521917	-0.147853
H	-3.348213	3.582296	1.367093
H	-3.089595	1.264437	-2.830695
C	-3.452694	-1.856127	-1.480445
H	-3.460603	-2.892329	-1.798109
C	-3.281547	-0.837434	-2.447673
H	-3.173593	-1.121709	-3.491201
C	-3.235951	0.488944	-2.088513
O	-3.059294	3.120859	-1.293272
O	-3.739527	-2.422746	0.866626
C	-3.627142	-3.807030	0.559895
H	-4.418710	-4.129006	-0.129313

H	-3.742423	-4.330282	1.510710
H	-2.642546	-4.035966	0.137469
C	-2.759384	4.461574	-0.928147
H	-3.615468	4.947388	-0.441421
H	-2.538873	4.980947	-1.862909
H	-1.886845	4.499776	-0.264946
H	-0.897821	1.114935	1.347220

Dimer of **6-4** edge to face (B3LYP/6-31G*)

Atom	X	Y	Z
H	-1.966608	-1.870259	0.616005
C	-2.785626	-1.178504	0.584245
C	-3.981797	-1.580662	0.063530
C	-3.674217	1.012928	1.033470
C	-5.071993	-0.686603	0.012824
C	-2.629870	0.135345	1.075788
C	-4.917636	0.615706	0.499640
C	-6.315870	-1.084260	-0.520333
H	-1.691441	0.454265	1.485978
C	-7.360405	-0.206992	-0.561726
H	-8.299692	-0.525535	-0.970281
C	-7.204232	1.107396	-0.070608
H	-8.023640	1.798744	-0.101870
C	-6.007911	1.509922	0.449145
C	-3.509835	2.398905	1.551315
C	-5.850701	2.899143	0.966876
C	-6.480006	-2.470657	-1.037522
C	-4.138495	-2.969914	-0.454482
N	-5.380815	-3.311886	-0.968085
N	-4.608180	3.240533	1.481358
O	-6.754271	3.679391	0.938772
O	-2.476787	2.782960	2.011648
O	-3.234006	-3.749286	-0.426851
O	-7.512953	-2.855846	-1.496868
C	-4.409123	4.596018	2.002428
H	-3.615382	5.082921	1.455197
H	-4.132021	4.547437	3.045263
H	-5.328428	5.140127	1.887064
C	-5.579733	-4.667881	-1.488118
H	-5.857209	-4.620294	-2.530923
H	-6.373190	-5.154428	-0.940169
H	-4.660279	-5.211705	-1.372530
H	6.264584	0.754324	2.988784
C	5.877333	0.720605	1.988997
C	5.629324	-0.488662	1.407029
C	5.132468	1.869083	0.008040
C	5.119365	-0.556509	0.093664
C	5.626175	1.915114	1.279826
C	4.869040	0.627310	-0.608242
C	4.857442	-1.798121	-0.523033
H	5.820896	2.866808	1.734555
C	4.362255	-1.844249	-1.794324
H	4.168125	-2.796008	-2.249121
C	4.108369	-0.649773	-2.502439
H	3.718887	-0.683509	-3.501378
C	4.357039	0.559574	-1.920748
C	4.870694	3.134807	-0.735043
C	4.088621	1.819733	-2.666664
C	5.123787	-3.063957	0.218254
C	5.894448	-1.748648	2.154295
N	5.625837	-2.943527	1.505840

N	4.362859	3.014374	-2.020623
O	3.653571	1.815228	-3.778962
O	5.088993	4.201061	-0.243824
O	6.321863	-1.744330	3.269530
O	4.913370	-4.130267	-0.276355
C	4.087036	4.233276	-2.786444
H	4.688402	4.243697	-3.683893
H	4.325519	5.080291	-2.169728
H	3.044478	4.256859	-3.067490
C	5.900793	-4.162552	2.272038
H	6.942608	-4.185492	2.555897
H	5.664514	-5.009521	1.654507
H	5.297139	-4.173708	3.167843

Dimer of **6-4** face to face (B3LYP/6-31G*)

Atom	X	Y	Z
H	2.257975	2.990603	1.323349
C	1.417652	2.316423	1.450775
C	1.668941	0.984089	1.737413
C	-0.972481	1.904590	1.449889
C	0.594010	0.079589	1.911717
C	0.094838	2.777189	1.308159
C	-0.740044	0.544270	1.762843
C	0.827039	-1.282997	2.213904
H	-0.108931	3.815835	1.071175
C	-0.241185	-2.150656	2.377869
H	-0.037093	-3.190576	2.608884
C	-1.563847	-1.692589	2.223708
H	-2.403143	-2.371692	2.328872
C	-1.814393	-0.365773	1.910926
C	-2.361904	2.395597	1.243477
C	-3.211519	0.098806	1.700871
C	2.220345	-1.795328	2.322183
C	3.069711	0.494466	1.831715
N	3.251897	-0.860627	2.128503
N	-3.393147	1.454256	1.401567
O	-4.169045	-0.661023	1.767262
O	-2.601310	3.554678	0.941463
O	4.032086	1.226864	1.641886
O	2.460956	-2.970609	2.552083
C	-4.774497	1.896722	1.158660
H	-5.094907	1.576008	0.163133
H	-4.792707	2.982398	1.220447
H	-5.424759	1.447278	1.908963
C	4.641662	-1.340317	2.163057
H	5.046200	-1.355402	1.147295
H	4.636379	-2.344747	2.579748
H	5.237872	-0.664485	2.777307
H	0.119636	3.188556	-2.614136
C	-0.087406	2.147249	-2.392141
C	0.977383	1.293483	-2.150978
C	-1.667843	0.344822	-2.027311
C	0.739794	-0.070837	-1.859462
C	-1.411909	1.673409	-2.327794
C	-0.595435	-0.551643	-1.802236
C	1.810892	-0.961405	-1.607035
H	-2.249685	2.341716	-2.495896
C	1.556364	-2.295813	-1.333024
H	2.393865	-2.958183	-1.141245
C	0.232606	-2.772788	-1.282541
H	0.025569	-3.813001	-1.055592
C	-0.832755	-1.913911	-1.501308
C	-3.070500	-0.136359	-1.913094
C	-2.226943	-2.421585	-1.390999
C	3.208169	-0.453559	-1.602166
C	2.368200	1.823112	-2.164671
N	3.394102	0.903331	-1.887514

N	-3.255972	-1.492853	-1.620505
O	-2.472746	-3.583144	-1.103695
O	-4.030113	0.611433	-2.048794
O	2.610043	2.999342	-2.388498
O	4.164253	-1.172128	-1.340904
C	-4.645209	-1.952030	-1.470313
H	-4.647262	-3.037439	-1.539704
H	-5.250064	-1.504499	-2.258661
H	-5.031482	-1.640754	-0.495471
C	4.776006	1.400388	-1.810265
H	4.781985	2.422292	-2.181993
H	5.422767	0.761353	-2.413258
H	5.111474	1.373973	-0.770180

Dimer of **6-3** edge to face (B3LYP/6-31G*)

Atom	X	Y	Z
C	3.043639	1.228176	-0.001044
C	1.633026	1.441693	0.135417
C	0.811297	0.445105	0.625651
C	1.363388	-0.803445	0.998655
C	2.711906	-1.050611	0.885409
O	1.200257	2.676067	-0.254036
C	-0.184263	2.970368	-0.134158
H	-0.256573	0.598164	0.723077
H	0.694559	-1.573743	1.372420
H	3.131484	-2.006617	1.175372
H	-0.795618	2.302320	-0.753519
C	3.575556	-0.039976	0.385230
C	4.986237	-0.250755	0.249997
C	5.807824	0.745400	-0.240627
C	5.254609	1.992501	-0.617158
C	3.906869	2.237769	-0.503660
O	5.420581	-1.487322	0.639594
C	6.804996	-1.772571	0.542455
H	6.875449	0.588059	-0.341843
H	5.917390	2.763611	-1.001196
H	3.486284	3.193840	-0.791378
H	7.400788	-1.097252	1.171053
C	-2.918733	-1.179845	-0.071089
C	-1.911854	-1.539041	-1.026173
C	-1.717079	-0.782408	-2.165738
C	-2.517046	0.361200	-2.397903
C	-3.490529	0.745892	-1.505158
O	-1.192566	-2.654102	-0.709160
C	-0.152890	-3.056598	-1.590019
H	-0.953252	-1.046701	-2.887167
H	-2.351841	0.939139	-3.303603
H	-4.102572	1.621013	-1.688794
H	-0.543192	-3.284715	-2.590338
C	-3.708748	-0.016794	-0.326645
C	-4.711628	0.343786	0.630922
C	-4.909010	-0.415356	1.768157
C	-4.114295	-1.563358	1.996272
C	-3.139855	-1.945081	1.104982
O	-5.424257	1.467476	0.320745
C	-6.440960	1.885085	1.215911
H	-5.666874	-0.146370	2.494682
H	-4.285996	-2.147410	2.896643
H	-2.536464	-2.827373	1.282307
H	-6.033012	2.119405	2.208085
H	-0.518472	2.899238	0.909145
H	-0.300189	3.998769	-0.482152
H	-6.872557	2.787867	0.779598
H	-7.222779	1.121176	1.320136
H	0.272796	-3.961602	-1.152989
H	6.926048	-2.797826	0.897697
H	7.159092	-1.702287	-0.494732

H	0.624980	-2.287229	-1.662746

Dimer of **6-3** face to face (B3LYP/6-31G*)

Atom	X	Y	Z
H	5.685694	0.155279	2.988895
C	5.223427	0.179509	2.005516
H	3.399396	1.065808	2.703618
C	3.954289	0.685438	1.854433
C	5.389344	-0.294991	-0.362232
C	3.354902	0.716721	0.566984
C	5.953041	-0.315756	0.898714
C	4.069746	0.224754	-0.567586
C	2.033559	1.234756	0.363094
H	6.951863	-0.705927	1.056832
H	4.028054	-0.117350	-2.705605
C	1.470063	1.255635	-0.899053
H	0.467974	1.636548	-1.055928
C	2.201871	0.763558	-2.005588
H	1.740581	0.791519	-2.989353
C	3.471681	0.258124	-1.855257
O	6.007501	-0.750080	-1.492390
O	1.413487	1.682850	1.493079
C	7.319048	-1.274153	-1.376104
H	7.613909	-1.571544	-2.384228
H	7.344973	-2.150958	-0.715480
H	8.021849	-0.519391	-0.999003
C	0.104051	2.222069	1.375950
H	-0.606075	1.475758	0.999976
H	0.091776	3.099791	0.716624
H	-0.185428	2.521862	2.384671
H	-5.685694	-0.155279	2.988895
C	-5.223427	-0.179509	2.005516
H	-3.399396	-1.065808	2.703618
C	-3.954289	-0.685438	1.854433
C	-5.389344	0.294991	-0.362232
C	-3.354902	-0.716721	0.566984
C	-5.953041	0.315756	0.898714
C	-4.069746	-0.224754	-0.567586
C	-2.033559	-1.234756	0.363094
H	-6.951863	0.705927	1.056832
H	-4.028054	0.117350	-2.705605
C	-1.470063	-1.255635	-0.899053
H	-0.467974	-1.636548	-1.055928
C	-2.201871	-0.763558	-2.005588
H	-1.740581	-0.791519	-2.989353
C	-3.471681	-0.258124	-1.855257
O	-6.007501	0.750080	-1.492390
O	-1.413487	-1.682850	1.493079
C	-7.319048	1.274153	-1.376104
H	-7.613909	1.571544	-2.384228
H	-7.344973	2.150958	-0.715480
H	-8.021849	0.519391	-0.999003
C	-0.104051	-2.222069	1.375950
H	0.606075	-1.475758	0.999976
H	-0.091776	-3.099791	0.716624

H	0.185428	-2.521862	2.384671

Dimer of **6-3** and **6-4** (M06-2X/6-31G*)

Atom	X	Y	Z
H	1.988256	2.955796	1.312916
C	1.224909	2.184758	1.331409
C	1.613847	0.863225	1.336927
C	-1.099511	1.528237	1.317710
C	0.648686	-0.168259	1.353906
C	-0.143722	2.520074	1.322661
C	-0.721396	0.167469	1.338682
C	1.027530	-1.529107	1.338525
H	-0.466028	3.555345	1.289777
C	0.072149	-2.521071	1.326844
H	0.395272	-3.556288	1.299984
C	-1.296932	-2.185940	1.310626
H	-2.059507	-2.957424	1.280947
C	-1.686097	-0.864510	1.305249
C	-3.125048	-0.516148	1.187539
C	-2.536147	1.895951	1.210562
C	2.466369	-1.896283	1.259810
C	3.055660	0.515281	1.257560
O	-2.904086	3.049585	1.129463
O	-3.995420	-1.359937	1.073008
O	2.835770	-3.049124	1.177931
O	3.928169	1.359558	1.167935
N	-3.454098	0.837674	1.197728
C	-4.870468	1.155374	1.034054
H	-5.189852	0.915876	0.015601
H	-5.001406	2.216856	1.226399
H	-5.453341	0.554296	1.731219
N	3.384383	-0.838176	1.276316
C	4.803918	-1.156350	1.145499
H	5.143628	-0.930938	0.130283
H	4.932203	-2.215013	1.354429
H	5.371528	-0.544815	1.846084
H	-3.072251	1.764338	-1.935719
C	-2.222273	1.087193	-1.941488
H	-0.767949	2.659752	-1.936947
C	-0.948482	1.591257	-1.945149
C	-1.398283	-1.184205	-1.913821
C	0.158496	0.701288	-1.940795
C	-2.461331	-0.308621	-1.919636
C	-0.051301	-0.700077	-1.943583
C	1.505744	1.185766	-1.899170
H	-3.482297	-0.671827	-1.884222
H	0.875295	-2.658938	-1.937035
C	2.568375	0.310205	-1.898044
H	3.588847	0.673580	-1.852565
C	2.329366	-1.086198	-1.926817
H	3.178953	-1.763543	-1.917562
C	1.056046	-1.590433	-1.941356
O	-1.514343	-2.533068	-1.846052
O	1.619971	2.534692	-1.826776
C	2.924170	3.069536	-1.701432

H	3.418152	2.692206	-0.798156
H	2.799217	4.150227	-1.633399
H	3.532178	2.829394	-2.581542
C	-2.820942	-3.069432	-1.759126
H	-3.344870	-2.692018	-0.873183
H	-2.696371	-4.149679	-1.684857
H	-3.402121	-2.831214	-2.657700

Dimer of **6-3** and **6-4** in water (M06-2X/6-31G*) SM8 solvent model

Atom	X	Y	Z
H	-1.045886	-2.116036	-3.583081
C	-0.765011	-2.070125	-2.536178
H	-2.787247	-2.016396	-1.837666
C	-1.736567	-2.014462	-1.572508
C	0.984829	-1.952676	-0.877044
C	-1.367417	-1.957770	-0.202808
C	0.607695	-2.042909	-2.197710
C	0.002553	-1.944004	0.165639
C	-2.350980	-1.900876	0.834712
H	1.347822	-2.067674	-2.988014
H	1.420629	-1.898854	1.800039
C	-1.976810	-1.887987	2.158705
H	-2.719752	-1.837444	2.944857
C	-0.604460	-1.902539	2.498505
H	-0.326300	-1.883365	3.547307
C	0.370288	-1.911154	1.534995
O	2.275907	-1.862151	-0.451066
O	-3.637083	-1.844699	0.395941
C	3.290486	-1.967883	-1.440126
H	4.238208	-1.883034	-0.909676
H	3.217527	-1.158411	-2.173821
H	3.236214	-2.936363	-1.947453
C	-4.663981	-1.805456	1.378548
H	-4.574597	-0.908598	1.998504
H	-4.637343	-2.704947	2.002357
H	-5.601752	-1.777164	0.824890
H	-0.092156	1.175720	-3.498326
C	0.275530	1.224569	-2.479279
C	-0.631383	1.224539	-1.442971
C	2.112308	1.286543	-0.909584
C	-0.185877	1.283470	-0.103712
C	1.659353	1.254016	-2.210796
C	1.198474	1.315501	0.166623
C	-1.100931	1.283816	0.972432
H	2.380643	1.240436	-3.020897
C	-0.647656	1.349455	2.271124
H	-1.369760	1.344258	3.079897
C	0.735488	1.393111	2.540948
H	1.099626	1.431092	3.561360
C	1.644334	1.364562	1.506572
C	3.566438	1.253958	-0.628443
C	3.097691	1.353736	1.802262
N	3.963422	1.304057	0.708046
C	-2.557354	1.175586	0.704670
C	-2.083328	1.121843	-1.726028
O	3.526407	1.383244	2.947829
O	4.407217	1.183537	-1.513697
O	-3.377458	1.145439	1.609660
O	-2.529347	1.045439	-2.861652
N	-2.951395	1.129187	-0.633479
C	5.409698	1.261034	0.947370

H	5.889153	2.094476	0.434612
H	5.818466	0.329452	0.554779
H	5.577901	1.325824	2.017779
C	-4.371056	0.933732	-0.938790
H	-4.700526	1.700800	-1.639045
H	-4.926981	1.005506	-0.008272
H	-4.514316	-0.049313	-1.390070

Dimer of **6-4** face to face (M06-2X/6-31G*)

Atom	X	Y	Z
H	2.439537	2.791991	1.169131
C	1.555337	2.173106	1.287136
C	1.709926	0.831207	1.562045
C	-0.846796	1.912313	1.220792
C	0.577255	-0.001136	1.716537
C	0.265844	2.716979	1.109402
C	-0.712228	0.545414	1.551805
C	0.713587	-1.380636	1.987187
H	0.134493	3.760050	0.839934
C	-0.400321	-2.178082	2.135132
H	-0.265325	-3.237378	2.328179
C	-1.690405	-1.629728	1.977444
H	-2.573567	-2.255929	2.056046
C	-1.843292	-0.294779	1.667186
C	-3.203834	0.255197	1.412874
C	-2.192795	2.462586	0.904144
C	2.071437	-1.989155	2.009344
C	3.078756	0.247156	1.627779
O	-2.343886	3.595411	0.494079
O	-4.198858	-0.439798	1.471662
O	2.243337	-3.183527	2.143407
O	4.070677	0.932138	1.475503
N	-3.283943	1.607564	1.076581
C	-4.609155	2.150369	0.768355
H	-4.811161	2.040550	-0.299613
H	-4.618863	3.202891	1.043430
H	-5.344792	1.586983	1.337979
N	3.159400	-1.132153	1.827470
C	4.477149	-1.768759	1.797183
H	4.487605	-2.530932	1.017418
H	4.677197	-2.238840	2.761610
H	5.212354	-1.000121	1.577049
H	-0.123381	3.236217	-2.344284
C	-0.257285	2.175131	-2.160835
C	0.853447	1.393489	-1.929819
C	-1.705073	0.272870	-1.796437
C	0.716749	0.012246	-1.668672
C	-1.548086	1.608792	-2.100423
C	-0.573930	-0.551501	-1.595769
C	1.846206	-0.804472	-1.431349
H	-2.430630	2.222785	-2.249553
C	1.690491	-2.148460	-1.167095
H	2.572551	-2.753802	-0.981749
C	0.399227	-2.710688	-1.085995
H	0.262320	-3.756145	-0.828512

C	-0.713123	-1.920474	-1.276400
C	-2.071259	-2.488077	-1.061732
C	-3.074031	-0.295143	-1.647916
C	3.208239	-0.201751	-1.396866
C	2.200811	2.020797	-1.850963
O	-4.067898	0.381962	-1.823335
O	-2.244023	-3.634045	-0.699413
O	4.194443	-0.872172	-1.165373
O	2.364568	3.218612	-1.963037
N	-3.158206	-1.634952	-1.264326
C	-4.481498	-2.210986	-1.017932
H	-4.701884	-2.963091	-1.778236
H	-5.208084	-1.404234	-1.049700
H	-4.483125	-2.680742	-0.034912
N	3.285182	1.177608	-1.598321
C	4.587348	1.832978	-1.464554
H	4.809330	2.384837	-2.378882
H	5.329738	1.061325	-1.282161
H	4.556631	2.525477	-0.621939

Dimer of **6-4** slip face to face (M06-2X/6-31G*)

Atom	X	Y	Z
H	-1.065404	-4.042798	1.372646
C	-1.279739	-3.136545	0.815577
C	-0.323507	-2.652200	-0.050665
C	-2.752808	-1.305221	0.256577
C	-0.557859	-1.472937	-0.791525
C	-2.504104	-2.455527	0.972776
C	-1.789049	-0.798914	-0.643849
C	0.422243	-0.946479	-1.663819
H	-3.265963	-2.818385	1.654811
C	0.172489	0.204550	-2.379781
H	0.945990	0.590207	-3.035975
C	-1.060376	0.875897	-2.235737
H	-1.264992	1.794264	-2.777720
C	-2.019691	0.391031	-1.372267
C	-3.298581	1.136604	-1.196395
C	-4.048588	-0.594399	0.423764
C	1.757112	-1.602106	-1.758900
C	0.976384	-3.360348	-0.184664
O	-4.933376	-1.008768	1.139075
O	-3.516475	2.174239	-1.791539
O	2.662009	-1.116911	-2.410751
O	1.226645	-4.384992	0.412031
N	-4.220994	0.590045	-0.305285
C	-5.505090	1.261909	-0.111890
H	-5.505040	2.167940	-0.712307
H	-5.632543	1.492733	0.947263
H	-6.314195	0.597883	-0.421640
N	1.924960	-2.787639	-1.040767
C	3.195778	-3.506224	-1.142015
H	3.841671	-2.946496	-1.813859
H	3.011819	-4.508607	-1.532986
H	3.638630	-3.592375	-0.147345
H	1.268148	-1.790342	2.784114
C	1.063500	-0.871913	2.242246
C	2.022716	-0.387008	1.378671
C	-0.419191	0.950513	1.670655
C	1.792004	0.803033	0.650424
C	-0.169306	-0.200512	2.386582
C	0.560778	1.476985	0.798219
C	2.755765	1.309559	-0.249884
H	-0.942675	-0.586131	3.042955
C	2.506940	2.459877	-0.966016
H	3.268794	2.822906	-1.647965
C	1.282442	3.140679	-0.808891
H	1.067972	4.046878	-1.366000

C	0.326262	2.656206	0.057340
C	-0.973806	3.364078	0.191172
C	-1.754052	1.606135	1.765984
C	4.051672	0.598952	-0.417007
C	3.301487	-1.132696	1.202373
O	-2.658760	1.121038	2.418165
O	-1.224413	4.388367	-0.405986
O	4.936598	1.013708	-1.131920
O	3.519250	-2.170685	1.796981
N	-1.922127	2.791542	1.047678
C	-3.193025	3.510009	1.148987
H	-3.837788	2.951681	1.823089
H	-3.637637	3.593696	0.154868
H	-3.008624	4.513340	1.537245
N	4.224012	-0.585744	0.311647
C	5.507956	-1.257801	0.117961
H	5.508223	-2.163400	0.719028
H	6.317288	-0.593597	0.426739
H	5.634758	-1.489396	-0.941096

Dimer of **6-3** slip face to face (M06-2X/6-31G*)

Atom	X	Y	Z
H	-3.930231	-2.468667	2.134006
C	-3.479367	-1.884074	1.337908
H	-1.687861	-3.056218	1.259773
C	-2.241101	-2.215819	0.858104
C	-3.645925	-0.026405	-0.193599
C	-1.657932	-1.443036	-0.179365
C	-4.196306	-0.779782	0.816525
C	-2.353467	-0.334762	-0.723177
C	-0.343547	-1.726916	-0.667869
H	-5.172451	-0.544093	1.223297
H	-2.302071	1.299592	-2.145554
C	0.228921	-0.939420	-1.639036
H	1.241445	-1.120044	-1.981676
C	-0.492996	0.153703	-2.173669
H	-0.014919	0.770862	-2.928332
C	-1.755721	0.456260	-1.739577
O	-4.241846	1.065717	-0.750939
O	0.257005	-2.795907	-0.086236
C	-5.513447	1.429192	-0.264217
H	-5.815273	2.310349	-0.830027
H	-5.474029	1.675082	0.804179
H	-6.242863	0.625755	-0.421012
C	1.565230	-3.116053	-0.507303
H	2.265141	-2.303495	-0.281626
H	1.589083	-3.337571	-1.581419
H	1.851717	-4.006163	0.053305
H	0.014919	-0.770862	2.928332
C	0.492996	-0.153703	2.173669
H	2.302071	-1.299592	2.145554
C	1.755721	-0.456260	1.739577
C	0.343547	1.726916	0.667869
C	2.353467	0.334762	0.723177
C	-0.228921	0.939420	1.639036
C	1.657932	1.443036	0.179365
C	3.645925	0.026405	0.193599
H	-1.241445	1.120044	1.981676
H	1.687861	3.056218	-1.259773
C	4.196306	0.779782	-0.816525
H	5.172451	0.544093	-1.223297
C	3.479367	1.884074	-1.337908
H	3.930231	2.468667	-2.134006
C	2.241101	2.215819	-0.858104
O	-0.257005	2.795907	0.086236
O	4.241846	-1.065717	0.750939
C	-1.565230	3.116053	0.507303

H	-1.851717	4.006163	-0.053305
H	-1.589083	3.337571	1.581419
H	-2.265141	2.303495	0.281626
C	5.513447	-1.429192	0.264217
H	6.242863	-0.625755	0.421012
H	5.474029	-1.675082	-0.804179
H	5.815273	-2.310349	0.830027

Dimer of **6-3** face to face (M06-2X/6-31G*)

Atom	X	Y	Z
H	2.508003	-2.563617	1.725657
C	1.879453	-1.677508	1.704312
H	0.041737	-2.779593	1.693314
C	0.516762	-1.806012	1.696410
C	1.721332	0.729964	1.618718
C	-0.296170	-0.643546	1.679543
C	2.497585	-0.405410	1.646876
C	0.296170	0.643546	1.679543
C	-1.721332	-0.729964	1.618718
H	3.579199	-0.341059	1.612683
H	-0.041737	2.779593	1.693314
C	-2.497585	0.405410	1.646876
H	-3.579199	0.341059	1.612683
C	-1.879453	1.677508	1.704312
H	-2.508003	2.563617	1.725657
C	-0.516762	1.806012	1.696410
O	2.214182	1.992976	1.519878
O	-2.214182	-1.992976	1.519878
C	3.578060	2.119553	1.187201
H	3.751854	3.181647	1.012129
H	3.806040	1.547699	0.278782
H	4.224532	1.778626	2.005339
C	-3.578060	-2.119553	1.187201
H	-3.806040	-1.547699	0.278782
H	-4.224532	-1.778626	2.005339
H	-3.751854	-3.181647	1.012129
H	-0.244490	-3.577945	-1.671017
C	-0.002204	-2.519609	-1.665344
H	-2.046304	-1.884888	-1.636859
C	-1.004268	-1.587674	-1.645408
C	1.690809	-0.801272	-1.628396
C	-0.677335	-0.206587	-1.645596
C	1.359108	-2.135306	-1.659849
C	0.677335	0.206587	-1.645596
C	-1.690809	0.801272	-1.628396
H	2.124048	-2.902754	-1.646897
H	2.046304	1.884888	-1.636859
C	-1.359108	2.135306	-1.659849
H	-2.124048	2.902754	-1.646897
C	0.002204	2.519609	-1.665344
H	0.244490	3.577945	-1.671017
C	1.004268	1.587674	-1.645408
O	2.965717	-0.324498	-1.574545
O	-2.965717	0.324498	-1.574545
C	3.999709	-1.272758	-1.453501

H	4.927465	-0.704841	-1.374535
H	4.046578	-1.925786	-2.333297
H	3.864389	-1.886476	-0.554119
C	-3.999709	1.272758	-1.453501
H	-4.046578	1.925786	-2.333297
H	-3.864389	1.886476	-0.554119
H	-4.927465	0.704841	-1.374535